Minnesota Department of Transportation

RESEARCH SERVICES & LIBRARY

Office of Transportation System Management

Evaluation of the Effect of MnPASS Lane Design on Mobility and Safety

John Hourdos, Principal Investigator
Minnesota Traffic Observatory

June 2014

Research Project
Final Report 2014-23

To request this document in an alternative format call 651-366-4718 or 1-800-657-3774 (Greater Minnesota) or email your request to ADArequest.dot@state.mn.us. Please request at least one week in advance.

Technical Report Documentation Page

1. Report No.	2.	3. Recipients Accession No.	
MN/RC 2014-23			
4. Title and Subtitle Evaluation of the Effect of MnPASS Lane Design on Mobility and Safety		5. Report Date June 2014 6.	
7. Author(s) Panagiotis Stanitsas, John Hourdos, and Stephen Zitzow		8. Performing Organization Report No.	
9. Performing Organization Name and Address Minnesota Traffic Observatory Department of Civil Engineering University of Minnesota		10. Project/Task/Work Unit No. CTS Project #2011094 11. Contract (C) or Grant (G) No. (C) 89261 (WO) 247	
12. Sponsoring Organization Name and Address Minnesota Department of Transportation Research Services & Library 395 John Ireland Boulevard, MS 330 St. Paul, MN 55155		13. Type of Report and Period Covered Final Report 14. Sponsoring Agency Code	
15. Supplementary Notes http://www.lrrb.org/pdf/201423.pdf			

16. Abstract (Limit: 250 words)

Dynamically priced High Occupancy Toll (HOT) lanes have been recently added to the traffic operations arsenal in an attempt to preserve infrastructure investment in the future by maintaining a control on demand. This study focuses on the operational and design features of HOT lanes. HOT lanes' mobility and safety are contingent on the design of zones ("gates") that drivers use to merge in or out of the facility. Existing methodologies for the design of access zones are limited to engineering judgment or studies that take into consideration undersized amount of observations. Case in point is the fact that the design philosophes between the two HOT facilities in Minnesota are diametrically opposed. Specifically, the I-394 freeway, the first dynamically priced HOT lane, was designed with a closed access philosophy, meaning that for the greater length of the roadway access to the HOT lane is restricted with only specific short-length sections where access is allowed. In contrast I-35W, the second HOT corridor, was designed with an open access philosophy where lane changes between the HOT and the GPLs are allowed everywhere except for a few specific locations. This contradiction generated questions as to effect each case has on safety and mobility. This study presents an assessment of safety and mobility on the two facilities as they operate today and highlights the issues present on either design. In addition, two design tools were developed, the first assisting in the optimal design of access zones based on traffic measurements, and the second allowing the assessment of the influence congested General Purpose Lanes can have on the mobility and safety of the HOT under different traffic conditions and utilization due to changes in pricing strategy.

17. Document Analysis/Descriptors		18. Availability Statement	
High occupancy toll lanes, high occupancy vehicle lanes, general purpose lanes, managed lanes, lane distribution, traffic congestion.		No restrictions. Document available from: National Technical Information Services, Alexandria, VA 22312	
19. Security Class (this report) Unclassified	20. Security Class (this page) Unclassified	21. No. of Pages 164	22. Price

Evaluation of the Effect of MnPASS Lane Design on Mobility and Safety

Final Report

Prepared by:

Panagiotis Stanitsas
John Hourdos
Stephen Zitzow

Minnesota Traffic Observatory
Department of Civil Engineering
University of Minnesota

June 2014

Published by:

Minnesota Department of Transportation
Research Services & Library
395 John Ireland Boulevard, MS 330
St. Paul, MN 55155

Acknowledgments

We would like to thank the Minnesota Department of Transportation for supporting this project. We would like to acknowledge the help we received from the Center for Transportation Studies (CTS) in coordinating and managing this project. We would like to acknowledge the help, support, and cooperation of Mr. Brian Kary, Ms. Julie Johnson, and others at the MnDOT Regional Traffic Management Center.

We would like to thank the Minnesota Traffic Observatory, especially Matthew Bonnema, Elizabeth Burton, Dan Chouinard, Adam Jessen, Michael Kronzer, Michael Kondziolka, Derek Lehrke, Robert Paquin, Gordon Parikh, Gwyneth Perry, Mark Powers, and Christopher Young, for extensive support in data collection and reduction.

Table of Contents

List of Figures

List of Tables

Executive Summary

Managed lanes have been implemented across the nation in various forms in an effort to increase efficiency and mobility on existing roadway networks. Depending on the type of restrictions implemented, managed lanes include exclusive lanes like bus or truck lanes, separation or bypass lanes, dual-use lanes, High Occupancy Vehicle (HOV) lanes, and value price or High Occupancy Toll (HOT) lanes. Under the context of HOV and HOT, a more concise way to describe these managed lanes is as a freeway within a freeway where lanes are reserved for particular groups of vehicles and are separated by the other General Purpose Lanes (GPLs). Dynamically priced HOT lanes have been recently added to the traffic operations arsenal in an attempt to preserve infrastructure investment in the future by maintaining a control on demand.

This study focuses on operational and design features of HOT lanes. HOT lanes' mobility and safety are heavily contingent on the design of zones ("gates") that drivers use to merge in or out of the facility. This can be attributed to the large speed differential that is observed between the HOT lane and its adjacent lane during traffic peak periods. Existing methodologies for the design of access zones are limited to engineering judgment or studies that take into consideration undersized amount of observations. Case in point is the fact that the design philosophes between the two HOT facilities in Minnesota are diametrically opposed. Specifically, the I-394 freeway, the first dynamically priced HOT lane, was designed with a closed access philosophy, meaning that for the greater length of the roadway access to the HOT lane is restricted with only specific short-length sections where access is allowed. In contrast I-35W, the second HOT corridor, was designed with an open access philosophy where lane changes between the HOT and the GPLs are allowed everywhere except for a few specific locations. Naturally this contradiction generated questions as to which design method is better and more importantly what are the safety and mobility considerations in each case.

This project was established to investigate these considerations, and since the two philosophes are different cases based on design preference, mainly to the level of service the facility owner wants to provide to the users, the second objective of the study was the creation of separate design tools for each alternative. In both cases, the approach was to decompose the studied phenomena in a manner that closely approximates reality. Shockwave characteristics were utilized as surrogates of both safety and mobility. Shockwave length was selected as a surrogate of safety and shockwave frequency as a surrogate for mobility.

The two facilities of I-394 and I-35W have been operating with no great safety or operational concerns; therefore, this study looked deeper into patterns of shockwave activity to uncover differences between the two design philosophies and potentially uncover areas of improvement now or in the future. With the help of MnDOT's Regional Traffic Management Center surveillance infrastructure combined with the advanced detection and measurement capabilities of the Minnesota Traffic Observatory (MTO) the length and breadth of the two corridors was observed and analyzed. For brevity, this report

concentrates only on the locations where mobility and safety patterns of interest were observed. These included four locations on I-35W and one location on I-394.

The first area of interest is on I-35W northbound between the Burnsville Pkwy and Cliff Road interchanges. This area is experiencing severe recurring congestion on the GPLs and has a large proportion of the entrance ramp volume heading for the HOT. Given the existing utilization on the HOT, the shockwaves observed, although large, have not generated any crashes. This can change if the utilization of the HOT lane increases following changes in the pricing algorithm or on the market characteristics of HOT demand. In addition, aggressive behavior by the commuter buses entering the freeway in this location accounts for a large number of the inappropriate lane changes observed. Considering mitigation strategies for this location, keeping in mind that they are not immediately needed, a first suggestion is to target bus driver behavior, requesting that bus drivers join the HOT less aggressively or a little later (after the Cliff Road bottleneck). Given that the demand on the intersecting roadways will not decline in the future, if the utilization of the HOT increases, there may be a need to restrict access to the HOT lane between TH-13 and Black Dog Road. This will hurt the service offered by the HOT so it should be considered only if conditions deteriorate significantly.

The second area of interest in northbound I-35W lies between 46th Street and 42nd Street closer to downtown Minneapolis. This last segment of open access delivered a very large amount of flow breakdowns numerically as well as a percent of the general lane change activity. This area is the last chance for vehicles to join the HOT and is an area where it would be very difficult to further restrict access. Specifically a large portion of the HOT traffic in the afternoon originates from the 46th Street ramp, which is already in the midst of the problem. If a closed access design were followed, there would still be the need for a gate north of 46th Street, generating the same issues we observe today. Restricting access south of 46th Street will not change the outlook much. A closer study of the origins of the demand on the HOT at this point could reveal some possible compromises.

On the southbound direction of I-35W there are two areas that could compromise safety and mobility. One is in the area of 98th Street and the other is the area of Blackdog Road. Although the congestion observed south of 98th Street (location 6101 SB) is a rare occurrence, it happens and when it does it generates quantifiable issues on the HOT. As seen in the following figure, it generated some of the biggest shockwaves among all locations on I-35W during all of the observed days. For the foreseeable future this is a location that needs to be watched for signs of deterioration. The areas close to the start of the open access south of I-494 (locations 6131 SB and 6130 SB) are operating fine today but are a good example of how the situation can change with the addition of just a few more vehicles in the HOT. The absolute values of the lengths of the waves signal a good standing in terms of safety, but if we take into account the high lane change activity of this segment, a future increase of vehicles on the HOT facility could result in greater disturbances.

The allowed access area around Louisiana Ave on the eastbound is the only area of interesting activity on I-394. This is the second to last gate before the HOT enters the

barrier separated reversible section. As it is characteristic of closed access design the "gates" experience very high lane changing activity. The average observed values reach 100 vehicles per 15 minute intervals during the morning peak hours and over 60 in the evening peak hours. The statistical characteristics of the observed flow breakdowns are on the higher end. The lengths of the recorded flow breakdowns reached a median value of 4 vehicles while the most extreme value was 12 vehicles. Despite the conservative design of the access segments on the HOT and the generally lower demand levels, very long shockwaves were generated due to the high speed differential, between the HOT and the adjacent GPL, at this part of the freeway.

It is difficult to compare the two design philosophies because they were devised to serve the needs of the two distinct roadways. I-394 is operating very well with the closed access design mainly because the majority of the demand originates from three distinct interchanges, I-494, TH-169, and TH-100. The rest of the ramps comparatively speaking have much lower demand. As illustrated in this report, this is not the case on I-35W. The interchange density is much higher with entrance ramps very closely spaced and with the majority of those ramps carrying large demands of HOT eligible vehicles. It would have been very difficult to follow a closed access design on I-35W, and given the results presented in this report, it would had made little difference in terms of mobility and safety.

Comparisons of shockwave characteristics of the four discussed zones are shown in the following figure. Although the volumes involved are different, the shockwave lengths observed are comparable signaling no difference in terms of safety between the two design philosophies.

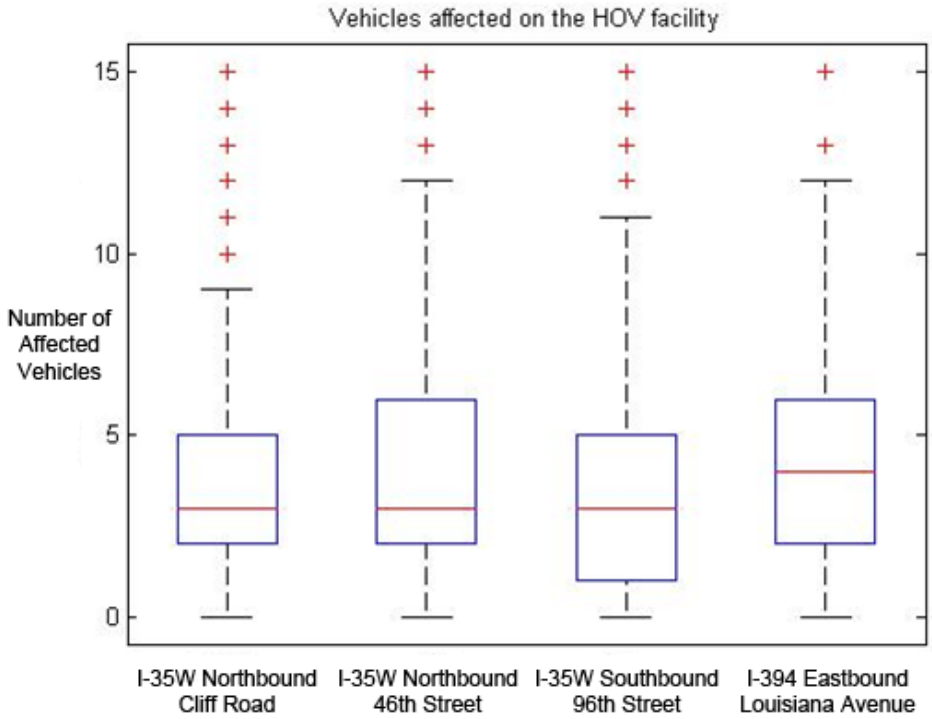

Following the assessment of the effect MnPASS has on the current mobility and safety of the HOT lane operations, this study continued with the development of two methodologies, which address design issues related to forthcoming and existing HOT facilities. The first methodology targeted forthcoming HOT facilities that adopt a closed access philosophy and derived a software tool capable of defining the Optimal Lane Changing Regions (OLCRs). The proposed methodology is capable of defining the OLCRs on forthcoming HOT facilities with respect to the positions of entrance or exit ramps.

Trajectories of vehicles merging from the entrance ramp to the freeway and moving toward the HOT lane were collected at a freeway segment of I-35W. A microscopic simulation model exploiting Monte Carlo techniques was developed and tested for its ability to capture the observed trajectory lengths. After the model's ability to regenerate realistic trajectories of vehicles was validated, the proposed methodology was compared to other commonly used practices. The main advantage of the proposed methodology is that it takes into account the traffic conditions on each lane between the entrance ramp and the HOT. This way the proposed model will design the OLCR at the location that the demand is expected to arrive. On the other hand, existing practices tend to overestimate the OLCR and place the gate up to 2000 feet further downstream than the vehicles are expected to arrive to the adjacent to the HOT lane.

The second methodology, proposed in this project, aims to support engineer decisions for planning access restrictions on existing HOT facilities; the core is a developed model capable of emulating shockwave propagation on the HOT lane given target densities and speed differential between the HOT and the adjacent GPL. This methodology and subsequent tool was focused on HOT facilities that follow an open access philosophy, and the outcome of this process can support the decision of engineers to restrict access for locations that will reach their operational limit in the future either as a result of increased demand or as a result of changes in the pricing strategy.

In particular, a shockwave propagation model was developed and captured the shockwave activity on three selected locations of interest on I-35W. After the model was calibrated to reproduce shockwave activity (shockwave lengths) at current traffic conditions, the same activity was reproduced for future demand levels until the examined facilities reached their operational boundary. The results support the validity of the process as the model replicated the distributions of shockwave lengths even at a 90% confidence interval. The developed mechanism was able to force the examined locations up to operational capacity by increasing the density of the simulated streams. The capacity was identified as the point in the density domain that the entire simulated stream experienced a disturbance after it was introduced.

In summary, the developed methodologies were derived so that their transferability is not affected and hence they can potentially be used by agencies to design HOT lanes without compromising mobility or safety. Both methodologies were driven by an extensive and diverse data collection process and validated against actual observations.

1. Introduction

Managed lanes have been implemented across the nation in various forms in an effort to increase efficiency and mobility on existing roadway networks. Depending on the type of restrictions implemented, Managed Lanes include exclusive lanes like bus or truck lanes, separation or bypass lanes, dual-use lanes, High Occupancy Vehicle (HOV) lanes, and value price or High Occupancy Toll (HOT) lanes (Kuhn et al. 2005). Under the context of HOV and HOT, a more concise way to describe these Managed Lanes is as a freeway within a freeway where lanes are reserved for particular groups of vehicles and are separated from the other General Purpose Lanes (GPLs).

HOT lanes have been recently added to the traffic operations arsenal in an attempt to preserve infrastructure investment in the future by maintaining a control on demand; in most cases they are conversions of existing HOV lanes. HOT lanes are "oases" of free-flow conditions within congested freeways. Observations support the benefits of implementing HOT and HOV lanes, which in many cases can carry up to half of the people carried on the entire freeway.

This study focuses on operational and design features of HOT lanes. HOT lanes' mobility and safety are heavily contingent on the design of zones ("gates") that drivers can use to merge in or out of the facility. This can be attributed to the large speed differential that are observed between the HOT lane and its adjacent lane during peak traffic periods. Existing methodologies for the design of access zones are limited to engineering judgment or studies that take into consideration undersized observation samples. Case in point is the fact that the design philosophes between the two HOT facilities in Minnesota are diametrically opposed. Specifically, the I-394 freeway, the first dynamically priced HOT lane, was designed with a closed access philosophy, meaning that for the majority of the length of the roadway access to the HOT lane is restricted with only specific short sections where access is allowed. In contrast, I-35W, the second HOT corridor, was designed with an open access philosophy where lane changes between the HOT and the General Purpose Lanes (GPL) are allowed everywhere except a few specific locations. Naturally this contradiction generated questions as to which design method is better and, more importantly, what the safety and mobility considerations are in each case. This project was established to investigate these considerations and to develop a methodology to design the proper access depending on site characteristics. While evaluating the current state of each of the two sites in terms of mobility and safety, it became clear that the two philosophes are not the opposite ends of a continuum but different cases based on design preference and the level of service the facility owner wants to provide to the users. The objective of the study changed to include the creation of design tools for each alternative separately. In both cases an approach was taken that aimed at decomposing the studied phenomena in a manner that closely approximates reality. Shockwave characteristics were utilized as surrogates of both safety and mobility. Shockwave length was selected as a surrogate of safety and shockwave frequency as a surrogate for mobility.

This report is divided into two main parts. The first part is the evaluation of the existing facilities, in terms of mobility and safety, in their present form and demand patterns. The

second part of the report describes the development of two new design tools. The first tool, targeting closed access facilities, utilizes historical or simulation based traffic measurements to design the optimal location and size of allowed access sections. The second tool, targeting open access facilities, utilizes similar information to identify sections where access should be restricted in order to preserve mobility and safety.

Traffic shockwave propagation and lane changing activity were decomposed to their fundamental components to emulate reality. The stochastic nature of the examined phenomena was incorporated in the developed models by implementing Monte Carlo techniques.

This effort opens the doors for a systematic treatment of access zones. It incorporates knowledge obtained from extensive periods of observations to the design of the Optimal Lane Changing Regions (OLCR) on forthcoming facilities and to the preservation of the quality of service on existing HOT lanes. This study was guided by an extensive and diverse data collection process capturing various traffic conditions. The constructed datasets provided all the necessary tools and insight for developing the constructed models.

2. Background

Managed Lanes

Managed lanes have been implemented on congested freeways as a strategy to balance the increase in the total number of vehicle miles traveled and slow highway capacity growth. Even though the total vehicle miles traveled in the United States have increased more than 70 % over the past 20 years, the corresponding increase in Highway capacity does not exceed 0.3 % (FHWA 2008). To address this issue agencies have implemented various types of managed lanes so that the person and freight moving capability of the highways could be increased.

Texas Department of Transportation defines a managed lane facility as one that increases highway efficiency by aggregating operational and design actions (Kuhn et al. 2005). Depending on the objective several types of managed lanes have been implemented in recent years including exclusive lanes, like bus or truck lanes, separation or bypass lanes, dual-use lanes, HOV lanes, and value price or HOT lanes (Kuhn et al. 2005). The most common operational strategies for managed lanes include:

- Pricing
- Access Control
- Eligibility

This study was centered around the HOT facilities in the State of Minnesota on Interstate 394 and Interstate 35W. The complexity of actively managing HOT lanes places them among the most demanding facilities to operate because of the dynamic character of their operational strategies. They not only have to be responsive to the changes in traffic demand for the facility but also need to account for a targeted level of service for users of the managed lane. Figure 1 was included in a report of the United States Department of Transportation in an effort to capture the management strategies that are related to the managed lanes.

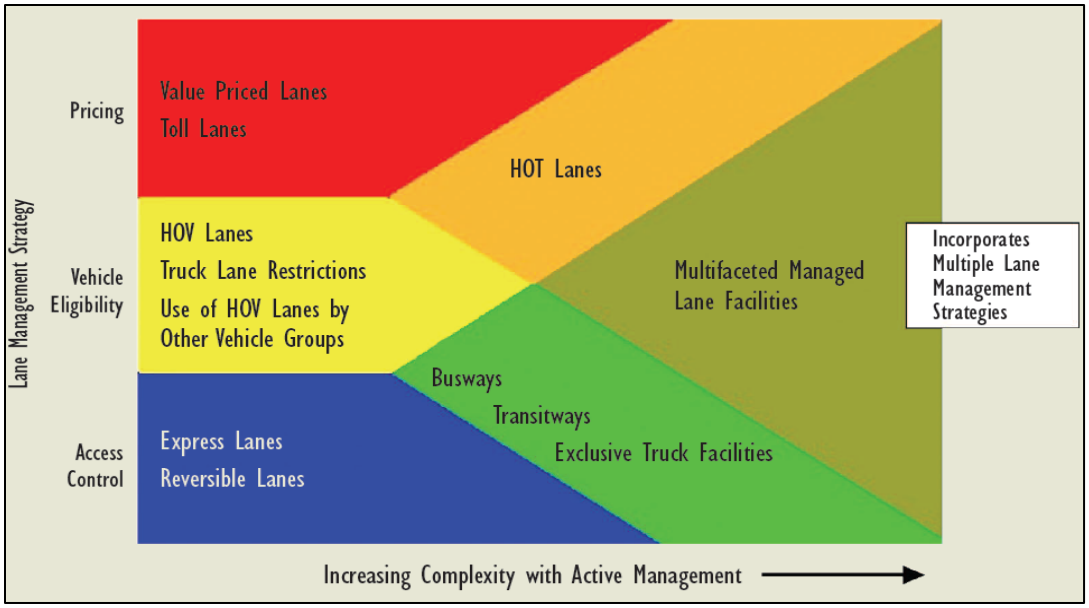

Figure 1. Active management strategies with varying goals and complexity (FHWA 2008)

HOV lanes are reserved lanes targeting vehicles with specified occupancy. In an attempt to preserve infrastructure investment in the future by maintaining a control on demand, HOT lanes have been implemented on exiting HOV facilities that were generally underutilized. The mobility and safety on the HOT/HOV facilities heavily relies on their interaction with their adjacent general purpose lanes. Different types of separating the HOT lane and its adjacent lane have been applied across the United States.

HOT lanes allow vehicles with lesser occupancy than the predefined to use the HOV facility. The HOT/HOV lanes are separated by either physical barriers (e.g. Interstate 394 Minneapolis, MN (Figure 2)) or a painted buffer (e.g. Interstate 35 W Minneapolis, MN, (Figure 3))

Figure 2. Interstate 394, Minneapolis, MN

Figure 3. Interstate 35W, Minneapolis, MN

Regarding the HOT lane on Interstate 394, there is a reversible section that accommodates inbound traffic during morning peak hours and outbound traffic for evening peak hours so that the maximum utilization of the lane can be achieved. Another example of a facility that utilizes a reversible section is that of Interstate 10 in Houston, TX (Figure 4). Facilities like I-394 and I-10 follow a closed access philosophy in their design and aim in minimizing the interaction between the HOT lane and its adjacent General Purpose Lane.

Figure 4. Interstate 10, Houston, TX

Design Guidelines

Several studies available in the literature were focused on the interaction between the HOT/HOV lane and the general purpose lanes of the freeway. Menendez and Daganzo (2007) simulated the interaction between GPLs and HOVs and provided results supporting the smoothing effect of HOV lanes on discharge flow rates at isolated interactions. This

positive effect was also supported by Cassidy et al. (2006). Even though the objective of those studies is not aligned with the main goal of the developed methodology, they share commonalities and were influential along the modeling efforts of this research.

Liu et al. (2012) measured the effect of lane changing activity between the HOT lane and the general purpose lanes using the VISSIM simulator and provided evidence about the negative effect of lane changing demand on the networks capacity. More factors connected to the frictional effect between the HOT and the GPL were identified by Liu et al. (2011). Two key factors include the tolling strategy and the separation type. The main objective here was not to derive design guidelines but to evaluate the performance of existing facilities and quantify the interaction between HOT/HOV lane and its adjacent lane and draws parallels with the model of this study. The amount of data that were used to calibrate the VISSIM simulation models was limited and difficult to obtain when designing a forthcoming facility.

As stated previously, the design aspects of HOV/HOT lanes that require the greatest amount of attention are the ones associated with the lane changing regions characteristics. The literature on this subject is limited and this is the point that this study aims in making a valuable contribution. The key characteristics of the proposed methodology for forthcoming closed access facilities aim in defining the distance of the merging area from the nearest entrance ramp as well as the length of the merging area.

Various efforts to derive methodologies for creating step wise processes with the potential of defining the length and the position of the OLCR are available in the literature and are presented below. In all cases the findings were based on either engineering judgment or simulation experiments that were calibrated at a level that was not able to capture individual driver behavior and vehicles' interactions.

Figure 5 presents the quantities of interest for the design process; L1 denotes the distance between the beginning of the entrance (or exit ramp in another scenario), L2 denotes the length of the merging area and Ltotal is the distance between the beginning of the entrance (or exit) ramp and the end of the proposed gate.

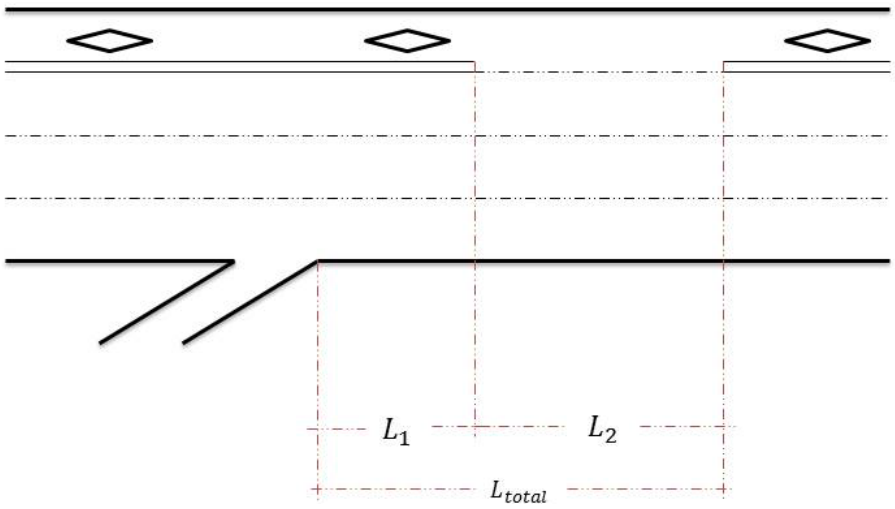

Figure 5. Design features of interest

The HOV Systems Manual (Texas Transportation Institute, 1998) proposes a distance of Ltotal equal to 2500 feet regardless of the number of General purpose lanes. This approach delivers a conservative design which in most cases would is able to accommodate the users of the HOV/HOT lane. It does not, however, take into consideration cases where the interaction between the HOT and its adjacent lane need to be minimized. In addition, traffic conditions and traffic patterns on the GPLs are not instilled in the design process.

Fuhs (1990) proposed a methodology that takes into account the number of lane changes that are necessary for vehicles to merge to the HOT lane after merging to the freeway from the nearest entrance ramp or vehicles that need to exit to the exit ramp downstream. The minimum proposed value for Ltotal was set to 500 feet for each lane change and the recommended value was equal to 1000 feet. In a similar vein, the California department of Transportation (1991) proposed a minimum distance of 660 feet per lane change. Regarding the length of the opening length, several values, which range from 900 feet to 1500 feet, have been proposed in an effort to accommodate the weaving demand of users of the facility (Fuhs (1990), Yang et al. (2011) , ASSHTO (2004) , Kuhn et al. (2005)).

Yang et al. (2011) proposed a probabilistic approach towards quantifying advisory designs utilizing gap acceptance theory. The core of their methodology was an analytical formulation that derives the probability that a weaving vehicle with critical gap equal to T will complete its weave successfully given the number of GPLs and Ltotal (Equation 1). E[D(q)] denotes the vehicles expected time for merging. s and sw represent the speed of the target lane and the speed of the subject vehicle respectively. The proposed model was calibrated based on the lane changing demand for zones that resulted after segmenting existing merging areas on Interstate 635 in Dallas, Texas.

$$P(N, L_{total}) = 1 - \sum_{k=0}^{N-1} \frac{\left(\frac{L_{total}}{S_W \ minE[D(q)]}\right)^k e^{\frac{L_{total}}{S_W \ minE[D(q)]}}}{k!} \qquad \textbf{(Eq. 1)}$$

Even though the proposed methodology by Yang derived results that were tailored to the characteristics of a potentially examined location its transferability is questionable because of the complex and time consuming data collection that is required for the calibration of the model. The results of the proposed methodology with respect to the length of the gate and Ltotal are summarized in Table 1. The advisory gate lengths varied between 900 and 1400 feet and were contingent to the weaving demand.

Table 1. Yang et al. (2011) design guidelines

Free Flow speed (miles/hour)	Minimum Ltotal for Number of GPLs			Desired Ltotal for Number of GPLs		
	3	4	5	3	4	5
55	2,000	2,500	3,000	2,400	2,900	3,500
60	2,100	2,600	3,100	2,500	3,000	3,600
65	2,300	2,800	3,400	2,700	3,300	3,900
70	2,400	3,100	3,700	2,900	3,600	4,200

Using data from I-635 in Houston Texas, Williams et al. (2010) developed a set of design guidelines based on the results of a simulation methodology developed in VISSIM simulator. The advisory lengths derived from the proposed process are summarized in Table 2 and rely once again on the merging demand for the HOT. The types of data that need to be harvested in this case are once again difficult to obtain and this was indeed the weak point of their methodology.

Table 2. Williams et al. (2010) design guidelines

Weaving demand (vehicle/hour)	Minimum Weaving distance per GPL
200	500
300	625
400	750
400	875

Wave Propagation

The second methodology developed in this study aims in access restriction on existing HOT lanes and was based on shockwave propagation on the HOT lane. The lane changing interaction between HOT and GPLs is the cause of flow breakdowns (shockwaves) on the HOT lane. Shockwaves create inconvenience to the commuters by forcing the traffic conditions of the HOT into transient congested traffic states. “Shockwaves are a boundary that shows discontinuity in the flow-density domain” (May, 1990); their propagation and the corresponding number of vehicles affected are surrogates for safety and mobility.

Traffic shockwaves have captured a great amount of research attention starting in 1950’s when Lighthill and Whitham (1955) introduced the hydrodynamic theory in traffic.

Realistic wave propagation has been the main goal of many traffic flow models. In lower order models (e.g. Newell, 2002) waves propagate as a simple random walk as supported by empirical findings from Windover and Cassidy (2001) for congested states. Models that influenced this study will be presented in a slightly higher detail even though the target was not to advance the car-following theory.

Car following models proposed by Gazis, et al. (1961), Gipps (1981) and Newell (2002) are among the most commonly used by commercial traffic simulation software. In the model proposed by Newel vehicle trajectories are approximated by piecewise linear extrapolations as presented in Figure 6. Vehicles will respond to their leader's deceleration if a minimum distance threshold is violated. Newell's model has been also verified by later studies using data from signalized intersections by Ahn, et al. (2004).

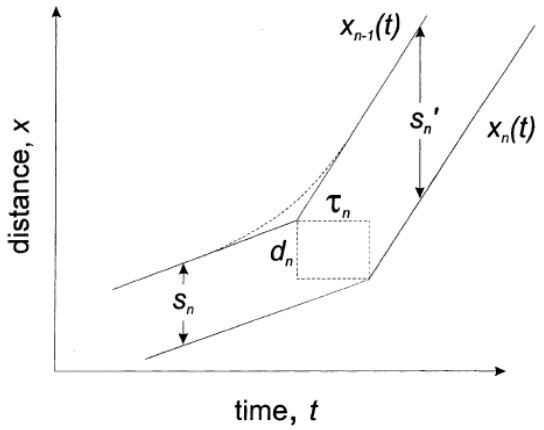

Figure 6. Piecewise linear trajectories in Newell's model (Ahn et al. (2004))

Vehicles in Gipps' (1981) model are assigned a desired speed Un which they do not exceed; Un is achieved at an acceleration rate that increases with speed and after Un is achieved the acceleration becomes zero. Equation 2 describes the speed of vehicle n at time t + T, where T is the driver's reaction time.

$$u_n(t+T) = \min\left(u_n(t) + 2.5 * a_n * T * \left(1 - \frac{u_n(t)}{U_n}\right) * \sqrt{0.025 + \frac{u_n(t)}{U_n}}, \right.$$
$$\left. -b * T + \sqrt{b^2 * T^2 + b\{2 * [x_{n-1}(t) - L_{n-1} - x_n(t)] - u_n(t) * T + \frac{u_{n-1}(t)^2}{b'}} \right)$$

(Eq. 2)

Where, $u_n(t)$ = speed of vehicle n

a_n = maximum desired acceleration of vehicle n

T = reaction time

U_n = desired speed of vehicle n

b,b' = deceleration parameters

L_{n-1} = length of vehicle n

$x_n(t)$ = position of vehicle n at time t

The General Motors Nonlinear Model proposed by Gazis, et al. (1961) is shown in Equation 3. α, β and γ are parameters of the model and the response is proportional to the speed of vehicle n at time and inversely proportional to the space headway. τn is the driver's reaction time while the speed difference is the stimulus for the implemented acceleration or deceleration. The model's connection to the Fundamental Diagram proposed by Greenshields, et al. (1935) is revealed by setting β equal to 0 and γ equal to 2. Chandler's model was the first car-following model and constitutes a special case of Gazis' model. Chandler's model is presented in Equation 4.

$$\dot{v}_n(t) = \alpha * \frac{U_n^{\beta}(t)}{\Delta X_n^{\gamma}(t-\tau_n)} * \Delta U_n^{front}(t-\tau_n) \quad \text{(Eq. 3)}$$

$$\dot{v}_n(t) = \alpha * \Delta U_n^{front}(t-\tau_n) \quad \text{(Eq. 4)}$$

Other models describing wave propagation at a car-following level were also proposed by Castillo (2001) or Kim and Zhang (2008) in a stochastic framework. In a stochastic manner wave propagation is also captured by traffic flow models proposed by Jabari and Liu (2012), Kuhne and Michalopoulos (1997) and Daganzo (1994). The latter (Cell Transmission Model) was the modeling base for multiple models that followed and utilizes the Godunov's scheme (Godunov 1959) to provide numerical solutions to the heat transfer equation capturing shockwaves and rarefactions. The aforementioned stochastic models deviate from the framework of this study and were presented briefly since they provided valuable insight for the modeling efforts of this research.

The aforementioned models could serve the purposes of this study but they come with complications which hamper the goal of the present study; a simpler and straight forward approach was therefore followed. Another reason for not implementing existing car following models was the fact that they do not ensure that the initial conditions of a potential car-following experiment will be preserved until a disturbance is introduced. Thus, the platoon formation of the examined stream would be reshaped until a shockwave initiates. Finally, the behavior that was mainly targeted was the variation of drivers' response as they exceed a threshold that describes their willingness to approach their leader. After this threshold is violated vehicles implement the highest possible deceleration and this was incorporated in the proposed model.

3. Description of Sites

This chapter offers a primer on the HOT lane facilities on Interstates 35W and 394. The objective is to present information about the facilities and their characteristics as well as provide further details for the selected segments used for developing and testing the models of this study. Both Interstate 394 and Interstate 35 W were examined for their potential in providing the necessary measurements; it was concluded that the I-35W corridor was more consistent with the objectives of this effort in terms of data collection while 394 was used to test the optimal lane changing region methodology.

I-394

The I-394 is a 9.5-mile freeway that serves as a major link connecting the western suburban communities and downtown Minneapolis. With an average three lanes in each direction, it carries an annual average daily traffic (AADT) of up to 151,000 vehicles (Cambridge Systematics, Inc. 2006). The posted speed limit is 55 mph. From its inception the freeway included an HOV lane in each direction. The I-394 MnPASS program was opened and became the first HOT lane in Minnesota in May 2005 (Cambridge Systematics, Inc. 2006). It converted the historical high-occupancy vehicle lanes into HOT lanes by equipping the lanes with sensors and leasing transponders to single occupancy vehicle (SOV) drivers. MnPASS Express lanes, designed as HOT lanes, provide up to two additional designated lanes on the I-394 between Wayzata and downtown Minneapolis. The general purpose lane (GPL) configuration remained unchanged. Figure 7 illustrates the schematic of I-394 Express lanes. The MnPASS lanes include two types of designs. From I-494 to Highway 100, the toll lanes were designed as diamond lanes (one lane per direction) following a closed access design. These lanes are separated from GPLs by double white lines and painted with diamond marks. The segment has designated access points that are controlled primarily by lane striping. There are 4 access points on the eastbound direction and 3 on the westbound. On the segment from Highway 100 to Downtown, two reversible lanes are present alongside the freeway separated from the GPLs by a concrete barrier.

I-394 MnPASS Express Lanes Pricing Zones

Direction	Limits	Hours
Eastbound	Wayzata Blve. to Hwy. 100	6AM - 10AM, Mon - Fri
Reversible lane Eastbound	Hwy. 100 to I-94	6AM - 1PM, Mon - Fri
Westbound	Hwy. 100 to Carlson Pkwy.	2PM - 7PM, Mon - Fri
Reversible lane Westbound	I-94 to Hwy. 100	2PM - 5AM Mon - Fri

Legend

- Message sign
- Toll rate sign
- Tolling location
- MnPASS open access (broken line)
- MnPASS restricted access (double solid line)

Figure 7. I-394 MnPASS map (MnDOT)

According to the MnPASS website (http://www.mnpass.org/), the current operation time for the HOT lanes is as follows. The eastbound of I-394 diamond lane section is operated Monday through Friday from 6 a.m. to 10 a.m. The westbound of I-394 diamond lane section is operated Monday through Friday from 2 p.m. to 7 p.m. Both eastbound and westbound lanes are open to general traffic for the rest of the day and on weekends. The eastbound of I-394 reversible section is operated from 6 a.m. to 1 p.m. The reversible lanes are closed from 1 p.m. to 2 p.m. for directional change. The westbound of I-394 reversible section is operated from 2 p.m. to 5 a.m. The reversible lanes are closed from 5 a.m. to 6 a.m. for directional change.

I-35W

I-35W is an Interstate Highway in the U.S. state of Minnesota, passing through downtown Minneapolis. It is one of two through routes for Interstate 35 through the Twin Cities of Minneapolis and Saint Paul, the other being Interstate 35E through downtown Saint Paul. I-35 splits into two branch routes: I-35W, which serves Minneapolis, and I-35E, which serves Saint Paul.

Traveling north, I-35 splits at Burnsville, where the I-35W route runs north for 41 miles, carrying its own separate sequence of exit numbers. I-35W runs through the city of Minneapolis before rejoining with I-35E to re-form I-35 in Columbus near Forest Lake. I-35W supplanted sections of old U.S. Highway 8 northeast of Minneapolis and old U.S. Highway 65 south of Minneapolis that have since been removed from the U.S. highway system. Following the implementation of HOT lanes on I-394, the MnPASS Lanes opened on I-35W on September 30, 2009. The project's goals were:

- Reduce congestion
- Improve transit service
- Increase attractiveness of transit service
- Provide alternatives to commuters to avoid congestion

The length of the HOT lanes on I-35W is 14 miles on the Northbound and 11.5 miles on the southbound. In both cases the HOT lanes are separated from the rest of the network using stripped lines. The northbound and southbound sections of I-35W south of I494 and the northbound section of I-35W at 42nd street are tolled during the following hours:

- Northbound from TH 13 to Hyw.62 from 6 a.m. to 10 a.m.
- Northbound from 42nd Street to downtown is always tolled when opened to traffic
- Southbound from I494 to TH 13 from 2 p.m. to 7 p.m.
- Lastly during off peak hours the lanes are not tolled and are open to general traffic with the exception of northbound from 42ne Street to downtown.

The I-35W MnPASS lanes follow the open access design philosophy. This means that lane changes between the HOT lane and the GPLs are allowed for most of the length of the facility (see Figure 8 below).

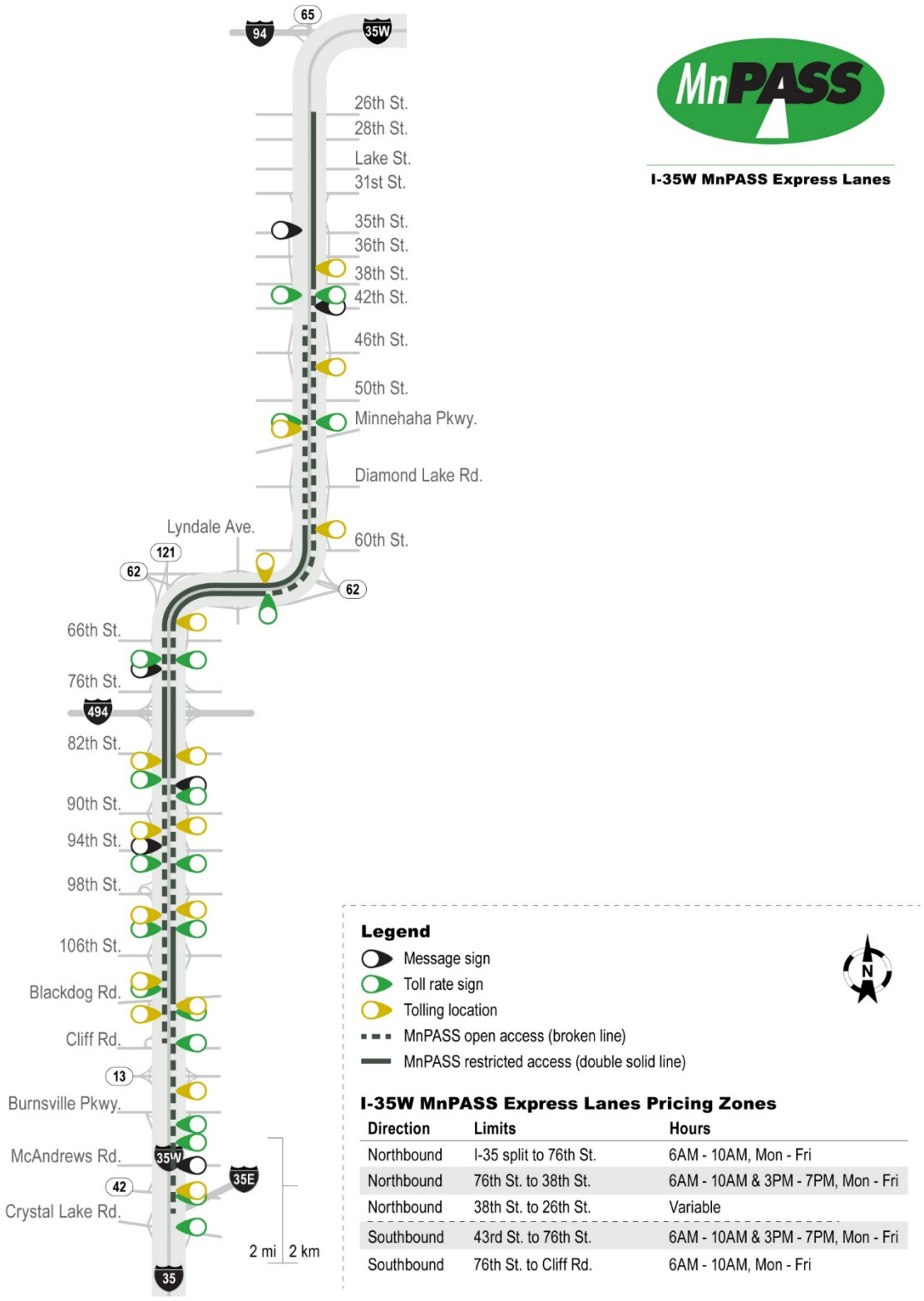

Figure 8. I-35W MnPASS map (MnDOT)

4. Evaluating Safety and Mobility under Present Demand Conditions

One of the original objectives of this project was to evaluate the two HOT lane designs and compare them in terms of safety and mobility. This step, in addition of being necessary in order to proceed in formalizing a methodology and/or general design guidelines, offers specific location evaluations and hopefully useful recommendations on where and when interventions are necessary to maintain the current, very successful, operation in both facilities. It is important to note that in this work there was no evaluation of the level of access to the HOT, meaning we did not evaluate the ability of the road users to reach the HOT as soon as they would like. Such evaluation would only apply to I-394 and to the best of knowledge other studies on that corridor have shown that this is not an issue.

The objective is accomplished by collecting observations of the current HOT lane facilities, extracting quantifiable measures of the level of interaction between HOT and GP lanes, and utilizing these measurements in judging current operations as well as estimating mobility and safety performance levels in the future. The following section describes the data collection effort.

Description of video data collection methodology

The first part of the video collection process started on June 21st 2011. During the first week camera operators got familiarized with the setup of the network as well as the capabilities of the RTMC cameras. Four people were responsible for completing the initial data collection task. They were trained by RTMC engineers on manipulating the RTMC cameras without affecting the incident detection procedures that take place. Cameras capable of providing intense lane changing activity were selected and transmitted back to the MTO. Once again, decisions were based upon the traffic conditions (congestion) for the selected segments and a set up for the cameras was selected so that it is as clear as possible the number of vehicles that are forced to decelerate when a vehicle enters or exits the HOT lane. Figure 9 through Figure 12 below present the locations and codes of MnDOT cameras used.

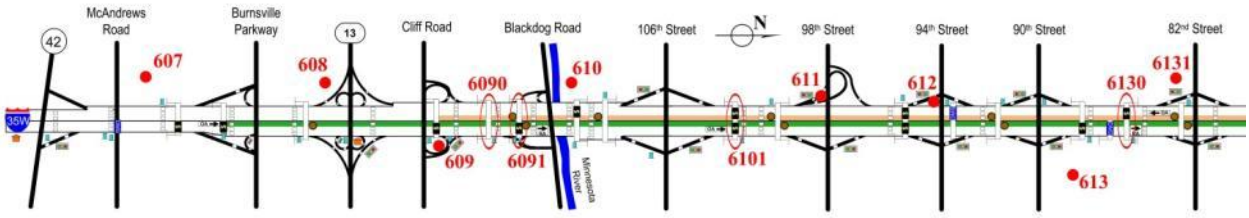

Figure 9. Location codes on I-35W

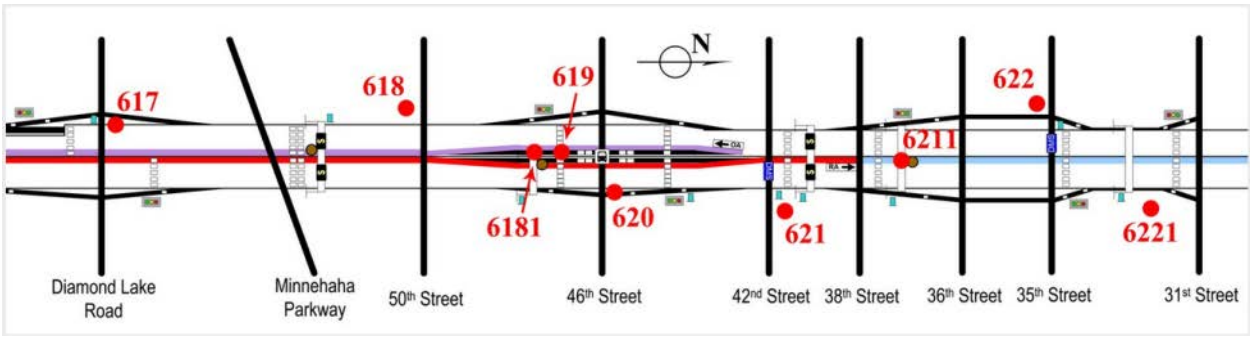

Figure 10. Location codes on I-35W

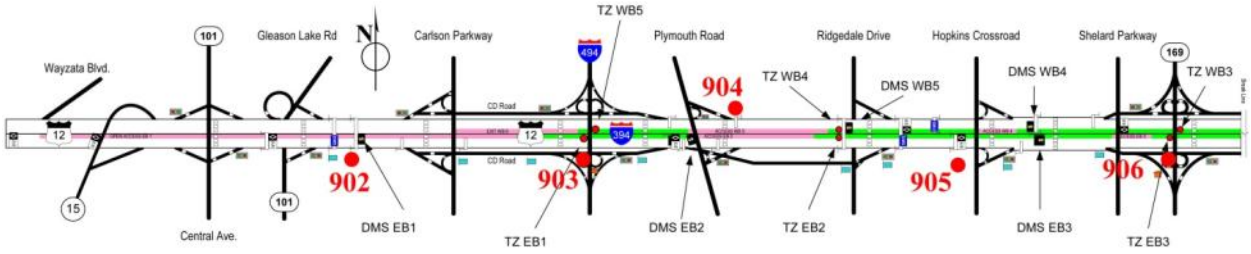

Figure 11. Location codes on I-394

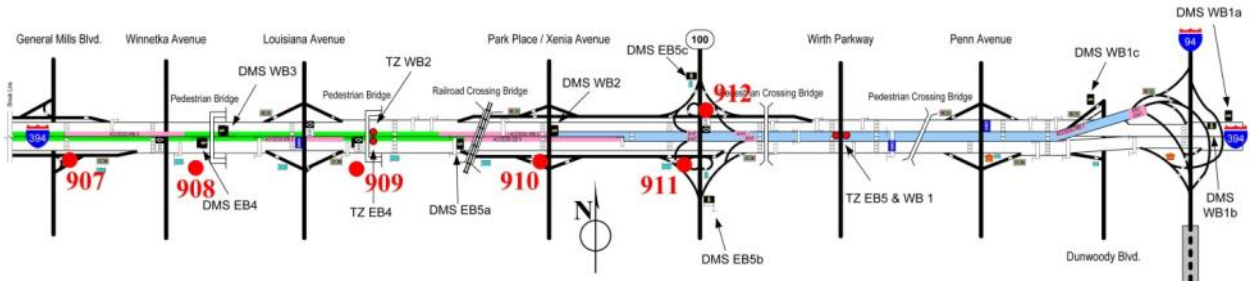

Figure 12. Location codes on I-394

Blind spot investigation

Both the cameras on I-394 and I-35W were tested for their capability of providing a clear view of the whole length of the road. In order to achieve that, vehicles were traced for the whole length of each road from camera to camera. In the case of I-394 no "blind" spot was identified. On the other hand in the case of I-35W a 10 second blind spot was identified in the beginning of the Northbound. It was decided later, that the specific part was not capable of producing a large amount of lane changing activity, thus further video collection was not necessary. In that way it was ensured that deploying additional surveillance equipment was not be necessary.

Table 3 presents the dates video data were collected as part of this objective. Most of the effort focused on retrieving data for typical week days (Tuesday, Wednesday, Thursday); also data for some days that were not considered as typical weekdays (Monday, Friday) were collected. The reason for recording data for non-typical weekdays was in order to identify the traffic conditions differences between the two. Table 4 aggregates the list of

RTMC cameras that we used for I-394 and I-35W while Figure 13 presents several sample camera views for both I-35W and I-394.

Table 3. Video recording days in summer 2011

June 2011	**July 2011**	**August 2011**
Tuesday 21st	Thursday 23rd	Tuesday 16th
Wednesday 23rd	Tuesday 26th	Wednesday 17th
Thursday 24th	Wednesday 27th	Thursday 18th
Monday 27th	Thursday 28th	Tuesday 23rd
Tuesday 28th		Wednesday 24th
Wednesday 29th		Thursday 25th
Thursday 30th		Friday 26th
		Tuesday 29rd
		Wednesday 30th
		Thursday 31st

Table 4. Cameras utilized in I-394 and I-35W

I-394	608	609	6091	610	6101	611	6130	6131	613	616	618	619	620	621
I-35W	904	905	906	907	908	909	910	911	912					

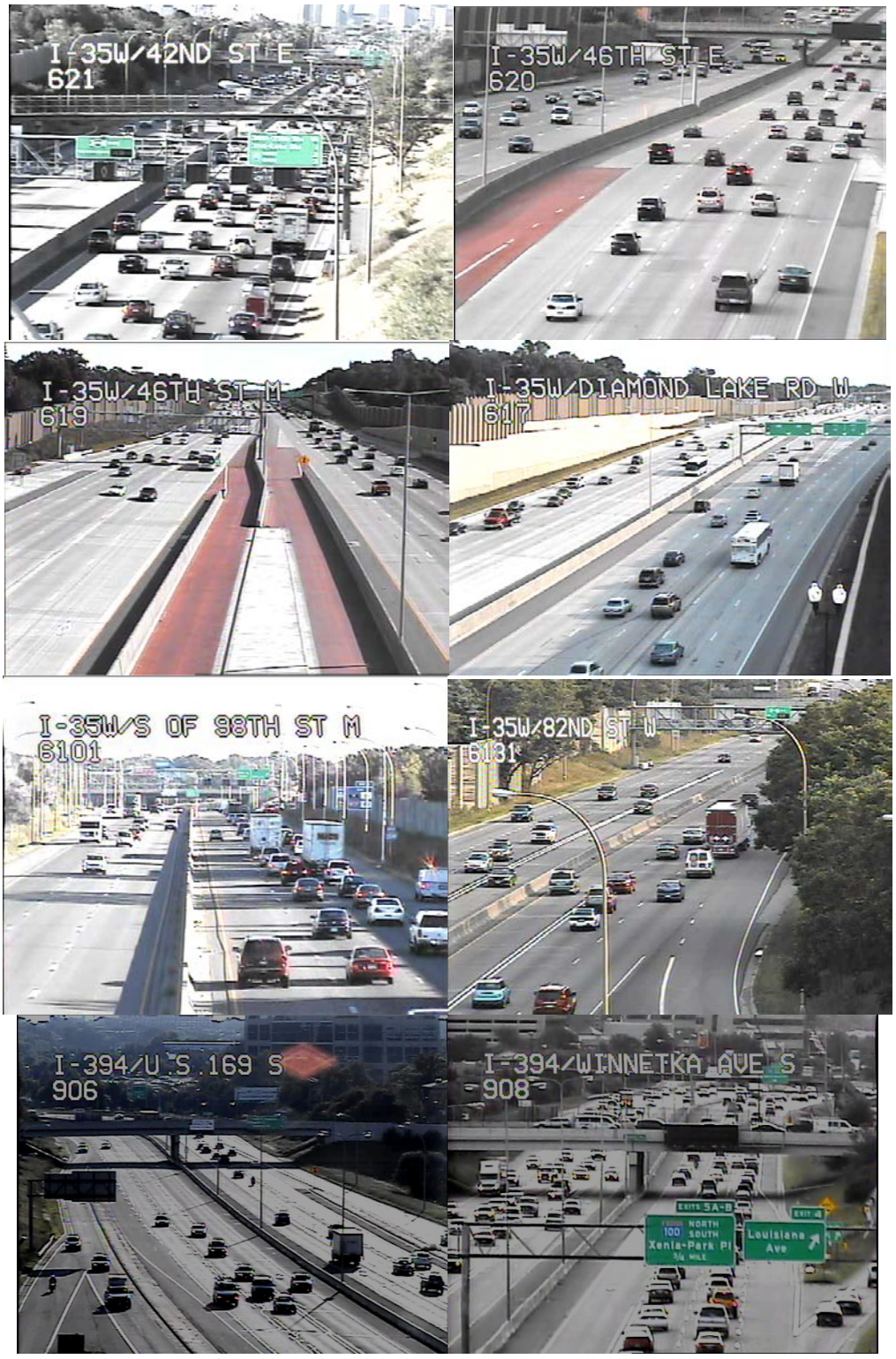

Figure 13. Sample camera views video was recorded

The goal in aiming the cameras was to balance the need from observing as much of the freeway segments as possible while being able to visually identify the signs of unsafe lane changes between the HOT lane and the general purpose lanes. These two goals are

countering each other and in many cases it was challenging to balance between the two. We believe that the amount of video collected assisted in balancing the two objectives and served the needs of the project.

Camera selection

The selection of cameras that were transmitted to the MTO was based upon the amount of lane changing activity that they were capable of capturing. In the case of I-394 the selection process was less demanding than in the case of I-35W. This conclusion lies in the fact the allowed access segments on I-35W are of greater length than the allowed access segments on I-394.

In the case of I-394 the design is more conservative than in the case of I-35W. More specifically, the HOT lanes on I-35W have open access segments of several miles in some cases. In that way the cameras that were selected to be observed and analyzed for I-394 required less effort to be determined since the lane changing activity is observed at the known allowed access points. On the other hand on I-35W further investigation was required in order to identify the segments that were capable of providing intense lane changing activity.

For this task several considerations were made. More specifically, the initial assumption was that lane changing activity occurs at a higher rate when drivers meet the "tail" of congestion. What is meant by "tail" of congestion is the transitional part of flow during which drivers are forced to join the stop and go waves that propagate upstream. At this point drivers are more likely to enter the HOT lane in order to avoid joining the stop and go waves. This initial assumption was also observed in the recorded data, verifying the assumption's validity. In the case of road segments providing higher lane changing activity, it was decided to dedicate more than one of the available cameras of the network so that the captured lane changes are recorded in the most possible detail. One example is the segment on the northbound of I-35W between 42nd and 46th street which was covered by both camera 620 and 621. One of the cameras is facing traffic approaching, while the other one faces the rear part of the vehicles. The intension was to have a clear view of both the initiation of the lane change from the one camera and the effect on the following vehicles from the other. In order to support our observations for segments of higher interest like the segment between 42nd street and 46th further investigation was conducted taking advantage of the available online detector databases on MnDOT's servers.

Two variables were selected to be used as indicators of severe lane changing activity; speed difference between the HOT lane and the adjacent lane, and flow balance. Severe lane changing activity indicates that discomfort will be observed for the drivers on the HOT lane, when a vehicle enters the HOT lane, forcing them to decelerate severely. In order to describe the values that speed difference and flow balance obtain in regards to the road segment as well as the time of the day, detector data were used.

Video reduction methodology

The research team responsible for this task viewed each one hour video in fifteen minute segments for data collection. The assistant researchers recorded the number of lane changes in and out of the HOT for each of the fifteen minute segments. Results were stored in a Google document spread sheet. While documenting the total number of lane changes, the assistant researchers were also watching to see if the lane changes created shockwaves in the traffic of the HOT and/or the adjacent GPL. Shockwave lengths were also documented in the Google documents spreadsheet.

The objective of this process was to deliver a collection of video clips that contain only the cases of Inappropriate Lane Changing (ILC) activity. In previous reports of this project and for the purposes of data collection the term Dangerous Lane Changes was used. The term may have been misleading since the observed lane changes collected are not actually dangerous but were isolated only if the lane change did generate an interaction between the subject vehicle and other vehicles in the HOT, the GPL or both. For clarity, in this final report the term "inappropriate lane change activity" is used to we refer to cases that generated shockwaves involving two or more vehicles. Video editing software was used to extract a video clip of each observed shockwave. The 40 seconds of total clip duration usually consists of 15 seconds before the vehicle enters or exits the HOT as well as another 25 seconds after. The reason for recording a longer period after the vehicle reaches the targeted lane is because we intend on focusing on the effect of the lane change on the drivers on the receiving lane (shockwave). In cases of substantially longer shockwave lengths, longer clips were created in order to observe the entire shockwave.

As already mentioned, the criterion for selecting a ILC was the effect that it had on the flow of the HOT. More specifically, if vehicles that followed the vehicle that changed lanes began to decelerate (even not very intensively) the clip of the LC was 'cut' and stored. An example at this point could be helpful in order to visualize the cases of interest. Let us assume that a driver intends to leave the HOT and enter the adjacent lane of traffic. In order to achieve that there should be an appropriate gap between the vehicles on the adjacent lane that he/she can move to. If the gap is not available the driver will need to decelerate and wait for an appropriate gap. If there were vehicles on the HOT that follow the driver of interest and they decelerated as well (creating inconvenience to drivers on the HOT) the ILC was stored.

On the other hand, if vehicles did not follow the driver of interest closely and none of the vehicles on the HOT was forced to decelerate then the specific lane change was not stored. A similar case would be when a vehicle entered the HOT. Once again, if the lane change forced the following drivers on the receiving lane to decelerate then the lane change was designated a ILC and was stored, otherwise it was discarded. One example of a documented shockwave is presented in Table 5 and Table 6.

Table 5. Example of data collected for a fifteen minute time block

Video File	Camera	Time Block	Dir	Dir2	Lane Changes into the HOV	Lane Changes out of HOV
DVR4-Cam3-Aug-31 at 17-02.avi	619	17:00-17:15	S	NB	6	3
DVR4-Cam3-Aug-31 at 17-02.avi	619	17:00-17:15	S	SB	3	4

Table 6. Example of a documented shockwave

File name	Camera Code (could be more than one within a single video file) [6xxx_I-35W/xxx xxx x]	Date (YYYYMMDD)	Complete (indicate if it is the last lane change contained in the file you are working on by L, otherwise NL))	Time (Use the time stamp in the title of the video file and add the time of the video so far-24h)	Direction (observe changes in the digital compass of the camera)
DVR3-Cam2-Aug-31 at 08-00	608	20110831	NL	8:27:43	N

Bound (NB/SB)	Vehicles Affected on the HOV(leader included)	Vehicles affected on the adjacent lane when the adjacent lane is the receiving lane (leader included)	Entering or Exiting HOV Lane (N/X)	Clip Name [freeway_ exit or entering the HOV(EN/EX)_Camera code_(3 or 4 digit code)_How many vehicles were forced to decelerate on the HOV lane including the vehicle that changed lane_Date(YYYYMMDD)_Time(start[24H])]
NB	4	0	N	I-35W_EN-608_4_20110831_082743.avi

5. Evaluation Results

For brevity this report focuses only on locations that there was interaction and friction between the HOT and GP lanes. A mid project deliverable presented preliminary results for all locations along the two freeways. To get a clear idea of how the designs on a whole are operating in comparison, cameras are grouped together into Zones. On I-35W there were three Zones under analysis. Zone 1 consists of NB traffic as viewed by cameras 608, 609, 6090, and 6091; Zone 4 consists of NB traffic as viewed by cameras 616, 6161, 617, 618, 619, 620, and 621; and Zone 7 consists of SB traffic as viewed by cameras 6131, 6130, 613, 612, 611, 6101, 610, and 6091. On I-394 Zone EB 4 is the only Zone under analysis and consists of cameras 908 and 909. The other Zones of I-35W and I-394 are not presented in this report as the data from these Zones yielded little interest. In this report results are drawn from the analysis of nine days of collected data, with at least four days of data for each Zone. All Zones of I-35W are represented by the dates Aug 31st, 30th, 25th, 24th, and 23rd as well as June 29th for Zone 1 only. EB 4 of I-394 is represented by the dates Aug 31st and 30th as well as July 27th and 26th. These dates have the most complete video coverage of their respective Zones, thus minimizing the amount of blind spots.

Lane Changing Frequency-Flow Breakdown Lengths

This section of the report provides findings from the analysis of all the aforementioned days of footage. The results obtained are presented for I-35W North, South, and I-394 East in that order. A comparison between locations on both facilities is provided in the end of this section.

Graphs of the inappropriate lane changes, as compared to total lane changes (TLCs) and volume of the HOT, for each specified Zone are provided, followed by an estimated percentage of vehicles in the HOT that experienced a shockwave. Box-plots presenting the observed lengths of the generated shockwaves are also provided. On each box, the central mark is the median, the edges of the box are the 25th and 75th percentiles, the whiskers extend to the most extreme data points not considering outliers, and outliers are plotted individually and are represented by red crosses. Based on this information, suggestions for improvement are discussed, motivated by results and the research's team observations during the data collection period. Finally, a comparison among all the examined Zones is presented identifying locations that may need further attention in the near future while Zones between the two facilities are compared based on the proportion of analyzed data.

Interstate 35 W Northbound

Contour plots are presented, providing information about the congested parts of the freeway during morning peak hours for the northbound direction (Figure 14 through Figure 19). The purpose of providing these plots is to support the identification of locations that require attention. I-35W North has two major bottlenecks and a third one which is less severe. Moving with the direction of traffic the first major bottleneck is on the Cliff Road interchange. The bottleneck seems to be the result of large inflows from closely spaced successive ramps from Burnsville Pkwy, TH-13, and Cliff Road. This bottleneck is in an Allowed Access segment of the HOT. Access is restricted about a half mile later at Black Dog

Road. At the interchange with I-494 a weak bottleneck is observed mainly affecting the rightmost lane but also due to the inflow and weaving from the I-494 ramps this location is under Restricted Access (double white line). The second major bottleneck is at 46th Street assisted by congestion from the downtown end of the roadway. This location is the beginning of the Priced Dynamic Shoulder Lane (PDSL) which is all restricted access north of 38th street.

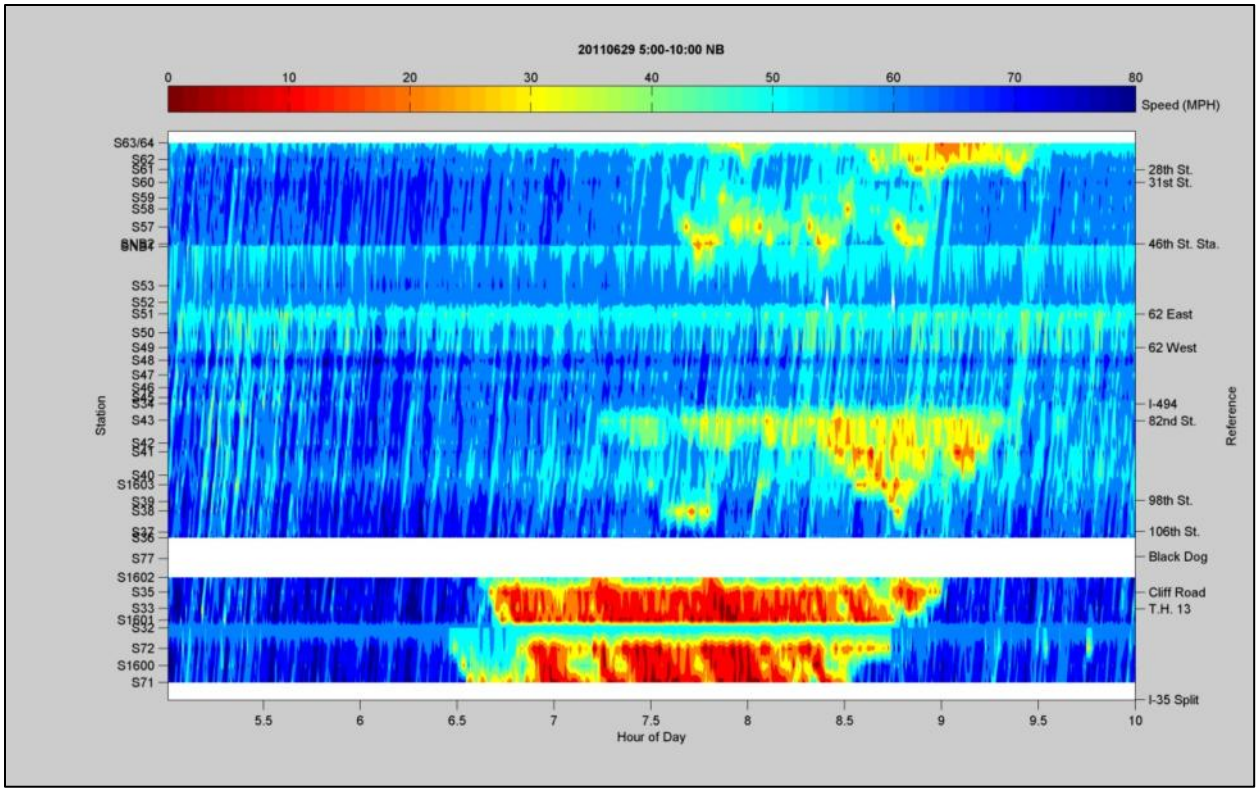

Figure 14. Speed contour plot June 29th Northbound direction

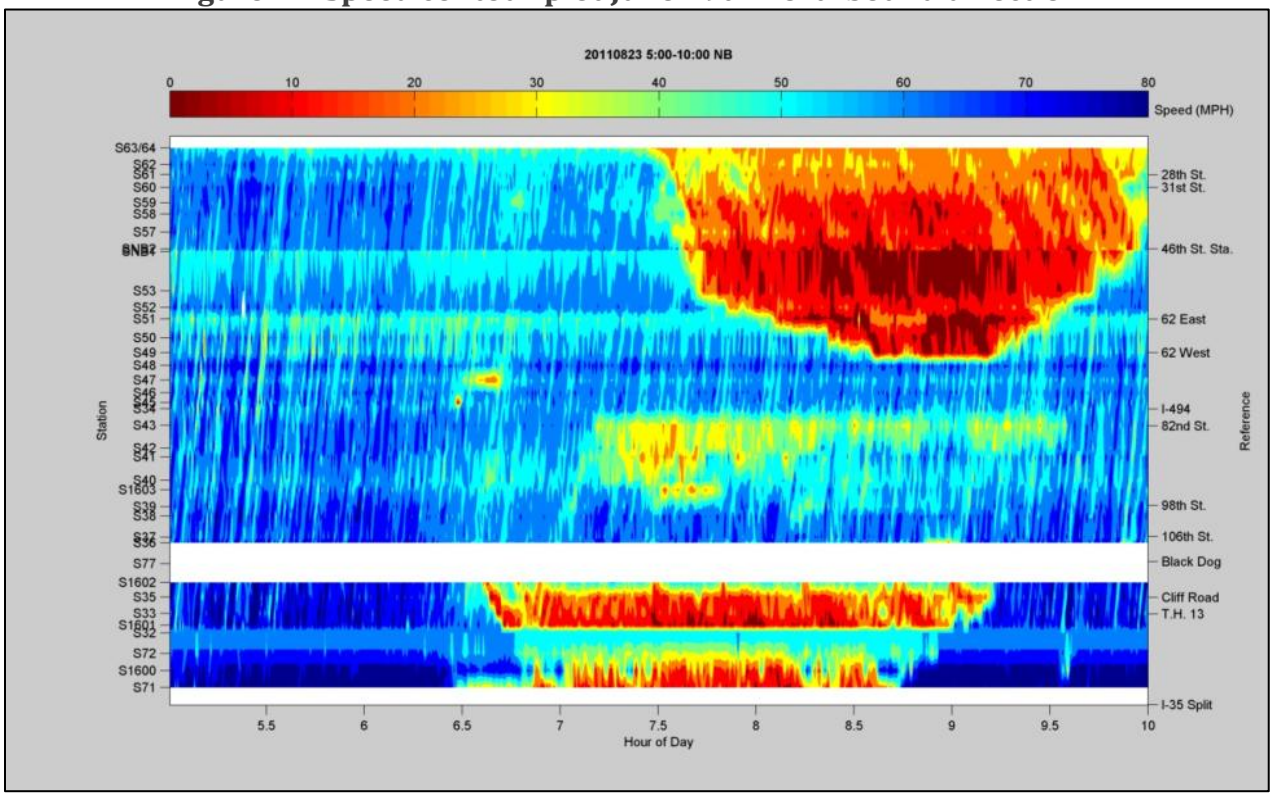

Figure 15. Speed contour plot August 23rd Northbound direction

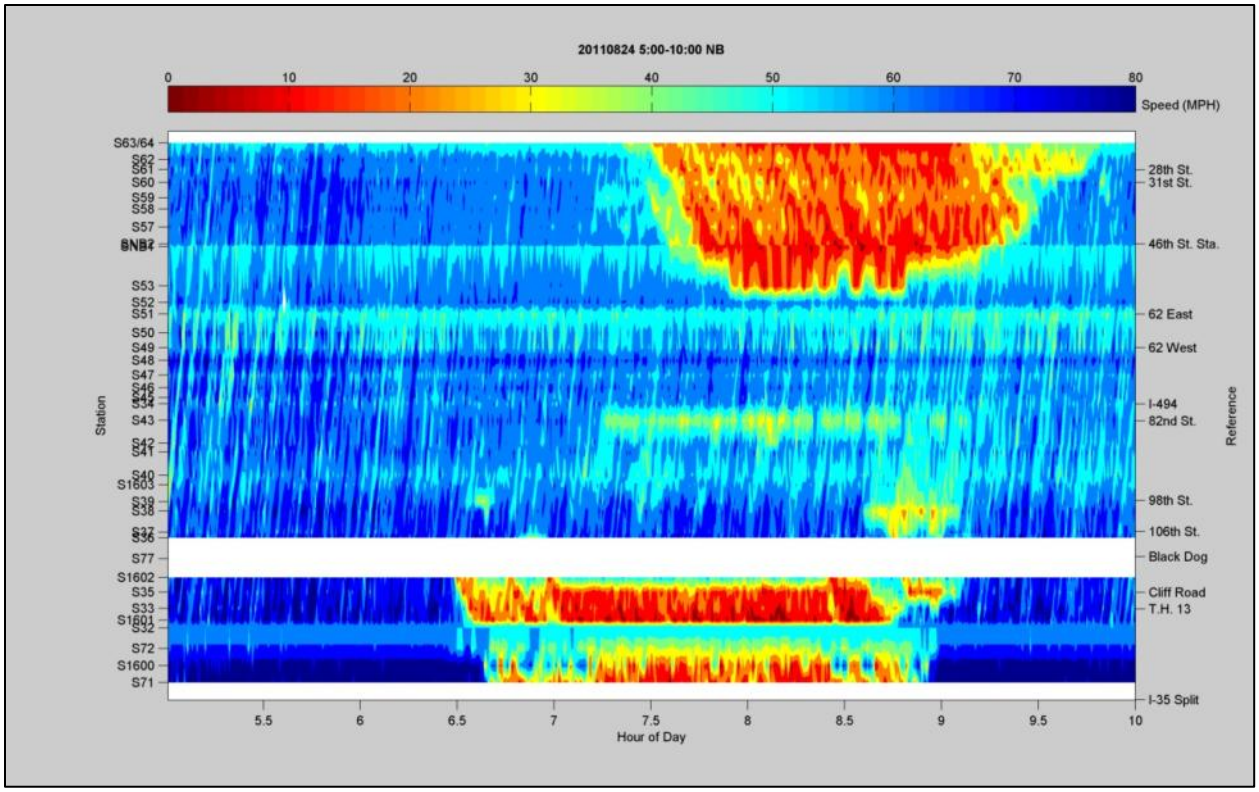

Figure 16. Speed contour plot August 24th Northbound direction

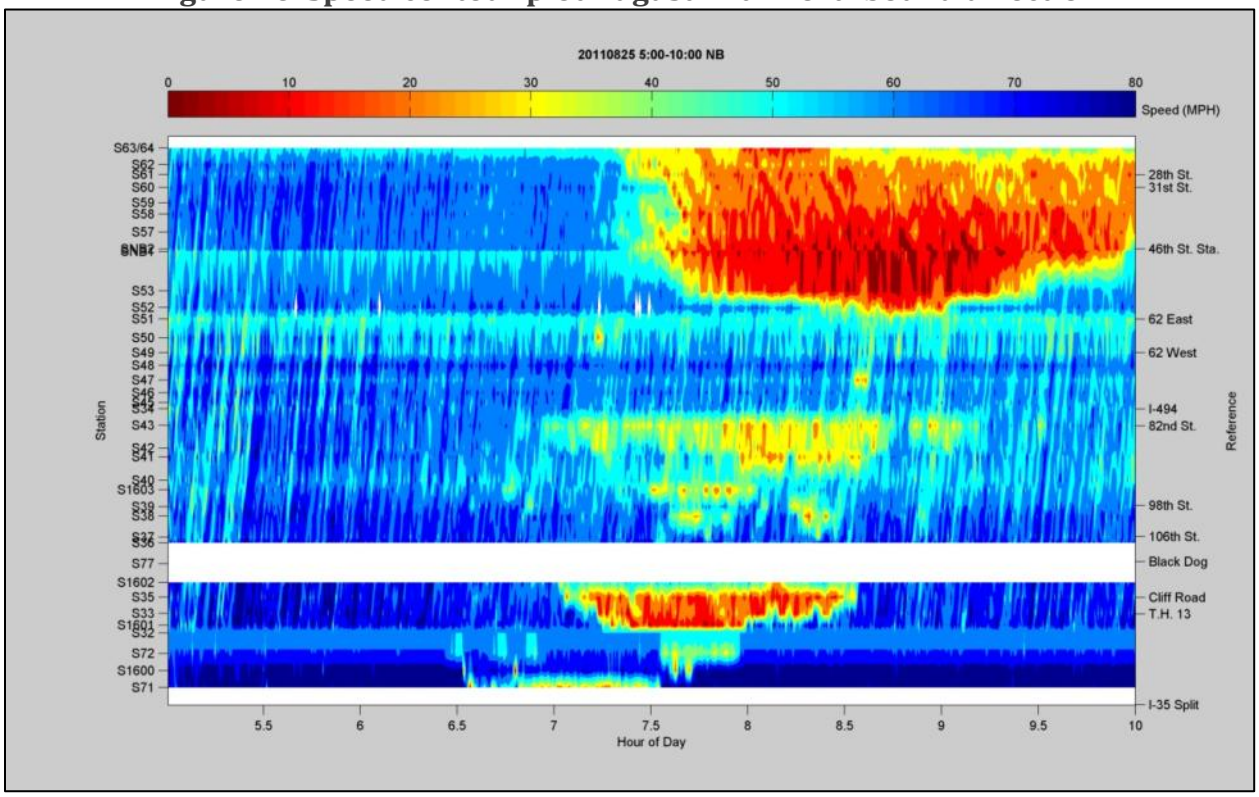

Figure 17. Speed contour plot August 25th Northbound direction

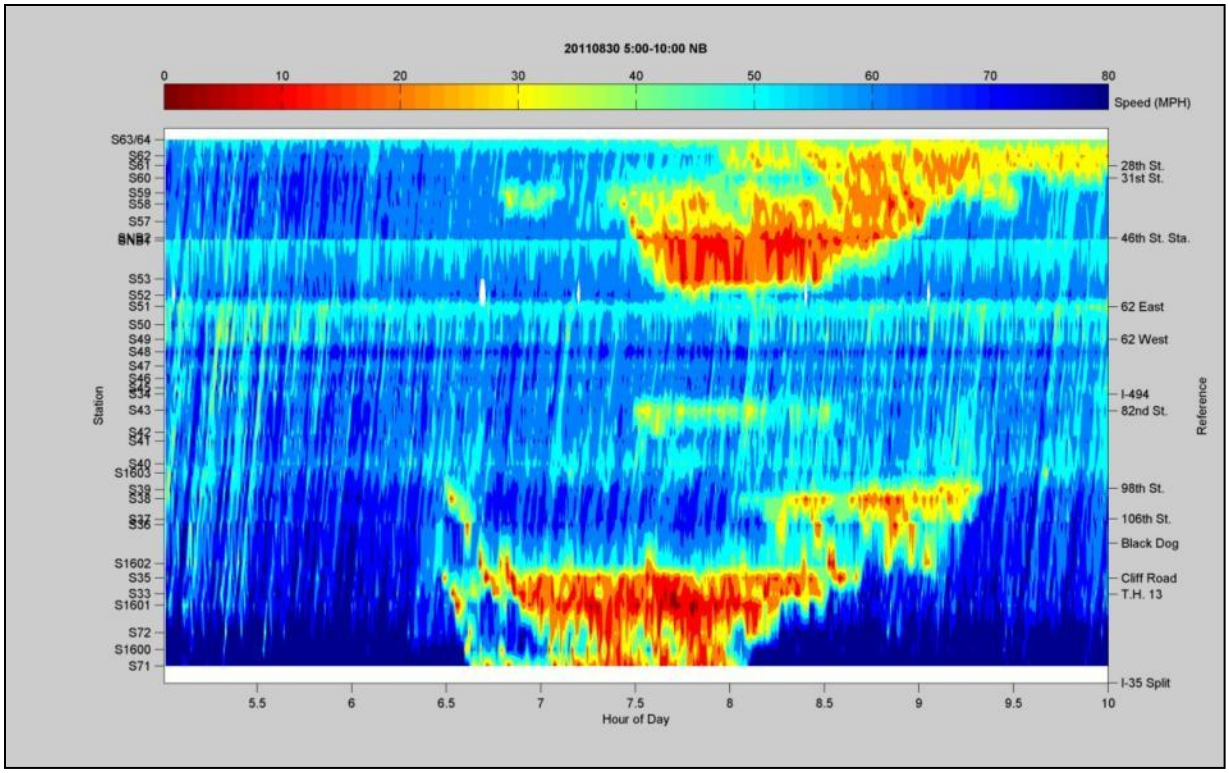

Figure 18. Speed contour plot August 30th Northbound direction

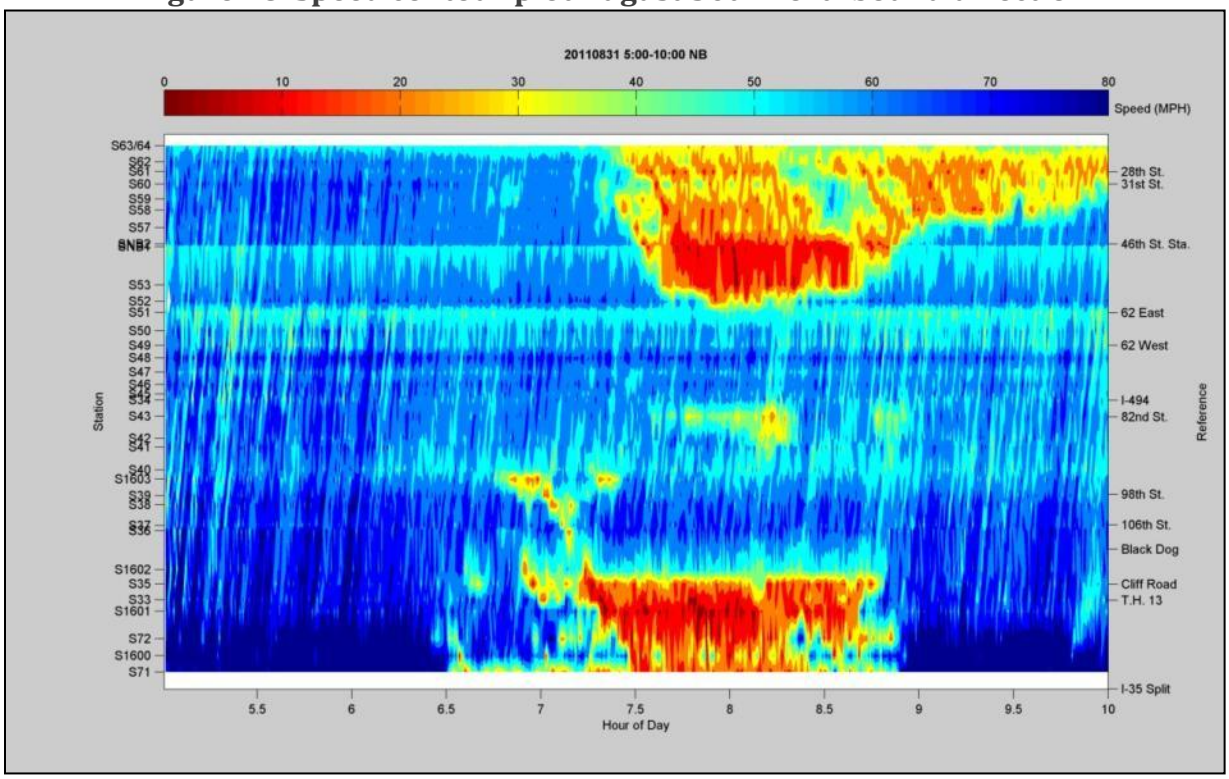

Figure 19. Speed contour plot August 31st Northbound direction

Zone 1: I-35W Northbound {Burnsville Pkwy to Black Dog Rd}

Figure 20. Location 608, example camera view facing north

Zone 1 is mainly an entrance point to the HOT lane since, in 2011, it was the beginning of the HOV lane. The primary point of activity is at the location of camera 608 (see Figure 20 above) at the major interchange of I-35W with TH 13. This can be seen in Figure 21 which presents the average amount of ILCs observed per day of data, as seen by each camera. Our observations are in accordance with the period that this particular section is tolled (morning peak). During the preliminary investigation of the network, this part was identified as one of the zones that would require a great amount of attention. This can be attributed to two reasons; first because of the large speed differential between the HOT and the adjacent GPL and second because of the entrance from TH 13 to I-35W which introduces into the stream a lot of vehicles destined to the HOT.

Data for six morning peaks were analyzed for this location during six typical weekdays on June 29th and August 23rd, 24th, 25th, 30th, and 31st 2011. Figure 22 presents the observed inappropriate lane changing activity as a percentage of total lane changes separated in 15 minute time blocks with respect to the time that they occurred. The graph displays the average percent of inappropriate lane changes over all the days of data at each 15 minute period as well as one standard deviation above and below the average. This figure along with Figure 23 support the fact that the segment around TH-13, camera 608, is mainly an entrance to the HOT since high peaks are observed for ILCs as well as ILCs per total lane changes.

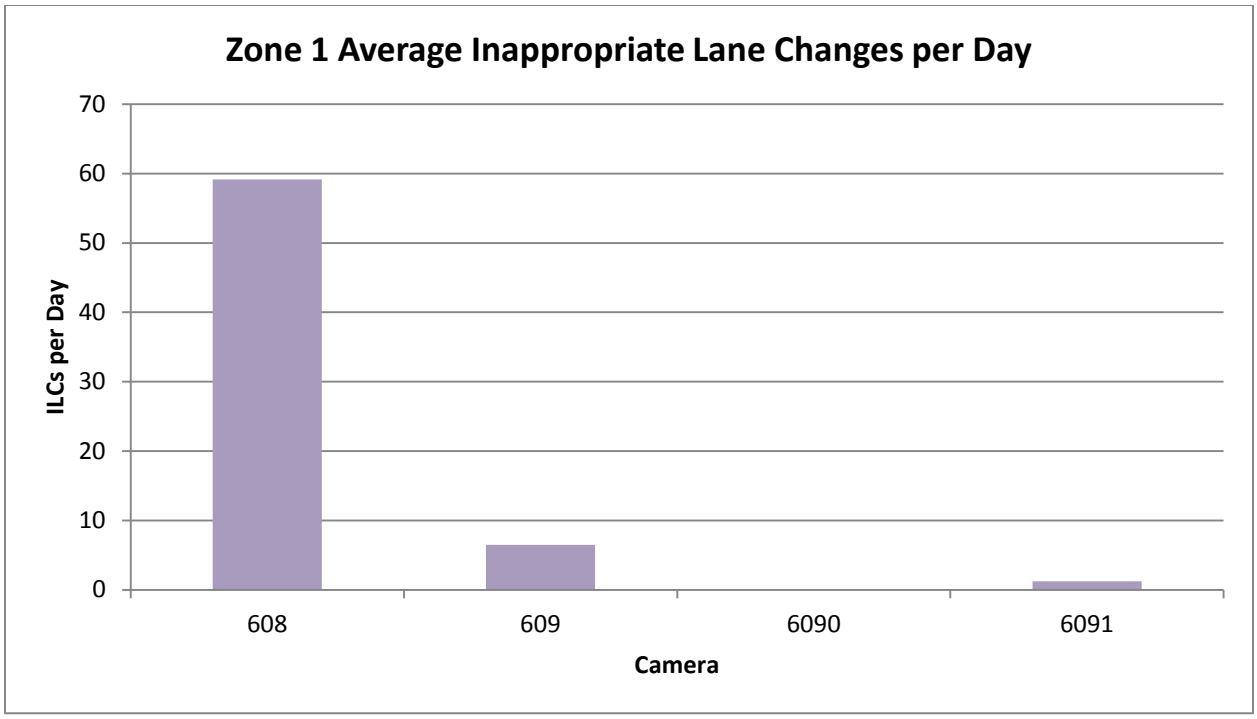

Figure 21. Average inappropriate lane changes from all days by observed camera

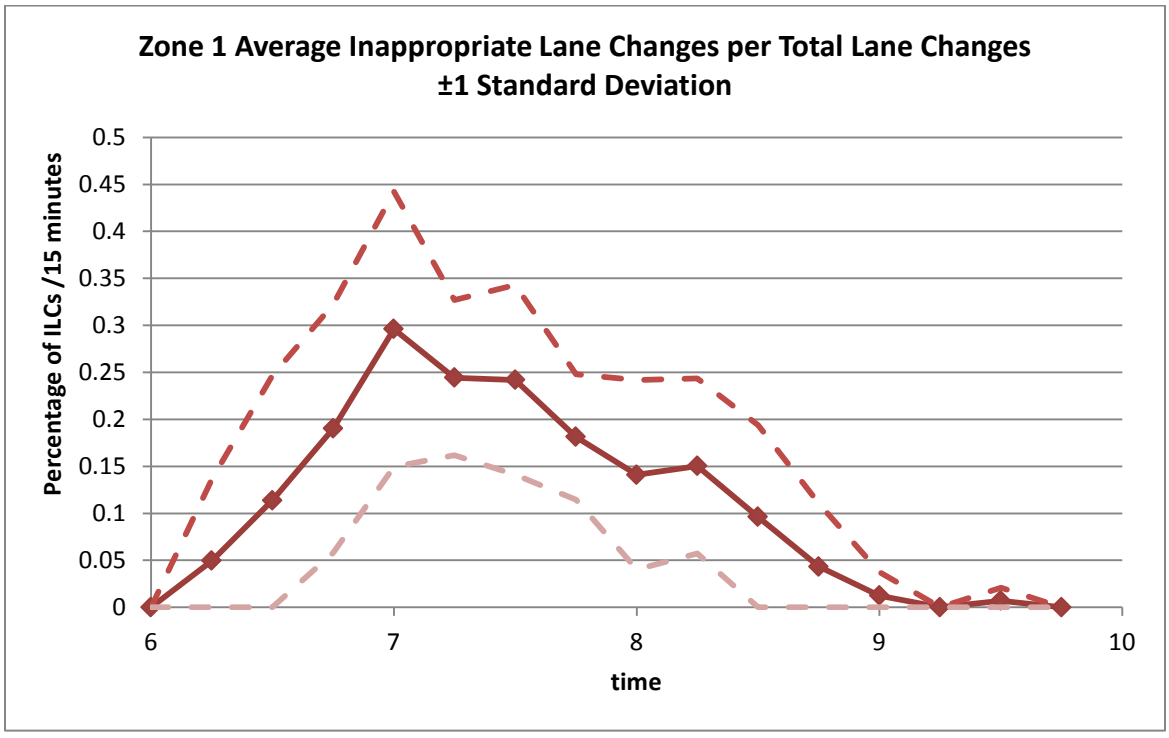

Figure 22. Inappropriate lane changes as a percentage of total lane changes

Figure 23 and Figure 24 present the number of the recorded flow breakdowns in relation to the volume on the HOT aggregated once again in 15 minute blocks. Observations are plotted with respect to the time of day that they occurred. As previously mentioned, the volume data were collected from MnDOT loop detectors. The detectors that were used to gather the data, for this zone and all others that will be discussed later, were just downstream of the zones' most significant area of activity. Figure 23 displays the proportion of drivers in the HOT that have committed a ILC. Figure 24 gives us the best look at the mobility of the Zone 1. In this figure we see the percentage of vehicles that experienced a flow breakdown while in the HOT through the zone. The total number of vehicles was accumulated by summing the size of all shockwaves that began in the specified time block. Vehicles that were involved in multiple shockwaves were not accounted for, and may be double counted. As seen in and Figure 24, nearly 15% of vehicles traveling on the HOT through Zone 1 experience a flow breakdown during the height of the morning peak on average.

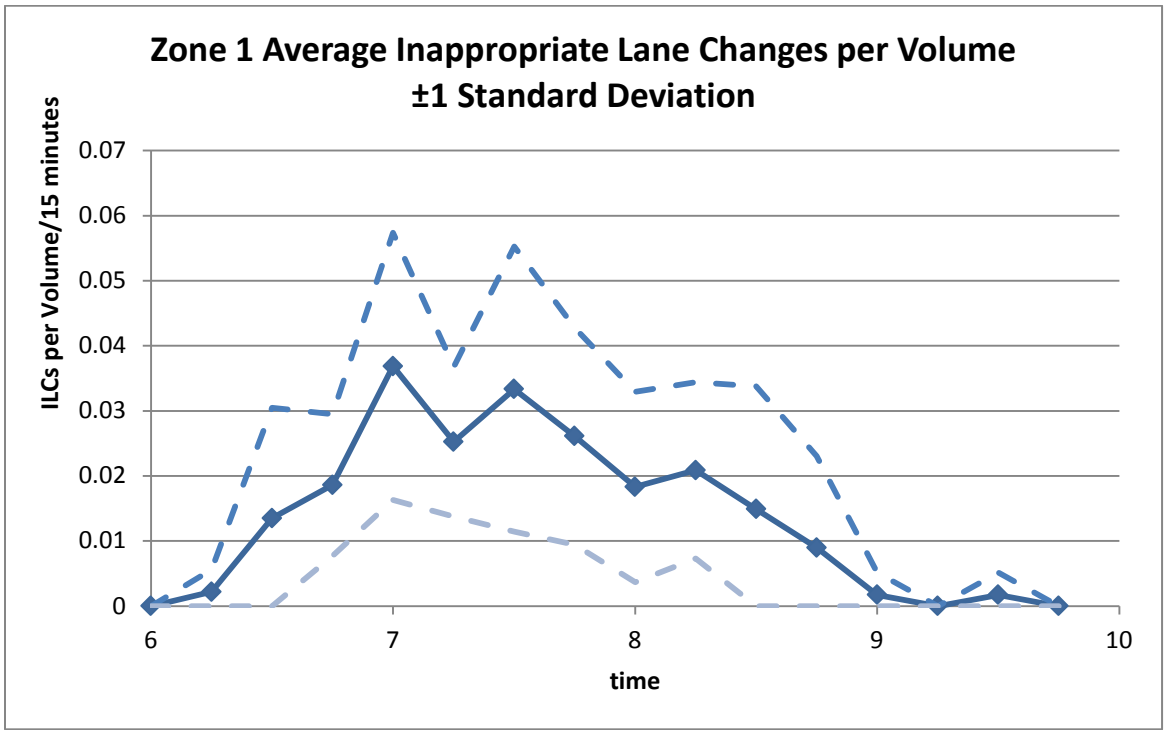

Figure 23. ILC activity as a proportion of the HOT volume

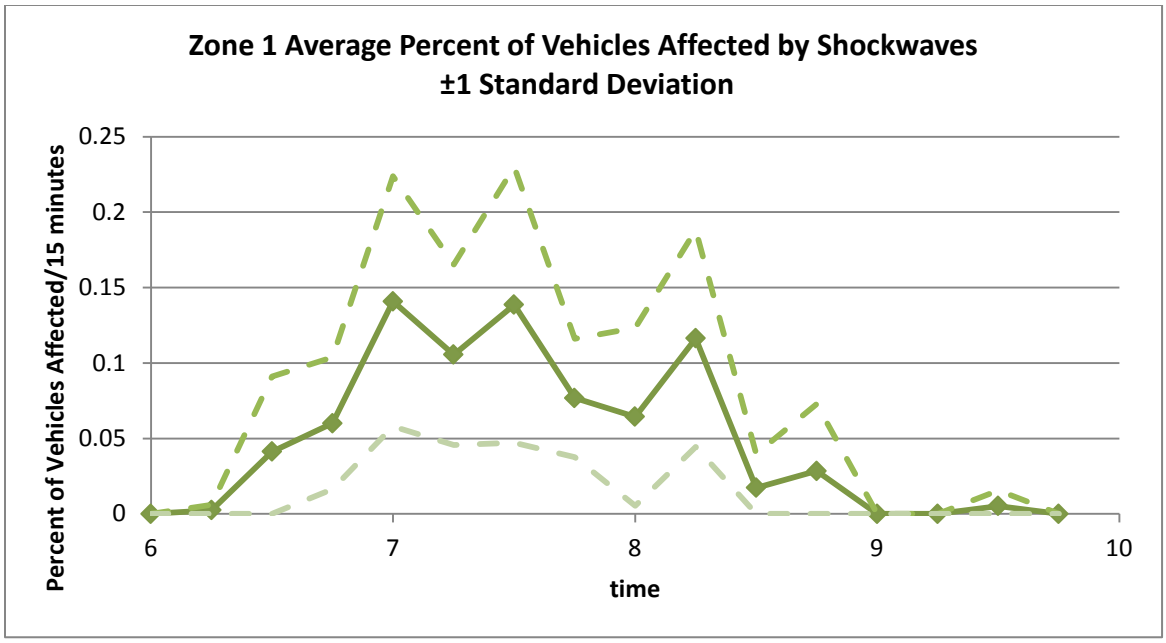

Figure 24. Average percent of vehicles affected by a shockwave through the zone

Shockwaves observed on this location were comparatively large in length with a median value of 3 vehicles and an extreme value of the constructed dataset reaching 9 vehicles. Figure 25 presents the statistical characteristics of the observed shockwaves. Very few vehicles were affected on the GPL since the speed of the adjacent lane during the time observations were collected was close to zero. This holds true for all the zones that will be discussed in this report.

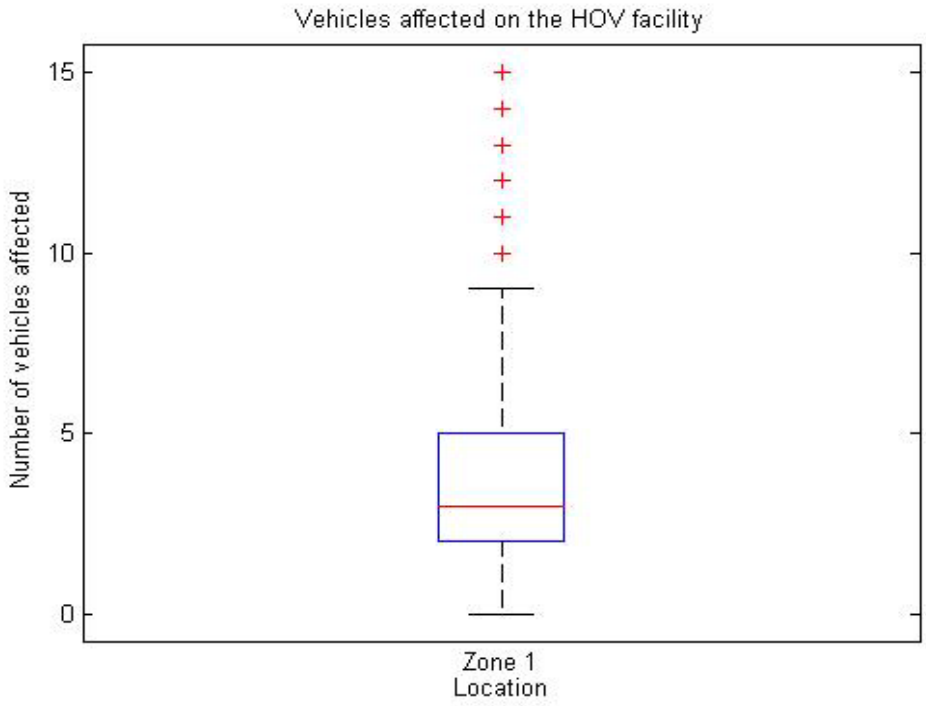

Figure 25. Box-plot of HOT Shockwave lengths on Zone 1

A closer look at the isolated ILC clips revealed that a great portion of the lane changes generating flow breakdowns on the HOT are a result of buses merging aggressively. An example of an observed situation involving two buses can be seen in Figure 26. The first bus performed a ILC generating a shockwave and immediately afterwards it reduced speed to allow for the second bus to change lanes. One effective solution that would improve the safety and mobility of the HOT at Zone 1 could simply be to instruct bus drivers to be less aggressive when merging to the HOT near TH-13.

Figure 26. Example of bus ILC on location 608

The situation on northbound 35W near camera 608, which spans from the on ramp from Cliff Road to upstream of the TH-13 interchange, is in need of attention. Although it is not the location of the biggest shockwaves observed they are consistent and there is no reason to believe that it would improve with time. Excluding the cases involving buses, there is no need for immediate action since the disruptions are not extreme and there have been no actual crashes on record. Given the current rate of utilization of the HOT the situation is stable but if that rate increases the condition could deteriorate.

This location is a candidate for reducing the amount of access to the HOT with the introduction of a double white line. Such change will come with a price. As the figures illustrate the inbound flow to the HOT is high in this location and therefore restricting it will reduce the overall benefit from the HOT. To sufficiently suppress a future ILC issue the Restricted Access would have to start downstream of Burnsville Pkwy and extend to Black Dog Road.

It is interesting to note that if the Closed Access design found on I-394 was followed; given the demand from TH-13 for the HOT a gate would have been located there generating the same issues.

Zone 4: I-35W Northbound {Highway 62 – 38th street}

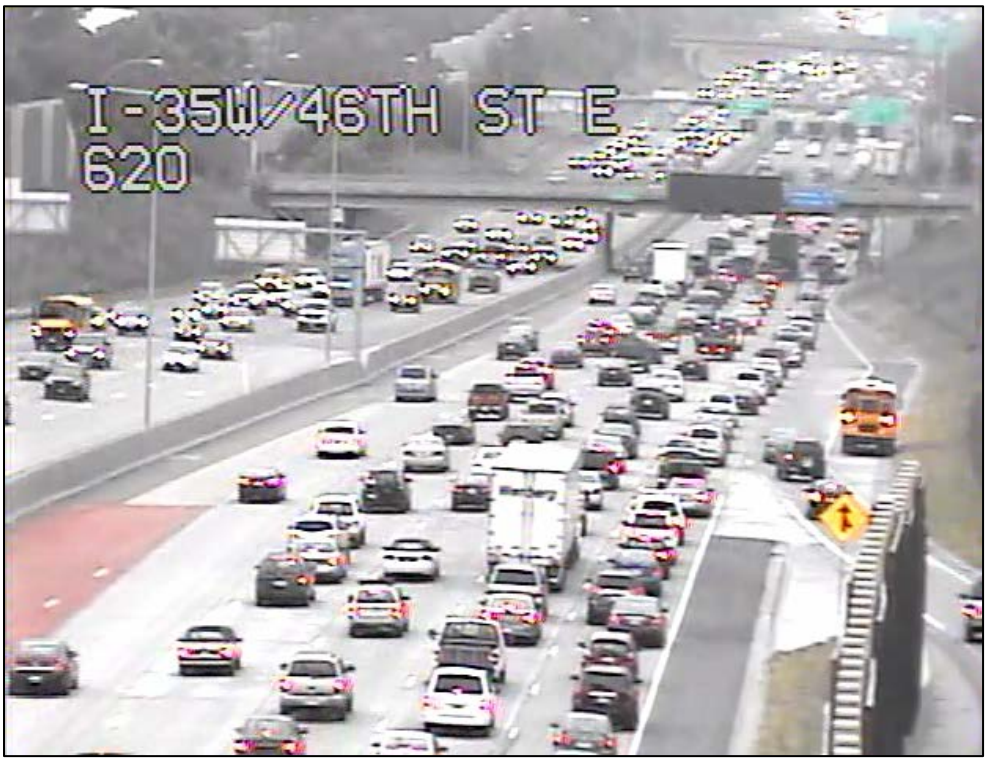

Figure 27. Location 620, example camera view facing north

Zone 4 is the last open area on northbound I-35W before downtown Minneapolis. Camera 620 provides footage for the segment between 46th street and 42nd street (see Figure 27 above), which has the most activity. This location is just upstream of the start of the PDSL segment of MnPASS and in extent the last area that drivers can join the HOT. The uniqueness of this location lies in the fact that it is at a segment where several streams merge; two entrance and one exit ramps are present downstream. The existence of the aforementioned ramps results in the initiation of many shockwaves which propagate upstream to the segment that camera 620 is covering. This creates unstable traffic conditions for all the GPLs and inevitably affecting the HOT as well. The presented results are drawn from five days of observation: August 23rd, 24th, 25th, 30th, and 31st. The observations indicate a location of severe lane changing activity with a great number of shockwaves generated on the HOT facility near camera 620.

The average inappropriate lane changing activity for the AM and PM peaks is shown on Figure 28 and Figure 29. This shows that the bulk of inappropriate lane changing activity in Zone 4 is occurring between 46th street and 42nd street. Figure 30 and Figure 31 show the percentage of ILCs per TLCs for the morning and evening peaks respectively. As seen in Figure 30, the average peak reaches over 30%. This is the highest percent of ILC per TLC observed in any of the four zones.

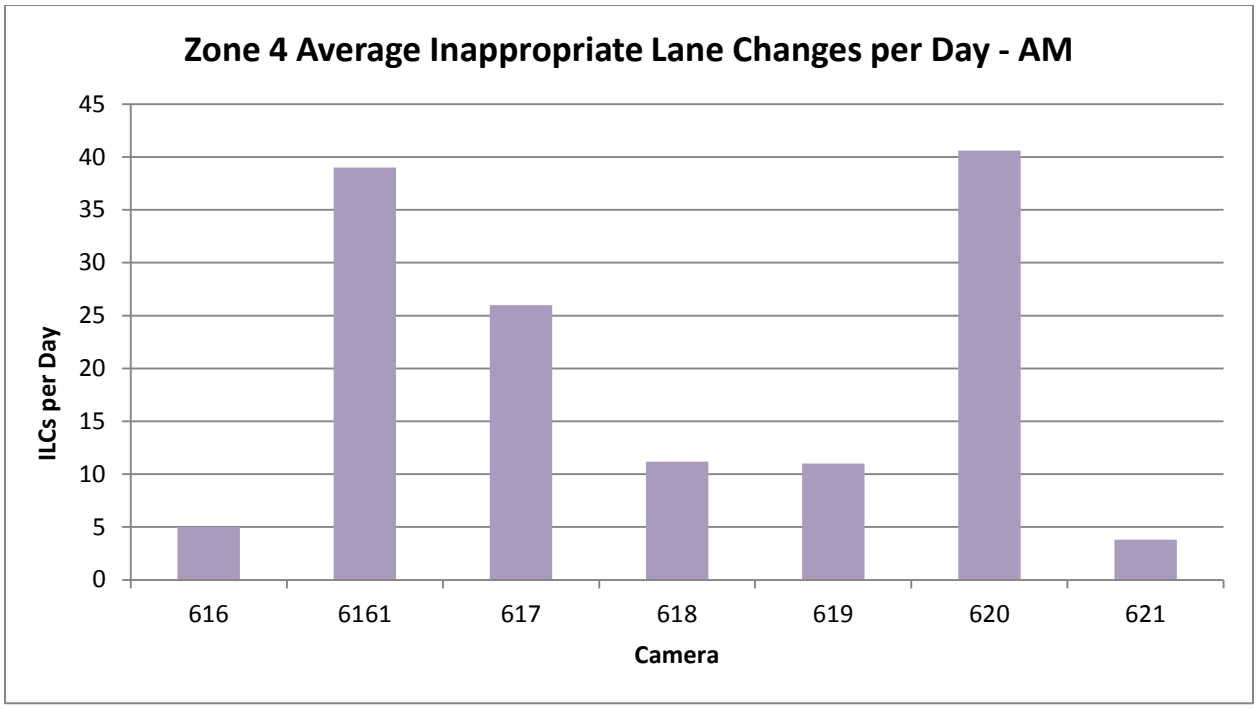

Figure 28. Average daily inappropriate lane changing activity for Zone 4 morning peak

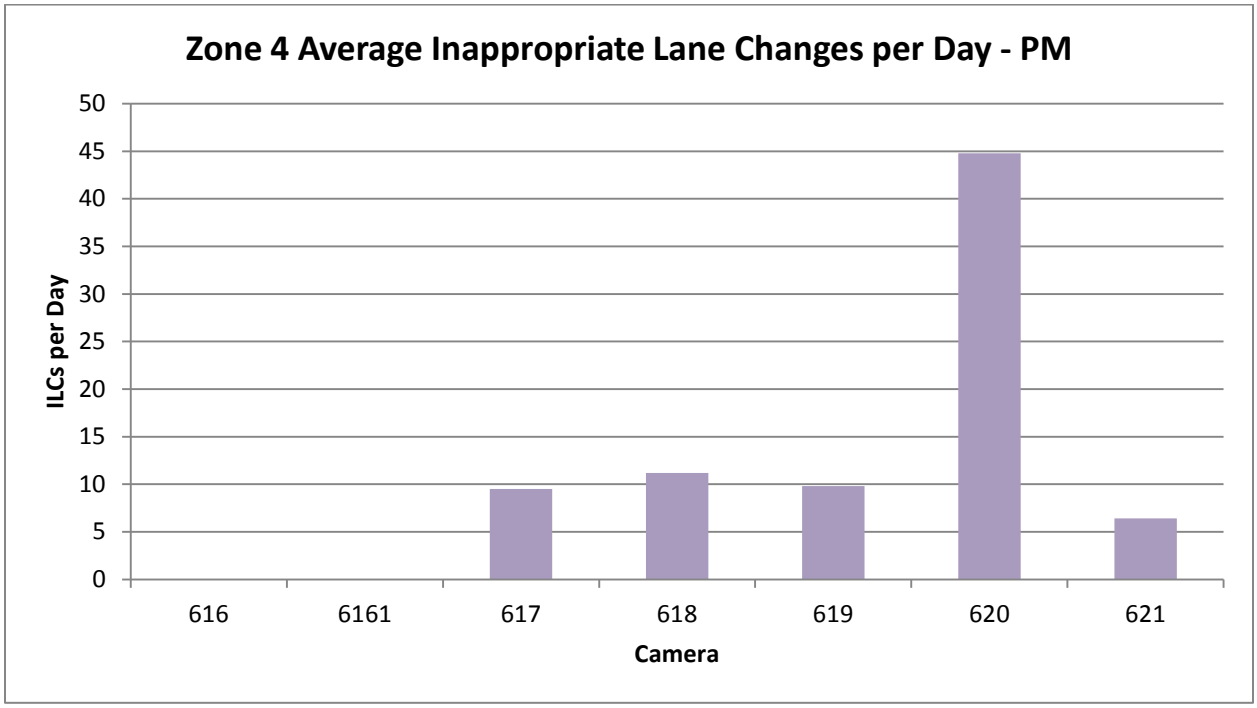

Figure 29. Average daily inappropriate lane changing activity for Zone 4 evening peak

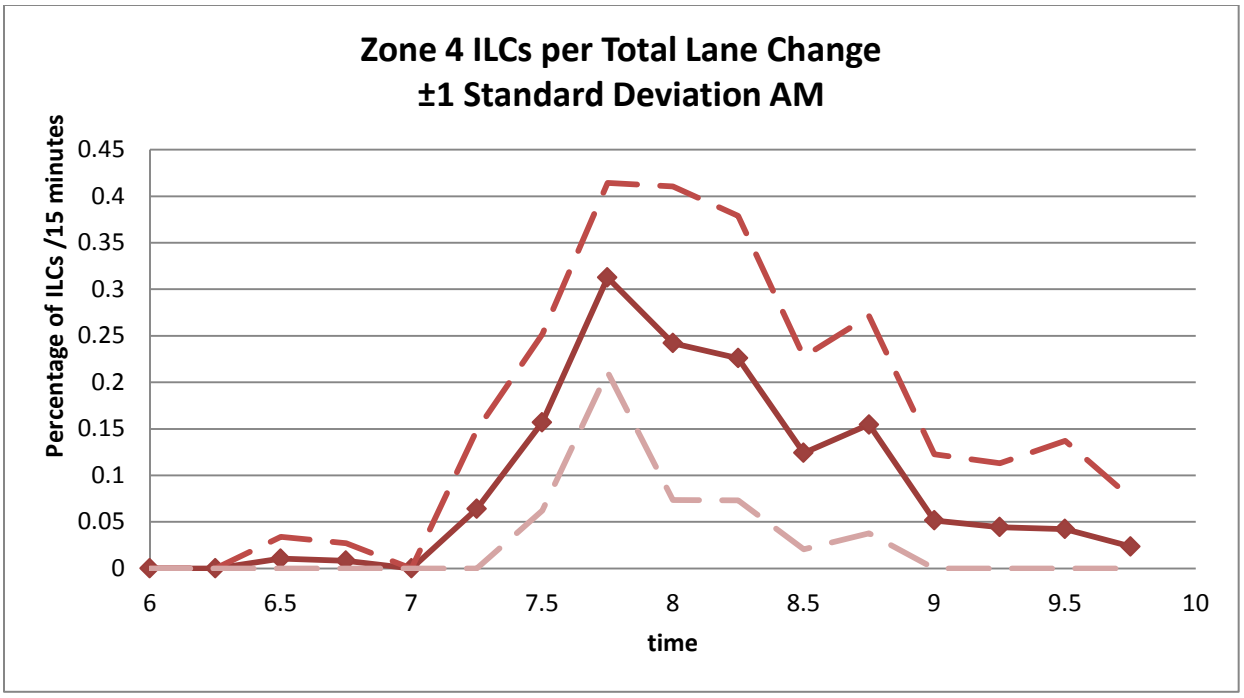

Figure 30. Average proportion of ILC of TLC for all days of Zone 4 during morning peak

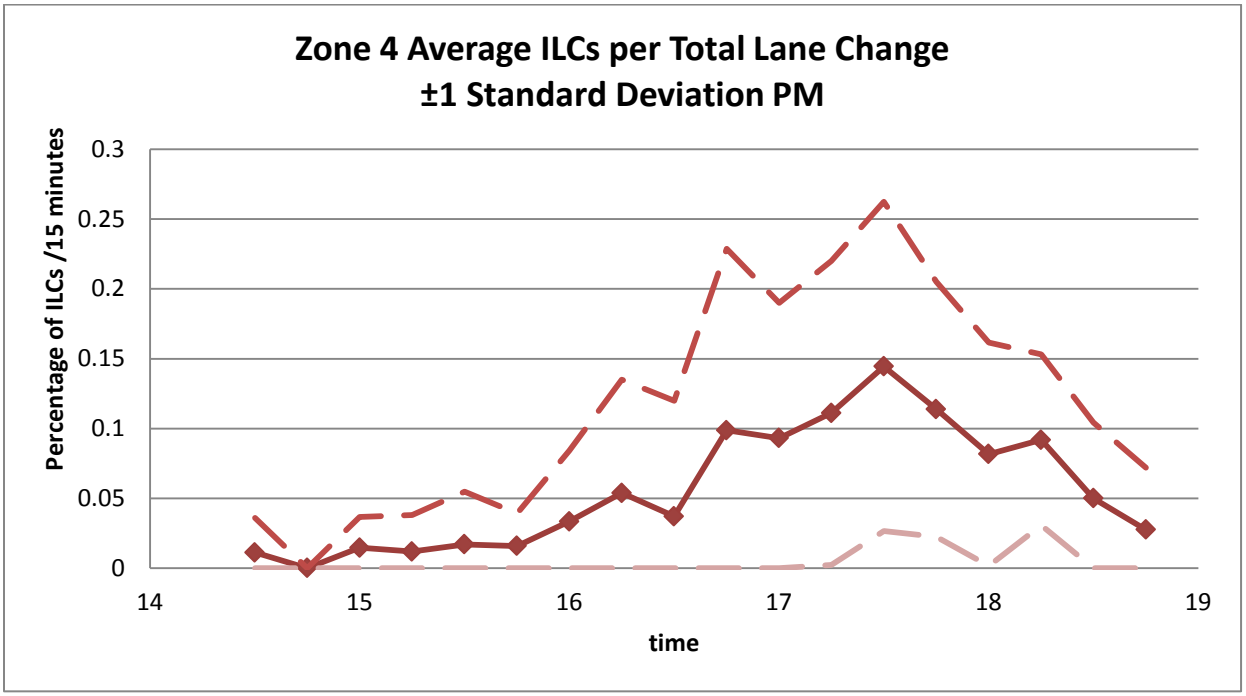

Figure 31. Average percentage of ILC per TLC for all days of Zone 4 during evening peak

However, Figure 32 and Figure 33 show that the ILC as a percent of the HOT volume is comparable to that of the other zones.

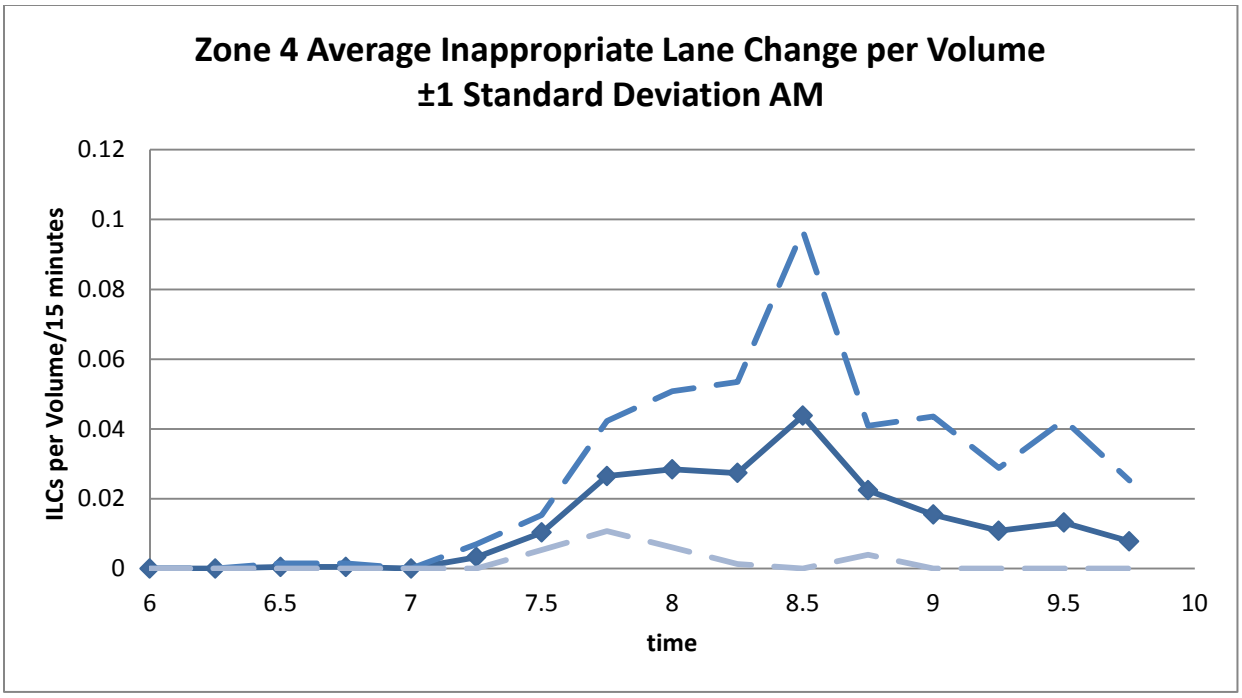

Figure 32. Average ILCs per HOT volume morning peak

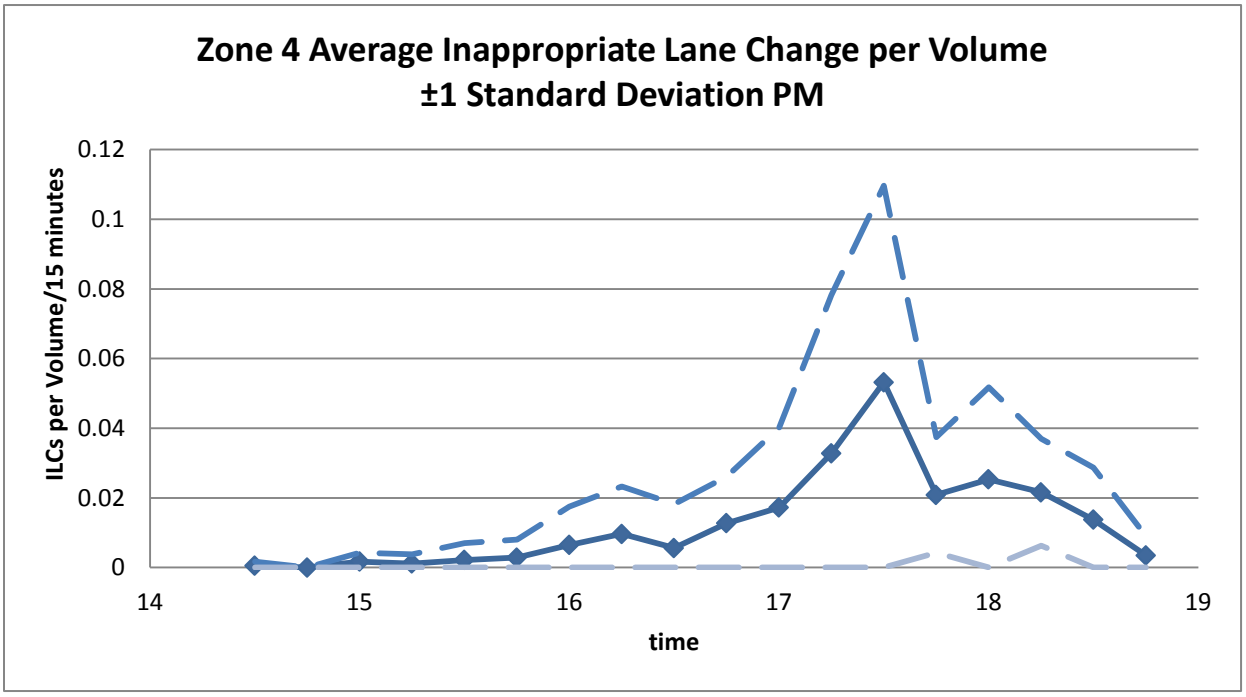

Figure 33. Average ILCs per HOT volume evening peak

Figure 34 and Figure 35 show the percent of vehicles that experience a breakdown in the flow of traffic. The values presented in the figures are on par with the values seen by the other zones. The standard deviations presented are a bit higher, but this is due to a handful of extreme outliers.

The median observed shockwave in this zone was also 3 vehicles. The extreme value was slightly larger than that of zone 1 at 12 vehicles. The statistical characteristics of observed shockwaves in zone 4 can be seen in Figure 36. Again, there were very few disturbances in the adjacent GPL due to the speed of the lane being close to zero.

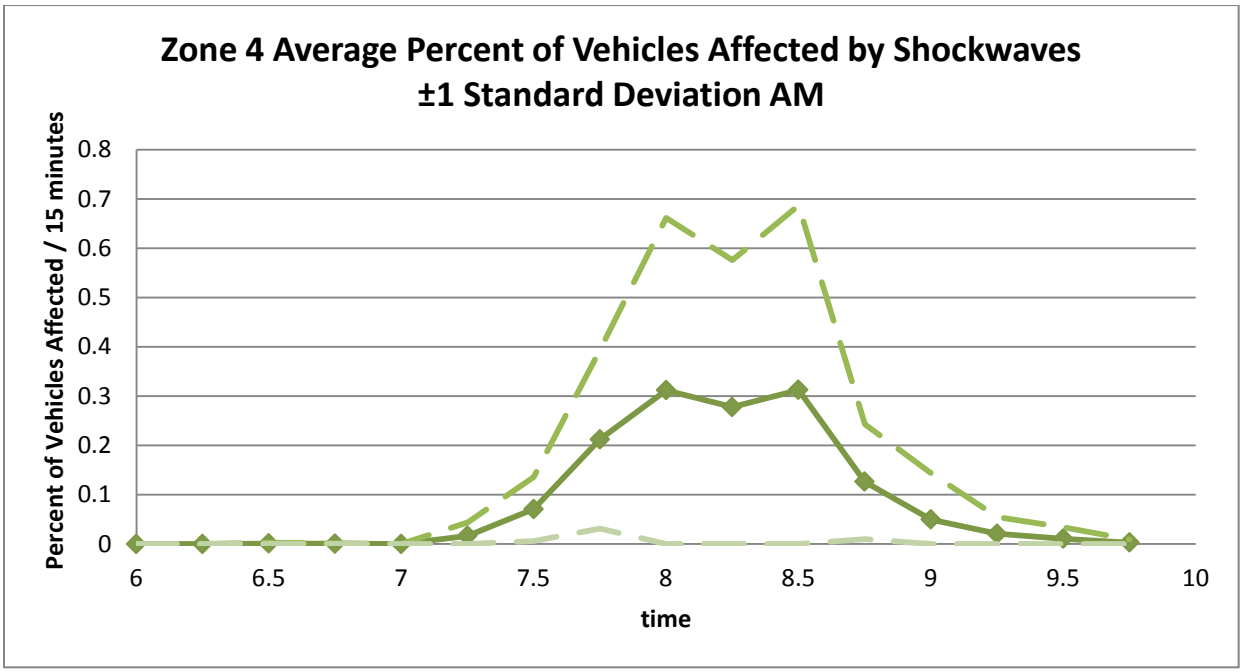

Figure 34. Percent of vehicles that experience a breakdown of flow during morning peak

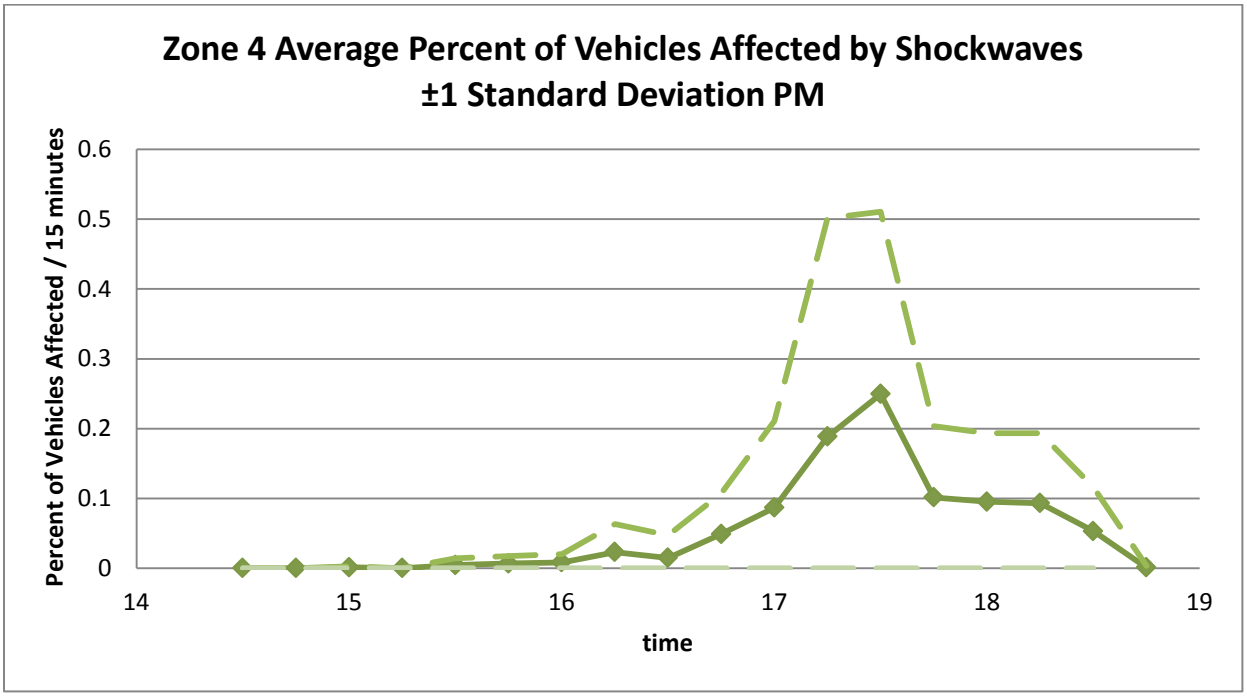

Figure 35. Percent of vehicles that experience a breakdown of flow during evening peak

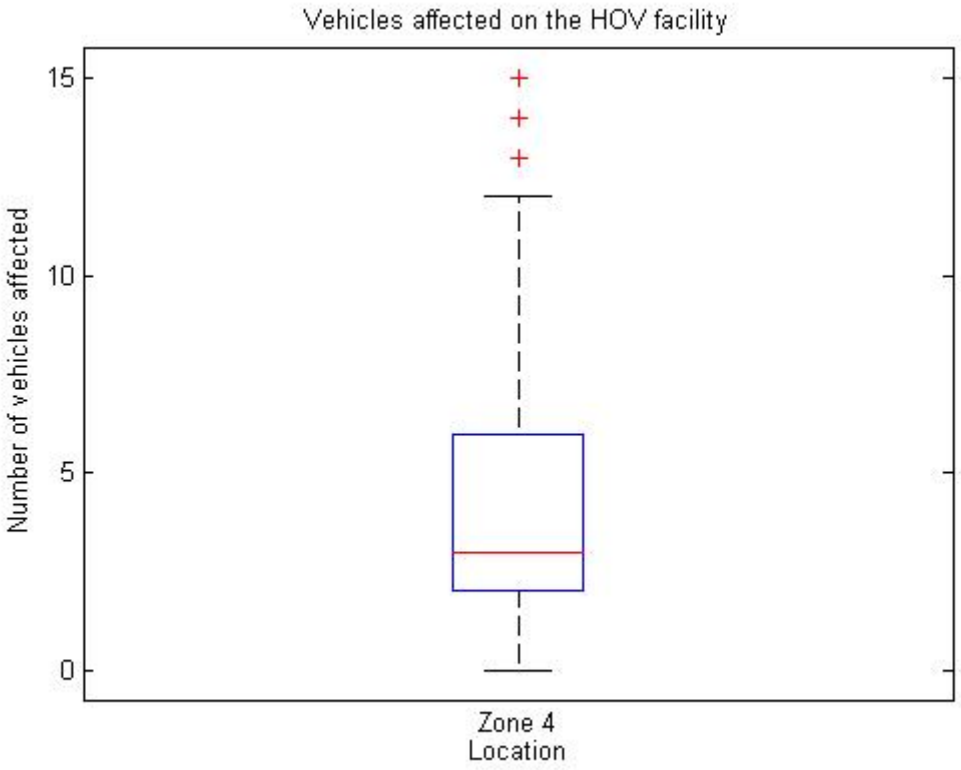

Figure 36. Statistical characteristics of observed shockwaves for Zone 4

In order to formulate an opinion as to potential changes in access for this location it was deemed important to understand what percent of the HOT traffic originates from 46th St. Although not offering a precise assessment, data from two consecutive loop detectors in the HOT are compared in Figure 37. Specifically the figure presents volume measurements for August 31st for two detectors on the HOT; D5967 before 46th street and D6792 at 38th street. In the morning very little traffic seems to originate from 46th St but in the peak of the afternoon period around 50% of the traffic of the HOT joins between 46th and 38th. This proportion renders difficult restricting access north of 46th St. If a Closed Access design was followed there would still be the need for a gate north of 46th St generating the same issues we observe today. Restricting access south of 46th St will not change the outlook much as it will be discussed in the next section.

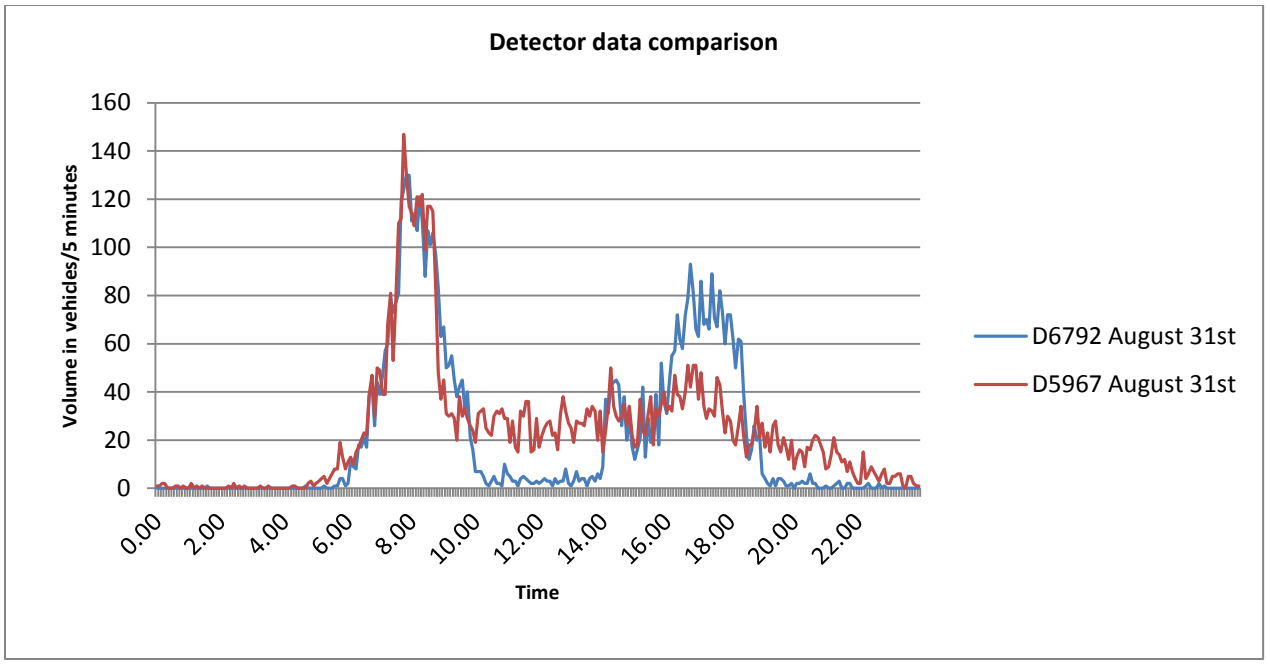

Figure 37. HOT detector data comparison

Interstate 35 W Southbound

Similar to the north direction contour plots are presented for the south direction, providing information about the congested parts of the freeway during the afternoon peak hours for the five days observed (Figure 38 through Figure 42). The purpose of providing these plots is to support the identification of possible solutions to locations that require attention. It is important to note that three of the five days (August 25th, 30th, and 31st) are outliers. They were selected to be during the State Fair because we desired the network to be as loaded as possible and therefore uncover lane changing behavior and more specifically inappropriate lane change behavior in as many locations as possible. In the days used in this report I-35W South exhibits two major bottlenecks and several minor ones. The two main bottlenecks in the supplied figures are on the TH-13 interchange and on the 98th St interchange. From the contour plots of the rest of the 2011 and 2012 till now we see that the TH-13 bottleneck is actually a rare occasion. The 98th St. bottleneck is a stable one that generates congestion as far back as I-494. The interchange on I-494 sometimes generates secondary congestion and the same is observed north of the TH-62 interchange with the latter being a result of congestion on TH-62 spilling over to 35W.

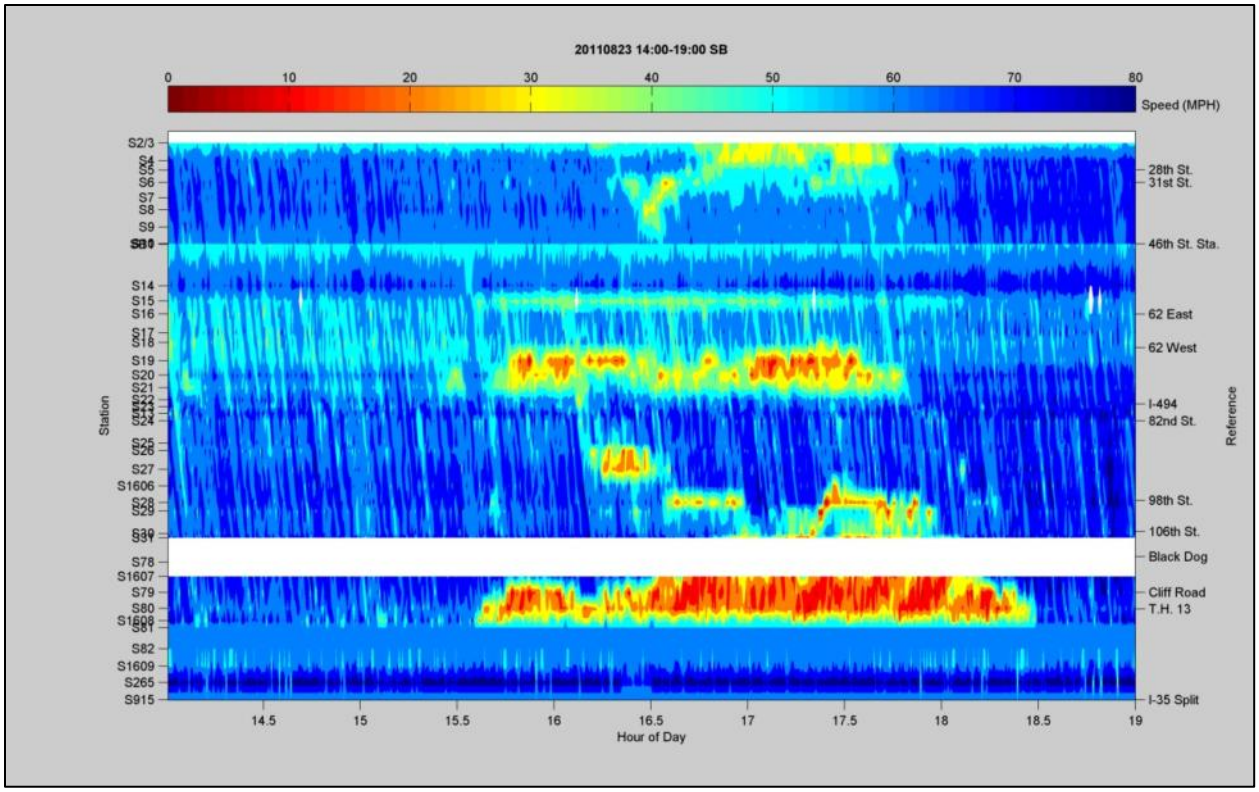

Figure 38. Speed contour plot August 23rd South direction

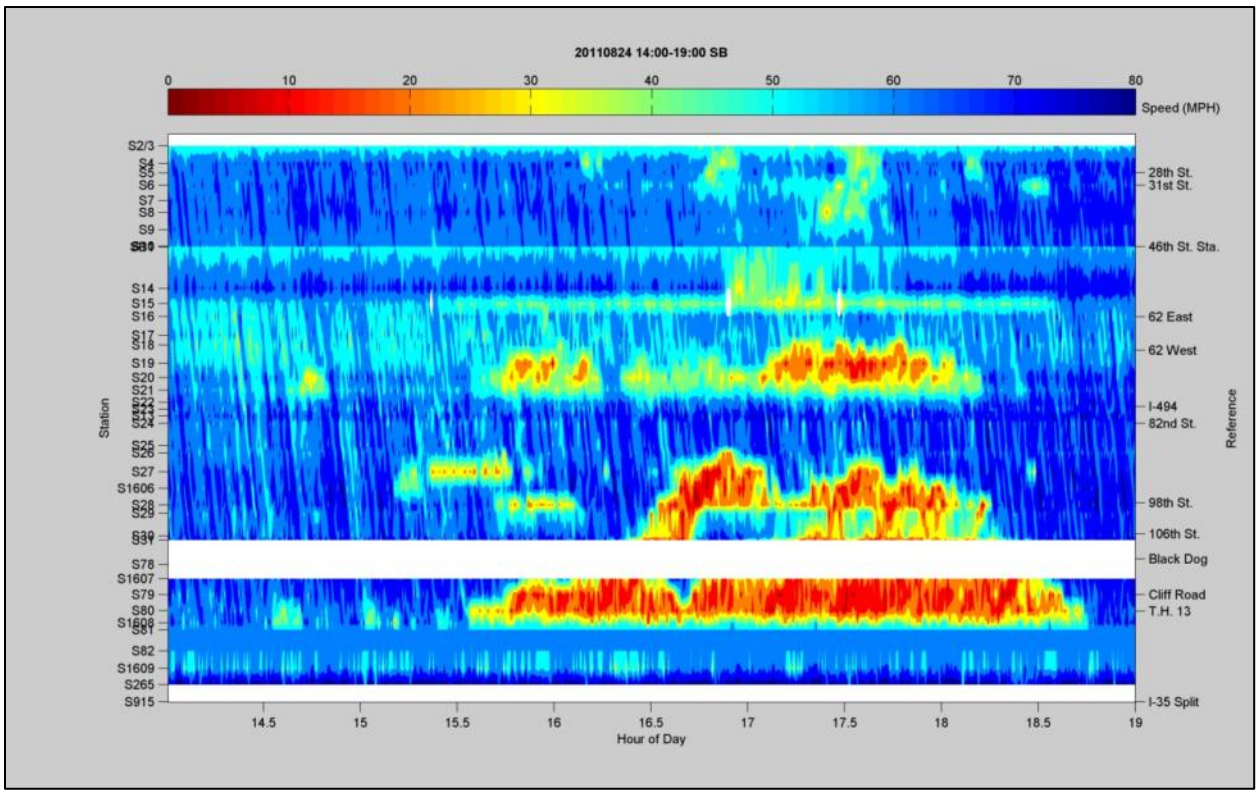

Figure 39. Speed contour plot August 24th South direction

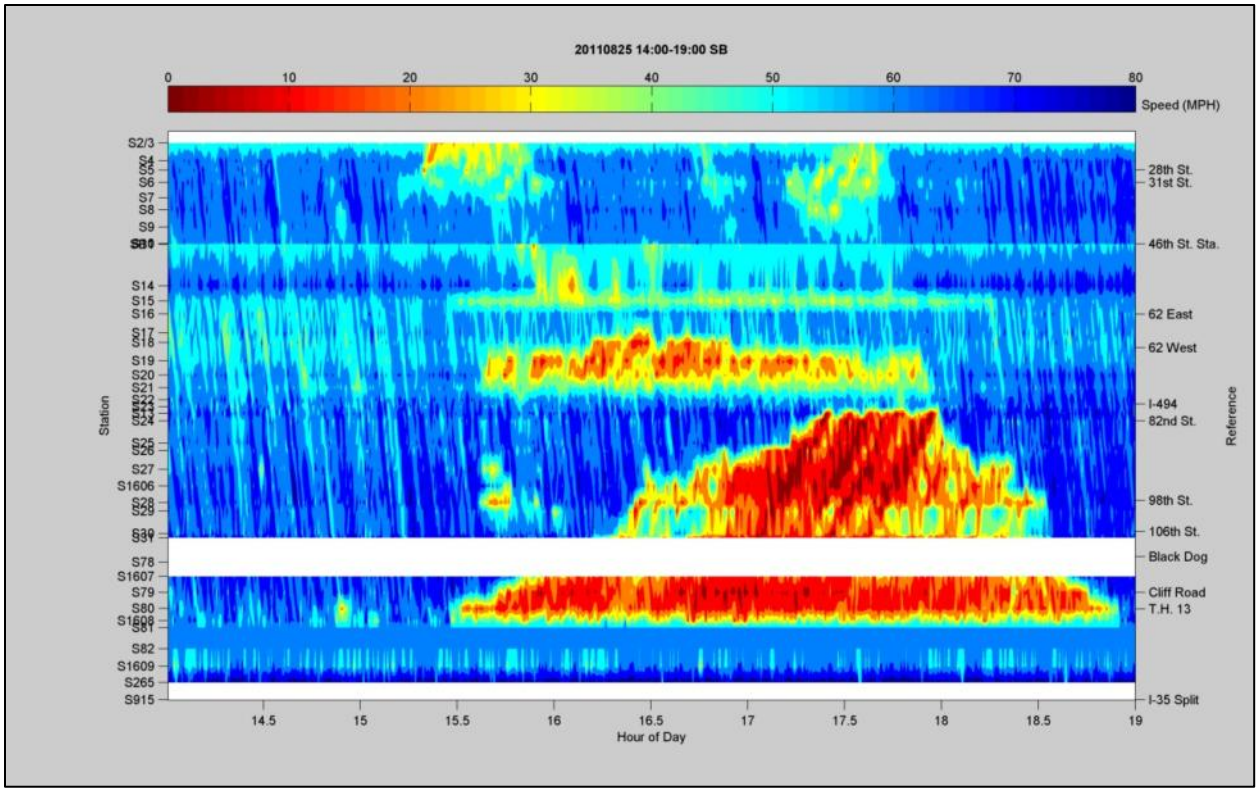

Figure 40. Speed contour plot August 25th South direction

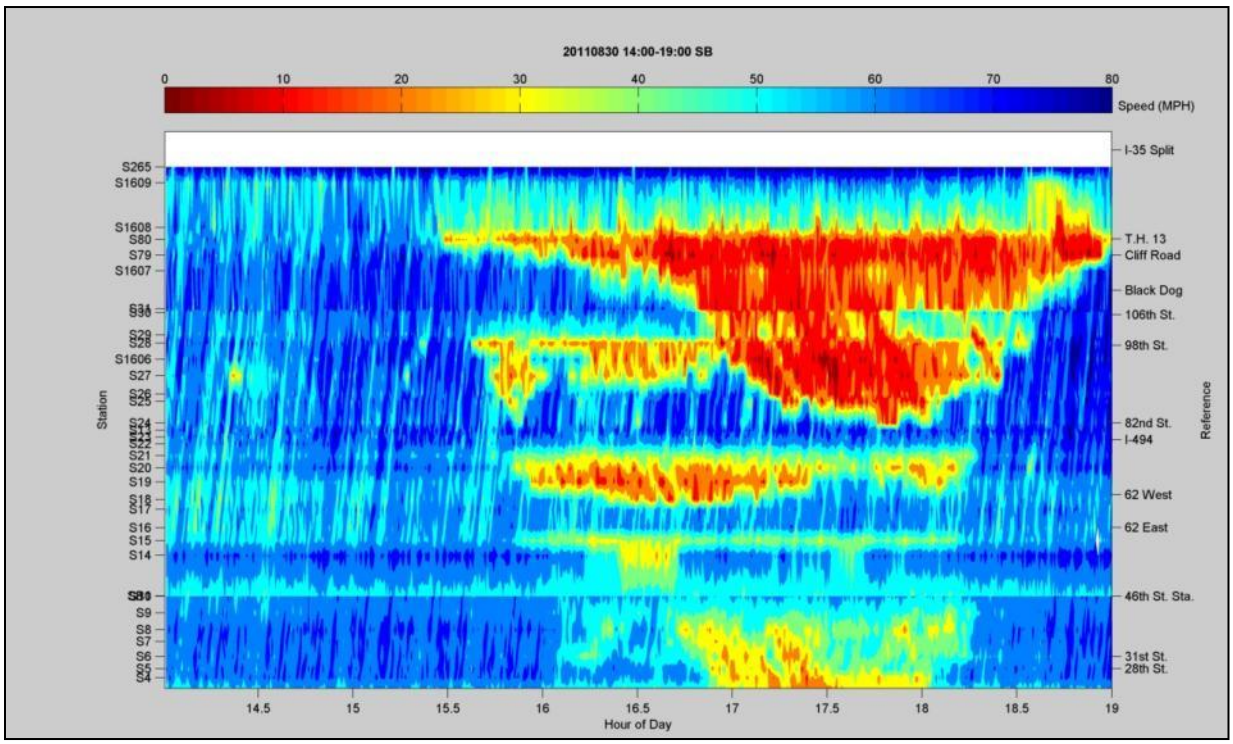

Figure 41. Speed contour plot August 30th South direction

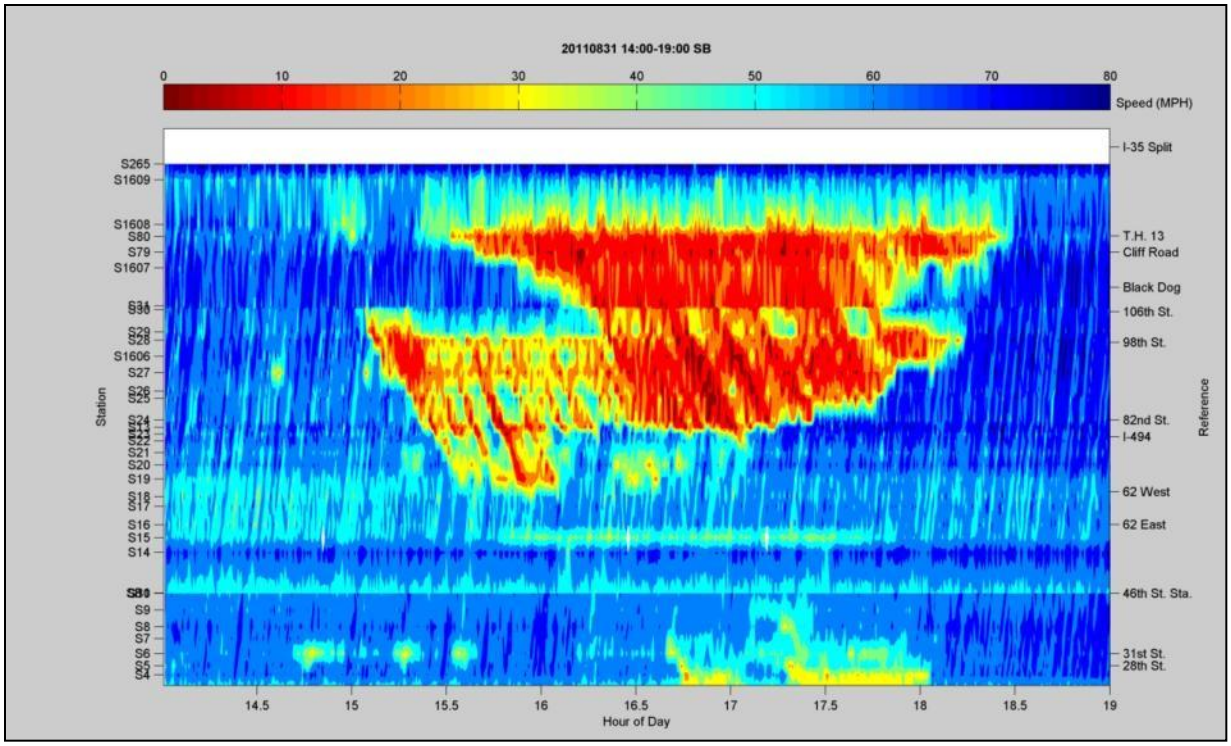

Figure 42. Speed contour plot August 31st South direction

Zone 7: I-35W Southbound (82nd Street – Cliff Road)

Figure 43. Location 6091 example of camera view facing south

Zone 7 has a segment of flow breakdown that once again is located between Cliff Road and Black Dog Road. It was primarily observed this time by camera 6091 facing south, which is shown in Figure 43. Figure 44 shows that location 6091 is the area with the most flow breakdowns in this zone, with location 6131 at the beginning of the zone being the only other location that comes close to matching the amount of breakdowns observed. Location 6091 is mainly an exit from the HOT with the shockwaves generated by HOT vehicles slowing down to select gaps on the slow moving GPL. There is not a specific location where these LCs are located since drivers, who we presume are mostly heading to TH-13, sometimes preemptively change lanes well upstream of the exit ramp and some others wait until the last moment. However, it was noted by the observers that gathered the data that a significant number of the larger shockwaves observed in this zone occurred near the bend in the roadway that is visible by camera 6091, and can be seen at the bottom of Figure 43. It is possible that drivers are having difficulty seeing merging vehicles just downstream of the bend. Further investigation of speeds in the region of camera 6091 showed that the congestion observed is not a frequent phenomenon. The days this congestion in the GPLs was observed demand was high possibly due to the Minnesota State Fair. For this reason we did not expand the evaluation on this particular location. Regardless, since the congestion was not the result of incidents it does indicate possible future conditions.

As previously mentioned, location 6131 had the second highest average amount of daily shockwaves. Location 6131 captures data for the segment between 82nd and 85th street

with emphasis given to the entrance ramp from 82nd street. The view of this camera overlaps with that of camera 6130, and ILCs that could be viewed by both were only counted for location 6131. In comparison to the area observed by camera 6130 this location offers observations right at the beginning of the Open Access part of the HOT. It was not uncommon for drivers to change lanes over the double white line since they were so close to the end of it. This location is the first opportunity traffic from I-494 has to enter the HOT. The lane changing activity was intense on most days of observation.

The interim report also identified locations 6101, 611, 613, and 6130 as locations of medium interest. Further analysis of zone 7 reaffirmed these descriptions. The activity of locations 6130 and 613 can be seen as separate continuations of the activity of 6131, where the frequency and severity of the observed shockwaves diminished as the distance from the opening of the HOT grew. Locations 6101 and 611 continued to follow the trend that was previously noted, in that there was a mild level of ILCs with shockwaves that were small in length. The activity experienced at these locations is largely affected by slowdowns from TH-13.

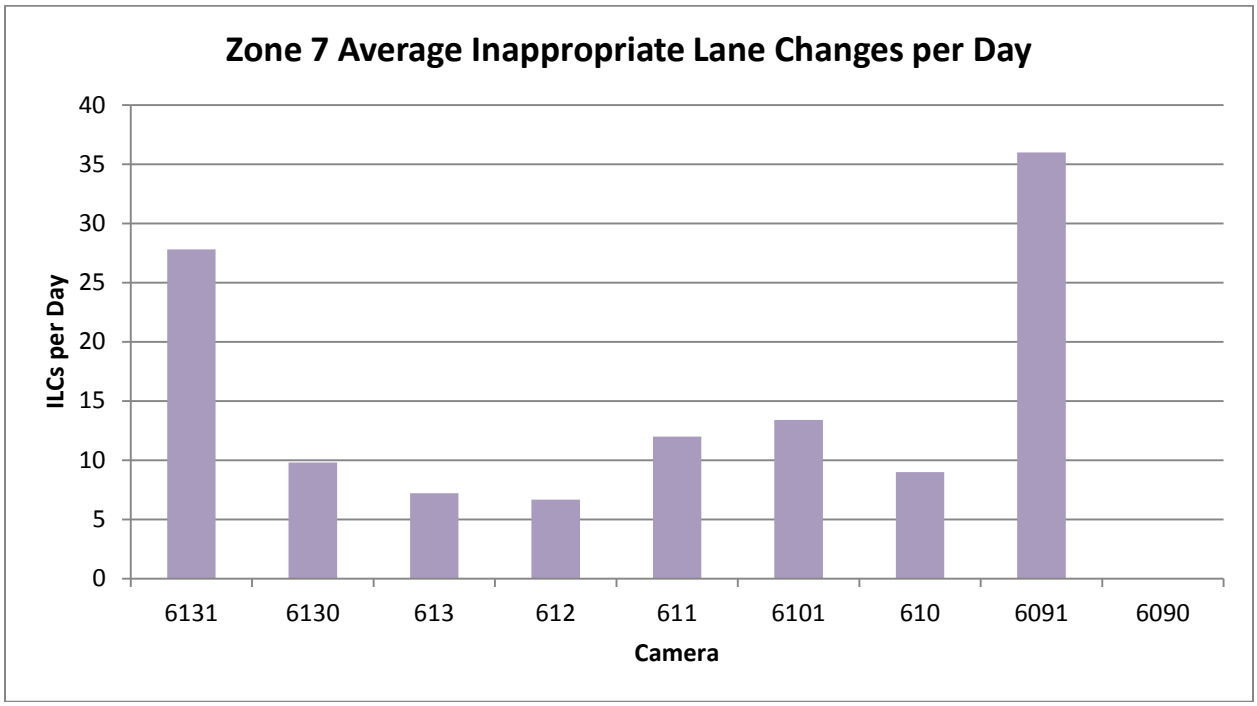

Figure 44. Average daily inappropriate lane changing activity for Zone 7

For the five afternoon peaks analyzed the ILCs per TLCs achieved relatively lower values zone wide compared to the other zones on I-35W with observations shown on Figure 45. The percent of vehicles in the zone that experience a breakdown of flow is comparable to that of zone 4, but more than zone 1. It should be noted that zone 7 is longer in length than zone 1, and therefore there are more opportunities for vehicles to experience a breakdown or multiple breakdowns as they are in the zone for a longer period of time.

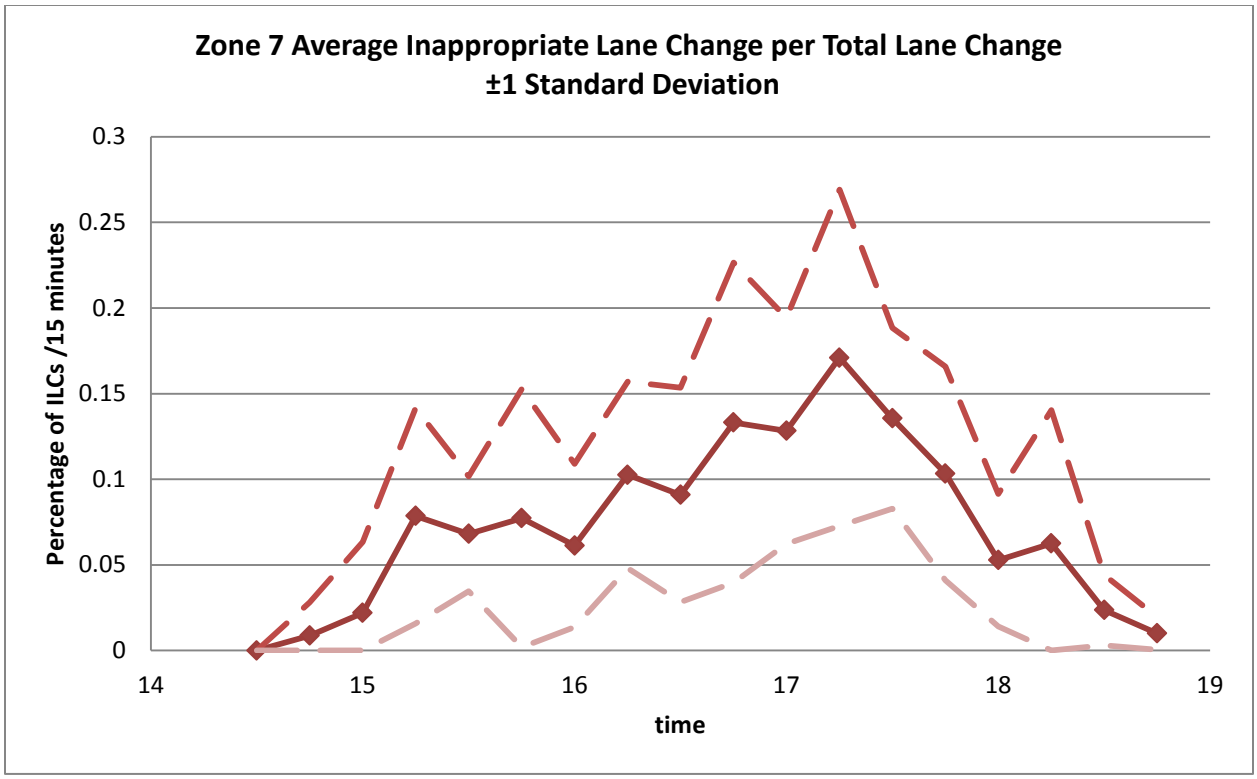

Figure 45. Average percentage of ILC per TLC for all days of Zone 7 during evening peak

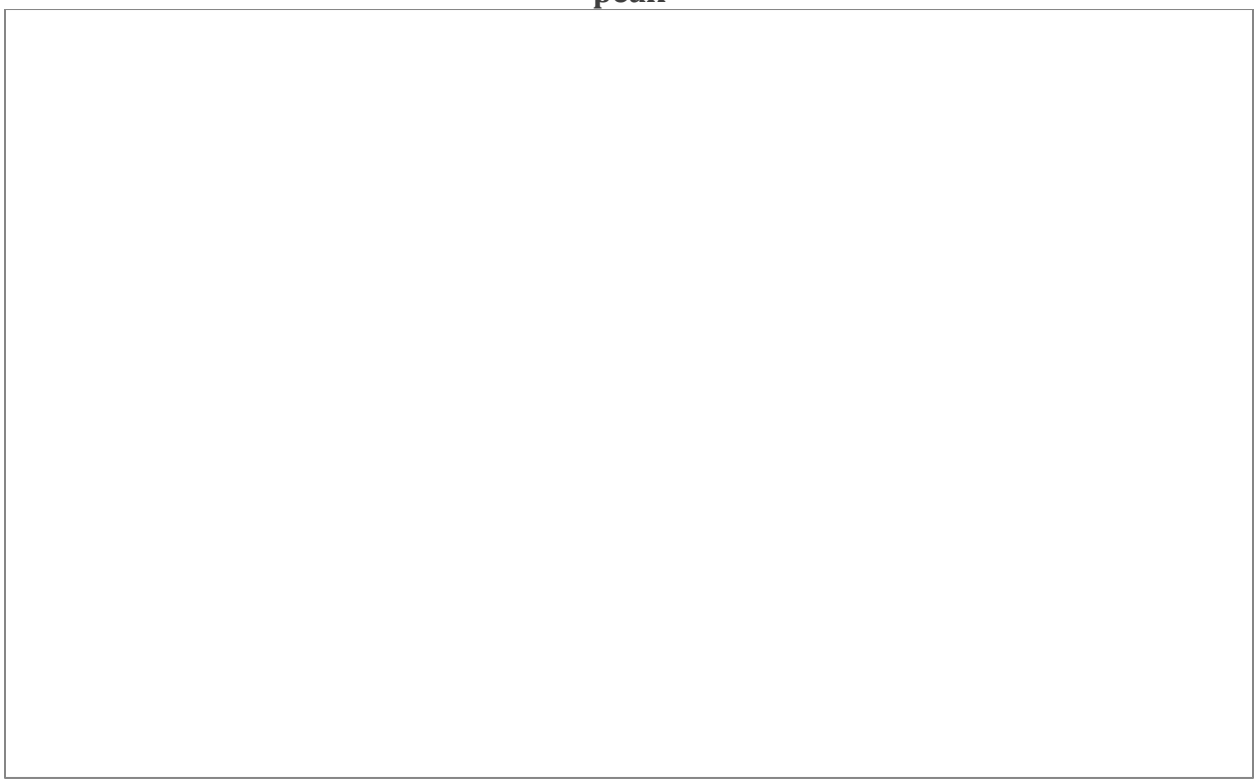

Figure 46. ILCs per HOT volume of zone 7

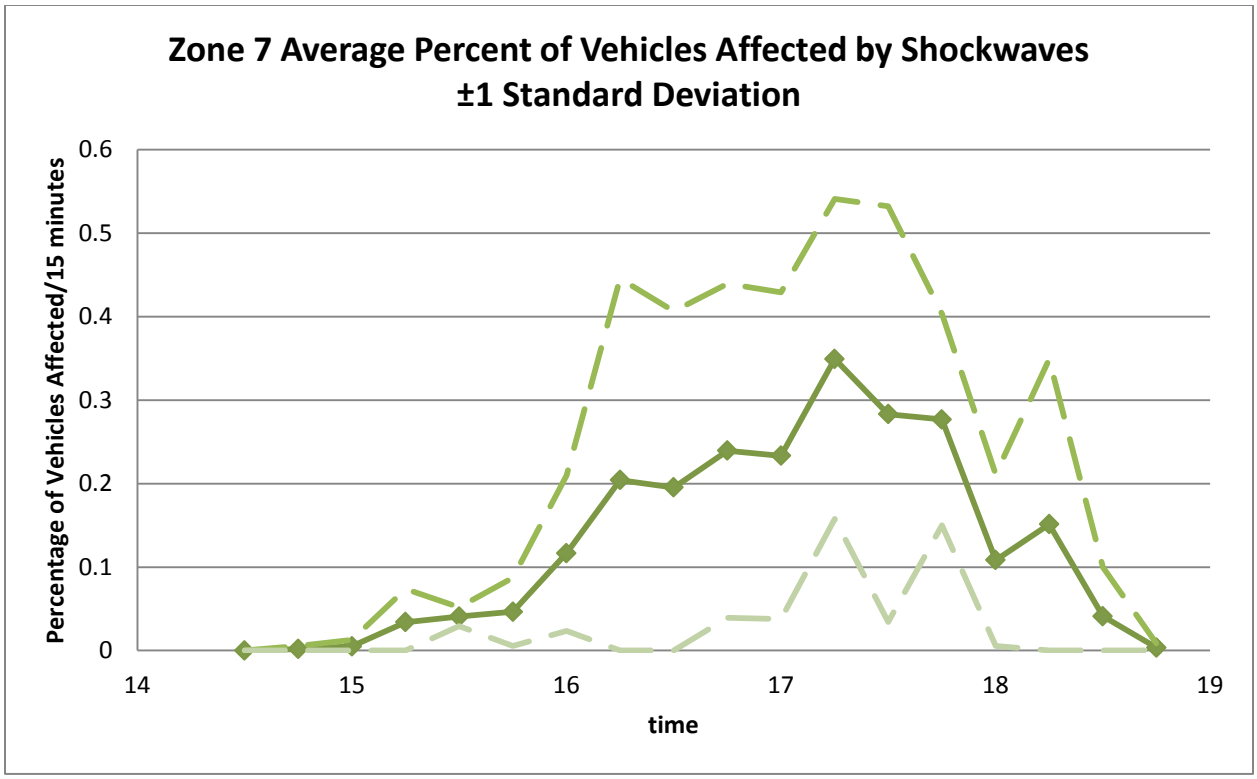

Figure 47. Percent of vehicles that experience a breakdown of flow

The characteristics of the observed shockwaves are shown in Figure 48. The figure shows that the shockwaves of this zone are smaller but comparable to those observed in zone 4. As with the two previously described zones the median observed shockwave length is 3 vehicles. The extreme value of 11 was slightly less than that of zone 4, and the 75th percentile value 5 was equal to that of zone 1.

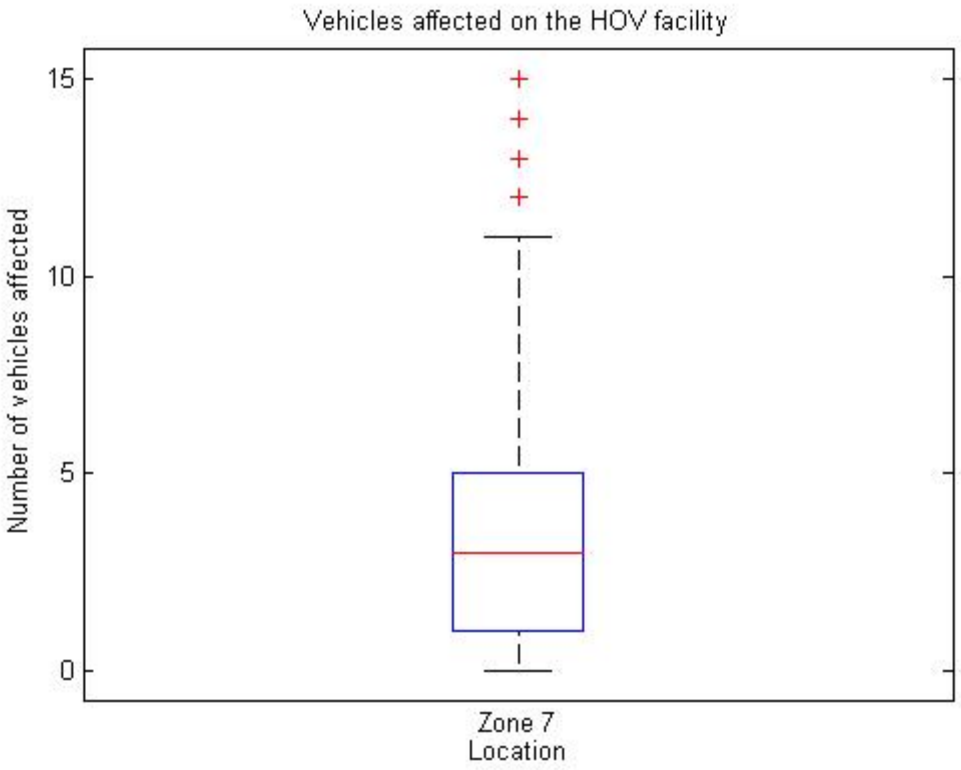

Figure 48. Statistical characteristics of observed shockwaves for Zone 7

On 6091 only 30% of the ILCs are inbound with most of the disruptions being caused by vehicles leaving the HOT. Considering the small amount of ILCs on 6101 restricting access would not make any difference. On 6091as observed the congestion on the GPLs forced the lane changes out of the HOT to spread over a wider area. Since this bottleneck is not a common occurrence there is no need for intervention. If we assume that such congestion was common the observed behavior would have dictated similar access geometry even if the Closed Design of I-394 was adopted. If in the future this location becomes a safety issue the more forceful consideration of having the TH-13 traffic leave the HOT much earlier can be considered but it would result in a fair number of violations.

I-35W safety and mobility assessment

This document so far presented our observations of the lane change activity on the I-35W MnPASS HOT Lane facility. On each location researched, evidence directing an assessment of the operations of the HOT in terms of safety and mobility were presented. Traffic flow interruptions (shockwaves) are undesirable since they affect both safety and mobility. The frequency of shockwaves eventually affects mobility since it increases density while lowering overall speeds. Such occurrences cause the price of the HOT to increase even if the overall demand is not high. Shockwaves are the instances where drivers are required to react to avoid collision. Due to the delay in human reaction, the larger the shockwave the higher the required deceleration required (assuming equally spaced vehicles). Therefore the larger the shockwaves in number of vehicles affected the greater the chances for a collision. This document cannot present a definite assessment of safety since this site has not been in operation long enough, but utilizes the size of the observed shockwaves as a surrogate in evaluating the safety of the different locations on the HOT. It is important to note that this research focused on the allowed access segments of the roadway. As mentioned in the earlier report of Task 4, there was one isolated case, 6130 NB, where an area with restricted access was covered, several violations of the double white line were noted and they generated shockwaves. This may be an isolated phenomenon or not. The way this research was conducted does not allow us to generalize.

In the northbound direction of I-35W two areas of concern were presented. The first area is between the Burnsville Pkwy and Cliff Road interchanges on zone 1. This area is experiencing severe recurring congestion on the GPLs and has a large proportion of the entrance ramp volume heading for the HOT facility. Given the existing utilization on the HOT, the shockwaves observed, although large, have not generated any crashes. This can change if the utilization of the HOT increases following changes in the pricing algorithm or on the market characteristics of the HOT demand. In addition, aggressive behavior by the commuter buses entering the freeway in this location attributes for a large number of the Inappropriate Lane Changes observed. Considering mitigation strategies for this location, keeping in mind that they are not immediately needed, we would first suggest targeting the bus driver behavior, requesting that they join the HOT less aggressively or a little later (after the Cliff Road bottleneck). Given that the demand on the intersecting roadways will not reduce in the future, if the utilization of the HOT increases there may be a need of restricting access to the HOT between TH-13 and Black Dog Road. This will hurt the service offered by the HOT so it should be considered only if conditions deteriorate significantly.

Since this project is also tasked to formulate an opinion regarding the comparison of the Close Access design used on I-394 with the generally Open Access design of I-35W an engineering assessment on that subject can be made for each location of interest. The access on I-394 is strategically located at the areas of high demand for the HOT. For the aforementioned area, given the importance and demand on the joining roadways, an open access “gate” would have been located there anyway. As we will see later on when observations on I-394 are presented, such “gates” experience comparable shockwave characteristics and therefore the issue discussed would have been the same. Closing access anywhere else around this area would have no effect in the safety and mobility of the HOT.

The second area of interest in northbound I-35W lies between 46th street and 42nd street in zone 7 closer to the downtown area of Minneapolis. This last segment of open access delivered a very large amount of flow breakdowns numerically as well as a percent of the general lane change activity. As discussed in the relevant section, this area is the last chance for vehicles to join the HOT and in extent an area where it would be very difficult to further restrict access. Specifically a large portion of the HOT traffic in the afternoon originates from the 46th St ramp which is already in the midst of the problem. If a Closed Access design was followed there would still be the need for a gate north of 46th St generating the same issues we observe today. Restricting access south of 46th St will not change the outlook much. A closer study of the demand of the origins of the demand on the HOT at this point may reveal some possible compromises.

On the southbound direction of I-35W there are two areas that could compromise safety and mobility. One is in the area of 98th St and the other is the area of Blackdog Road. Although the congestion observed south of 98th St (location 6101 SB) is a rare occurrence it happens and when it does it generates quantifiable issues on the HOT. As seen in the following figures it generated some of the biggest shockwaves among all locations on I-35W during all of the observed days. For the foreseeable future this is a location that needs to be watched for signs of deterioration. The areas close to the start of the open access south of I-494 (locations 6131 SB and 6130 SB) are operating fine today but are a good example of how the situation can change with the addition of just a few more vehicles in the HOT. The absolute values of the lengths of the waves signal a good standing in terms of safety but if we take into account the high LC activity of this segment, a future increase of vehicles on the HOT facility could result in greater disturbances.

Later in this report a tool aimed in forecasting at which level of HOT facility utilization the aforementioned areas will have to be mitigated is presented. The tool and methodology developed can guide mitigation strategies in terms of both access and control of the pricing of the HOT lane to keep the demand below the threshold at which this roadway geometry will start to experience serious problems.

As a closing note on I-35W, an assessment of the impact on the adjacent lane was made. For almost all the examined locations, our observations are very close to null values; the low speeds on the adjacent lane do not force drivers to decelerate during the LC activity which explains the observed small lengths of shockwaves.

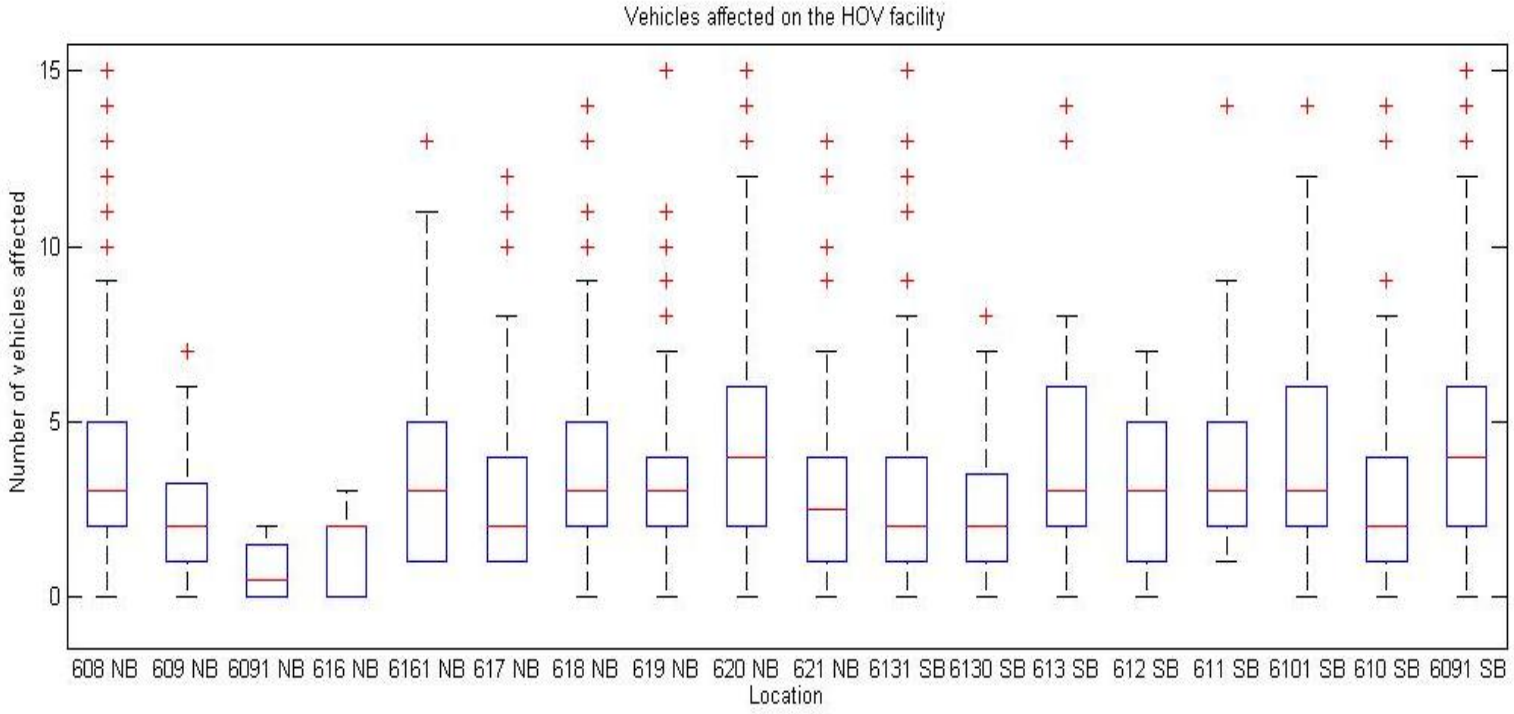

Figure 49. Observed flow breakdowns on the HOT

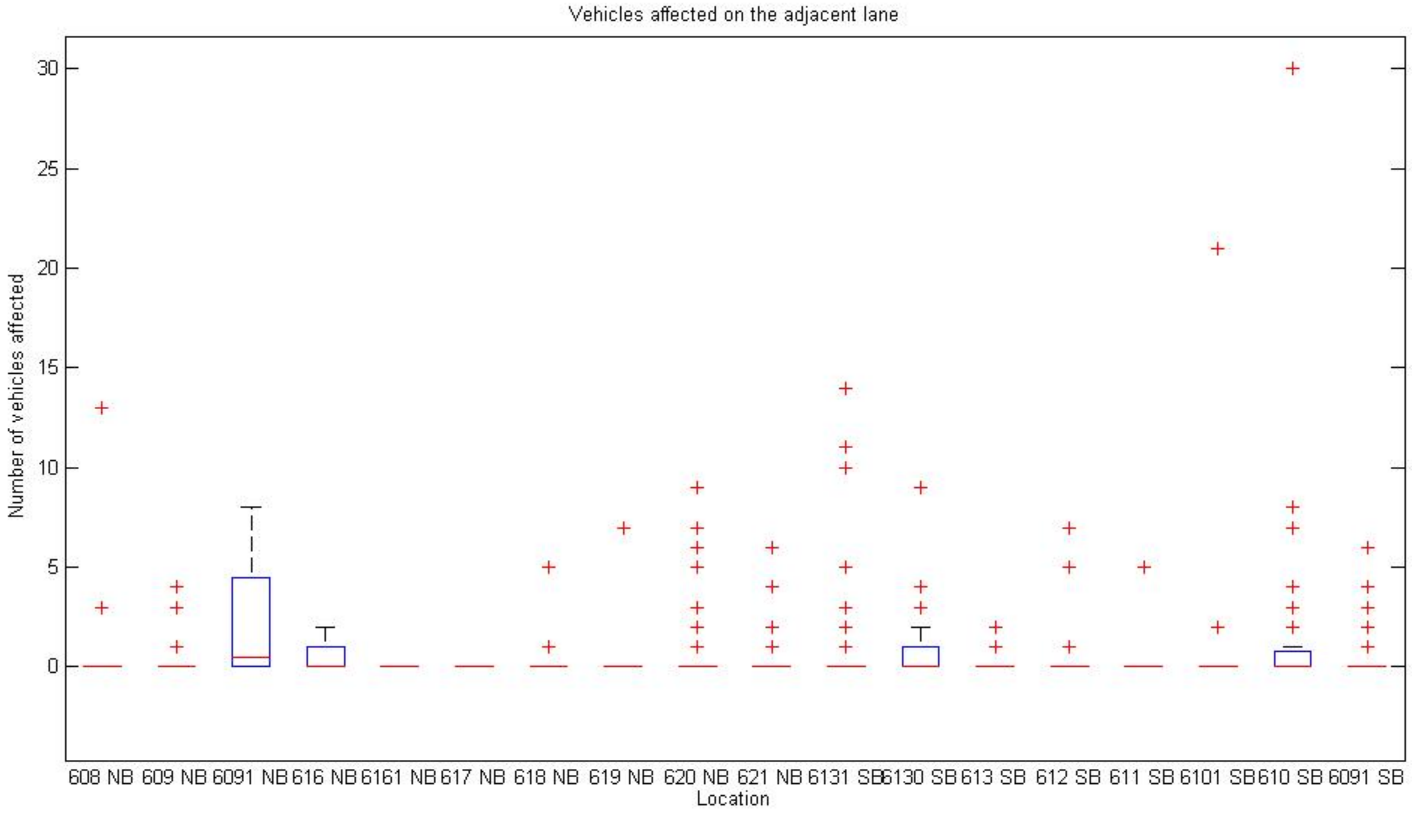

Figure 50. Observed flow breakdowns on the adjacent GPL

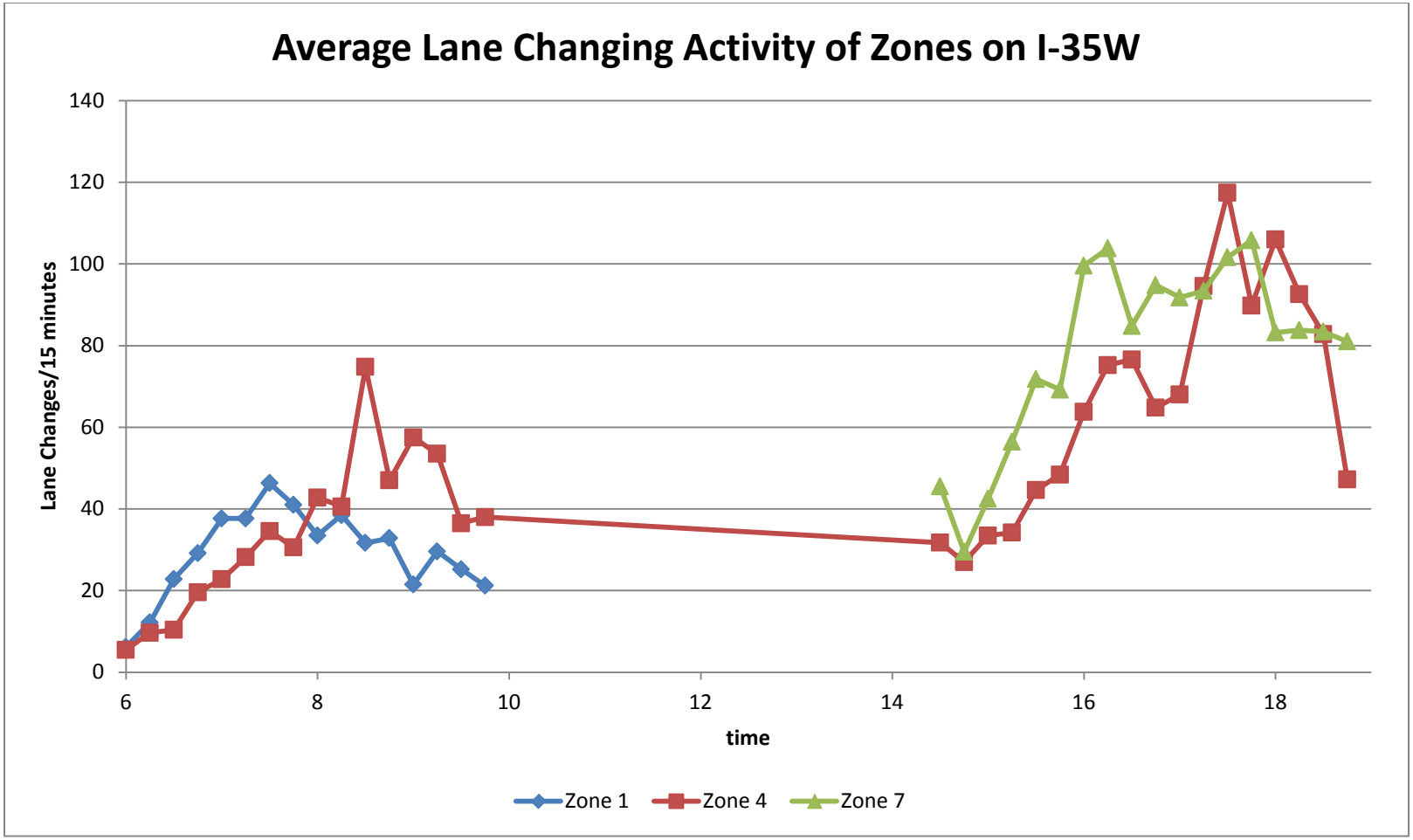

Figure 51. Average lane changing activity of I-35W

Interstate 394

The collected observations for interstate 394 are limited as compared to I-35W. I-394 in general has a lot less demand and congestion as compared to I-35W. In addition I-394 follows a Closed Access design with allowed access in the form of "gates" (areas of limited length) located strategically around the four major interchanges intersecting this roadway.

Following the same methodology as in I-35W, further investigation was only carried out on a single location of the eastbound direction. This is the only location with congestion in the GPLs. The objective is to assess the possible difference in safety and mobility of the Closed Access design paradigm. Four days of footage from I-394 have been analyzed and the collected observations will be presented in a subsequent report.

Access Eastbound 4: I-394 EB (Louisiana Avenue)

Figure 52. Location 908 example camera view facing east

Figure 53. Location 909 example camera view facing west

Access EB 4 is the second to last gate before the HOT enters the barrier separated reversible section. The gate is viewed by camera 908 for west of the Louisiana Ave bridge (see Figure 52), and camera 909 for east of the bridge (see Figure 53). This gate was identified as one of the most important for the I-394 corridor during the video collection task. As it is characteristic of Closed Access design the "gates" experience a very high lane changing activity. The average observed values reach 100 vehicles per 15 minute intervals during the morning peak hours (Figure 54) and over 60 in the evening peak hours (Figure 55). The statistical characteristics of the observed flow breakdowns (Figure 62) are on the higher end. The lengths of the recorded flow breakdowns reached a median value of 4 vehicles while the most extreme value was 12 vehicles. Despite the conservative design of the access segments on the HOT and the generally lower demand levels, very long shockwaves were generated due to the high speed differential, between the HOT and the adjacent GPL, at this part of the freeway.

Once again, the assumption that the optimal design should correspond to the individual needs of each segment is supported and that the individual lane changing characteristics should be taken into account in order to decide about the locations and lengths of the gates.

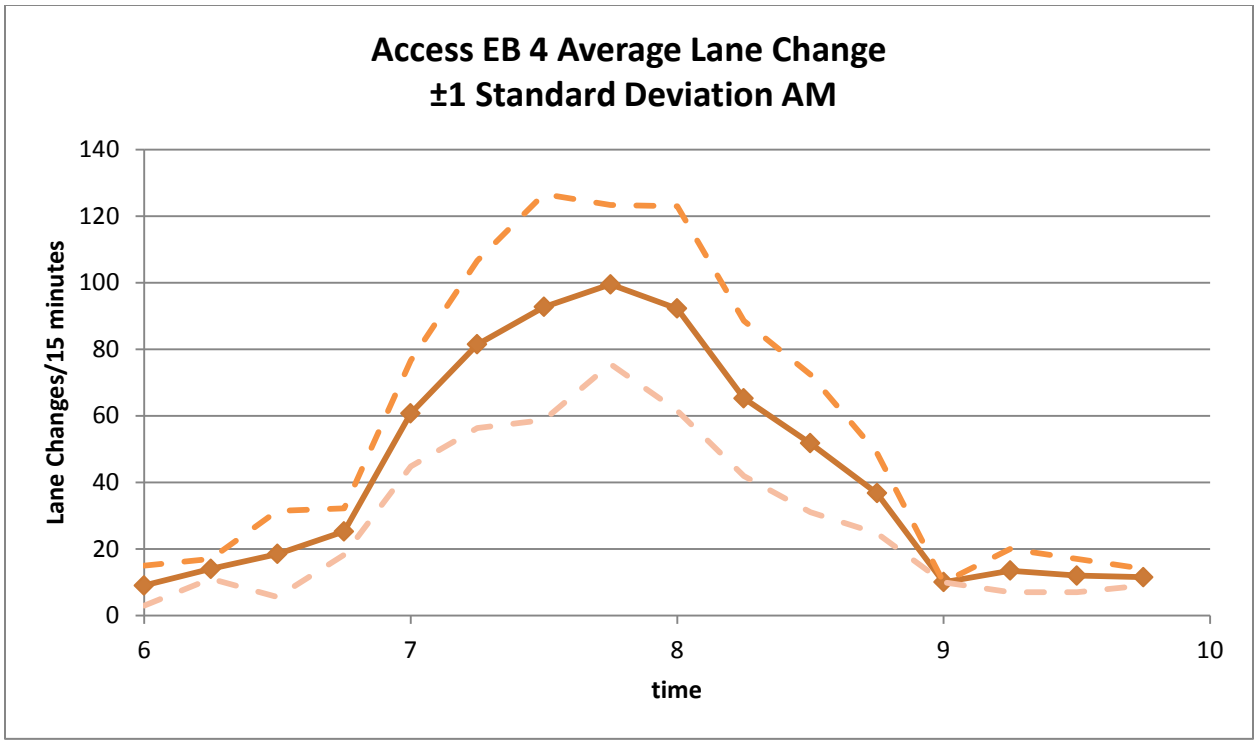

Figure 54. Average total lane changing activity Access EB 4 AM

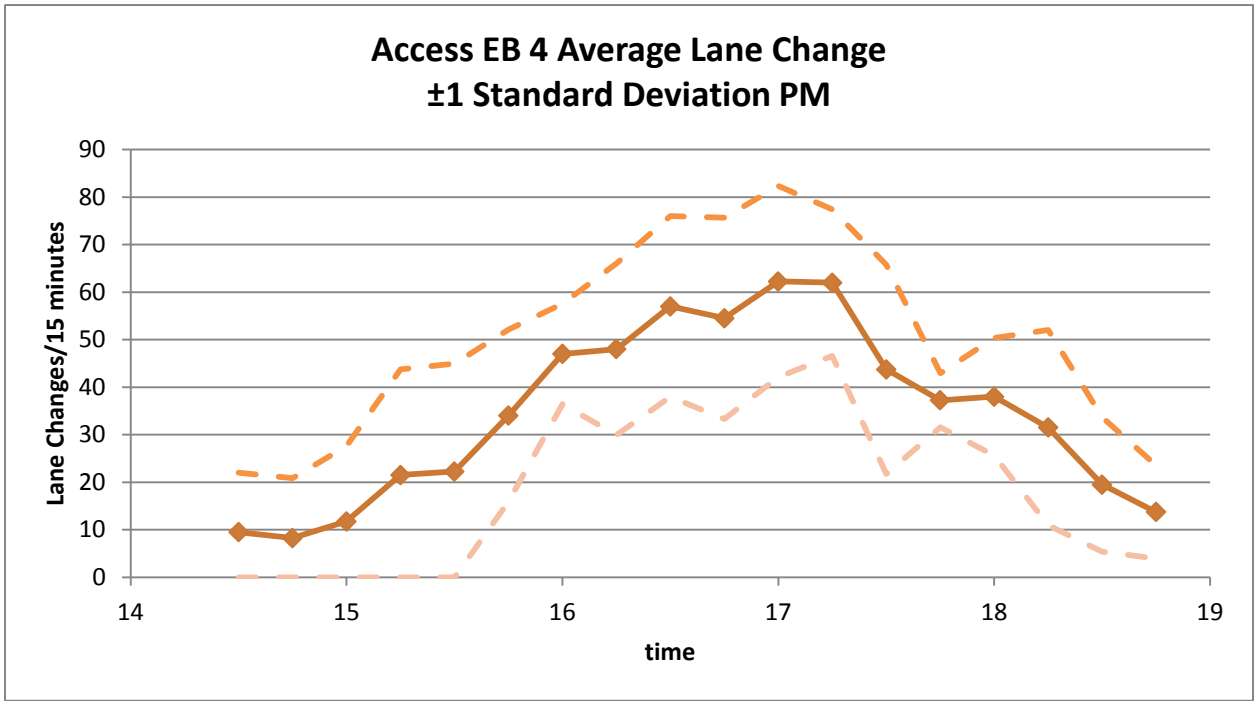

Figure 55. Average total lane changing activity Access EB 4 PM

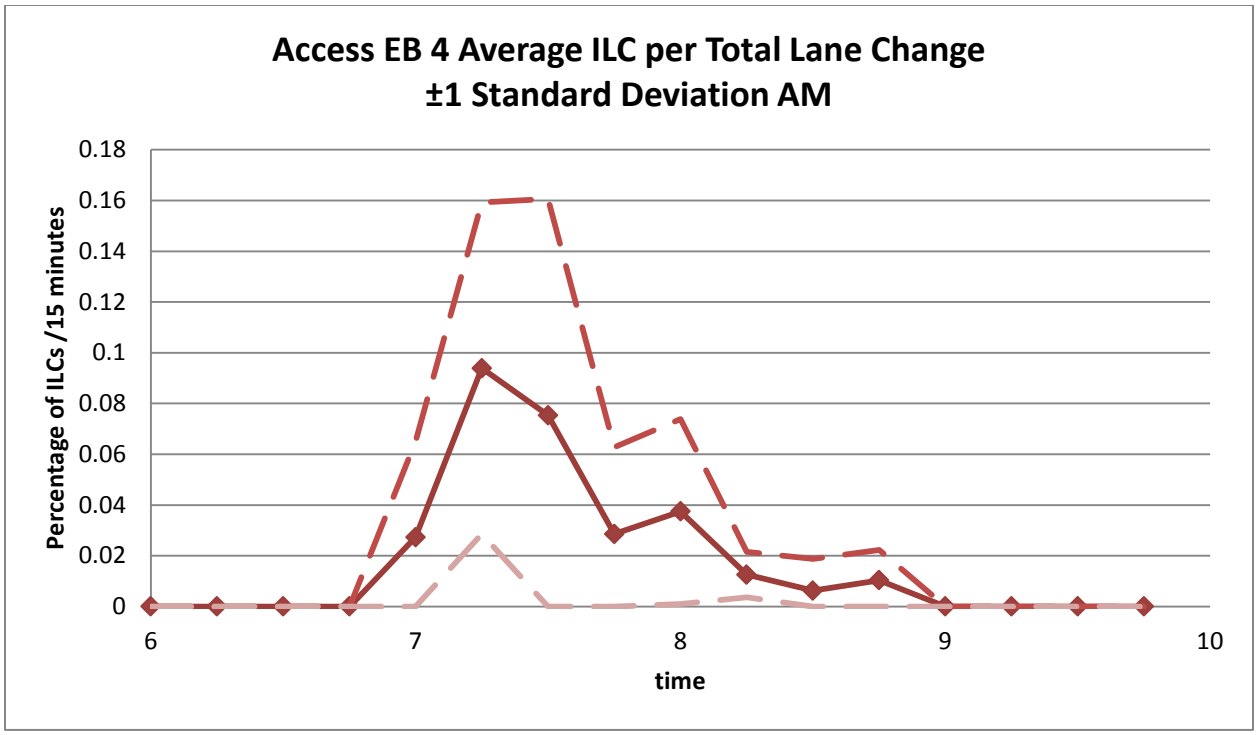

Figure 56. Average percentage of ILC per TLC for all days of Access EB 4 during morning peak

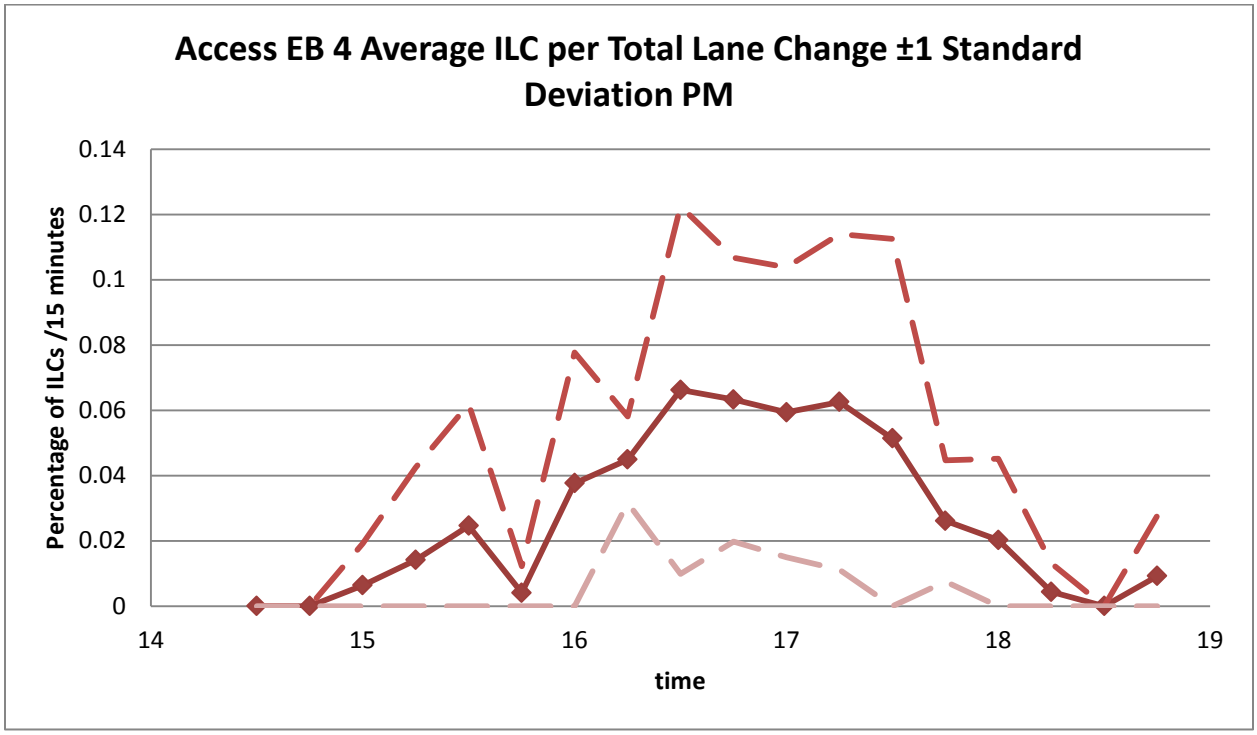

Figure 57. Average percentage of ILC per TLC for all days of Access EB 4 during evening peak

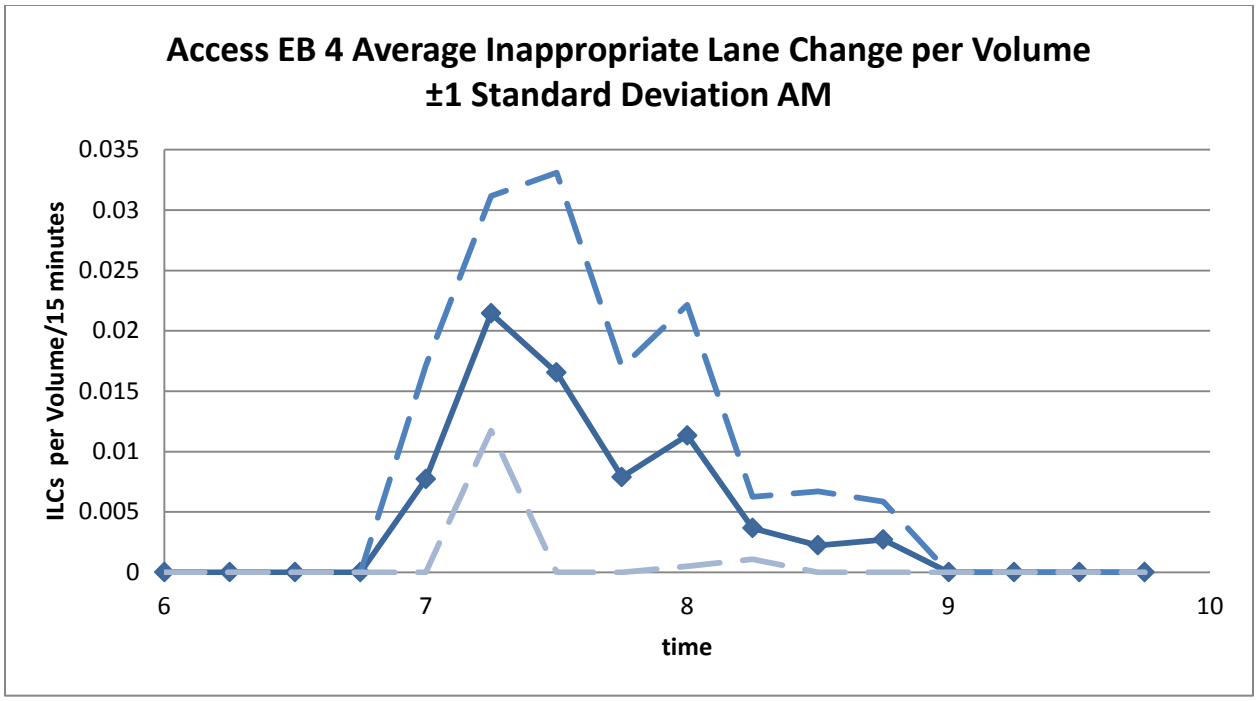

Figure 58. Total lane changing activity August 30th location 909 AM

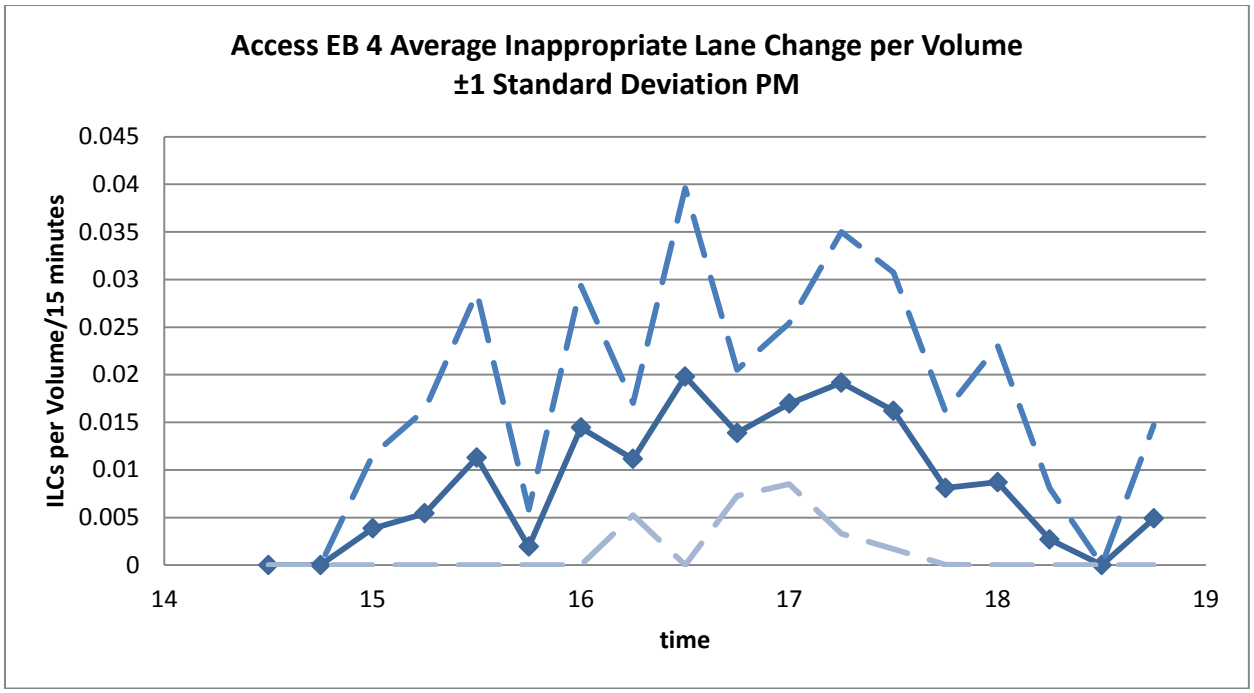

Figure 59. Total lane changing activity August 30th location 909 PM

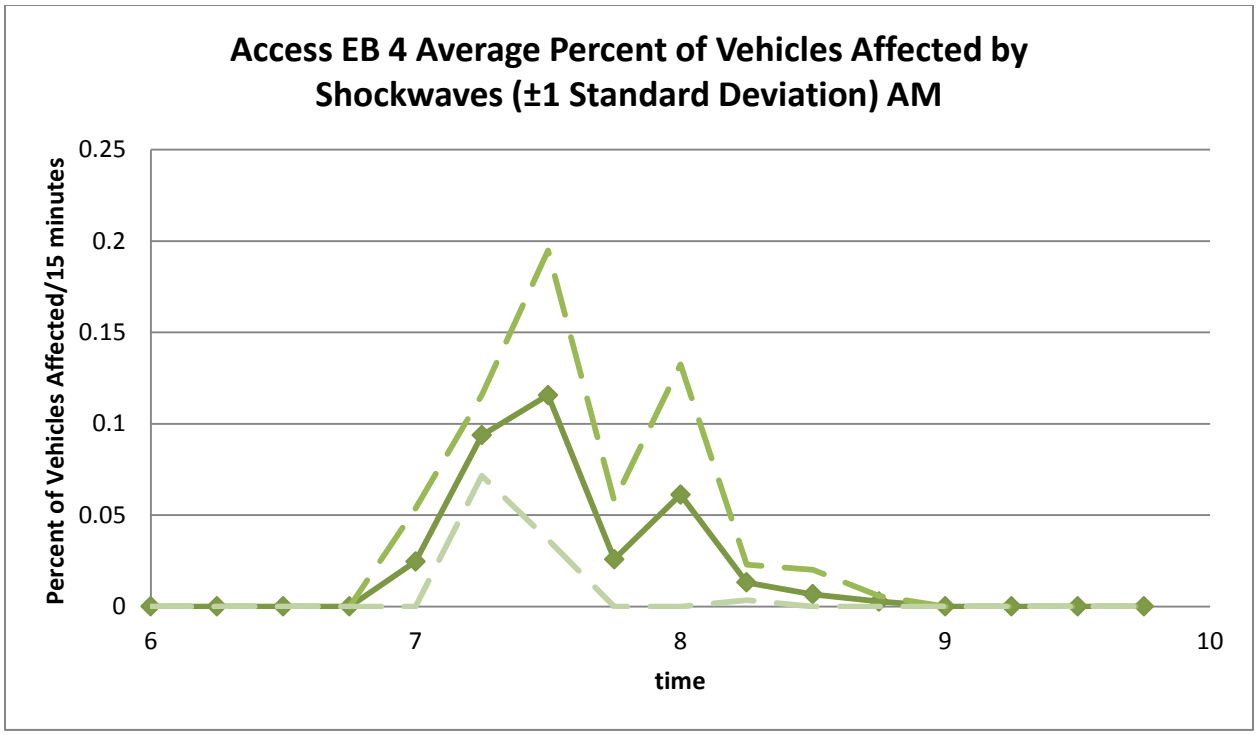

Figure 60. Average percent of vehicles that experience a breakdown of flow AM

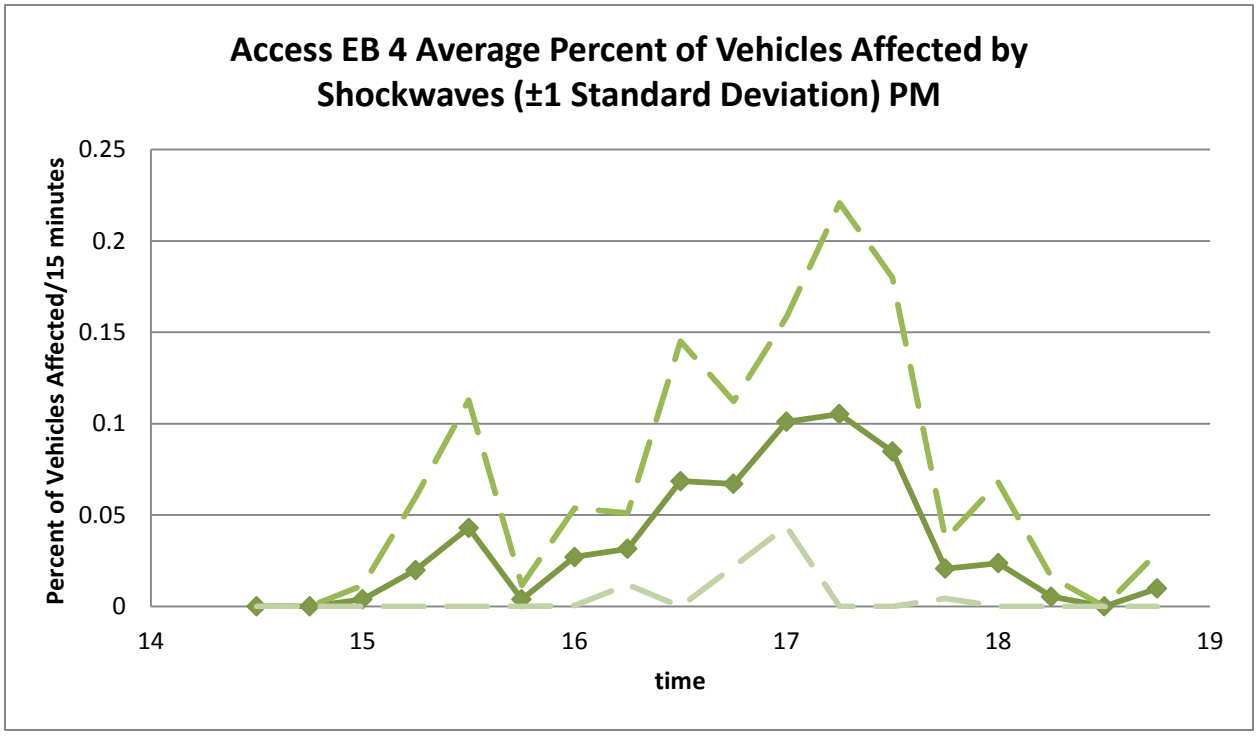

Figure 61. Average percent of vehicles that experience a breakdown of flow PM

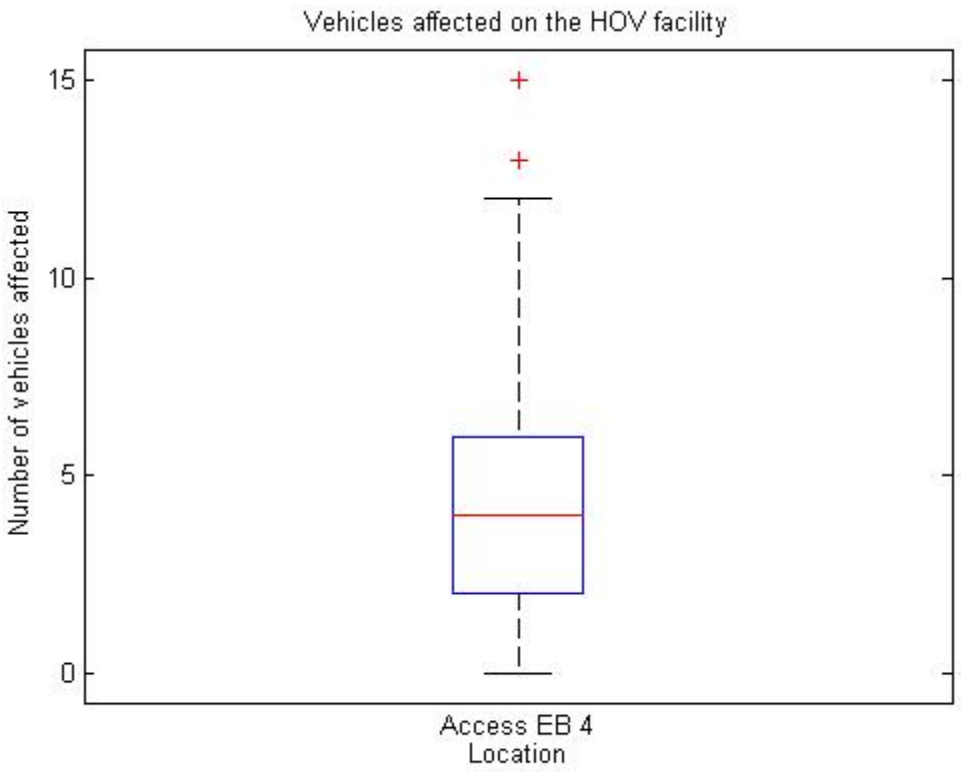

Figure 62. Statistical characteristics of observed shockwaves for Access EB 4

Comparison between locations on I-35W and I-394

A comparison can be conducted based on the findings for the two networks. I-394 has a much more conservative design of the access points of the HOT with gates to the facility of limited length (1000-3000 feet). On the other hand, access segments on I-35W follow an opposite design with only small areas of restricted access and long segments allowed lane changes between the HOT and GPL.

It is difficult to compare the two design philosophies because they were devised to serve the needs of the two roadways. I-394 is operating very well with the Closed Access design because the majority of the demand originates from three distinct interchanges, I-494, TH-169, and TH-100. The rest of the ramps comparatively speaking have much lower demands. As it was illustrated in this report this is not the case on I-35W. The interchange density is much higher with entrance ramps very closely spaced and with the majority of those ramps carrying large demands of HOT eligible vehicles. It would have been very difficult to follow a Closed Access design on I-35W and as it was pointed out in this report it would had made little difference in terms of mobility and safety.

In Figure 63, comparisons of the shockwave characteristics of the four discussed zones are shown. Although the volumes involved are different we can see that the shockwave lengths observed are comparable signaling no difference in terms of safety between the two design philosophies.

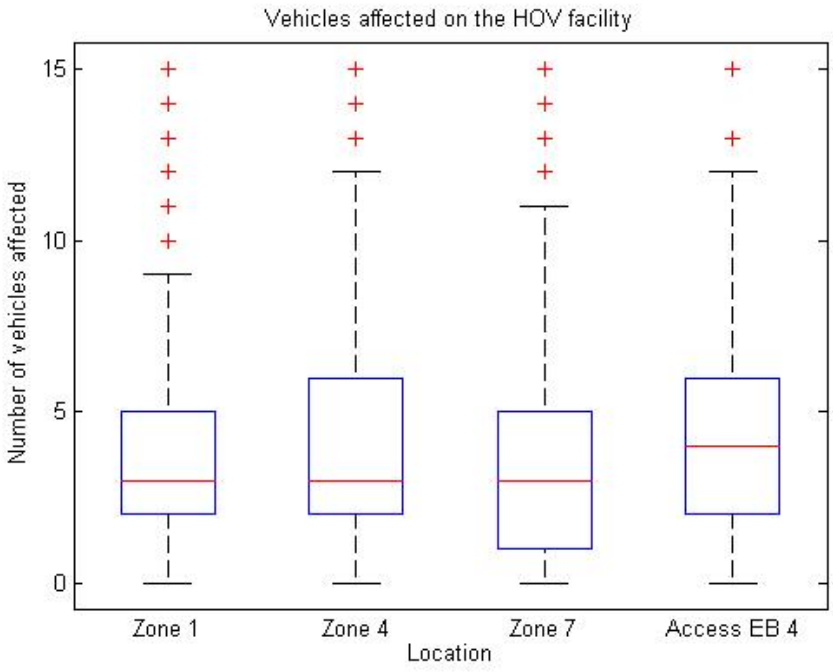

Figure 63. Comparison between facilities on I-394 and I-35W

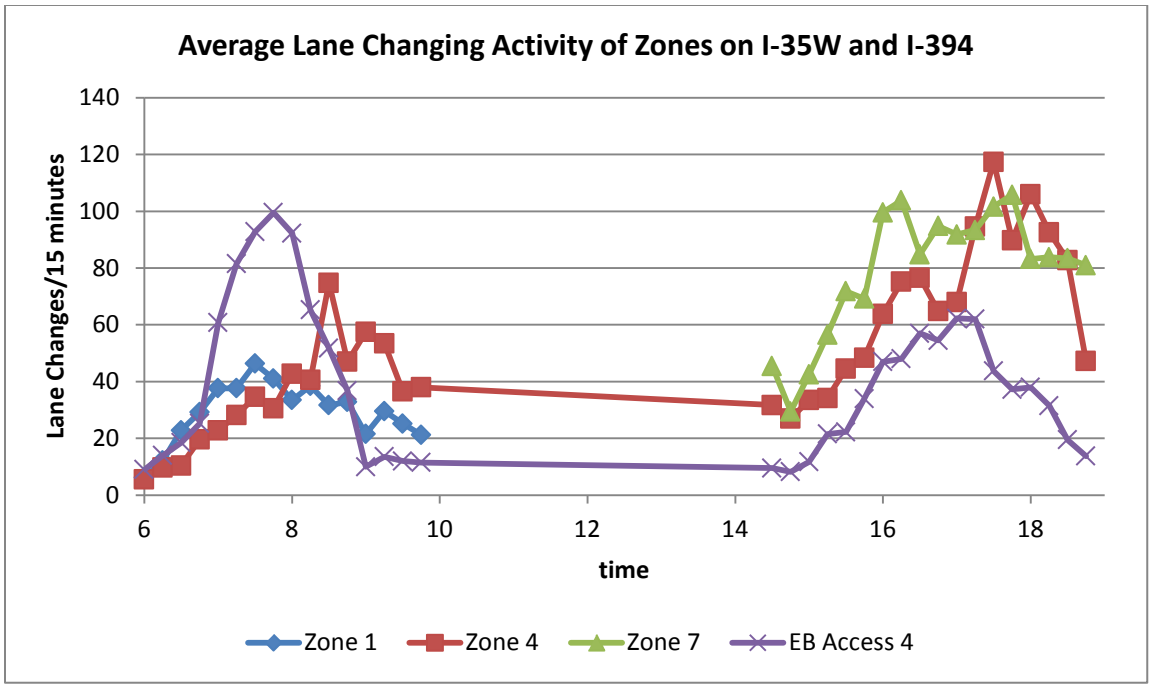

Figure 64. Comparison between lane changing activity on I-394 and I-35W

6. Development of HOT lane design tools

As discussed in the beginning of this report, the second objective was to develop a methodology and tool for the design of optimal access for shared lane HOT facilities. The way this objective finally evolved involves the development of two separate tools, one for the design of optimal lane changing regions in a facility following the Closed Access design and one for the forecasting of shockwave activity on an Open Access facility under hypothetical/future HOT utilization levels. We believe that this way the purposes and priorities of the project are better served.

The rest of this chapter is devoted in the presentation of the data collection process that covered the special needs of the aforementioned development as well as some basic modeling required by both methodologies. Following chapters describe the details of each of the two tools and their respective proposed uses.

Data collection

The necessary data for this study were collected in two stages in order to accommodate the needs of the two parallel modeling efforts. The data consisted mainly of video recordings for the locations of interest, which were later used for machine vision as well as manual data extraction. In addition to the harvested video recordings, inductive loop detector data was also collected using a database made available by the Minnesota Department of Transportation. The shockwave measurements presented in the earlier sections were also used in this stage.

Headway video recordings data collection

An additional video collection period took place on December 22nd, 2011 and January 12th, 2012. The objective of this task was to collect video-recordings that were later used for machine vision extraction of headways. The cameras used were ones placed on an Active Traffic Management (ATM) gantry; gantry cameras provide more accurate results during the headway collection process because they are situated directly above the roadway. The locations that headway measurements were extracted are presented in Table 7 along with the periods of data collection.

Table 7. Video data collection for headway extraction

+	+	+	+	
+	+			
+	+	+	+	
+	+	+	+	

Vehicle trajectories data collection

In an effort to describe the lane changing activity of vehicles merging to the HOT lane after entering the freeway from the nearest entrance ramp, six cameras were utilized for data collection; including one RTMC camera and five high resolution cameras deployed by the MTO personnel. The location of interest was a 2000 feet freeway segment of I-35W Northbound between the 46th Street entrance ramp and 41st Street.

The spacing for the five MTO units were set to be approximately 400 feet apart; this allowed a high level of continuity while tracking a subject vehicle through the series of cameras without blind-spots in the process. Taking weather considerations into account, it was decided to collect high resolution video data for the time period between October 30th 2012 and November 2nd 2012 for the time span between 5:00am to 11:00am in an effort to capture the morning peak hours.

Data Reduction

After all the necessary video data were collected, efficient methodologies were developed in order to retrieve all the necessary pieces of information that supported the models' development. The following datasets were delivered after taking advantage of the harvested data:

- A dataset including measured shockwave lengths for the locations of interest.
- A dataset including headway measurements for various traffic conditions and their corresponding loop detector data for the segments of interest.
- A dataset describing the accepted and rejected gaps for drivers merging in or out of the HOT from the adjacent to the HOT lane.
- A dataset consisting of trajectories for vehicles merging to the HOT lane after merging to the freeway from the entrance ramp of the 46th street; including measurements of speed, accepted and rejected gaps and time increments spent on each lane as well as between lanes.

Headway dataset construction

Video data collected on December 22nd were analyzed using AUTOSCOPE© machine vision equipment. The three I-35W locations examined in the mobility and safety assessment chapter were examined in order to identify their headway distributions and platoon characteristics. The results of this process were essential in simulating realistic representations of the HOT traffic stream.

Virtual detectors were created for each location. The measurements collected by the software consisted of consecutive detector activations and deactivations. In that way, headway measurements were obtained by taking the difference of consecutive detector activations. After the headway dataset was constructed headway measurements were related to corresponding detector density and speed measurements and were assigned a time stamp. In order to reduce the noise that was contained in the detector data a moving window filter of 5 minutes was implemented on the original 30 second counts. This way the scatter in the data was reduced.

Platoon characteristics and the process of platoon formation are key components towards a better understanding of traffic flow on any given site. Platoons were defined by Athol (1965) as the stable portion of traffic throughout the spectrum of traffic behavior. A later definition in the Highway Capacity Manual (2000) defines a vehicle platoon as a group of vehicles moving together. Several studies in the past have made an effort to categorize vehicles in groups. In most cases a critical headway was defined in order to separate drivers in followers and leaders and derive the platoon size distribution (Athol, 1965). The headway measurements were categorized based on those values. Gaur and Mirchandani (2001) used second-by-second loop detector density data to identify vehicle platoons.

Using a time threshold in platoon separation is an effective technique; though it does not capture the individual speed selection. In a more recent study Benekohal, et al. (2004) proposed a dual threshold of either a time headway of less than 4 seconds or a space headway of less than 250 feet as platooning criteria. Using the critical spacing in conjunction with speed data, fluctuations of higher resolution can be captured and different traffic states can be represented effectively using the same separation threshold.

Following the creations of the headway/speed/density data sets, they were processed to separate headways of platoon followers and leaders based on a predefined distance of 250 feet or a predefined time threshold of 4 seconds, taking into account prevailing speed conditions (Figure 65) the threshold is suggested in the literature.

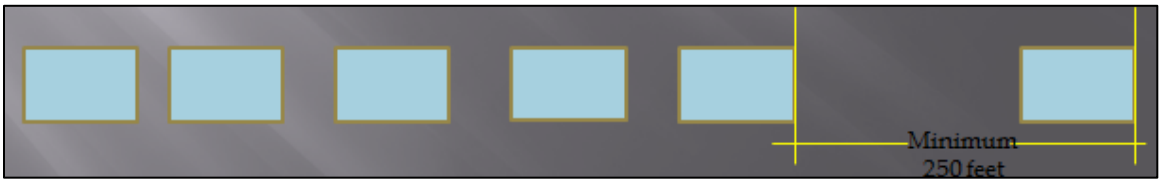

Figure 65. Vehicles separation in platoon leaders and followers

For the follower headways relatively small values were observed. Drivers decide to follow their leading vehicles at close distances because they do not have to be concerned with lane changing activities from both sides. Another reason could be attributed to the speed differential between the HOT and the GPL. Drivers decide to close the distances between them so that they do not give the opportunity to vehicles from the GPL to merge and cause them inconvenience. Finally, from the platoon size histogram we can observe that platoons on the HOT are short in length (approximately 1-3 vehicles) while the longer the platoon the smaller the probability of its formation. The platoon formation characteristics are presented separately for each site. For reasons explained later headway data were collected only on I-35W.

I-35W NB at Cliff road.

Figure 66 presents the platoon formation characteristics harvested on December 22nd, 2011 and January 12th, 2012 for the segment of I-35W between TH13 and Cliff Road. For this location, 45% of the collected observations corresponded to single vehicles; a fact that underlines the underutilization of the I-35W HOT. Furthermore, as in all the examined cases, the shape of the histogram of leader headways is governed by the choice of drivers

not to join a platoon and could be described by an exponential distribution. Finally, the peak of the histogram for follower headways for both days is between 0.75 and 1.15 seconds. This indicates that drivers tend to follow their leaders at relatively short distances. It is possible that drivers in the HOT in order to prevent slower moving vehicles joining from the GP lane decrease their following distances.

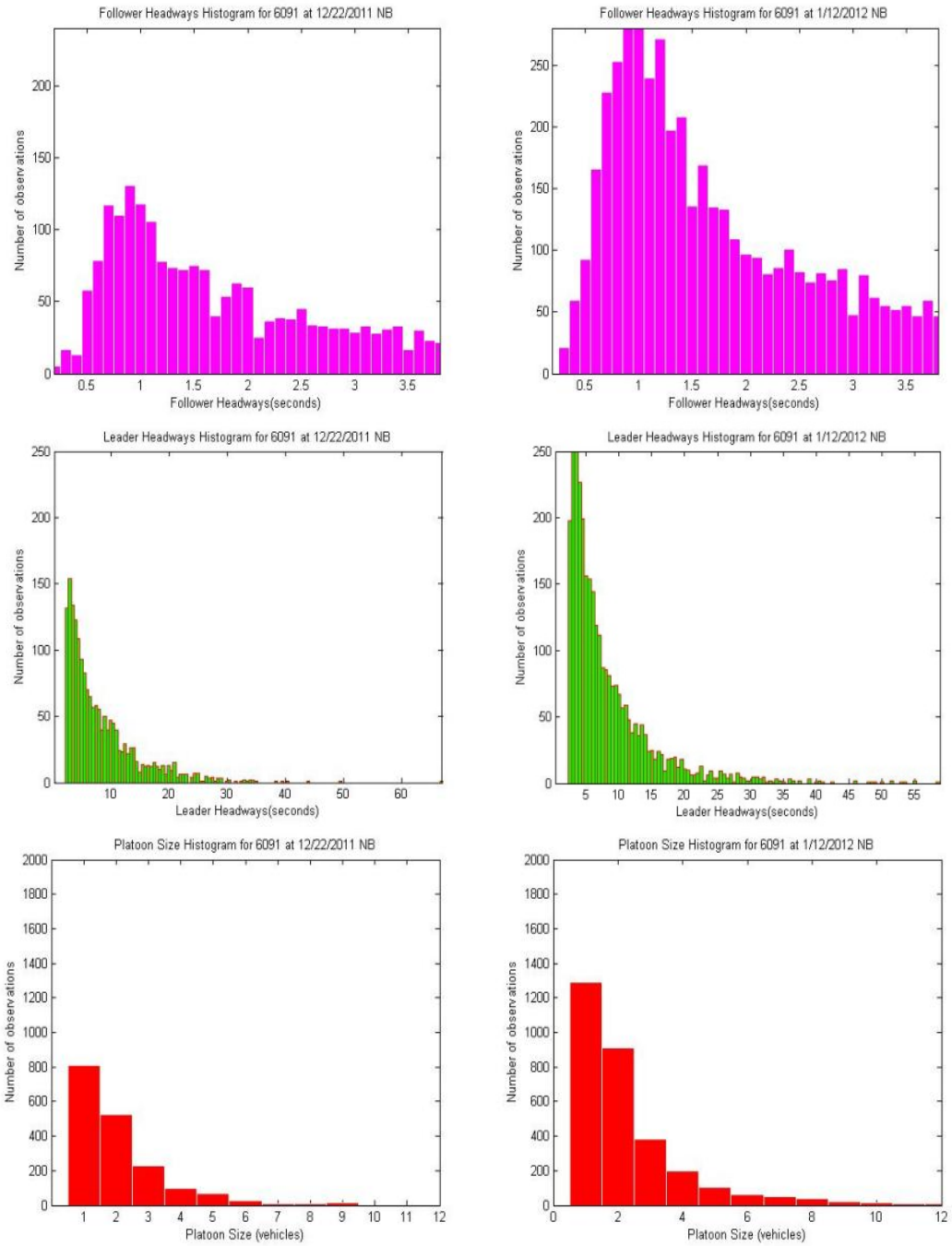

Figure 66. Platoon formation characteristics 1

I-35W SB between 98th St and 106th St.

For the segment between 98th street and 106th street data could only retrieved for December 22nd, 2011 (Figure 67). The percentage of the free flowing vehicles accounted for almost 50 % of the collected observations which again underlines the underutilization of the I-35W HOT lane today. Once again, the shape of the histogram of leader headways is governed by the choice of drivers not to join a platoon and could be described by an exponential distribution. Finally, the peak of the histogram for follower headways is between 0.95 and 1.25 seconds which is slightly higher than for the other two presented cases.

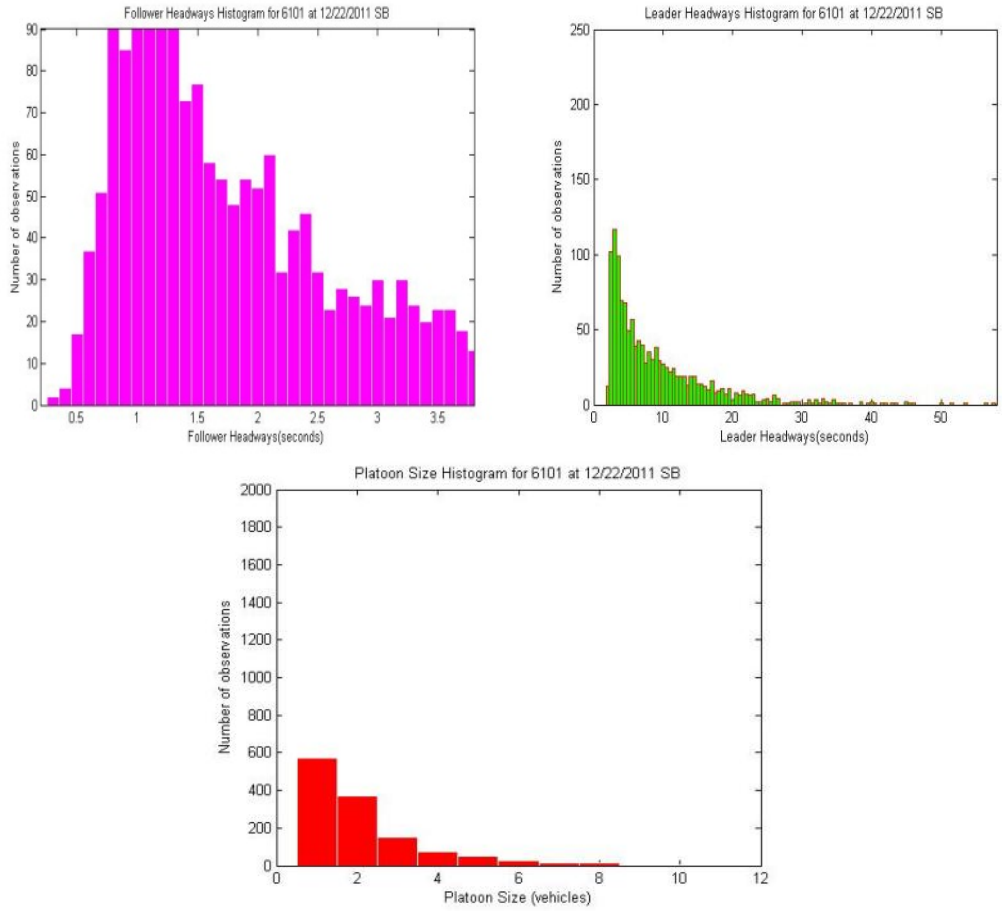

Figure 67. Platoon formation characteristics 2

I-35W NB between 82nd and 86th St and between 86th and 90th St.

The shape of the histogram of leader headways, as in the previous two cases, is governed by the choice of drivers not to join a platoon and could be described by an exponential

distribution. The peak of the histogram for follower headways for both days (Figure 68) was between 0.85 and 1.15 seconds.

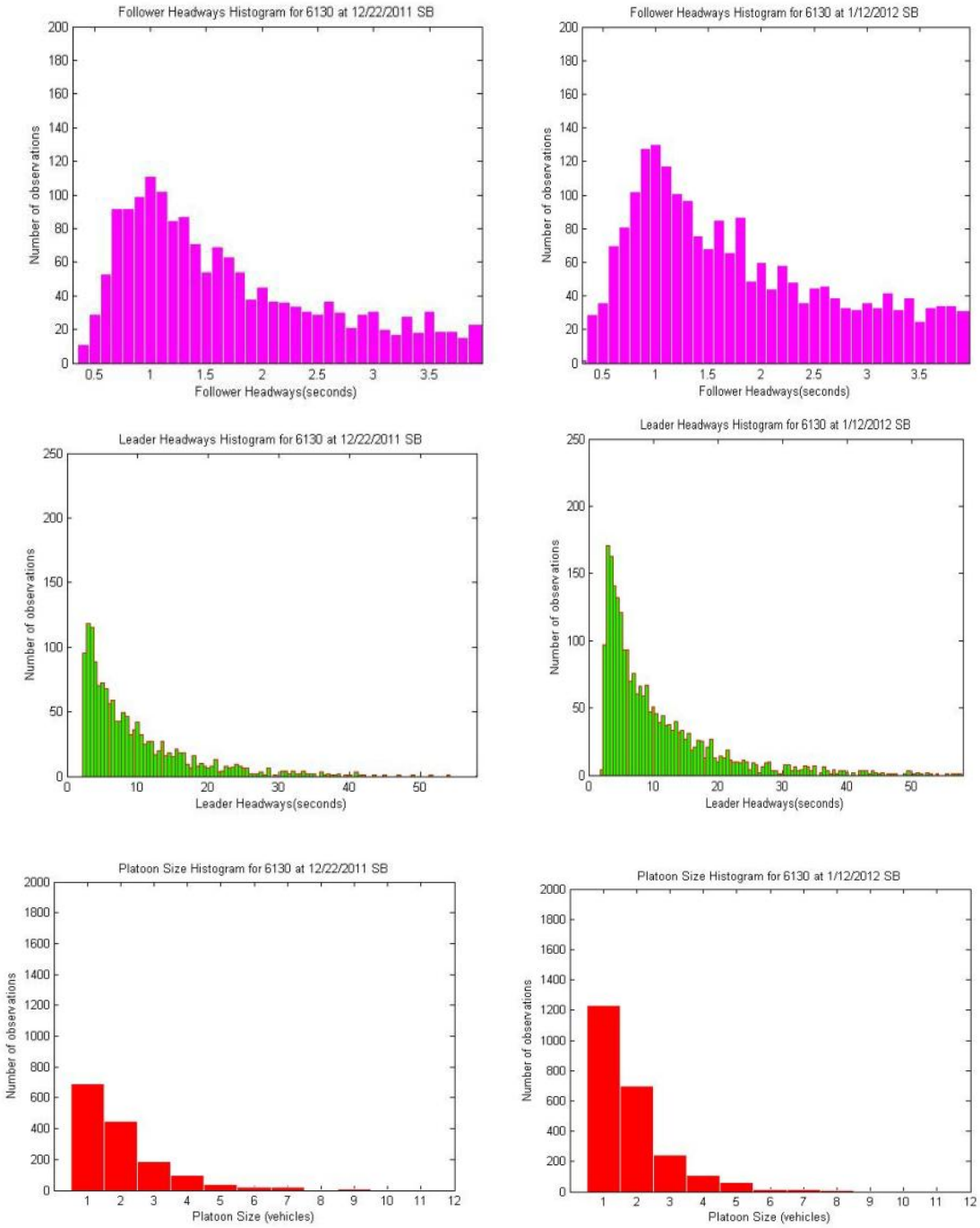

Figure 68. Platoon formation characteristics 3

Lane Change Trajectory Dataset

The lane change trajectory dataset required for the development the OLCR model was build based on measurements and observation from the segment of I-35W northbound between

46th street and 41st street. The location of interest is a 2000 feet freeway segment of I-35W Northbound. The segment of interest contains four general purpose lanes and one HOV/ HOT lane with an entrance ramp located at 46th Street as presented in Figure 69.

This segment of the freeway was identified as one that would be capable of providing a large sample of vehicle high resolution trajectories for drivers merging to the freeway from the entrance ramp of 46th street and moving all the way to the HOT. In that way, all the steps of the lane changing process would be captured so that all the necessary parameters of developing the OLCR model.

Ideally trajectories would have been collected for vehicles merging out of the HOT facility as well and several potential locations were examined for that reason on both I-35W and I-394. In the case of I-35W the great length of the merging areas to the HOT lane made it difficult to identify such a location where a large amount of vehicle trajectories for vehicles merging out of the freeway could be extracted.

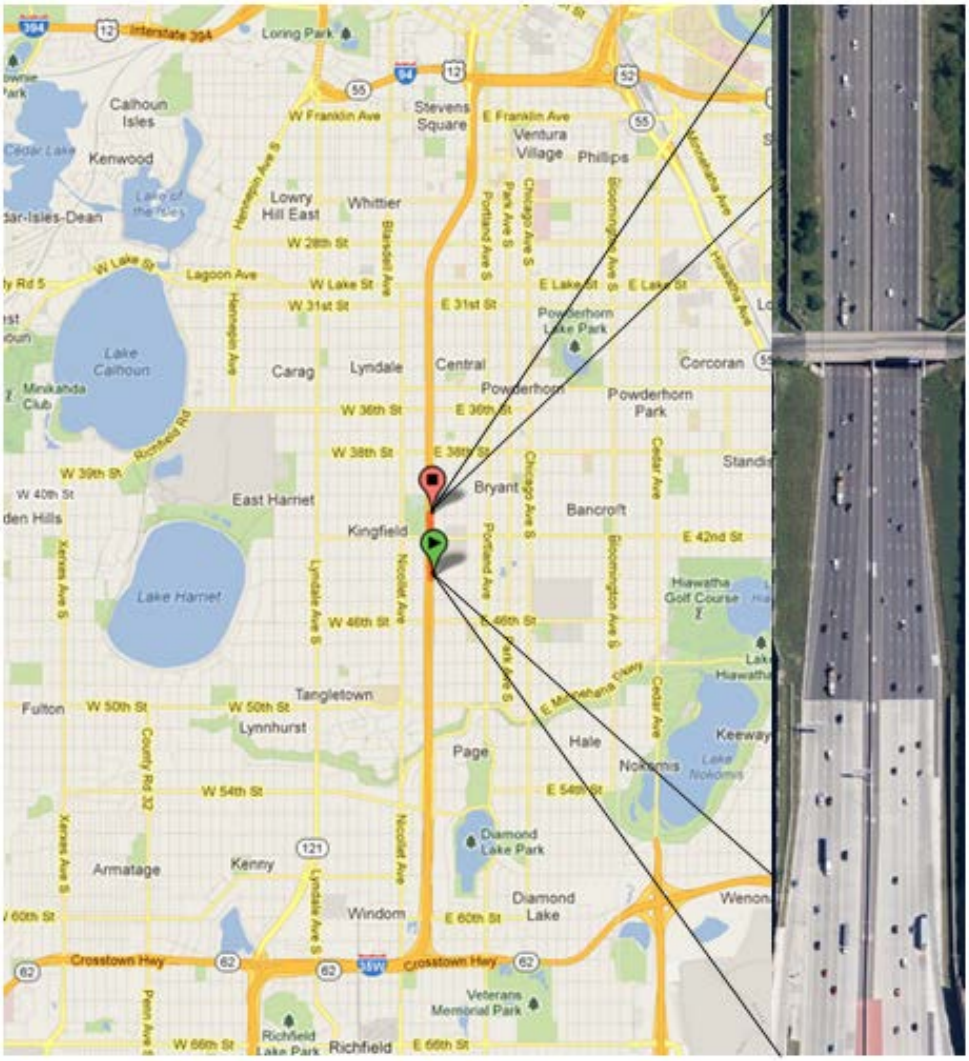

Figure 69. Freeway segment for trajectory extraction

In order to develop the optimal lane changing region tool observations of all the steps of the lane changing process after a vehicle merged in the freeway from the 46th street entrance ramp and all the way to the HOT lane were necessary along with the decisions associated with each step. For the construction of this dataset the analysis of three days' worth of data (October 30th 2012 to November 1st 2012) was sufficient to provide 50 accurate vehicle trajectories. For the three days of interest lane changing activity was investigated for the time period between 08:00 am and 10:00. This decision can be explained by the following considerations:

- For this time period the density fluctuated between congested states and free flow, providing a broad spectrum of density values for each lane.
- Lighting conditions were able to provide a clear view of the highway's lane dividers which was essential for measuring the quantities of interest.

The following measurements for each lane change were captured, along with the time increments that drivers spent on each lane as well as between the lanes:

- The exact location of the merging point to the freeway.
- Gap sizes (accepted and rejected lead and lag gaps) and vehicle lengths.
- Prevailing speed on the target lane and speeds of subject vehicles that desire to change lane.

This process began by developing a script that enables simultaneous viewing of the six different videos recorded from the location of interest as shown in Figure 70.

Figure 70. Trajectory extraction working environment

The first step was to synchronize the cameras so that a subject vehicle could be tracked through the series of cameras. Time stamps for individual cameras were not perfectly synchronized and a calibration step had to take place before extracting measurements. This was done by adjusting the offsets of each camera utilizing a feature of the written script. The optimal configuration was obtained through a trial and error process until the time stamps for all cameras were perfectly synchronized.

To obtain vehicle trajectories, lane changes were identified from the first camera (Camera 1) and then high resolution video data of the subsequent cameras was analyzed for measuring the necessary quantities. Vehicles desiring to merge to the HOT would use their indicator light after merging to the freeway in order to signal their intension to change lanes. Considering the lane dividers length and the spacing between them, traced the position of the subject vehicle while successively changing lanes.

Establishing a zero foot reference point, which is shown by the red line in Figure 71, was essential for recording the distances from the entering point. One example is illustrated in Figure 71 presenting a vehicle merging to the first lane after approximately 132 feet from the predefined position.

Vehicles were classified in two different types in order to establish vehicle lengths. Vehicle lengths were determined to be 17 feet for SUVs, vans or trucks and 14 foot length for cars. These assumptions were made from researching dimensions of different makes and models of vehicles. The accepted gap was derived by adding the lag gap, the lead gap and the vehicle's length.

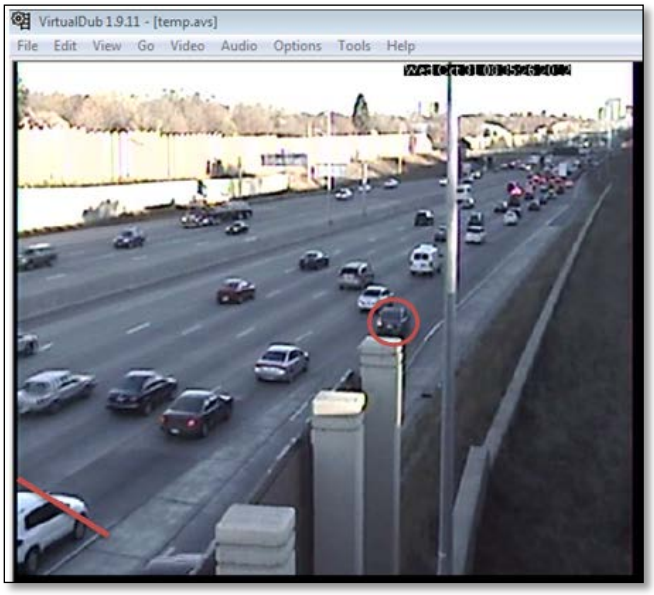

Figure 71. Defining the zero reference point

Figure 72 presents the moment that a subject vehicle is changing lane; the lag and lead gaps were measured at this point. In addition, the number and lengths of rejected gaps had to be measured as well.

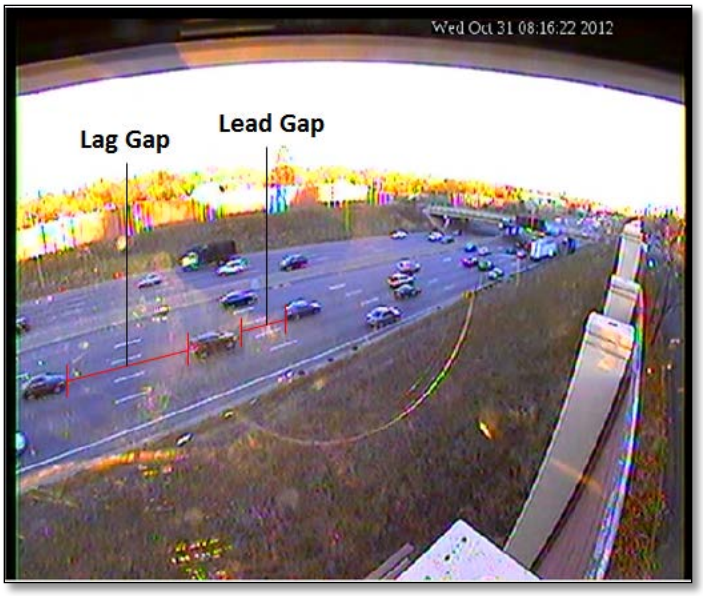

Figure 72. Lead and lag gap

The last piece of information collected was the speeds of vehicles participating in the lane changing process. In order to accomplish this, it was necessary to use a fixed length on the road determined by the lane dividers and spacing between them. A 100 ft. distance was used as the aforementioned fixed length and the amount of frames that it took the subject vehicle to traverse the section was recorded.

One frame in the recorded video corresponds to 1/15th of a second. Given the distance travelled and the travel time, the speed of the subject vehicle was determined. As illustrated in Figure 73, the process of collecting vehicles speeds starts by establishing a clear view of the road so that the front end of the vehicle was aligned with the beginning of the 100 ft. region. After the front end of the vehicle reaches the third white stripe, the travel time is recorded. Figure 73 presents an example of determining a vehicles speed in the second lane; this process is repeated until the subject vehicle reaches the HOT.

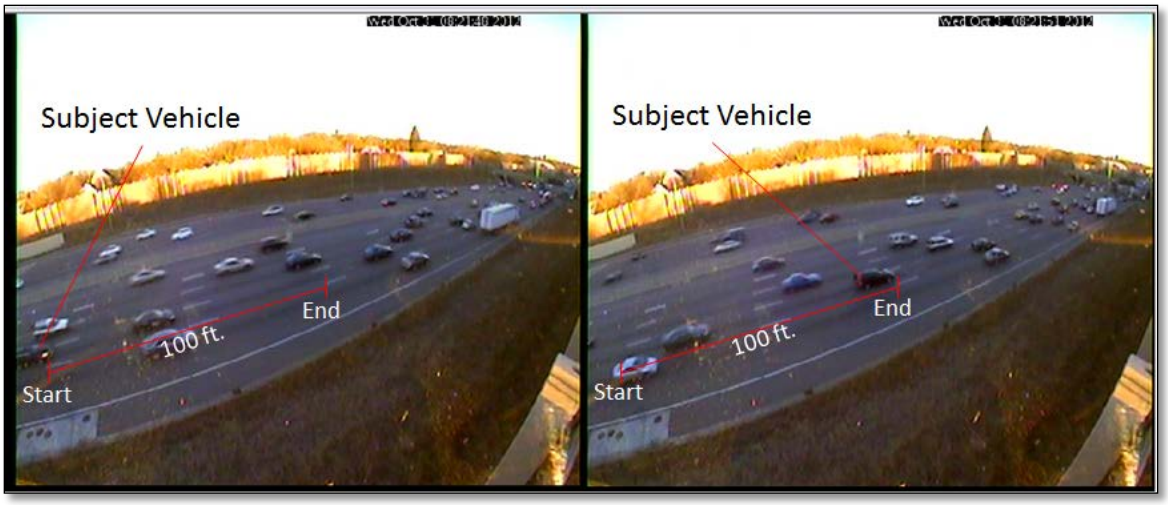

Figure 73. Obtaining speed estimates

Along the analysis process several difficulties were identified and were addressed. Video footage for the time period between 05:00am to 08:00am was discarded due to poor lighting conditions. The highway lane dividers were not clearly visible, thus the footage corresponding to this time span was not analyzed. Secondly, the time interval between 10:00am and 11:00am was also discarded since the HOT was closed to traffic.

In order to be consistent with the modeling efforts of this study it was necessary to identify trajectories of the highest possible quality. Specifically, cases where subject vehicles would experience shockwaves during the course of their trajectory were excluded. The exclusion rule was based on the percent error between observed and calculated distances exceeded 5%.

Observed distances were obtained by using GIS techniques. The exact merging points of each lane change were connected to their corresponding coordinates by utilizing the freeway lane dividers and other reference points of the freeway. Calculated distances were obtained by multiplying the time vehicles spent on each lane with their corresponding speed under the assumption that drivers did not change their speed over the interval of interest. Essentially the amount of error between the two distances is created by the fluctuations in speed of the traced vehicles; fact that does not coincide with this study's modeling efforts.

The task of discarding trajectories was not limited to a percent error, but was also subject to the type of interaction of drivers along the merging process. More specifically, for congested traffic conditions that prevailing speeds are below 10 miles/hour, gaps on the target lane are undersized and thus drivers need to collaborate and create an appropriate gap so that the vehicle can merge. If subject vehicles performed such maneuvers, these cases were not subject to further examination. The reason for rejecting cooperative lane changes lies in the limitation of gap acceptance models to accommodate this phenomenon.

Figure 74 presents the boxplots of the collected time increments that vehicles spend on each lane in their effort to reach the HOT lane. On each box, the central mark is the median, the edges of the box are the 25th and 75th percentiles, the whiskers extend to the most extreme data points not considered outliers, and outliers are plotted individually. It can be seen that as vehicles move to the right the time they spend on each lane is decreasing which can be intuitively explained by the fact that traffic is lighter as vehicles move to the left.

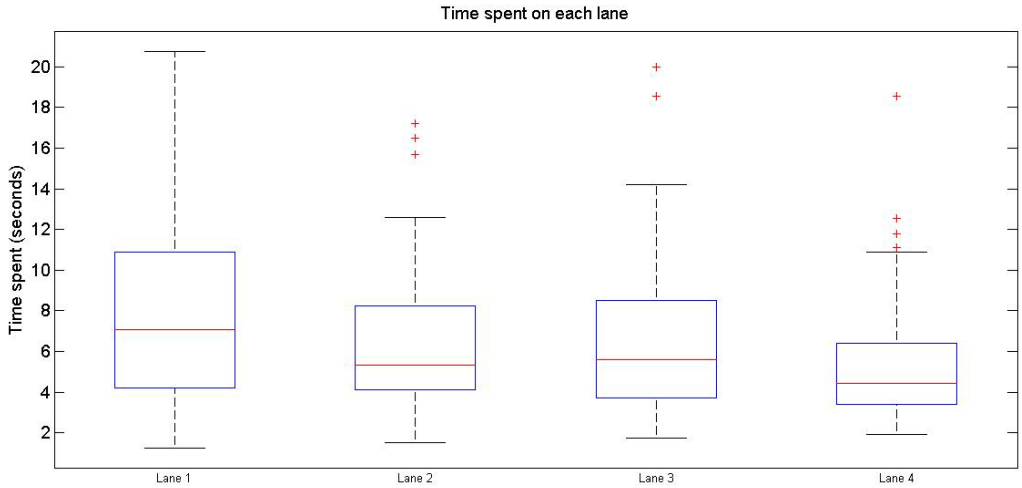

Figure 74. Time increments' box plots

Separating the time vehicles spent on each lane based on a threshold in speed is presented in Figure 75 and Figure 76. It can be seen that the decreasing pattern observed in the aggregated boxplots is eliminated after separating the observations in two groups based on a threshold of 30mph. This reveals the random character of the time increments spent on each lane if speed is controlled.

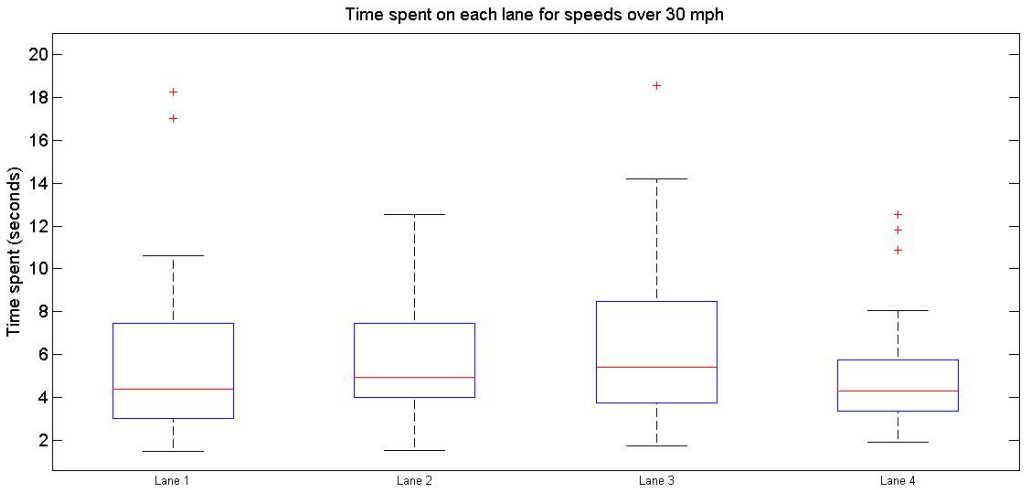

Figure 75. Time increments' box plots for speeds over 30 MPH

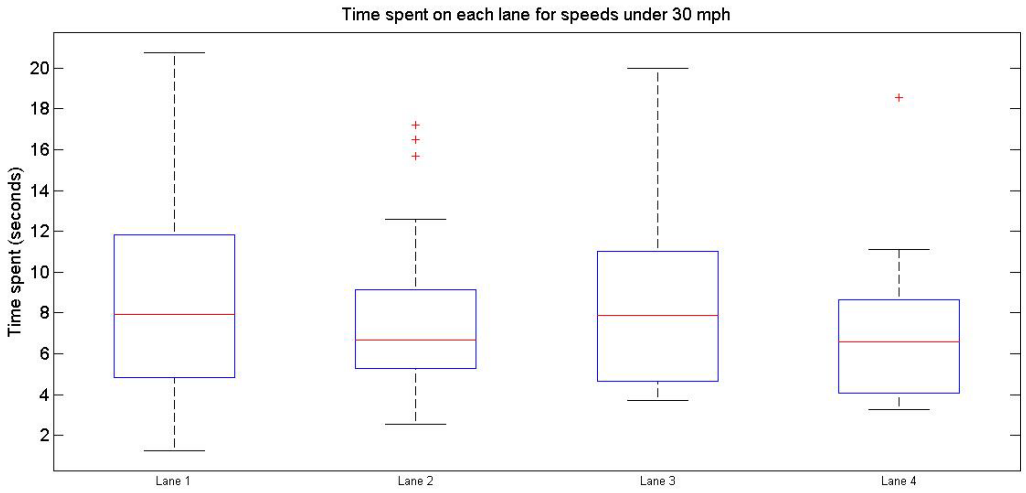

Figure 76. Time increments' box plots for speeds less than 30 MPH

Furthermore, Figure 77 presents the distance that vehicles cover on each lane in their effort to merge to the lane on their left. Figure 77 is derived from Figure 74 by incorporating the obtained speed measurements for the vehicles of interest. The distance that drivers spend on each lane increases as vehicles move from the most left to the right which can be explained by the increase in speed from lane to lane. This increasing trend does not apply to the distance vehicles cover on the 4th lane. The deviation from the general trend is not as conspicuous because of the availability of gaps on the HOT which, despite the higher speeds, results in a smaller distance than drivers cover on the 3rd lane.

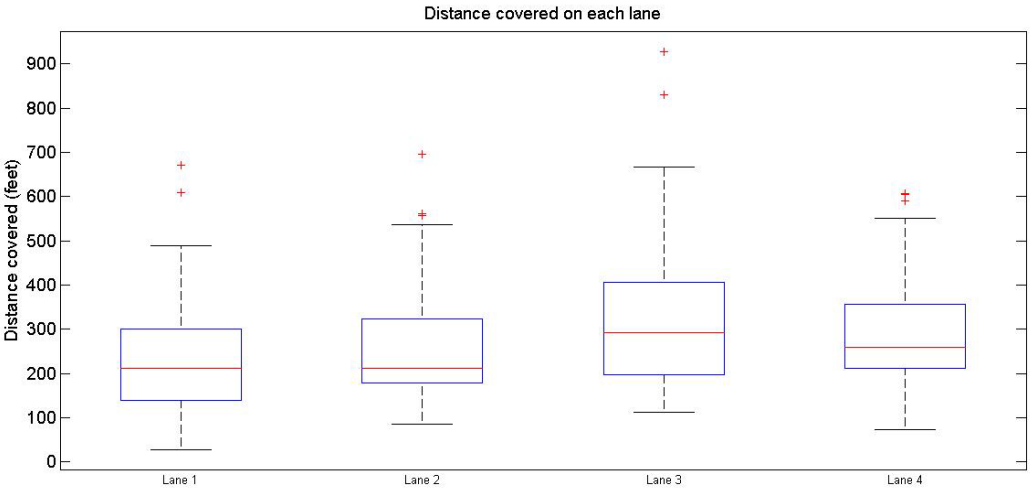

Figure 77. Distance covered on each lane

Separating distance vehicles cover on each lane is based on a threshold in speed of 30 mph and is presented in Figure 78 and Figure 79. It can be seen that the increasing pattern observed in the aggregated boxplots remains for observations captured when the speed conditions are exceeding 30 mph. In the case that speeds are lower than 30mph, the character of the distance vehicles cover on each lane does not follow the aforementioned decreasing pattern and appears to be more random depending on the driver.

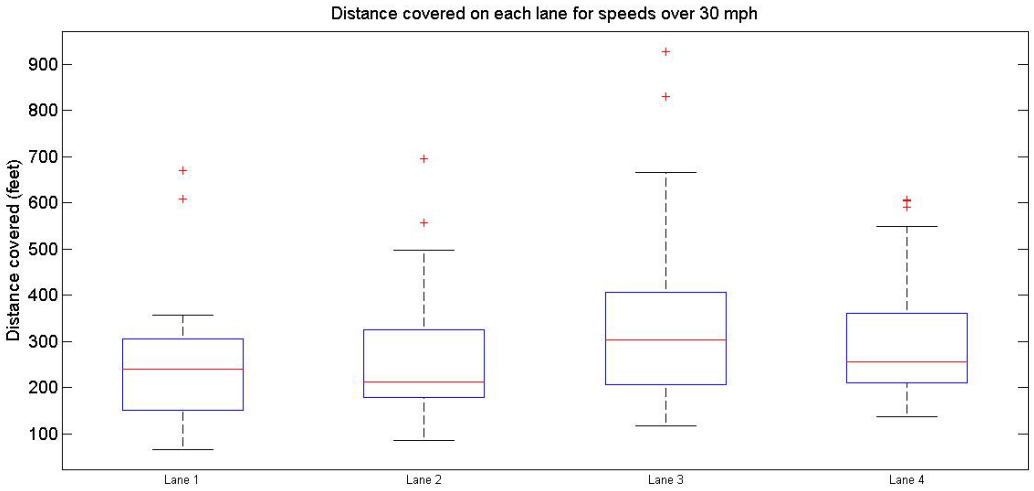

Figure 78. Distance covered on each lane for speeds over 30 MPH

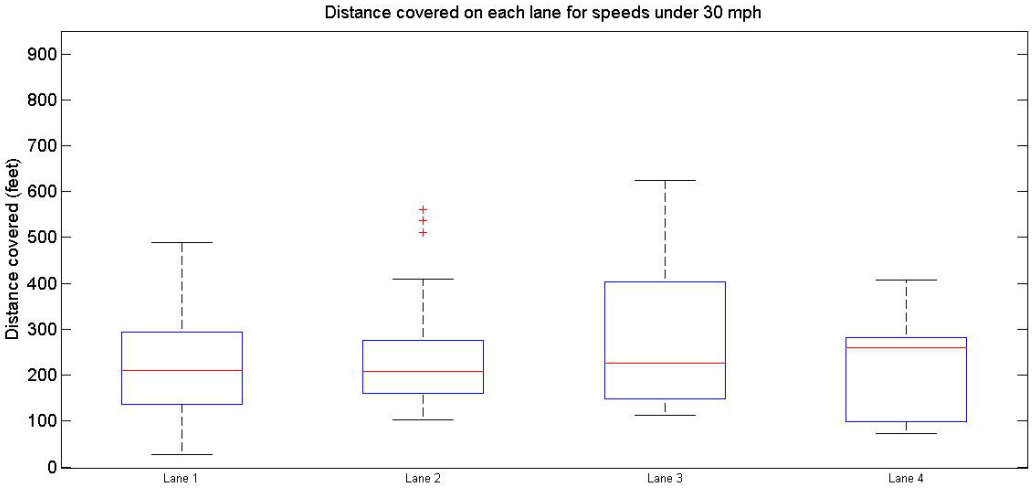

Figure 79. Distance covered on each lane for speeds less than 30 MPH

Finally, Figure 80 presents two boxplots of the gaps that drivers rejected or accepted in their effort to join the HOT lane after merging to the highway from the 46th street entrance ramp. It can be seen that the data point corresponding to the 75th percentile for the rejected gaps does not exceed the 25th percentile of the accepted gaps sketching the boundary between accepted and rejected gaps (approximately 95 feet). Further discussion about the gap acceptance modeling will be presented in the next section.

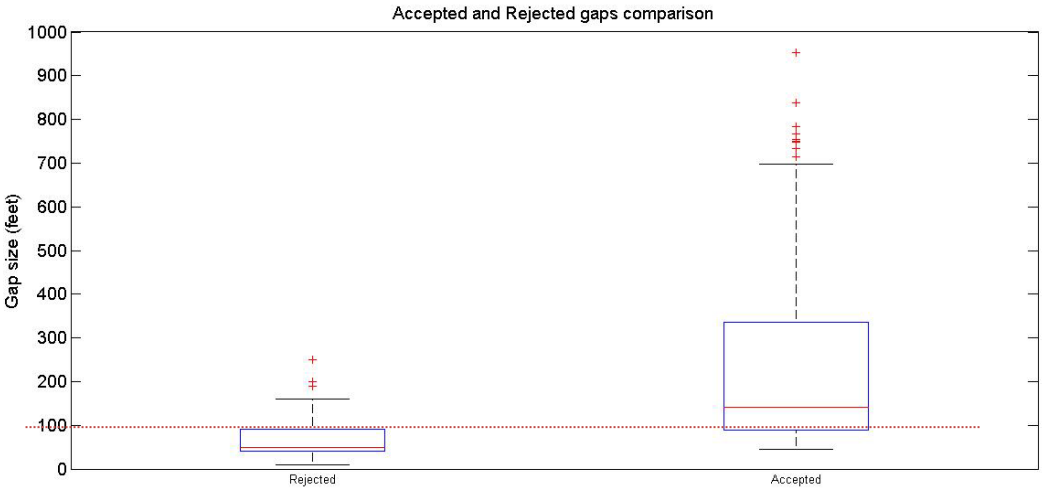

Figure 80. Accepted and rejected gaps

Gap Acceptance Modeling

In this section the development of a gap acceptance model used in both tools is presented. In the shockwave propagation model disturbances are introduced to positions of the simulated vehicle sequences using the results of the developed Gap Acceptance model. In that way, the decision process is emulated in the same fashion that occurs in reality; gaps are evaluated and are either rejected or accepted, with the first accepted gap initiating the lane change. For the OLCR model gap acceptance is once again crucial and used to shape the time increments that drivers spent on each lane along their subsequent decisions. Conceptually the process of Gap Acceptance is one that involves several gaps of interest. From these set of gaps the driver rejected all but the one that was finally accepted.

A study that draws many parallels with the proposed model was developed by Kita (1993). Kita used a logit model to describe driver's willingness to either accept or reject a gap at merging areas between freeways and on-ramps.

Model selection

The developed Gap Acceptance model is a logit model that derives the probability of accepting a gap based on a set of measurements. For each lane change quantities of interest for describing the Gap Acceptance were harvested. More specifically the measurements that were used to describe the decision were the speed of the subject vehicle, the prevailing speed on the target lane and the sizes of the lead accepted gap, the lag accepted gap and the rejected gaps.

Since the collected data were connected with a binary response variable, a Generalized Linear Model (GLM) was used. GLMs are extensively used, after they were introduced by Nelder and Wedderburn (1972) in an effort to extend ordinary linear regression so that response variables can be described by a distribution other than the normal. The distribution describing the response variable for this modeling effort is binomial (Bernoulli

since the gaps are either accepted or rejected). The following equation describes the probability of accepting a gap given a set of explanatory variables X and their corresponding fitted parameters β in logistic regression.

$$\Pr(acceptance|\mathbf{X}) = \frac{e^{(\boldsymbol{\beta}\mathbf{X})}}{1 + e^{(\boldsymbol{\beta}\mathbf{X})}} \quad \text{(Eq. 5)}$$

The first step was to decide about the parameters that have a significant effect on the shape of the response variable and then evaluate several proper link functions to describe the data before concluding that the logit function derives the best fit. Using R software, a first attempt to describe the collected binary decisions using all the collected explanatory variables was conducted. Table 8 presents the fitting results for this first approach taking account of all the collected explanatory variables. It can be concluded based on the obtained p-values that three parameters have a statistically significant effect on describing the binary dataset; the speed of the subject vehicle, the prevailing speed on the target lane and the size of the lag gap.

Table 8. Fitting results for all the available parameters

Parameter	Value	Standard Error	z value	Pr(>|z|)
β0 (Intercept)	-1.391	2.272	-0.612	0.540
β1 (Lag Gap)	0.054	0.012	4.494	0.000
β2 (Lead Gap)	0.002	0.007	0.257	0.798
β3 (Target Lane Speed)	-0.088	0.042	-2.098	0.036
β4 (Subject Speed)	0.120	0.044	2.722	0.007
β5 (Vehicle Length)	-0.014	0.125	-0.108	0.914
AIC	172.61			

The size of the leading gap was proven to be statistically insignificant and this can also be explained intuitively. When a driver evaluates gaps in order to join the target lane, the leading gap is less important than the lag gap because the vehicles speed can be adjusted to match the leaders speed while evaluating constantly its reactions (acceleration, deceleration). In the case of the lag gap estimating the following vehicle's reactions and speed is more challenging and more difficult to adjust the subject vehicle's speed so that a "safe" transition to the target lane can be achieved. Thus the lag gap has a greater effect on the shape of the decision. It can also be shown from the sign of the corresponding parameter that the greater the length of the lag gap, the higher is the probability of being accepted.

It can also be seen that the length of the vehicle does not have a significant effect either. This can be attributed to the fact that the plethora of the harvested observations corresponded to vehicles that their length were either 14 feet (car) or 17 feet (SUV) and very few observations corresponded to buses. In that way most of small difference in vehicle's length (3 feet) was not reflected in the value that the predicted response obtained.

Furthermore, the sign of the parameter corresponding to the target lane was negative. As such, the faster the target lane moves the lower the probability of accepting a gap. In most cases the speed of the target lane was higher than of the speed of the subject vehicle and thus the observed speed difference makes a gap on the target lane less attractive for a driver. Finally the sign of the parameter for the subject vehicle's speed is positive and opposite from the one of the target lane's parameter. The two observations combined reveal the aforementioned effect of the speed difference in the probability of accepting a gap.

The logit model that was selected presents the probability of accepting a gap given the subject vehicle's speed, the target lane's speed and the size of the leading gap. The fitting details are presented in Table 9.

$$\Pr(acceptance|\, Gap_{lag}, V_{target}, V_{subject}) = \frac{e^{(-1.49 + 0.05*Gap_{lag} - 0.09*V_{target} + 0.12*V_{subject})}}{1 + e^{(-1.49 + 0.05*Gap_{lag} - 0.09*V_{target} + 0.12*V_{subject})}} \quad \text{(Eq. 6)}$$

where Gaplag is the size of the lag gap in feet,

Vtarget is the speed of the target lane in miles/hour and

Vsubject is the speed of the subject vehicle in miles/hour.

Table 9. Fitting results using a Logit link function

Parameter	Value	Standard Error	z value	Pr(>|z|)
β0 (Intercept)	-1.493	0.736	-2.027	0.043
β1 (Lag Gap)	0.054	0.011	4.676	0.000
β3 (Subject Speed)	0.119	0.043	2.748	0.006
β4 (Target Lane Speed)	-0.088	0.041	-2.163	0.031
AIC	166.71			

7. Optimal Lane Changing Region Design Tool

In this chapter the developed methodology for computing the optimal location and length of merging areas is presented. This methodology was constructed to support engineers' decisions on defining the Optimal Lane Changing Regions (OLCRs) on forthcoming HOT lane facilities that adopt a Closed Access philosophy. For most of their length, facilities following that design philosophy, restrict the interaction between vehicles on the HOT lane and its adjacent GPL and allow access only at selected areas usually between important exit and entrance ramps (e.g. I-394 Minneapolis, MN).

Utilizing the harvested trajectory data, as presented in the previous chapter, a methodology emulating the process drivers follow to traverse between the GPLs to join the HOT lane was developed. The goal of this methodology was to reproduce the observed travel distances that drivers covered during their movement between the entrance ramp and the HOT lane.

After the proposed model's ability to emulate the desire lane changing activity was validated, an implementation strategy was developed so that engineers in the future can identify the OLCRs by evaluating the model's output at various demand levels. Demand for all lanes is considered to be equivalent to traffic density. In addition, under the assumption that lane changing is the same between cases that drivers move to their left and to their right the process was also able to account for vehicles desiring to merge out of the HOT lane so that they can exit the freeway at the following exit ramp.

First, traffic flow was reconstructed for all the general purpose lanes; headways were sampled using the findings of a Fundamental Diagram investigation for each lane. In this process the Gap Acceptance model presented earlier was used to shape the time increments that vehicles spent on each lane. In addition, the time drivers spent between lanes after accepting a gap was replicated by drawing random numbers from a Log-normal distribution fitted to the corresponding measurements. Finally, an additional behavioral parameter describing the time that drivers spend before looking for an appropriate gap was also taken into account. The final outcomes of this methodology are advisory positions and lengths for merging areas on HOT facilities.

Ahmed, et al. (1996) developed a lane changing model that shares commonalities with the proposed methodology. In the proposed methodology in order to define the OLCR, drivers do not need to select a lane of their choice as in the model proposed by Ahmed et al. (1996); the examined drivers' sample solely includes drivers that intend to use the HOT lane and will always move to the lane on their left.

Traffic Flow reconstruction

Reconstructing traffic flow on the GPLs was based on the findings of a Fundamental Diagram investigation, under the validated assumption that headways are following the Lognormal distribution for densities below capacity. This effort mainly considers density levels below the critical density for the sake of simplicity. Results will also be presented though for density levels exceeding the critical density of the facility by relaxing the condition of independent selection of headways as will be demonstrated in a later section.

Based on the harvested trajectory measurements, it was shown that working with densities below the critical density does not affect the value of the results significantly. Figure 81 presents two boxplots, one for observed trajectory lengths for traffic conditions below capacity and another for traffic conditions exceeding capacity. As observed, the ranges of the two sub-datasets as well as the 75th percentiles are equal while the 25th percentile for the distances harvested for prevailing conditions above the critical density is significantly lower than for the cases corresponding to traffic conditions below the critical density.

Therefore, the difference between the two conditions can be overseen since this discrepancy will result in vehicles merging before the proposed position of the gate for traffic conditions above the critical density. Thus, drivers will reach the adjacent lane to the HOT before the proposed gate and they will be able to merge as soon as an opening becomes available. Figure 82 presents the Cumulative Distribution Function of the constructed dataset and will be later used to evaluate the output of the OLCR model.

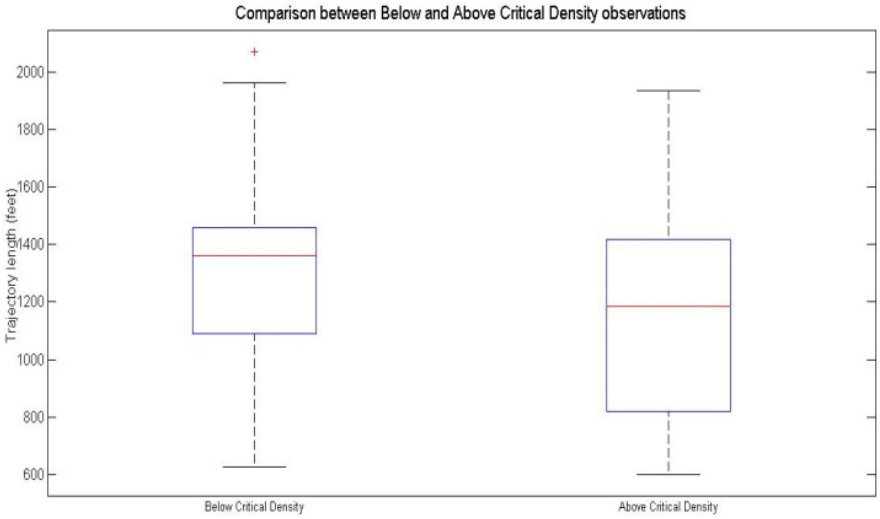

Figure 81. Comparison between trajectory lengths for cases above and below capacity

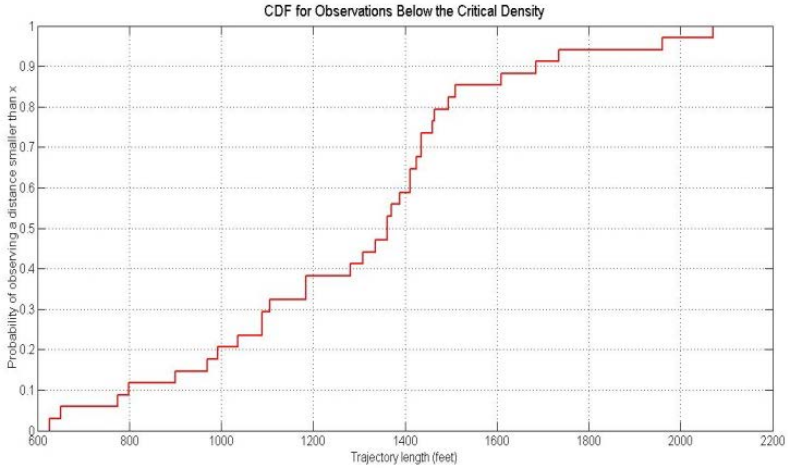

Figure 82. Cumulative distribution function for of the harvested trajectory lengths

Fundamental Diagram investigation

As mentioned above, a fundamental diagram investigation first took place in order to define quantities such as free flow speed and jam density for each lane. The bell-shaped FD proposed by Greenshields, et al. (1935) was fitted to data extracted for each lane of the examined freeway segment. The decision for using Greenshield's model instead of another FD, such as the Triangular shaped FD (Newell, 2002), was motivated by the fact that a mild speed differential was desired between the general purpose lanes. Using the triangular shaped FD would assign only the free flow speed to the simulated streams and thus a miniscule speed differential would be achieved between the GPLs; the modeling efforts of this study are mainly bounded by the capacity of each lane. Figure 83 demonstrates the aforementioned speed-density, flow-density and speed flow relationships for the FD proposed by Greenshield's.

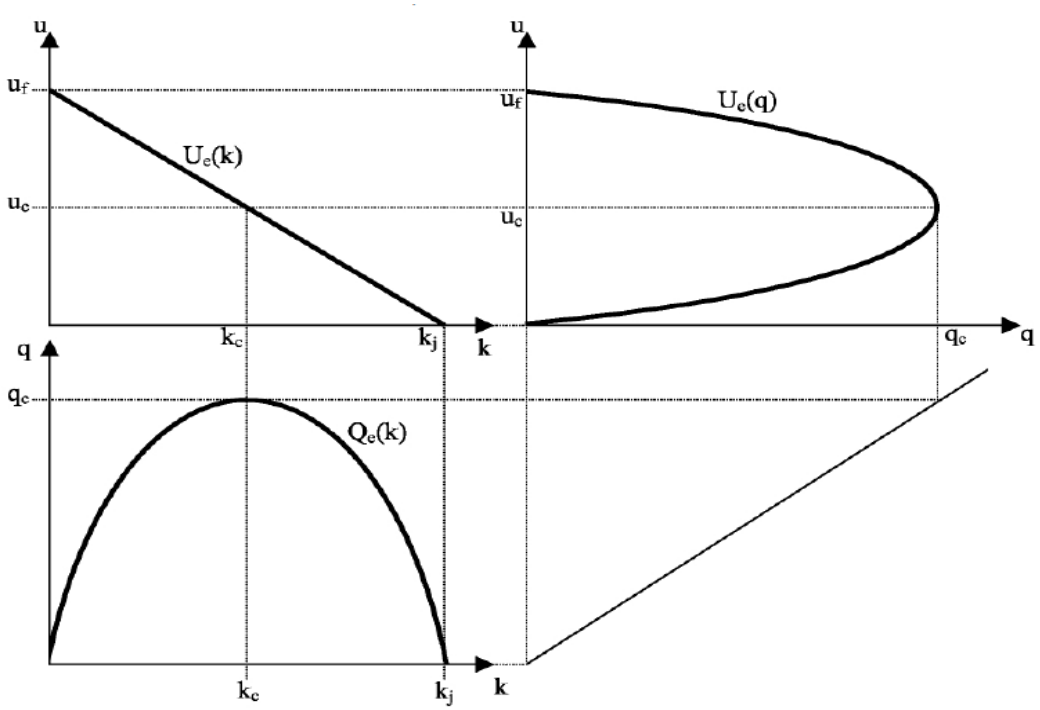

Figure 83. Fundamental relationships (Immers and Logghe 2002)

For Greenshield's model the speed – density relationship is described by Equation 7, while the flow – density and flow-speed relationships are presented in Equations 8 and 9.

$$u = U_e(k) = \frac{u_f}{k_j}(k_j - k) \qquad \text{(Eq. 7)}$$

$$q = Q_e(k) = \frac{u_f}{k_j}k(k_j - k) \qquad \text{(Eq. 8)}$$

$$q = U_e(q)^{-1} = k_j u\left(1 - \frac{u}{u_f}\right) \qquad \text{(Eq. 9)}$$

The fitted parameters for the FD of each lane are presented in Table 10 while Figure 84 to Figure 87 present the fitted curves with the harvested data being superimposed. As shown a very high R Squared value was achieved in all cases with the lowest being close to 86 %. The lowest value was achieved for the most right lane and stems from the larger amount of congestion that this lane experienced compared to the rest four lanes. This lead to a more disperse scatter in the right side of the parabola. For the rest of the lanes the R2 value obtained was over 90 % capturing the collected data with high accuracy. The fitted curves were used instead of raw data to derive the corresponding speed and flow given the desired value of density.

Table 10. Fundamental diagram fitted parameters

Lane	$u_f\ (miles/hour)$	$k_j\ (vehiles/\ mile)$	R2 (%)
1	70.6	102.7	86.4
2	69.2	112.1	99.5
3	72.3	99.4	90.3
4	77	101.2	99.6

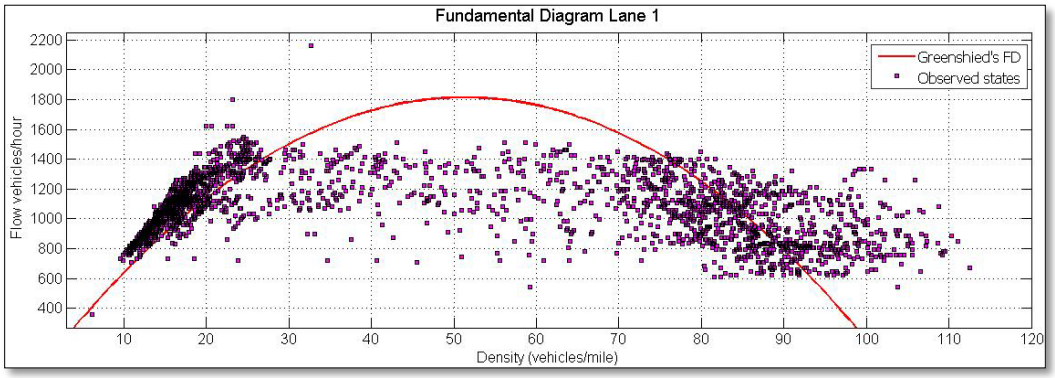

Figure 84. Fitted fundamental diagram lane 1

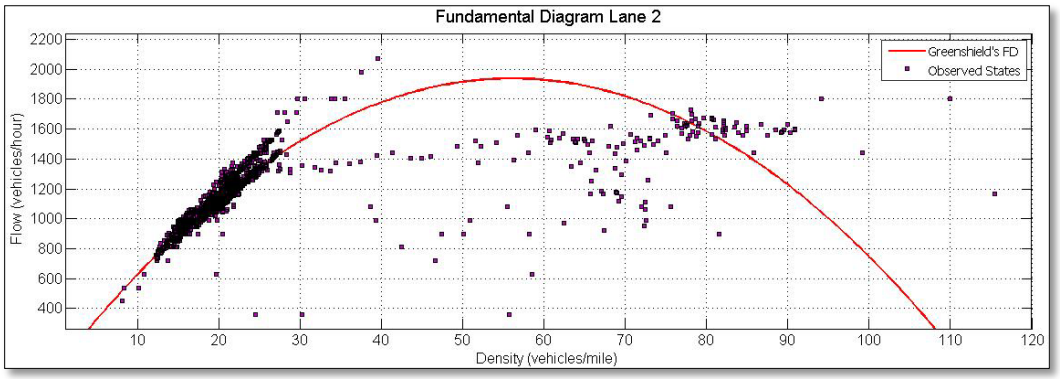

Figure 85. Fitted fundamental diagram lane 2

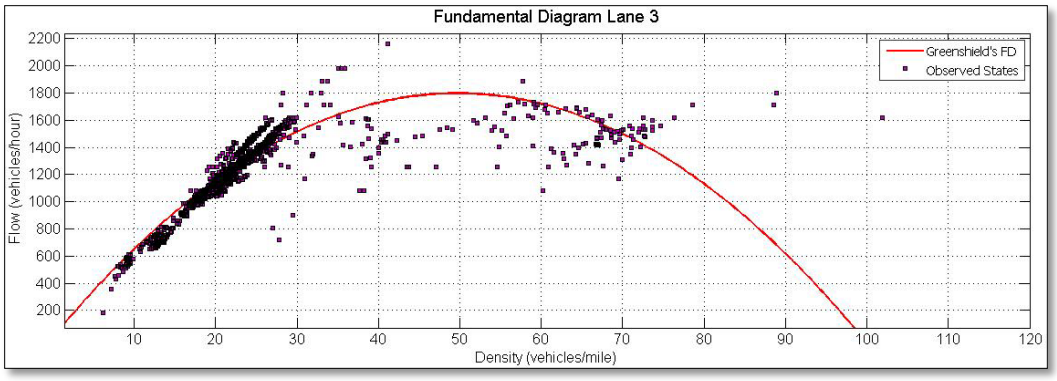

Figure 86. Fitted fundamental diagram lane 3

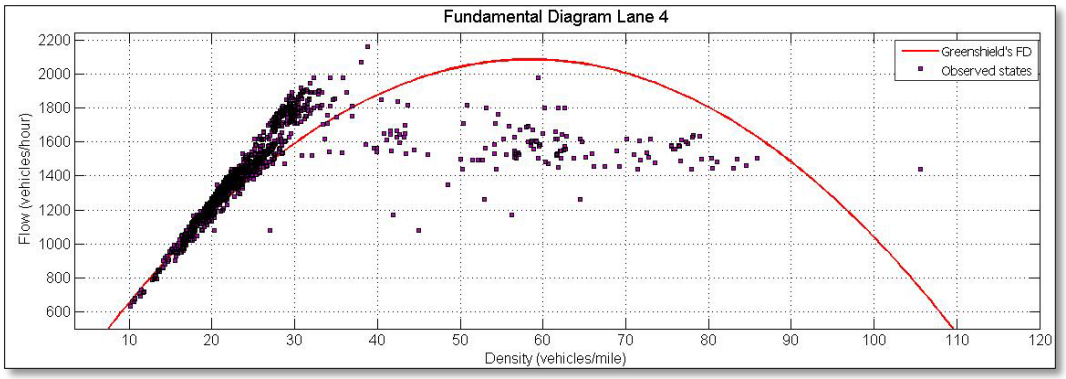

Figure 87. Fitted fundamental diagram lane 4

To address what is the most appropriate distribution for describing the collected headway measurements, several distributions were tested including the Exponential, the Normal the Weibull and the Lognormal. Headway measurements were first connected to their corresponding density measurements. For this step only headways corresponding to traffic conditions below capacity were considered. The Lognormal distribution provided the best fit based on the Maximum Likelihood value among the tested distributions (Exponential, Normal and Weibull).

A mixed programming formulation was constructed to partition headways based on their corresponding density so that a more accurate fit could be achieved using more than one set of parameters of the Lognormal distribution. The reason for developing such a methodology was that the most accurate Coefficient of Variation for the fitted Lognormal distribution could be computed.

This formulation aimed in minimizing the infinity norm between the empirical distribution of the observed data and the fitted distribution using a set of Lognormal distributions. The infinity norm is the maximum difference between the two distributions as described in Equation 10. Ideally, if the norm converges to zero then the two distributions are the same as proved by the Glivenko-Cantelli Theorem (Wellner, 1977). Figure 88 illustrates an example of the aforementioned sup-norm.

$$\|F_n - F\|_\infty = \sup_{x \in \mathbb{R}^+} |F_n(x) - F(x)| \qquad \text{(Eq. 10)}$$

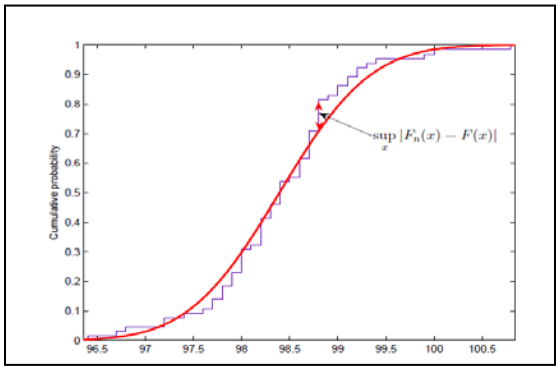

Figure 88. Sup-Norm

In the following formulation the boundaries between subsequent partitions are denoted by u_i, the number of partitions is denoted by N with Nmax being the maximum number of partitions examined. Dmax is the density at capacity and K is the value that the sup-norm obtains. The obtained value of the sup-norm is proportional to the length of the density region the problem becomes:

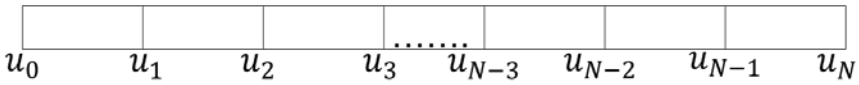

$$minimize \sum_{i=0}^{N} (u_i - u_{i-1}) * K_i \text{ , } \textbf{subject to}$$

$$N \leq N_{max}$$

$$u_0 \leq u_1 \leq \cdots \leq u_N$$

$$u_i \in [0 \ , \ D_{\max}]$$

$$where\ K_i = f(u_i, u_{i-1})$$

Computing the sup-norm between the two distributions was performed using a Monte Carlo framework. The initial conditions were values for $u_1 \ldots u_N$. For those conditions the Lognormal distribution was fitted to the headway subset for each region and based on the estimated parameters a large sample was generated. Subsequently, the sup-norm between the empirical distribution of measured headways and the fitted distribution was computed. The constructed formulation utilizes the Optimization Toolbox in Matlab and aims in shifting the boundaries between the density regions in order to minimize the difference between the two distributions.

Deciding about the optimal number of partitions was conducted by interpreting the output of the algorithm. Specifically, after optimal values for the boundaries of each number of partitions were obtained, a weighted sum of the sup-norms for the different subsets of each partition was computed. The partition with the minimum value for the sup-norm was the solution to the problem. Despite the simple formulation and the limitations of the optimization toolbox a decrease in the sup-norm was observed and finally the optimal partitioning was concluded to correspond to two regions with a breakpoint in the density domain at 29.6 vehicles/mile. The corresponding value for the sup-norm was 2.1 % (Table 11). The largest number of partitions tested was 5 due to high computational effort that was required. Figure 89 presents the comparison between the estimated and the empirical cumulative distribution function for the two selected regions with a very accurate fit being achieved.

Table 11. Optimal Sup-Norm values for various partitions

Number of Partitions	Sup-norm (percentage)
1	3
2	2.1
3	3.4
4	3.3
5	3.8

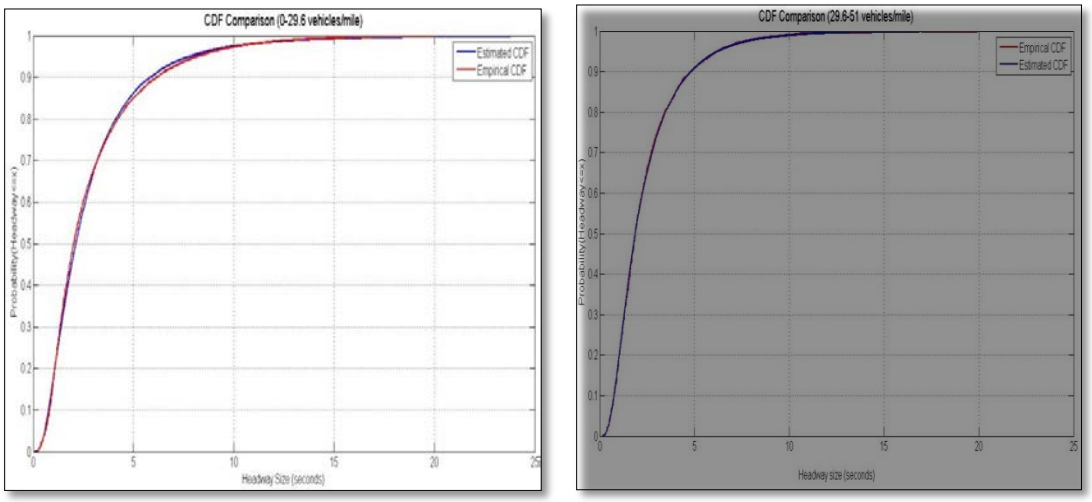

Figure 89. Comparison for optimal partitioning between estimated and observed CDFs

Under the assumption that headways are independent and identically distributed, a random number generator following a lognormal surface of distributions was responsible for reconstructing the desired headway sequences. The mean value of the generated headway sample had to vary, reflecting the fluctuations in density. Given the Fundamental relationship between flow and density as derived from Greenshield's FD the mean value for the headway sample is presented in Equation 11 as the inverse of flow:

$$\bar{h} = \left(u_f * k * \left(1 - \frac{k}{k_j} \right) \right)^{-1} \quad \text{(Eq. 11)}$$

The second parameter that had to be computed was the standard deviation of the simulated sample; this step utilized the findings of the partitioning problem. The Coefficient of Variation (CV) for each region was computed in an effort to connect the mean of the distribution with its variance based on the collected data. Equation 12 presents the estimator that derives the CV based on the standard deviation of the two samples (Koopmans, et al. 1964).

$$\widehat{C_{vln}} = \sqrt{e^{s_{ln}^2} - 1} \quad \text{(Eq. 12)}$$

where S_{ln} is the sample standard deviation of the data after a natural log transformation.

For the density region between 0 and 29.6 vehicles the samples estimated CV was 0.98 and for the region between 29.6 vehicles/mile and 51 vehicles/mile (critical density) was equal to 0.82. The CV used for computing the standard deviation of the sample was decided to be equal to the average of the two computed values (0.88). Equation 13 gives the standard deviation for a selected mean value given the CV.

$$\widehat{stdev} = \bar{h} * \widehat{C_{vln}} \quad \text{(Eq. 13)}$$

Thus, for the given mean and the estimated standard deviation, the parameters for the Lognormal distribution were computed by Equations 14 and 15.

$$mu = \ln\left(\frac{\bar{h}}{\sqrt{\widehat{stdev} + \bar{h}^2}} \right) \quad \text{(Eq. 14)}$$

$$sigma = \sqrt{\ln\left(\frac{\widehat{stdev}}{\bar{h}^2 + 1} \right)} \quad \text{(Eq. 15)}$$

Figure 90 presents the surface of probability density functions for the range of the examined traffic conditions based on the results of this investigation. The presented surface covers the whole spectrum of density that this step covers ranging between 5 vehicles/mile and 51 vehicles/mile. It can be seen that as density values increase, the mode of the distribution is shifting to the right delivering larger headway values. This is intuitively explained by considering that vehicles follow their leaders in shorter distances as density increases.

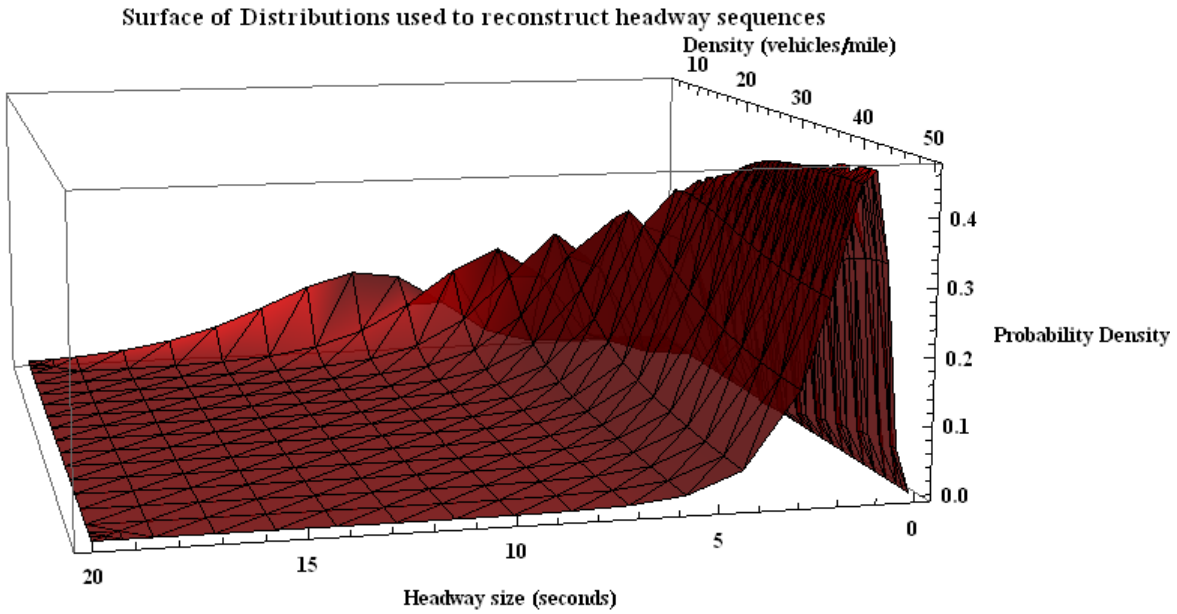

Figure 90. Surface of lognormal distributions for headway sequence reconstruction

The assumption of independence was tested empirically using Autocorrelation functions (Box, et al. 2011) for a number of different sequences of observed headways. One example is presented in Figure 91 for a time series of headways covering densities between 20 and 25 vehicles/mile; it can be seen that the autocorrelation function exceeds the computed 95 % confidence intervals only for two lags supporting the lack of dependence between successive headway selections. Those two values do not have a particular meaning in affecting decisions between drivers since a driver that is 15 positions upstream in the sequence (observed lag) cannot be affected by a vehicle that is 15 positions ahead of it. The assumption of independence was not supported for headway sequences exceeding the critical density. Simulation results will be presented for both conditions below the critical density as well as conditions that exceed the critical density.

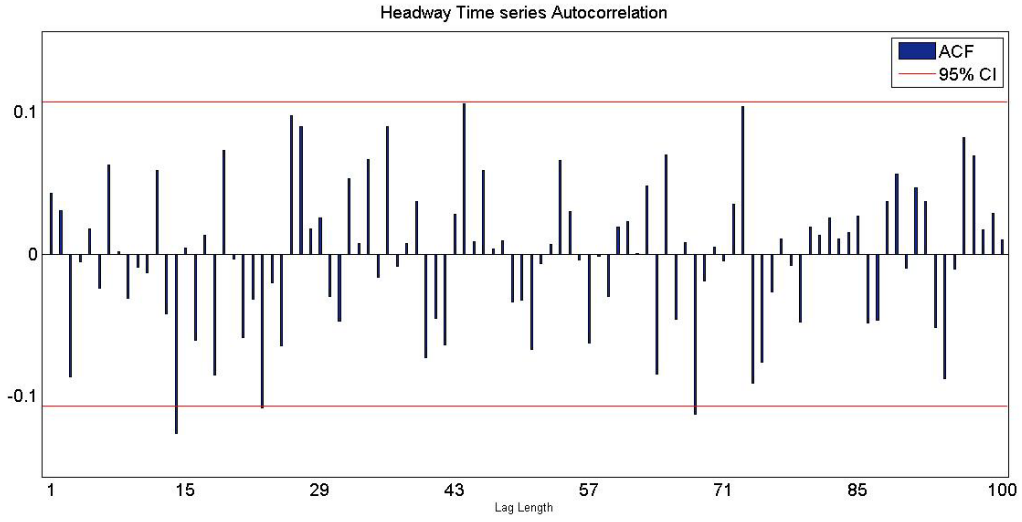

Figure 91. Autocorrelation function for headway time series with 95% confidence intervals

Car following

After the mechanism responsible for reconstructing headway sequences was described, a fairly simple, rule based, car-following mechanism was developed so that trajectories can be generated. More specifically, vehicles moving faster than their leader would match their leaders' speed if a headway threshold was violated.

Quantifying the aforementioned headway threshold was conducted by separating vehicles in platoon followers and platoon leaders based on either a space threshold of 280 feet or a time threshold of 3.1 seconds. Previous studies have used the same manner of distinguishing vehicles in the two aforementioned groups by either a space threshold of 250 feet or a time threshold of 4.0 seconds (Benekohal, et al. 2004). In the present study, the two separation parameters were tuned in order to separate headways. Figure 92 presents the resulting histograms of headways corresponding to platoon follower and platoon leaders while Figure 93 presents a boxplot in an effort to present the characteristics of the follower headways sample.

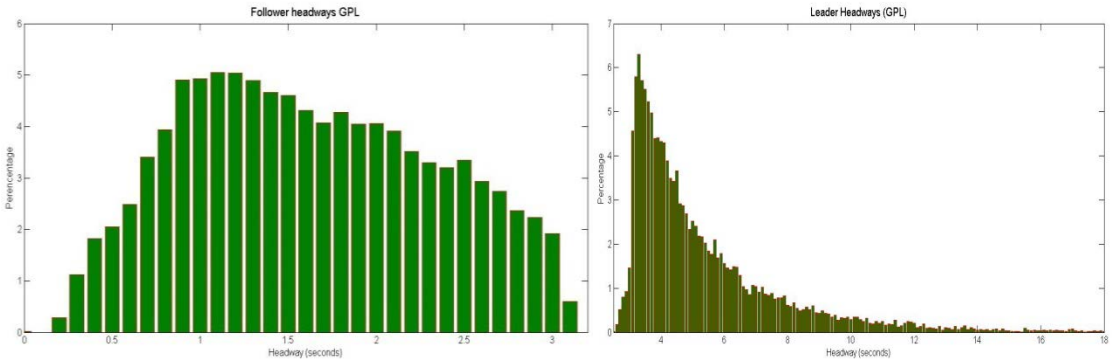

Figure 92. Follower and leader headway histograms

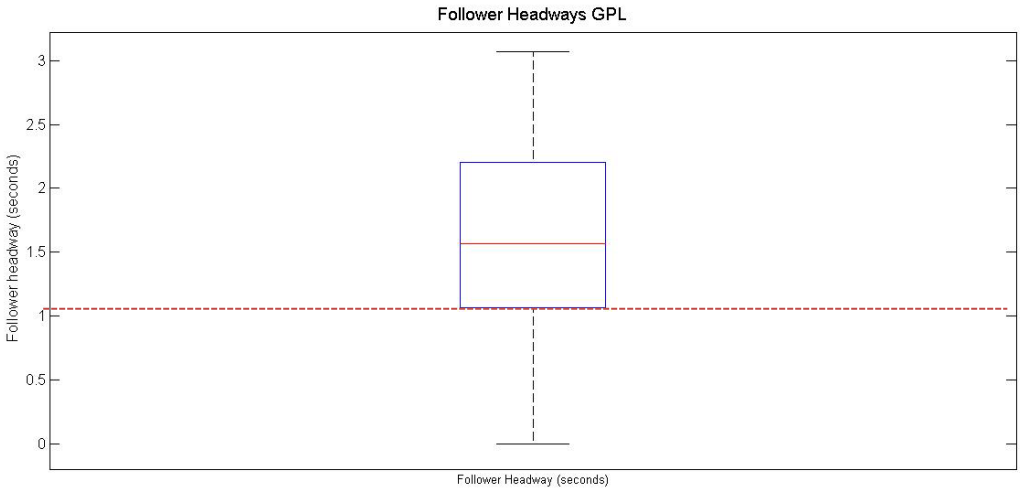

Figure 93. Follower headways boxplot

To replicate drivers' willingness to approach their leader a stochastic threshold was used for each driver of the simulated stream. In particular, using the 25th percentile of the followers' headways as the mean of an exponential distribution the aforementioned threshold was sampled for each vehicle. If the followers moved at a higher speed than their leaders and the headway threshold was violated, then followers would match the speed of their leaders.

Individual vehicle speeds were derived by sampling from a normal distribution with a mean equal to the prevailing speed of the GPL and a standard deviation equal to 3 feet/second. The reason supporting this desired variation in speed was based on the need for gaps to fluctuate over time. Figure 94 presents generated trajectories for a 5 minute interval for the most right lane, while Figure 95 presents the multilevel field of trajectories for all the GPLs participating in the experiment.

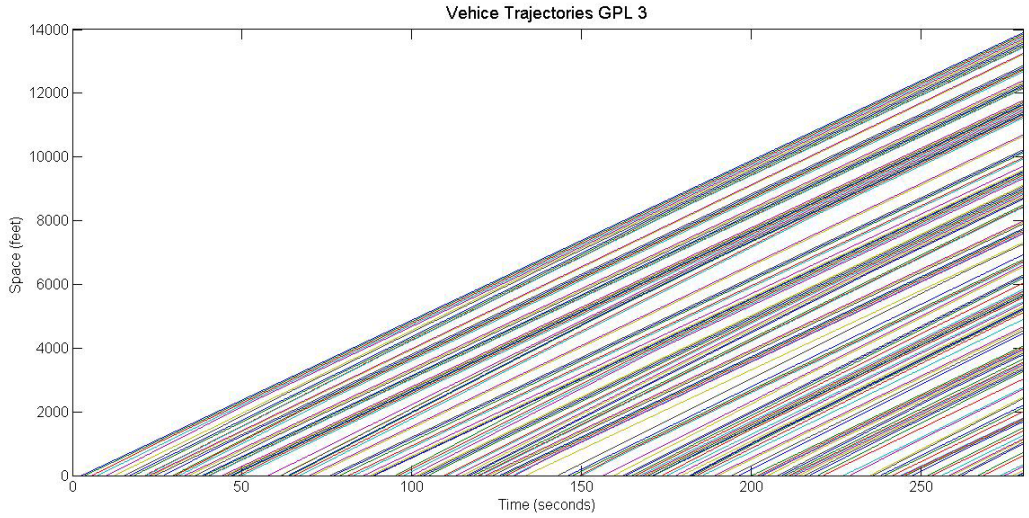

Figure 94. Sample vehicle trajectories for lane 3

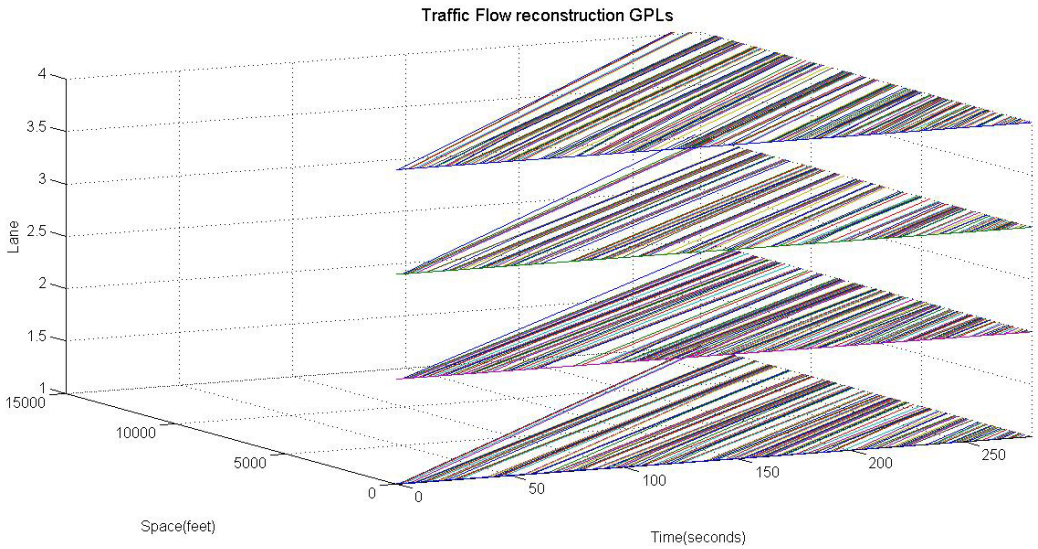

Figure 95. Sample multilevel vehicle trajectories for the 4 GPLs of the examined network

Modeling duration of drivers movement between lanes

Another quantity of interest for the development of the OLCR model was the time that drivers spend between lanes after they finally accept a gap on the target lane. Specifically, the time which drivers consume between making a decision and repositioning their vehicles in the middle of the target lane had to be quantified as well. Additional data was extracted from the trajectory dataset and a distribution was fitted to the resulting dataset to capture the randomness of this quantity.

The best fit to the harvested data was a normal distribution with mean equal to 2.79 seconds and variance equal to 0.6 seconds2 (Figure 96). Among the different distributions that were tested, the normal best fit to the data based on the log-likelihood of each estimated distribution. The fitting results are summarized in Table 12.

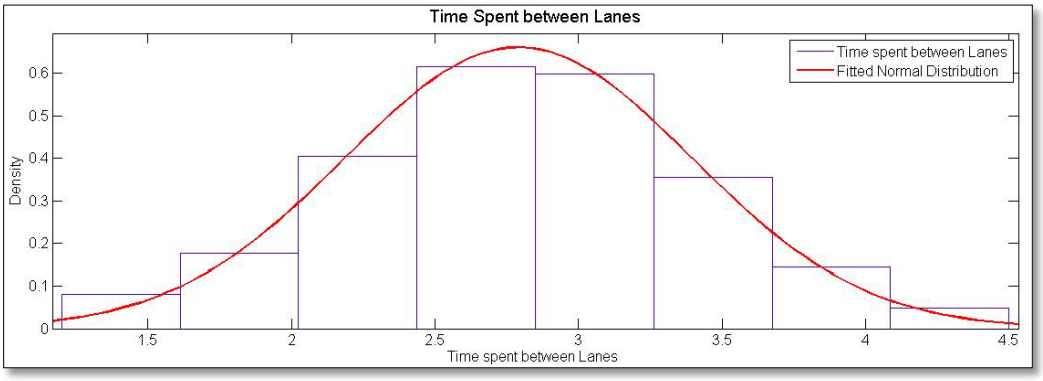

Figure 96. Distribution fitting results for the time drivers spend between lanes

Table 12. Distribution fitting results for the time that drivers spend between lanes

	2.79	
	Estimate	Std. Error
	0.60	0.04

Traffic Assessment Parameter (TAP)

One more quantity that was incorporated in this methodology is the time that drivers spend on each lane before starting to evaluate the available gaps on their target lane. This time lag is justified by the time that drivers need to evaluate the traffic conditions on the lane that they have just joined before beginning the process of moving to the lane on their left. The Traffic Assessment Parameter (TAP) is an unobserved behavioral parameter and the subsequent steps towards quantifying TAP will be presented in the Simulation Results section.

The methodology developed to define advisory designs for OLCRs on freeway facilities, utilizes the traffic flow reconstruction tool presented in the previous section of this Chapter along with the developed Gap Acceptance model and a set of behavioral parameters. More specifically, given the desired demand level, trajectories for the vehicles of the GPLs are generated. Trajectories are generated in five minute blocks and can accommodate either a level demand or a time series of different demand states for the examined network.

Detector data was retrieved from MnDOT's database and the density evolution for the days of interest was used as the input to the validation experiment. For the first step in order to validate the models output, only sections of the time series that were below the critical density were taken into account. Further numerical details are presented in the section describing the conducted experiment. The following steps are being followed in order to formulate the advisory lane changing regions for the HOT lane:

1. Trajectories for the vehicles on the General Purpose Lanes are generated based on the parameters of the FD and the desired demand level.
2. A numerical value was sampled for the TAP parameter for each driver and each lane change; when vehicles switched lanes form the acceleration to the lane on their left the TAP was set equal to zero since there is no need for drivers to evaluate the conditions on the lane before start searching for an appropriate gap.
3. The time increments that subject vehicles spend on each lane are shaped by the output of the Gap Acceptance model and the time drivers spend between lanes; the same process is repeated for all the lanes of interest.
4. Given the speed of each lane involved in the process and the simulated time subject vehicles travel, the total distance traveled between the entrance ramp and the HOT lane is computed.
5. Another quantity that had to be defined in this effort is the percentage of drivers that the design targets to provide service to. For the purposes of this study the target percentage of drivers desiring to provide service to was set equal to 90 %; this is something that design engineers can tune in the future to obtain results tailored to the needs of their network.

Figure 97 illustrates a schematic representation of the various steps the process towards achieving the advisory OLCR. The results are projected taking advantage of the image processing toolbox offered in MATLAB. In that way, it is easier to visualize the output of the simulation. First, an image of the segment of interest along with two reference points on

the facility is required. In that way, distances on the image can be correlated to actual lengths; the proposed design is superimposed (Figure 98).

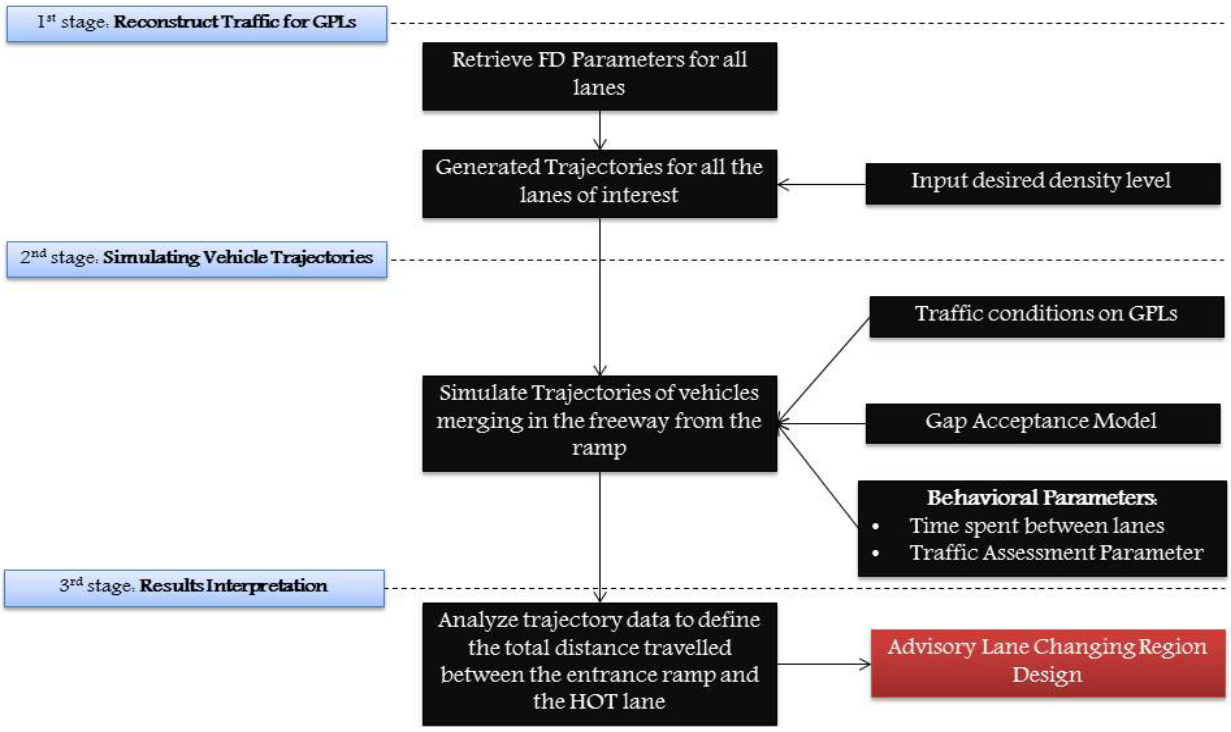

Figure 97. Schematic methodology of defining the OLCRs

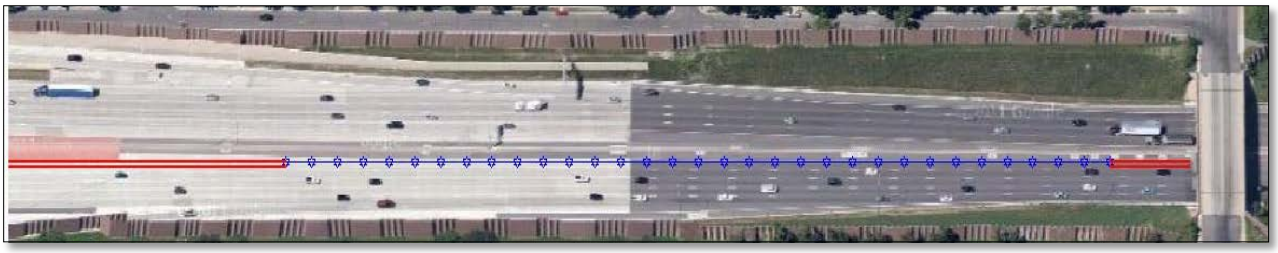

Figure 98. Visualizing the output of the proposed methodology

Experiment

Evaluating the output of the constructed methodology was based on the demand input derived from the corresponding inductive loop detectors. More specifically, the density evolution for the days between October 30th and November 1st was used for the time between 08:00am and 09:00am using 5 minute intervals; this is in accordance with the fact that most of the observations were captured during this time period. As stated in a previous section density values exceeding the critical density of each lane were not taken into account at this first step.

Given the density evolution, trajectories corresponding to the prevailing density conditions were generated for all the GPLs. Following the steps of the developed methodology, trajectories of vehicles entering the freeway form the entrance ramp and moving all the

way to the HOT lane were simulated in response to the given traffic conditions. The main quantity of interest was the total distance that vehicles traveled along the freeway.

Simulation results

After the information described in previous section were incorporated in the process a comparison between the harvested trajectory lengths and the simulated trajectory lengths was necessary in order to conclude about the validity of the developed methodology. The comparison between the simulated and the observed data is presented through their corresponding Cumulative Distribution Functions (CDFs) as well as Probability Density Functions (PDFs). Since the harvested dataset was limited to 50 vehicle trajectories it was decided to use 95% Confidence Intervals (CI) around the empirical CDF for the collected data in an effort to take into consideration unobserved trajectories. Specifically, the 95% CIs were computed based on Greenwood's formula (Greenwood, 1926).

The first effort to replicate the observed trajectory lengths was not successful and the simulated vehicles reached the HOT lane long before they did in reality. Figure 99 presents the CDF of the simulated trajectory lengths (red color), the CDF of the collected trajectory lengths (blue color) and the 95% CI corresponding to the empirical CDF of the collected observations (green color).

This observation underlined the need of incorporating the Traffic Assessment Parameter (TAP) in the process as described in an earlier section of this Chapter. TAP is an unobserved behavioral parameter that describes the time that drives spend on the lane they have just joined evaluating the conditions of the lane before they try to find an appropriate gap and merge to the lane on their left.

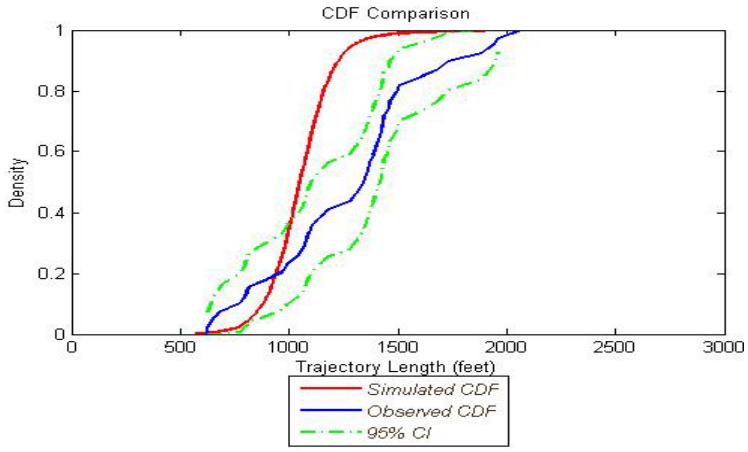

Figure 99. CDF comparison between observed and simulated trajectory lengths with 95 % confidence intervals without TAP

The first step towards identifying the characteristics of this unobserved parameter was to assume that it is constant for all drivers and observe the impact of this assumption to the results of the simulation. Specifically, TAP was assumed to be equal to 0.9 seconds for all drivers. The results of the simulation experiment under this assumption are presented in Figure 100. Even though the gap between the two CDFs was decreased the need of a larger

variance for the simulated trajectories was identified; this underlined the stochastic nature of TAP.

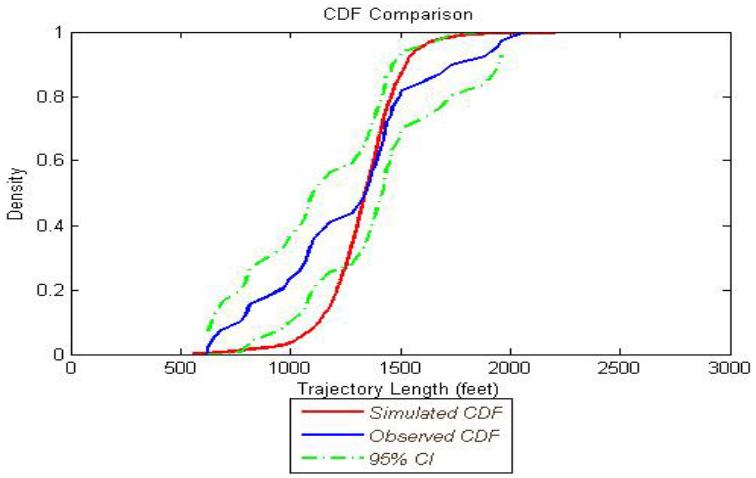

Figure 100. CDF comparison between observed and simulated trajectory lengths with 95% confidence intervals with constant TAP = 0.9 seconds

The next step was to sample values for TAP from a unimodal distribution (a truncated Normal with mean equal to 0 seconds and standard deviation equal to 2.2 seconds) so that the stochasticity of the parameter can be accommodated. This modification resulted in a major improvement of the results as supported by Figure 101. The variance of the resulting distribution was increased and it can also be seen that the CDF of the simulated trajectories lies in the region defined by the 95% confidence intervals.

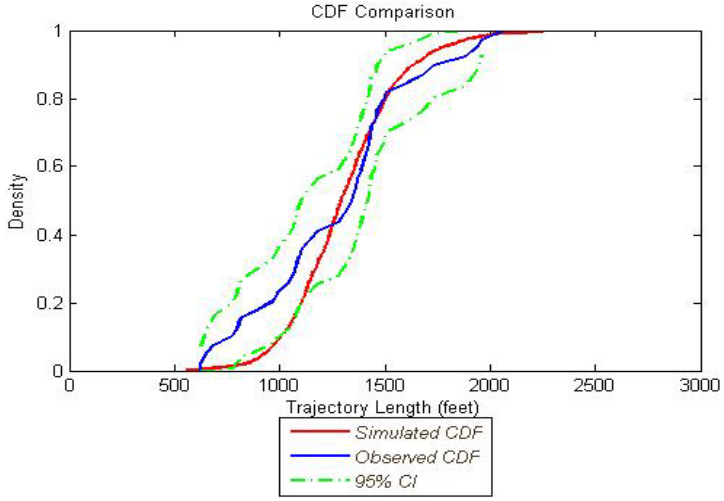

Figure 101. CDF comparison between observed and simulated trajectory lengths with 95% confidence intervals with sotchastic TAP

It can be seen that for the whole spectrum of the observed data the simulation results are within the region that the CI define. Especially for outputs that exceed 1300 feet in length, the model captures the character of the observed distances with great accuracy.

To support this observation, both the collected and the simulated trajectories were separated based on the threshold of 1300 feet. For the resulting subgroups a comparison based on their estimated kernel smoothed density is illustrated in Figure 102 and Figure 103. The estimate is based on a normal kernel function, and is evaluated at 100 equally spaced points that cover the range of the given vector each time. Figure 102 presents the comparison for the group of simulated and collected trajectories exceeding 1300 feet in length. Clearly, the model closely captured the character of the collected data in great detail.

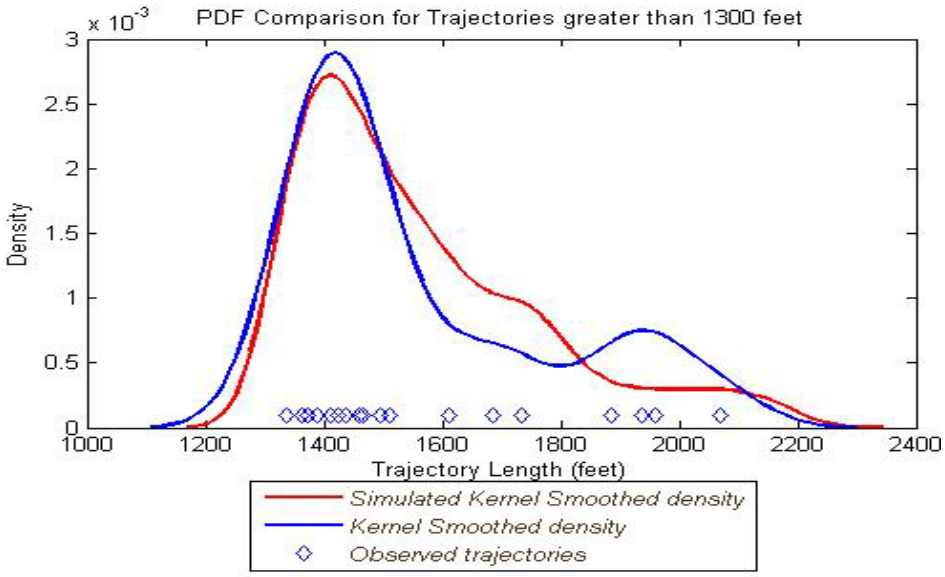

Figure 102. PDF comparison between the observed and the simulated Kernel smoothed density of trajectory lengths for lengths over 1300 feet

For trajectories that are below the threshold of 1300 feet the performance of the proposed methodology is not as accurate as in the previous case. While experimenting with the developed model, it was observed that short trajectories in length are likely to be reproduced for traffic conditions close to the critical density. The modeling efforts are bounded by the critical density and thus lower speeds than 35 miles/hour cannot be simulated.

Figure 103 presents a PDF comparison between the observed and simulated trajectories that are lesser than 1300 feet. Even though the model is not performing accurately for this region, simulated vehicles will reach the HOT lane later compared to what has been observed in reality. In a hypothetical design based on the output of the model this will result in vehicles reaching the adjacent lane to HOT lane earlier than the "gate" and thus they will have the opportunity to merge as soon as they are beside the proposed access zone. Once again the 95 % CIs presented in Figure 104 support the fact that the simulated trajectories are within an acceptable region for this group as well.

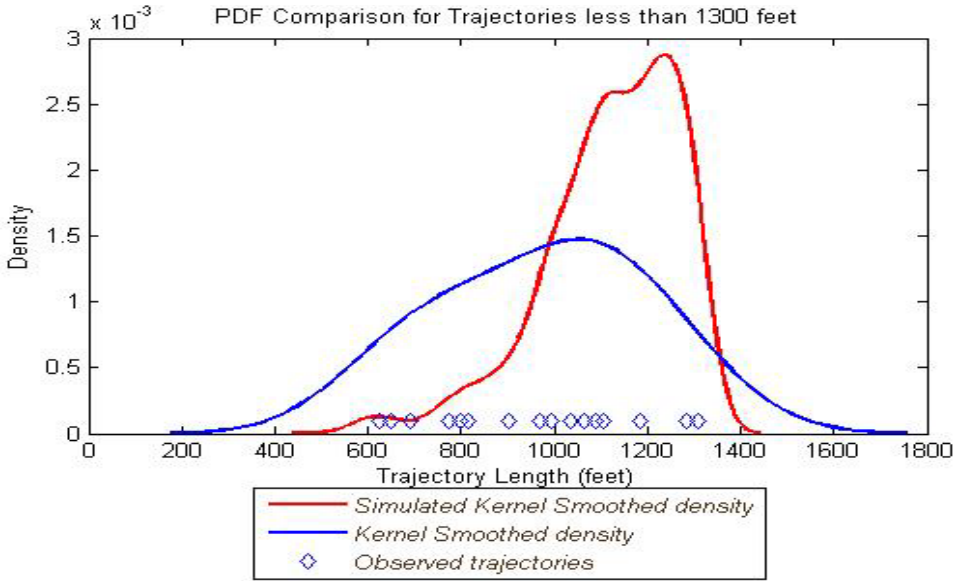

Figure 103. PDF comparison between the observed and the simulated Kernel smoothed density of trajectory lengths for lengths less than 1300 feet

Expanding this simulation to densities exceeding the critical density

In an effort to examine the model's behavior at densities exceeding the critical density, detector signal for the dates that the trajectory extraction took place were used but this time signal was used for the desired traffic conditions. The trajectory lengths that were used to validate the models output in this step corresponded to the same traffic conditions as the ones used in the input of this experiment; densities over 75 vehicles/mile were not used since attractive gaps are not available and thus drivers need to cooperate with vehicles on the lane that they wish to join.

First, headways were partitioned in two regions using the same optimization formulation described earlier in this chapter. The optimal partitioning was obtained for separating headways in two groups with a break point at 18.5 vehicles/mile. The same process was followed to obtain the corresponding CV as well as the new surface of distributions used in the experiment. Figure 104 presents the output of the model for the selected input as well as the corresponding trajectory lengths harvested for the aforementioned density levels with 95 % confidence intervals. Once again the models performance is supported by field observations.

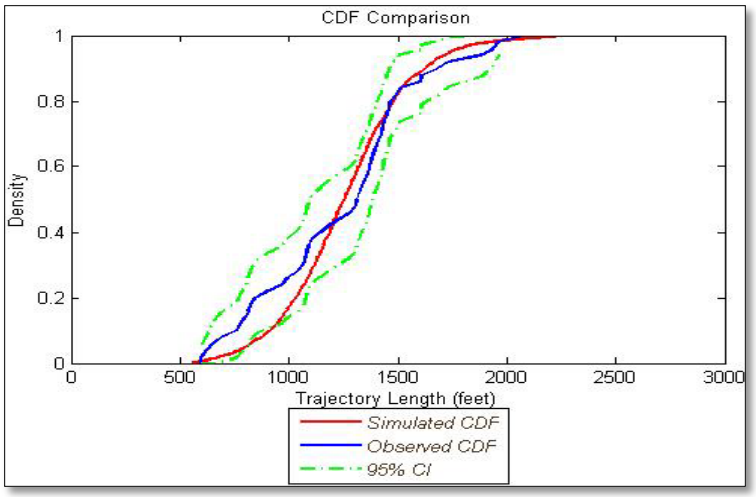

Figure 104. CDF comparison between observed and simulated trajectory lengths with 95% confidence intervals with stochastic TAP

Comparison with commonly used practices

In this section, a hypothetical scenario aiming in identifying the OLCR for a freeway with 4 GPLs and one HOT lane is presented. Figure 105 presents a schematic representation of the hypothetical freeway segment. Here, it is assumed that only the location of the entrance ramp to the freeway shapes the length and position of the proposed merging zone. For purposes of simplicity the FDs of the GPLs of the hypothetical freeway are identical to the characteristics of the examined segment earlier in this Chapter. The goal is to define the quantities L1, L2, Ltotal, as they are presented in Figure 105, so that potential users merging from the entrance ramp can achieve to join traffic on the HOT lane within the boundaries of the merging zone.

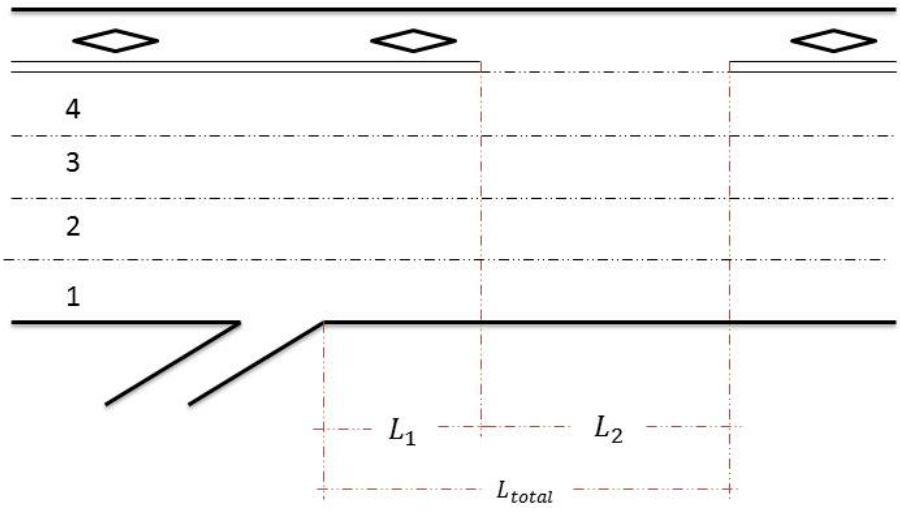

Figure 105. Test Site

Several studies in the past have derived guidelines to define the aforementioned quantities of interest. A discussion can be found in the background chapter; their findings with respect to the quantities of interest are briefly repeated. Specifically, the HOV Systems Manual (National Research Council, 1998) proposes a distance of Ltotal equal to 2500 feet regardless of the number of General purpose lanes. Two limitations were identified in this approach; it does not take into account cases that the interaction between the HOT and its adjacent lane need to be minimized and traffic conditions and traffic patterns of the GPLs are not instilled in the design process.

Fuhs (1990) proposed a methodology that accounts for the number of lane changes that are necessary for vehicles to merge to the HOT lane after merging to the freeway from the nearest entrance ramp or vehicles that need to exit to the exit ramp downstream. The minimum proposed value for Ltotal was set to 500 feet for each lane change and the recommended value was equal to 1000 feet. In a similar framework the California department of Transportation (1991) proposed a minimum distance of 660 feet per lane change. Regarding the length of the opening length several values have been proposed in an effort to accommodate the weaving demand of users of the facility and all range between 900 feet and 1500 feet (Fuhs (1990), Yang et al. (2011), ASSHTO (FHWA, (2004)), Kuhn et al. (2005)).

Yang et al. (2011) proposed a probabilistic approach towards quantifying advisory designs utilizing gap acceptance theory. The results of the proposed methodology with respect to the length of the gate and Ltotal varied between 2000 feet and 4200 feet depending on the free flow speed of the GPLs and their number. The advisory gate lengths varied between 900 feet and 1400 feet and were contingent to the weaving demand.

Using data from I-635 in Houston Texas Williams et al. (2010) developed a set of design guidelines based on the results of a simulation methodology developed in VISSIM simulator. The advisory lengths derived from the proposed process are varied between 500 feet per GPL and 875 feet per GPL depending on the weaving demand.

The limitations of the aforementioned processes are either based on the fact that are very generic or require data that are difficult to obtain for their implementation. An effort to compare the OLCRs resulting from the proposed methodology with the results of the methodologies available in the literature is presented. For the designs that provide minimum and recommended lengths two hypothetical designs will be derived for each one of them. Table 13 summarizes the findings of this investigation and will be the foundation for the ensuing discussion.

Table 13. Comparison of the proposed methodology to common practices

	2000 - 4000	900 - 1400	1100 - 3100
	2500 - 3600	900 - 1400	1600 - 2700

In all cases the length of L1 is overestimated and thus this we result in drivers reaching the adjacent to the HOT lane long before the merging zone becomes available; it varies between 40 and 2000 feet. This is a common problem observed in various locations that a closed access design philosophy is implemented.

One example can be found on the HOT lane of Interstate 394 in Minneapolis, MN prior to the exit ramp towards Louisiana Avenue Eastbound. Here, drivers are forced to wait until they perform their lane changing maneuver; this has a negative impact on the critical gap that will be accepting after the merging opening becomes available. In addition, this impatience can result in violators merging to the HOT lane while the painted buffer (if there a concrete barrier is not used to separate the lanes) is present. This endangers the safety conditions on the HOT lane since it is possible that drivers will ignore the lane changing restriction and merge to the HOT lane. At this point, drivers that are already on the HOT lane are not expecting vehicles to merge and consequently are not alerted.

Implementing the proposed methodology on I-394

As mentioned above, a location on Interstate 394 was identified for which the gate is placed downstream of the location that the actual need for merging is observed empirically. Figure 106 presents the segment of interest which lies downstream of the entrance ramp merging from Louisiana Avenue to I-394 Eastbound. The distance between the beginning of the gate and the entrance ramp to the freeway is approximately 2200 feet.

Figure 106. Test Site on I-394

In order to demonstrate the potential of the proposed tool, Fundamental Diagram characteristics were identified for the examined location following the same procedure described for the validation experiments. Table 14 summarizes the FD characteristics for

the examined location. Accounting for the delay that selecting a gap on the HOT lane when desiring to merge from its adjacent lane is infused in the process by including the particular lane change in the process as well.

Table 14. Fundamental diagram parameters GPLs on test site

Lane	u_f $(miles/hour)$	k_j $(vehiles/mile)$
1	63.78	130.9382
2	71.52	112.1531
3	71.29	134.3067
4	69.48	111.6145

Drivers will need to perform three lane changes to reach the HOT lane and this three-step process was simulated to define the optimal location of the gate. Data for 10 typical weekdays were extracted representing both winter days as well as summer days were used to conclude about the optimal gate design. Specifically, the density evolution for 5 morning peak periods (07:00am - 09:30am) was used as the input to the experiment; the objective was to capture a large number of traffic patterns so that the design can accommodate a broad range of traffic conditions.

The developed tool suggests the starting point of the examined gate should be placed 750 feet after the entrance ramp to the freeway so that 95% of the users can receive access to the HOT lane; this is significantly different to the implemented design. The difference between the OLCR tool design and the implemented design is 1450 feet. Figure 107 presents the resulting histogram of the simulated distance that vehicles covered between the entrance ramp and the HOT lane. The proposed starting point as derived from the OLCR tool as well as the implemented design is also illustrated in Figure 108.

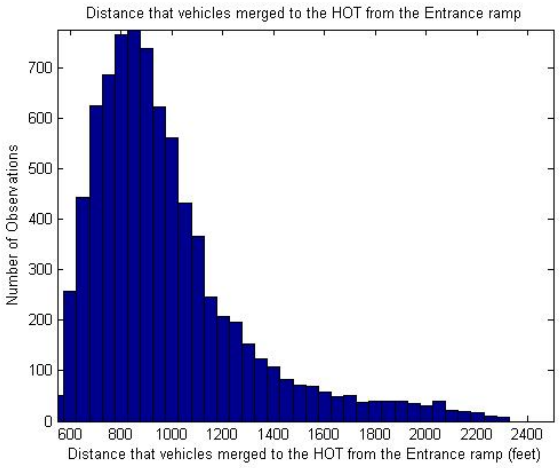

Figure 107. Simulated trajectory lengths

The suggested length for the OLCR is 1100 feet. For the examined case, a comparison for the length of the gate cannot be made since the reversible segment of the HOT lane starts

exactly after this gate. The results of this example support the claim that existing methodologies suggest OLCR designs downstream of the location that the actual need for merging is expected to appear.

Figure 108. Proposed design

Figure 109 presents flow (vehicles/hour) evolution for a typical weekday for the detectors on the adjacent to the HOT lane at the examined segment; one prior to the entrance ramp (red line), one at the OLCR proposed beginning of the gate (green line) and one at slightly downstream of the implemented beginning of the gate (blue line). It can be seen that for most of the length of the examined morning peak, flow at the OLCR proposed beginning of the gate is consistently higher than prior to the entrance ramp; this can be translated into vehicles that merge in the freeway from Louisiana Avenue and have to wait until the gate becomes available and merge to the HOT. As mentioned above they have to wait for up to 1450 feet before the gate becomes available. In that way the adjacent to the HOT lane is receiving traffic that is not intended to use it and waits for the opening to the HOT lane. Using the proposed methodology this pattern between the detector signals would not have been observed since drivers would get service at the location that they need it.

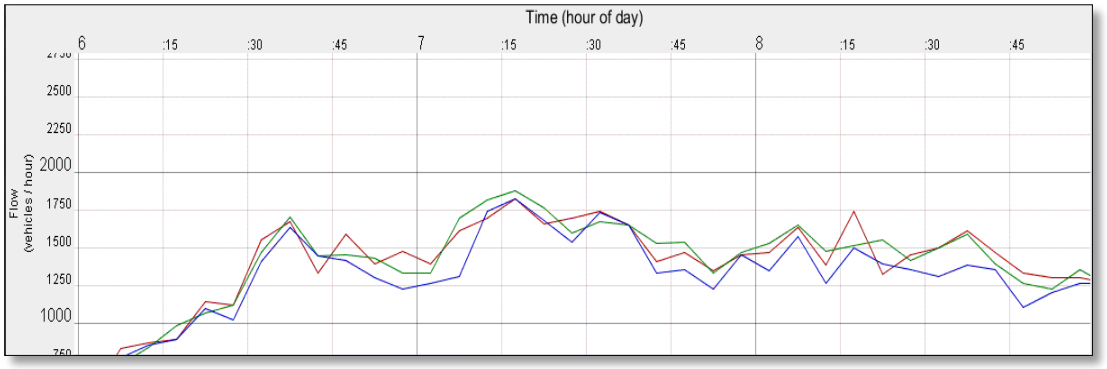

Figure 109. Detector signal comparison - flow (vehicles/hour)

Proposed implementation

The proposed methodology was developed to guide engineers' decisions in defining OLCRs on a forthcoming closed access design facility. The first step towards implementing the OLCR methodology is to fit a set of Fundamental diagrams to the GPLs of the examined network and identify their parameters. Once the parameters are defined, the proposed

implementation methodology requires the demand signal for typical weekdays during peak hours. In a more refined implementation of the model demand signal derived from a simulation experiment would take into account the expected density reduction of the GPLs in response to the HOT lane's implementation. This process lies heavily on the selection of the demand input provided to the model in order to output advisory designs. A large number of typical weekdays should be used in the input matrix of this methodology so that a broad spectrum of traffic patterns can be considered towards defining the OLCR. Finally, after the input is defined and the simulation is performed engineers will need to provide a desired percentage of the drivers sample that they aim in providing service for.

8. Planning for Access Restrictions

This chapter describes the formulation of a methodology to emulate shockwave propagation on the HOT lane. All the subsequent steps of this modeling effort will be presented in detail along with the developed mechanism that was constructed for simulating shockwave propagation at increased demand levels. The developed methodology facilitates decision making regarding access restriction for locations where the interaction between the HOT lane and its adjacent lane impacts the safety conditions on the HOT lane.

Compression shockwaves or flow breakdowns are caused when vehicles either join traffic on the HOT lane facility or decide to leave the HOT lane and join the GPL. Flow breakdowns force traffic conditions on the HOT lane into transient congested states creating inconvenience to the commuters who have paid extra to avoid congestion. Although currently rare, flow breakdowns can be observed during peak hours because of the large speed differential between the HOT lane and its adjacent GPL at certain locations.

The importance of flow breakdowns is also signified by the fact that the greater their length the higher the probability of an incident occurring. Thus, observed wave lengths are a key component in assessing network safety; simulating realistic wave propagation on the HOT lanes and evaluating safety for increased demand levels was the main goal of this effort after calibrating the developed model using observed shockwave lengths.

Compression waves were introduced to the simulated streams of vehicles based on a variation of the previously developed gap acceptance model. Simulated shockwave length distributions were derived and compared to actual observed shockwave activity, while the same methodology was implemented for artificially increased demand levels.

Traffic stream reconstruction

Reconstructing realistic traffic streams, using the obtained headway is the first step towards developing a methodology for shockwave emulation. The tool that was used to this end was along the lines of microscopic traffic simulation. Using a Monte Carlo sampling methodology the platoon characteristics identified earlier as well as individual driver's characteristics were utilized to generate realistic traffic streams.

Monte Carlo sampling methodology

Monte Carlo simulation is a powerful iterative tool that has been widely applied in studies emulating complex physical phenomena. The stochastic aspects of the informative parameters of such phenomena are replicated through proper sampling methods from descriptive distributions.

Using Monte Carlo sampling a more realistic representation of traffic streams with location specific platoon characteristics was achieved. On a single driving lane vehicles congregate in platoons, therefore a random sequence of vehicles moving at the same speed will have them separated either by leader headways or follower headways. In addition, for each of

these vehicles, behavior characteristics like reaction time and deceleration are selected as presented in Figure 110.

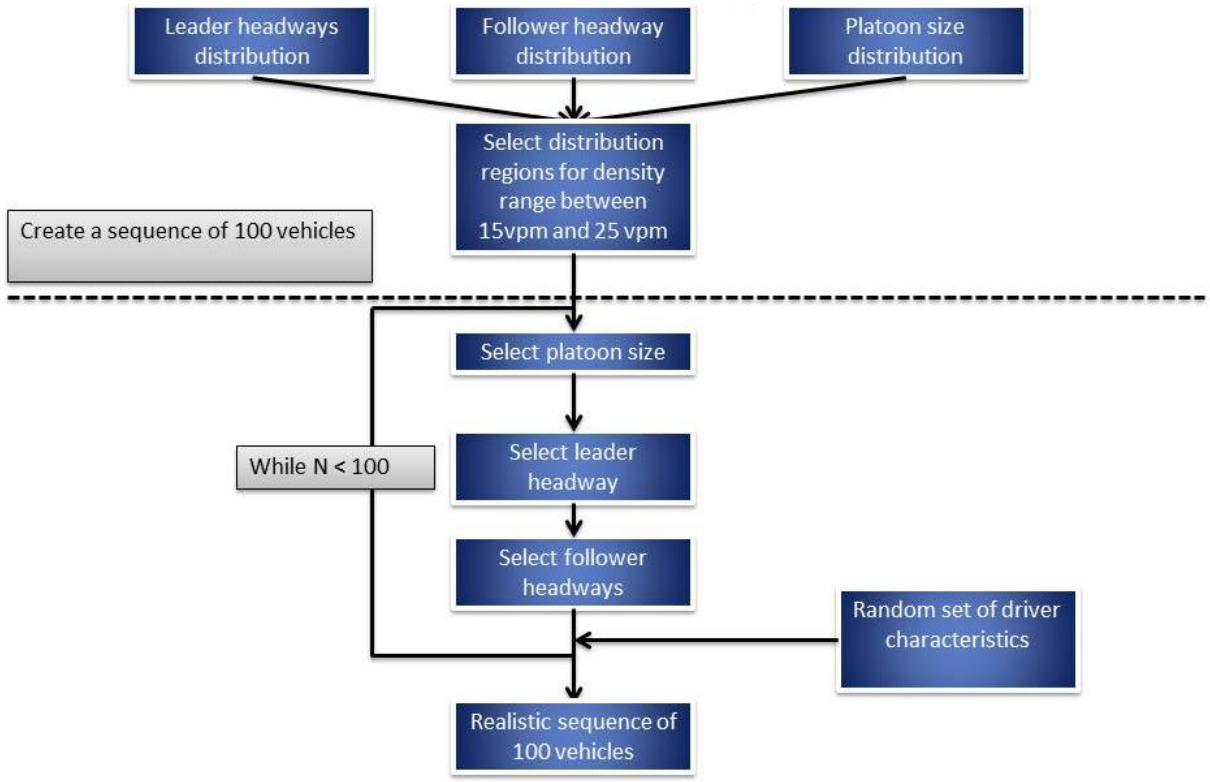

Figure 110. Monte Carlo sampling methodology

Sampling distributions

For platoon characteristics the sampling distributions were derived through the platoon formation analysis described earlier. Follower headway, leader headway, and platoon size empirical distributions were used to construct the initial spacing conditions. In an effort to have homogeneous headway selection and exclude cases that corresponded to disturbed traffic a specific region of density was selected with range between 15 and 25 vehicles per mile.

In order to create the initial spacing conditions of the simulated vehicle sequence the 'dice' is rolled at least three times for each platoon. First using a uniform integer random number generator with range of outcomes between 1 and the total number of observed platoons for the selected density region the size of the platoon was selected. Given that, the leader of this platoon was assigned a headway based on a uniform integer random number generator with range between 1 and the total number of observations for platoon leaders. Finally for each follower in the platoon a headway was selected from a set of distributions based on the predefined platoon size.

Each vehicle in the sequence was assigned a random set of driver characteristics. Distributions for these were derived either from the literature or from observations. Table 15 summarizes the selected distributions.

Table 15. Sampling distributions

Parameter	Distribution
Follower headway	Empirical distribution for the examined location
Leader headway	Empirical distribution for the examined location
Platoon size	Empirical distribution for the examined location
Reaction time	Truncated Normal (1.01,0.37) seconds (Johansson et al. (1971))
Acceleration rate	Normal (5.6,1) feet/sec^2 (Gipps (1981))
Deceleration rate	2 * Acceleration rate (Gipps (1981))
CDP	Normal(35,2.25) feet (observation)

Shockwave propagation model

The core of this methodology is a wave propagation model based on one-dimensional kinematic equations. The reason for developing a new model, instead of using one of the established car-following models available in the literature, was to ensure that the initial conditions selected will not be "reshaped" and the simulated sequence of vehicles will propagate intact until a disturbance is introduced; this is a major assumption in the proposed process. Despite the headway oscillations observed in real traffic streams this assumption can be justified by the claim that this experiment aims in isolating instances of disturbances, like isolated lane changes into the HOT.

The main behavior of the model is based on a parameter assigned to drivers describing the smallest distance each follower is willing to approach its leader while experiencing a shockwave. The Comfort Deceleration Parameter (CDP) is stochastic and was assumed to be normally distributed.

After a disturbance (deceleration) is introduced each driver will act one reaction time later than the leading vehicle and will implement the assigned deceleration rate. For every interval later than the reaction time of each follower the position of both the leader and the follower in each pair is estimated under the assumption that they will maintain their speed. If vehicles, based on their estimated positions, will come closer than the CDP then a more severe deceleration is applied; 50 % higher than the one assigned originally. The increase by 50 % was once again based on observations as derived from the recordings in December and January and is a part of the calibration process that will be presented later in this chapter.

Finally, the model gives drivers the capability of recovering after experiencing a shockwave. This is achieved by another check according to which if the leading vehicle has

a greater speed than the follower and the distance between them is more than CDP then acceleration is implemented until the speed prior the event is reached again. The acceleration is deterministic and is derived from the average acceleration capabilities of a vehicle, as used in previous simulation experiments (Gipps, 1981). A more detailed graphic representation of the model is presented in Figure 111.

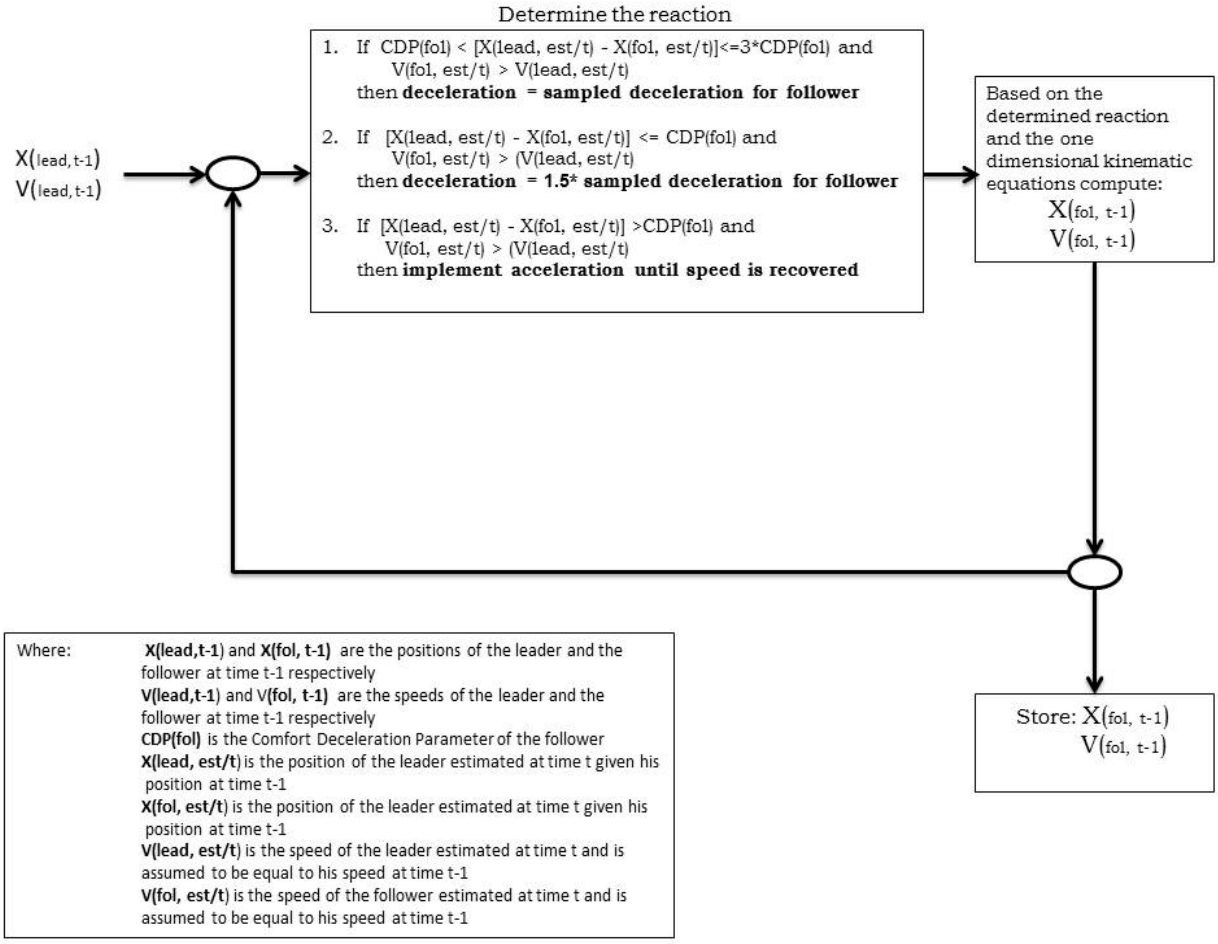

Figure 111. Shockwave propagation model structure

Methodology Structure

In order to simulate the desired wave propagation a scenario was designed capable of combining all the aforementioned tools towards computing shockwave histograms. The simulation horizon was set to 100 seconds and was sufficient to accommodate all generated shockwaves. Using the Monte Carlo sampling techniques described above a realistic sequence of 100 vehicles was constructed.

Since the empirical distributions for leader headways, follower headways and platoon sizes corresponded to a density region between 15 vehicles per mile and 25 vehicles per mile, the simulated stream was tested in each iteration to verify that the density region condition was satisfied. If the sampling process did not result in a traffic stream with corresponding density within the desired region, the step was repeated until the condition was satisfied.

According to the simulation scenario, for the 5 first seconds all vehicles moved without any change in their speeds. Using the developed gap acceptance model, headways were examined so that the first accepted gap could be identified. At that point the selected vehicle was forced to execute a predefined decrease in its speed followed by an immediate recovery with the given acceleration. The speed drop which vehicles had to execute was stochastic and was the result of the calibration process that is presented in the following section.

After the disturbance was introduced vehicles experienced the shockwaves based on rules underlined by the shockwave propagation model. When a vehicle in the sequence did not have to implement deceleration the iteration was terminated and the number of vehicles affected ahead of it was stored.

Figure 112 presents the space and speed trajectories for one iteration of the experiment. In the presented example the shockwave length was equal to 7 vehicles. Some oscillations can be observed in the speed trajectories after the vehicles recover their initial speeds. This noise was not considered to be significant and did not contaminate the results of the process. After a minimum number of 4000 iterations were completed the two sample Kolmogorov Smirnov test would decide about the proper termination of the whole process.

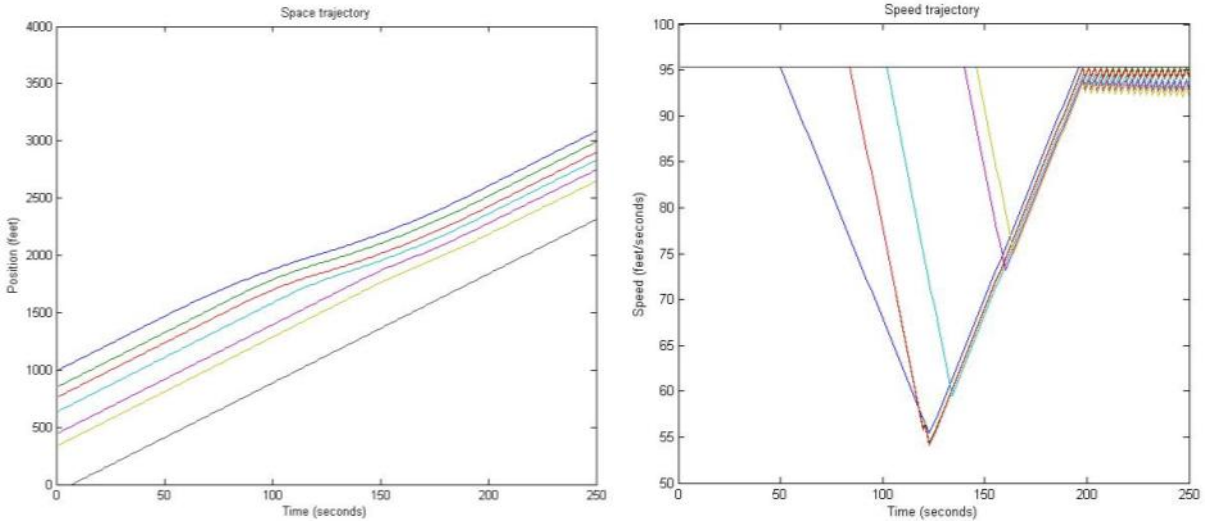

Figure 112. Example space and speed trajectories for seven vehicles

Gap Acceptance refinement

Focusing on the interaction solely between the HOT lane and its' adjacent GPL an additional data collection was completed beyond the one described in Chapter 5. The outcome of this process was used in order to introduce a disturbance in specific points of a simulated sequence of vehicles in the effort to explore the future behavior of shockwaves in the present HOT facilities.

From the set of collected gaps for each driver, it rejected all but one, the one that was finally accepted. In this study the turn light indicator was used to signal the intention of the driver

to make a lane change. Therefore, all gaps after the indicator light started flashing are considered gaps of interest. Following all the rejected gaps, the final one was accepted and the driver joined traffic on the HOT. Gaps were measured each time between the rear of the front vehicle and the rear of the following vehicle. In that way, each time one vehicle length was included.

The measured gaps were the ones related to the lane changing maneuver and included gaps that the driver rejected before changing lane and finally the gap that he accepted and joined traffic on the HOT lane. The clips that were analyzed only included cases that vehicles joined the traffic on the HOT lane. Totally 116 gaps were measured and 55 of them were accepted. Additionally, the relative speeds of the subject vehicle as well as the speed of the vehicles on the HOT were extracted.

The selected model is a logit model and the steps of selecting are following the process described in Chapter 6. After interpreting the fitting results for this model the number of rejected gaps was proved to be statistically insignificant as can also be seen from Table 16. Intuitively this can be explained from the fact that in the examined cases drivers decide not to allow their impatience to affect the risk of their selection and could be attributed to the high speed differential between the HOT lane and the adjacent lane.

Table 16. Fitting results for the 1 model

	Estimate	Std. Error	z value	Pr(>|z|)
(Intercept)	-3.0885	1.07851	-2.864	0.00419
gap	1.89607	0.35074	5.406	6.45E-08
Rejected before	0.23141	0.34389	0.673	0.50099
Relative speed	-0.0831	0.02926	-2.839	0.00453

Since the number of rejected gaps was not statistically significant the fitted model is described by Equation 16 while the results of the fitting process are aggregated in Table 17. After removing the third parameter of the model it can be seen that the coefficients that correspond to the other two parameters of the model experienced a minor change. Figure 113 presents the surface described by the fitted model.

$$\Pr\left(gap\ is\ accepted \middle|\ gap, v_{dif}\right) = \frac{e^{(-2.895+1.925*gap-0.085*v_{dif})}}{1+e^{(-2.895+1.925*gap-0.085*v_{dif})}} \qquad \text{(Eq. 16)}$$

Table 17. Fitting results for the gap acceptance model

	Estimate	Std. Error	z value	Pr(>|z|)
(Intercept)	-2.895	1.01128	-2.863	0.0042
gap	1.92532	0.35553	5.415	6.12E-08
relative.speed	-0.085	0.02944	-2.888	0.00388

It can also be seen that the parameter β1 that corresponds to the size of the gap has a positive sign which indicates that the probability of accepting a gap is increasing as the size of the gap increases as well. Relative speed between the two lanes has a negative effect to the probability of acceptance derived from the negative sign of the corresponding parameter β2. Both observations are reasonable and can be explained intuitively.

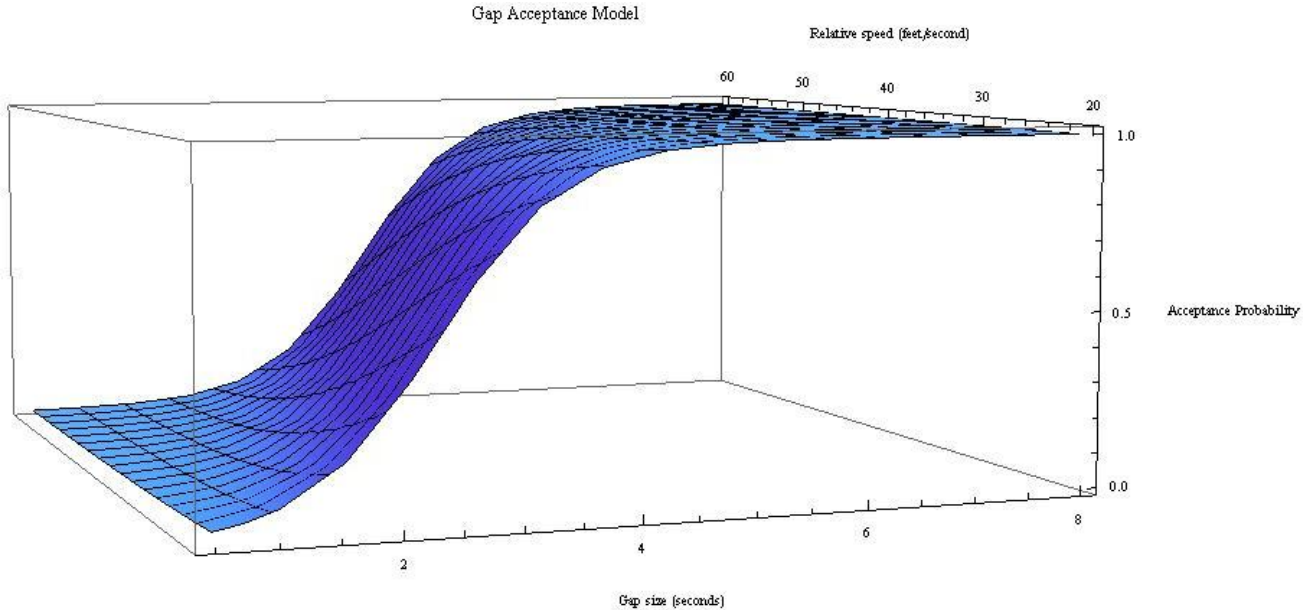

Figure 113. Surface plot of gap acceptance model

Calibration

The result of the proposed model is a distribution of simulated shockwave lengths. In order to match the observed results a calibration process was developed aiming in minimizing the sup-norm derived from the comparison of the simulated CDF and the CDF of the observed shockwave lengths.

The aforementioned test was performed in MATLAB using the command kstest2(x1,x2). In the examined case x1 was a vector of simulated shockwave lengths while x2 was a vector of measured shockwave lengths. This command gives three outputs denoted as h, p and ks2stat; where h is either 0 if the null hypothesis is rejected at a user-defined confidence interval and 1 otherwise, p is the asymptotic p value and ks2stat is the test statistic of the comparison.

The calibration process was formulated as a simple optimization problem with the objective function being the test statistic of the two sample Kolmogorov Smirnov test. The variables of the problem were the mean and the variance of the Normal distribution that describes the speed drop while the constraints were derived from the collected video recordings. The resulting formulation is:

$$minimize\ f(\mu,\sigma) \qquad \boldsymbol{subject\ to},$$

$$Lb_\mu \le \mu \le Ub_\mu$$

$$Lb_\sigma \le \sigma \le Ub_\sigma$$

where f(μ,σ) is the resulting test statistic for a given mean μ and variance σ of the distribution describing the speed drop.

Other parameters of the model such as the Comfort Deceleration Parameter, the deceleration rate and the amount of additional deceleration that drivers implement after the Comfort deceleration Parameter is violated, were calibrated based on observations and the process did not appear to be very sensitive to their selection.

The Comfort Deceleration Parameter is stochastic and was assumed to be normally distributed with a mean of 35 feet and a variance of 2.25. The parameters of the distribution were based on observations obtained during the two days in December 2011 and January 2012 and can be considered as part of the calibration process.

The acceleration is deterministic and is derived from the average acceleration capabilities of a vehicle, as used in previous simulation experiments. Finally, the amount of additional deceleration was 50 % higher than the one assigned originally. The increase by 50 % was once again based on observations as derived from the recordings in December and January.

In the case of speed drop, calibrating the parameters of the distribution was based on the described optimization problem. The results of this simulation experiment were sensitive even to the slightest changes in the speed drop distribution and this justifies the additional amount of effort placed on the calibration of the used distribution.

The problem was solved in MATLAB using the command fmincon of the optimization toolbox. fmincon(fun,x0,A,b) starts at x0 and finds a minimum x to the function described in fun subject to the linear inequalities A*x <= b. For the problem described above the resulting matrices A and b are:

$$A = \begin{pmatrix} -1 & 0 \\ 1 & 0 \\ 0 & -1 \\ 0 & 1 \end{pmatrix}, b = \begin{pmatrix} -Lb_\mu \\ Ub_\mu \\ -Lb_\sigma \\ Ub_\sigma \end{pmatrix}$$

while x0 is a vector with our initial guesses for the mean and the variance of the distribution which were a result of a trial and error process. The results obtained for the parameters of the speed drop distribution are summarized in Table 18.

Table 18. Speed drop calibrated parameters

Segment	Mean (miles/hour)	Variance (miles/hour)
6091|608 NB	38.7	4.5
6130 SB	34	4.9
6101 SB	37	2.45

Achieving increased demand levels

After the proposed model was successfully calibrated to describe shockwave propagation on all the selected locations, an investigation of wave propagation at artificially increased density levels was conducted. The purpose of this task was to evaluate safety conditions on the HOT lane for scenarios that the operation strategy of the HOT lane allowed more vehicles in the facility or operated for a longer period of time at the predefined density boundary of the pricing algorithm.

The operation strategy on the examined location is controlled by a pricing algorithm that is designed so that traffic on the HOT lane is kept below a threshold density level by changing the cost of use for the HOT lane. In that way, for more than 90 % of the time of lane operation time speeds are larger than 45 miles per hour. In this section, an estimate of shockwave length distributions will be produced for density levels slightly over 29 vehicles per mile so that the behavior of the network at the limit can be described.

First a mechanism was developed in order to create a realistic traffic flow representation at the desired demand levels. Starting with headways corresponding to uninterrupted conditions (between 15 and 25 vehicles per mile) a sequence of 100 vehicles was created with the same sampling process as described in a previous section. Once again the simulated sequence had to fulfill the density region condition and the corresponding density had to be within the region of 15 and 25 vpm.

The difference between the corresponding density of the sequence and the target density was then transformed into a desired reduction in seconds based on the speed of the sequence. In that way, the aggregated reduction for the sampled headways was computed. The corresponding speed of the increased density levels was assigned to all the vehicles of the stream.

The mechanism that was developed for this task was simple yet effective and was based on a scoring system that achieved the desired aggregated reduction iteratively. After implementing a uniform decrease by 10% in all headways of the sequence, their “score” was computed by assigning 5 points for each second of the headway size and subtracting 2 points for each vehicle ahead of the selected headway in the platoon. After the “score” for all the headways in the sequence was computed the headway with the maximum score was reduced by 10 % and after that the “score” was again computed for all headways. This process was repeated until the desired density was achieved.

Results

In this section results of all the steps described will be presented. First, the result of the calibrated model will be compared to observed shockwave lengths for all examined cases by comparing the cumulative distribution functions of the observed and the simulated shockwave lengths. Second, histograms of the simulated shockwave lengths at conditions corresponding to undisturbed traffic conditions will be presented. Third, boxplots and cumulative distribution fictions of simulated wave lengths at various increased density levels will provide a view of shockwave propagation at future traffic conditions.

Northbound between TH13 and Cliff Road.

As stated in the beginning of this section the presentation of the obtained results will start by providing the validation results. Figure 114 supports the fact that the proposed model captured the observed shockwave lengths at 90 % confidence interval while Figure 115 demonstrates the histogram of the simulated wave lengths and the density region validation. More specifically, Figure 115 demonstrates that all simulated cases corresponded to the density region that the headway measurements belonged to. The conclusion that the simulated shockwave lengths belong to the same distribution as the observed lengths, was supported by the two sample Kolmogorov Smirnov test as described in the calibration section at a 90 % confidence interval.

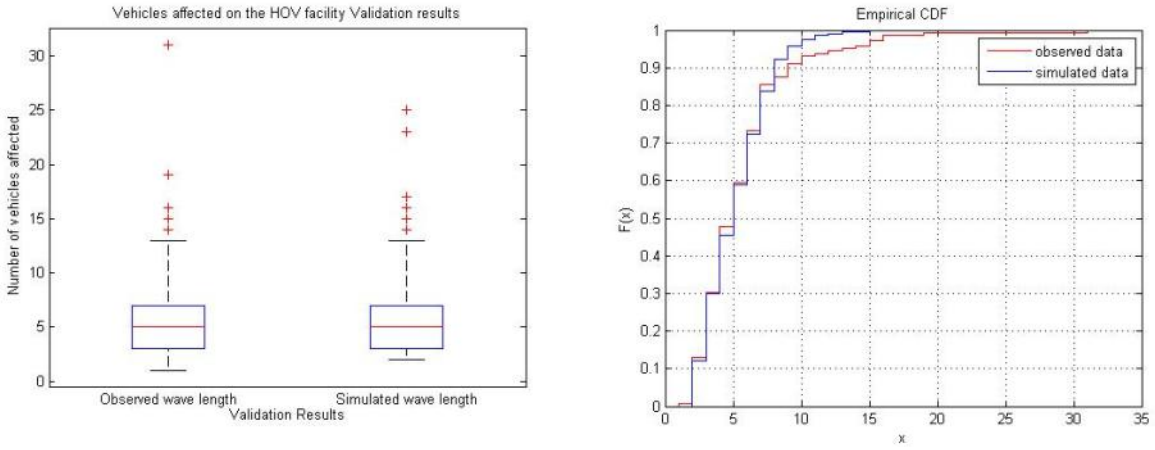

Figure 114. Validation results

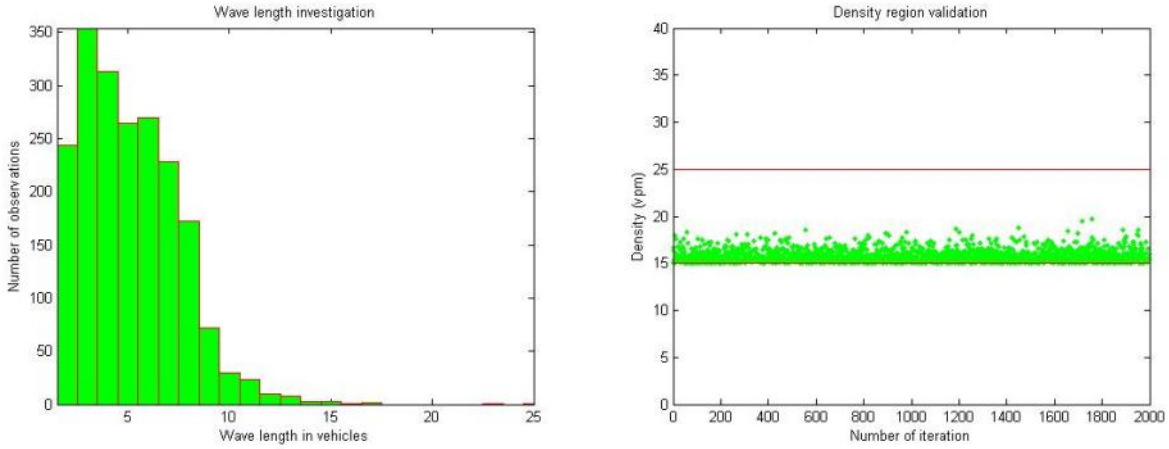

Figure 115. Shockwave length histogram and density region validation

Figure 116, Figure 117, Figure 118 and Figure 119 present the obtained histograms for the various density levels that the location was tested for. In that way first the density region between 15 vpm and 25 vpm was shifted by 50 % leading of a new region of 22.5 vpm and 37.5. Most of the simulated streams had a corresponding density closer to the lower bound of the region. The same process was also repeated for an increase of 75 %, 100 % and 150 %.

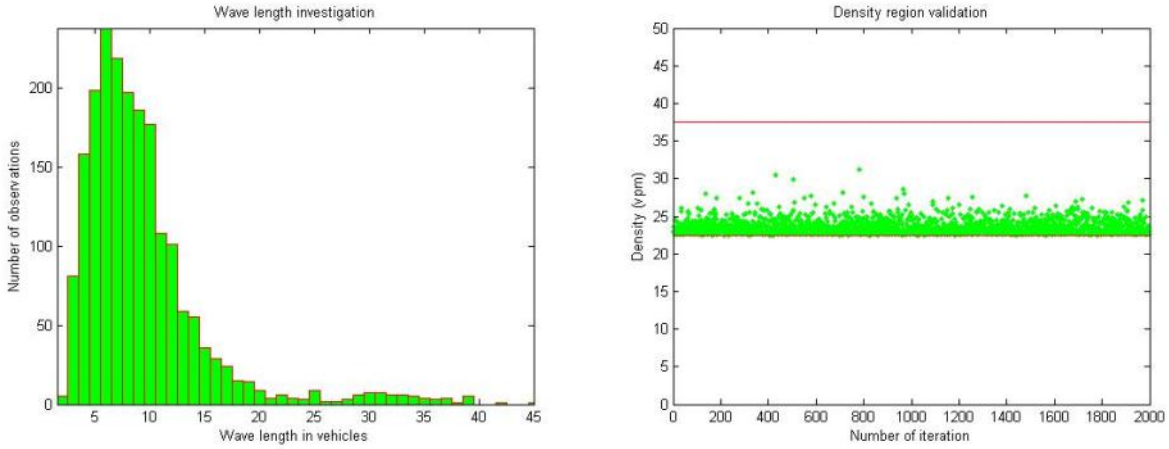

Figure 116. Resulting shockwave histogram for 50 % increase in density

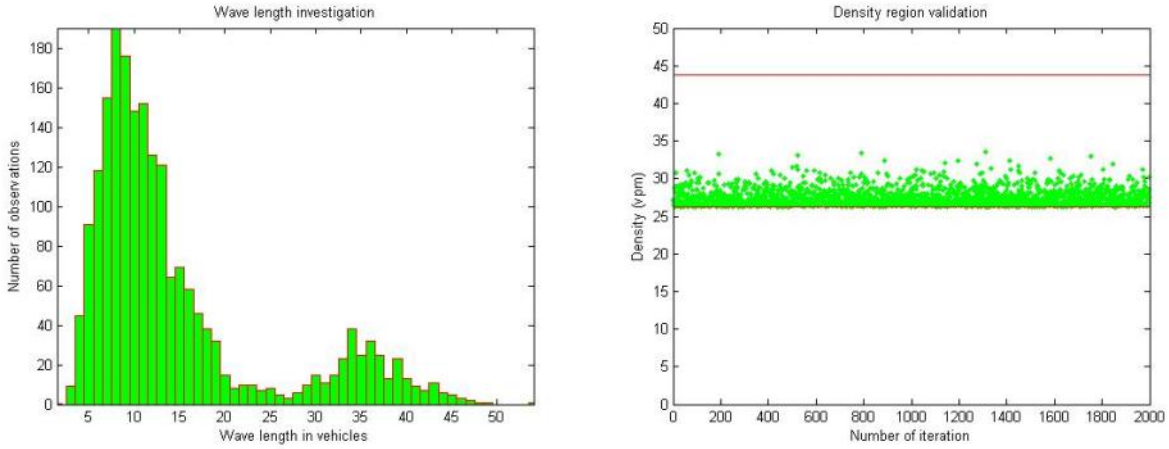

Figure 117. Resulting shockwave histogram for 75 % increase in density

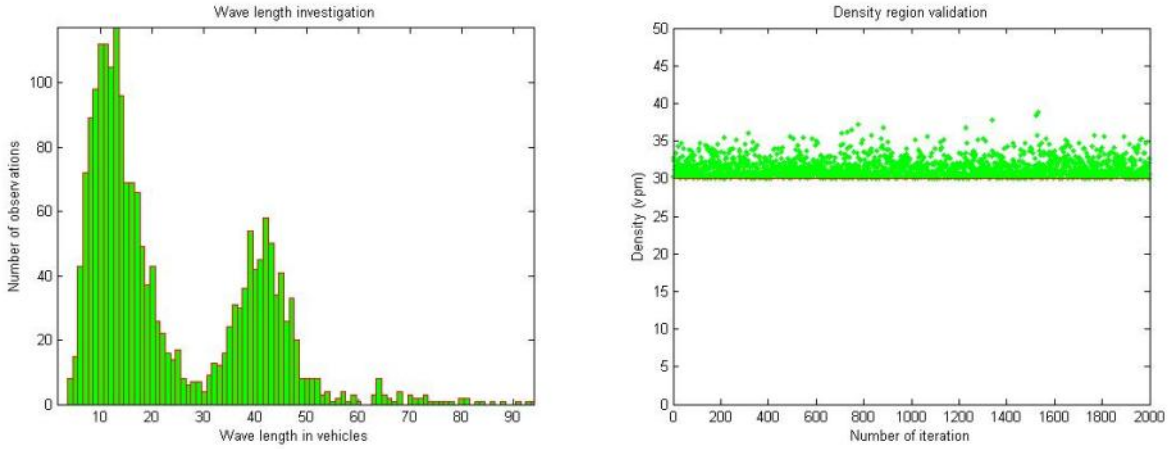

Figure 118. Resulting shockwave histogram for 100 % increase in density

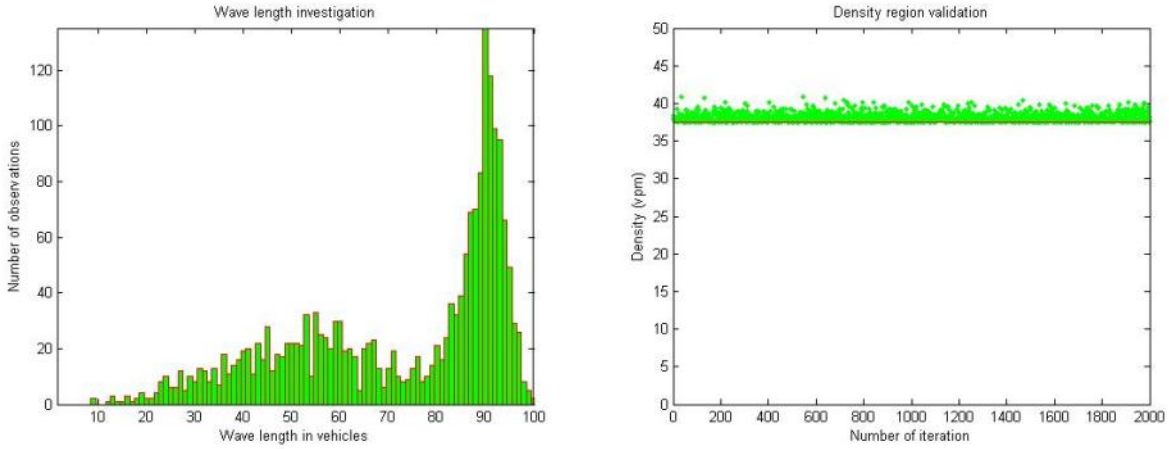

Figure 119. Resulting shockwave histogram for 150 % increase in density

It can be seen that for the uninterrupted initial conditions and the smallest of the tested increased demand levels (50 %), the resulting histograms depict an exponential distribution governed by the random character of the event. By further increasing the demand and shrinking the car-following distances a second peak in the distribution can be seen in the range of 30 to 50 vehicles. This is a concerning observation since shockwaves that are great in length have a great probability in resulting in a crash.

The observed peak is achieved at densities in the region of 35 vpm (LOS D) which cannot be reached under the current operational strategies. Another interesting observation is that by operating the facility for longer time at the boundary (29 vpm) would not affect safety significantly, a fact that can also be supported by observing Figure 116, Figure 117 and Figure 118. Finally, after density obtains values of 40 vpm the facility exceeds its boundary and all vehicles in the stream experience the disturbance (Figure 119).

The comparison between the various levels is illustrated in Figure 120 and Figure 121 by comparing the corresponding cumulative distribution function and the corresponding boxplots. It can be seen that for small increases reaching the operational boundary of the facility the length of the shockwaves does not reach concerning values while after the boundary it appears to become unstable and this results in the observed second peak of the simulated distributions.

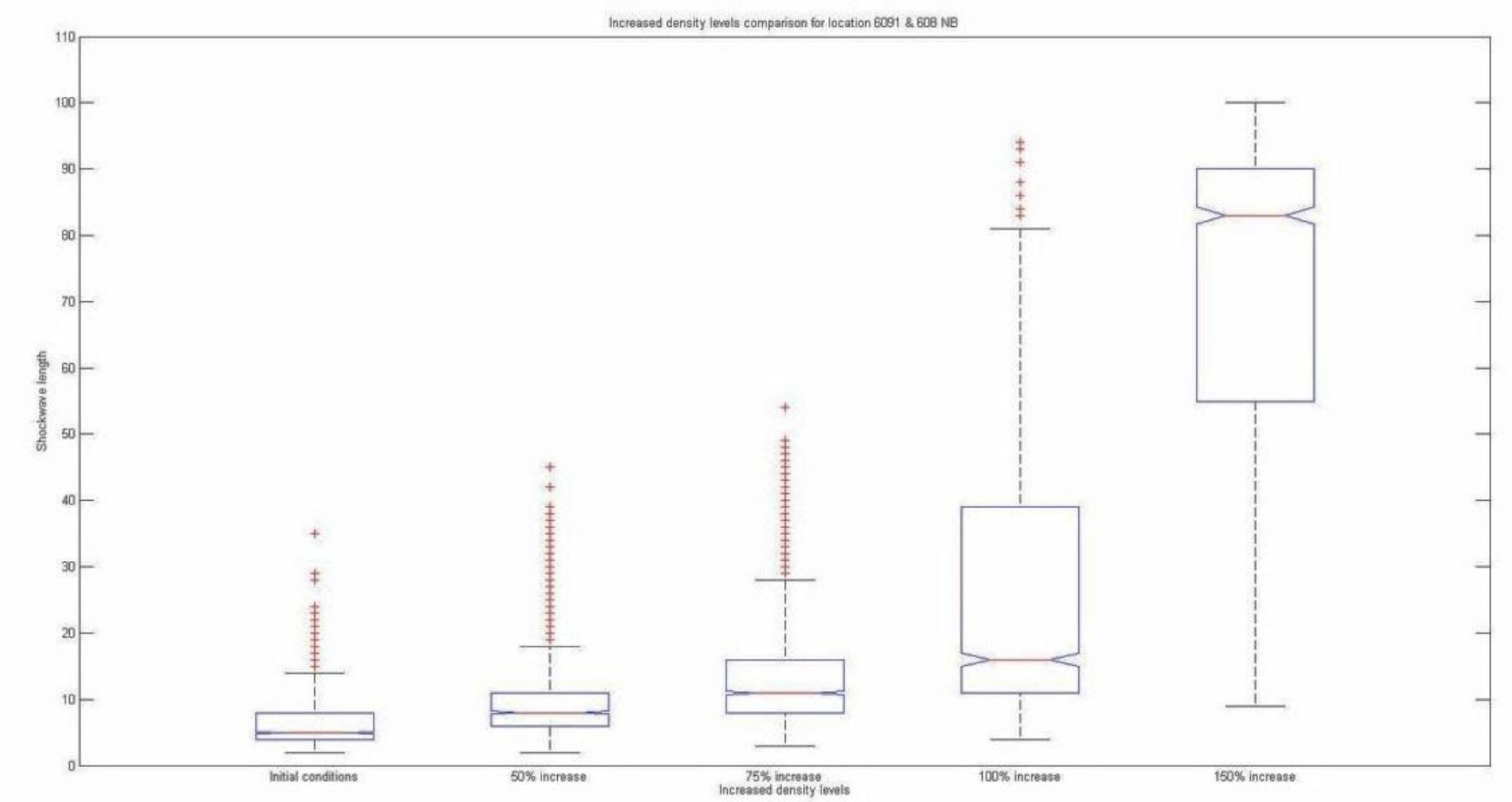

Figure 120. Boxplots of simulated shockwave lengths

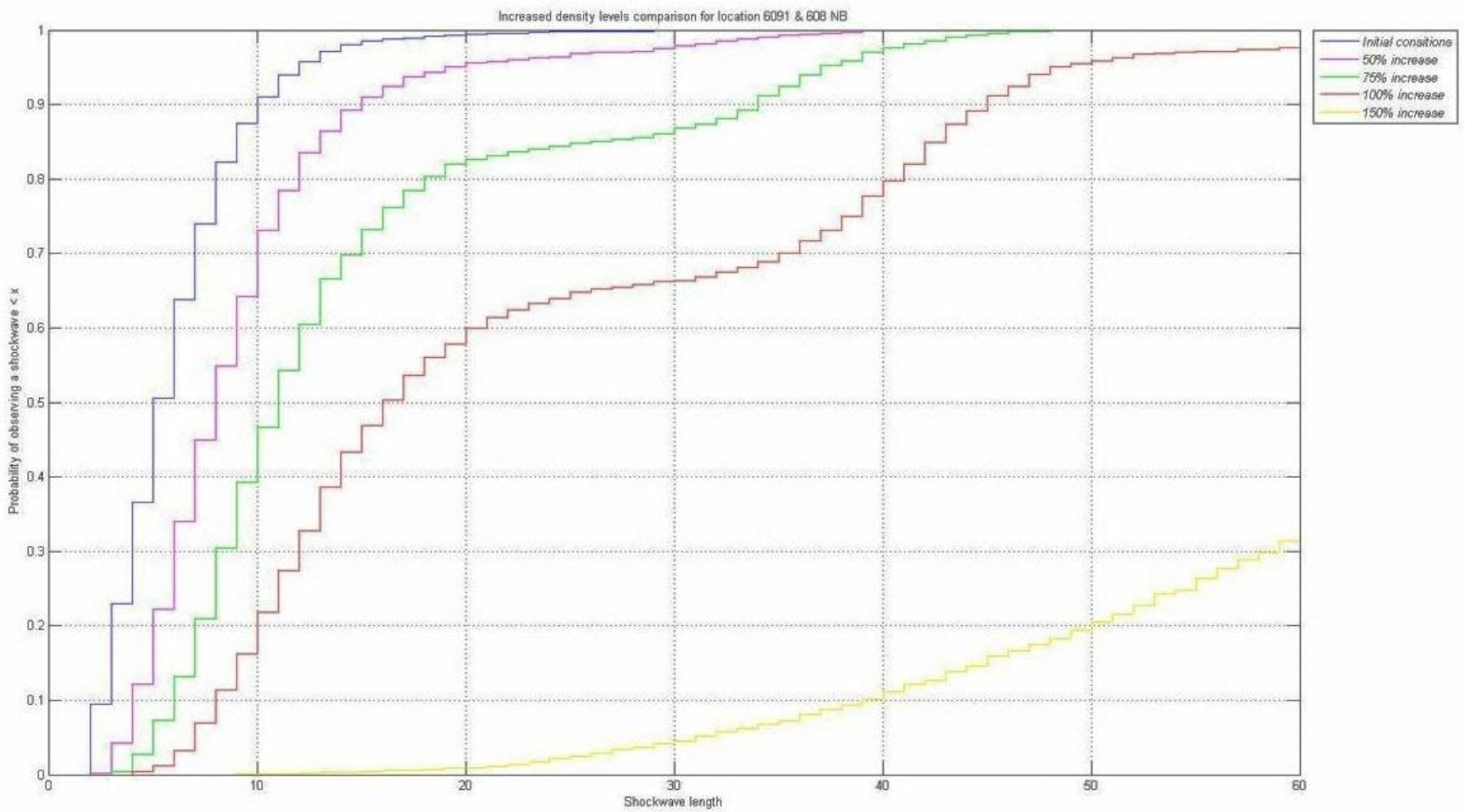

Figure 121. Cumulative distribution functions of simulated shockwave lengths

Southbound between 82nd and 86th and between 86th and 90th street.

As in the case of the segment between TH13 and Cliff Road a similar investigation was conducted for the segments between 82nd street and 86th street as well as 86th street and 90th street. Figure 122 presents a comparison between the simulate shockwave lengths and the observed shockwave lengths. In this case the model did not capture the observed lengths at the detail that it did for the previous case. Figure 123 depicts the histogram of the simulated wave lengths and the density region validation. Once again in order to make conclusions about the simulated results the two sample Kolmogorov Smirnov was used.

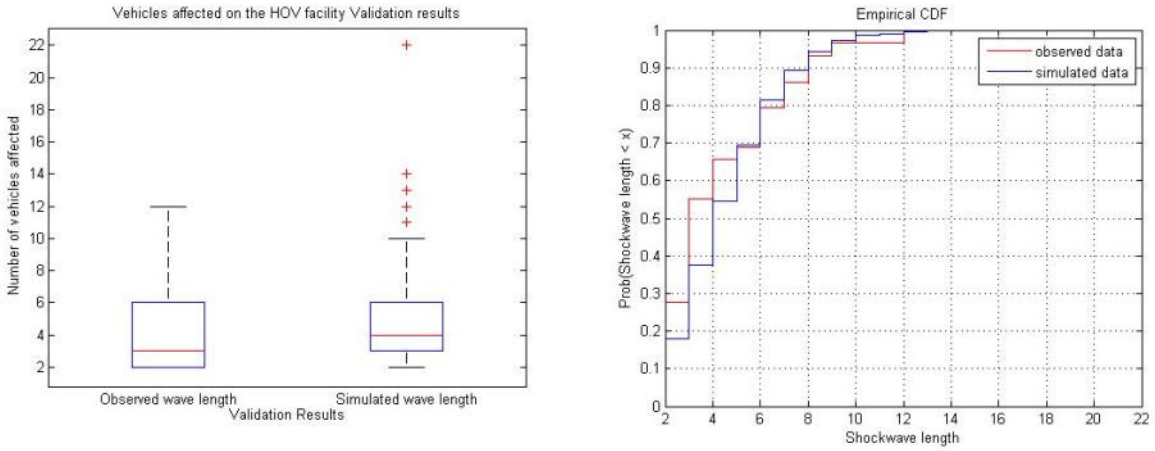

Figure 122. Validation results

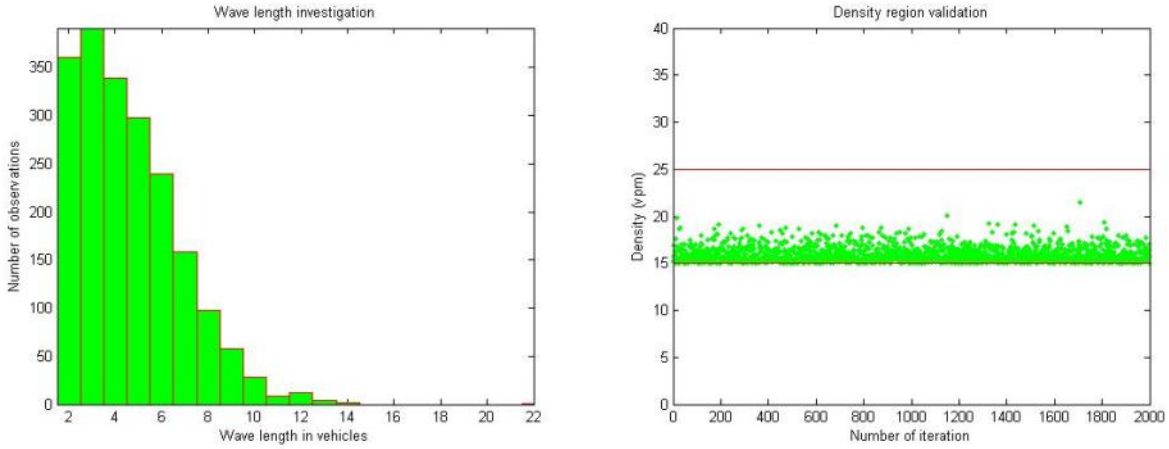

Figure 123. Shockwave length histogram and density region validation

Figure 124, Figure 125, Figure 126 and Figure 127 present the obtained histograms for the various density levels that the location was tested for; starting with a 50 % increase, then implementing a 75 % increase followed by a 100 % increase and finally a 150 % increase. Most of the simulated streams had a corresponding density closer to the lower bound of the region.

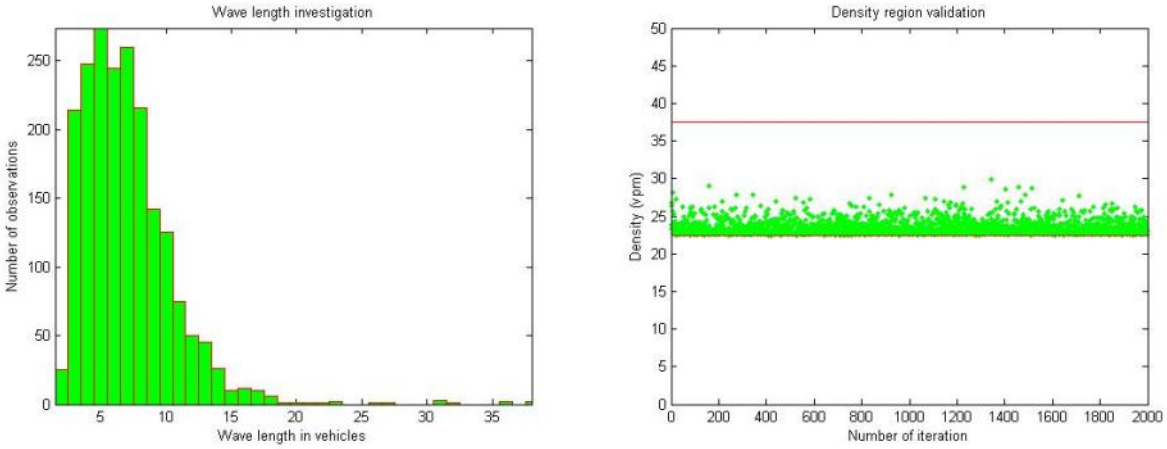

Figure 124. Resulting shockwave histogram for 50 % increase in density

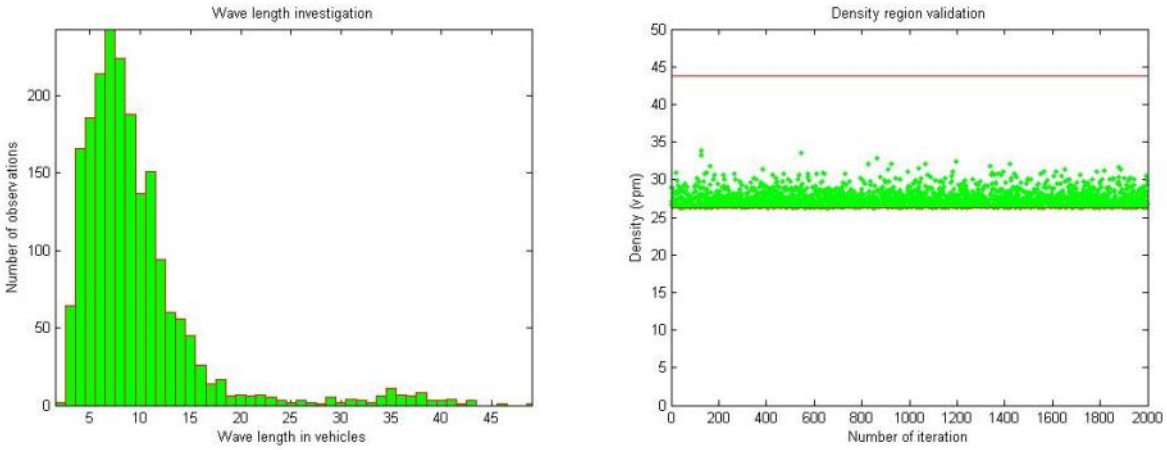

Figure 125. Resulting shockwave histogram for 75 % increase in density

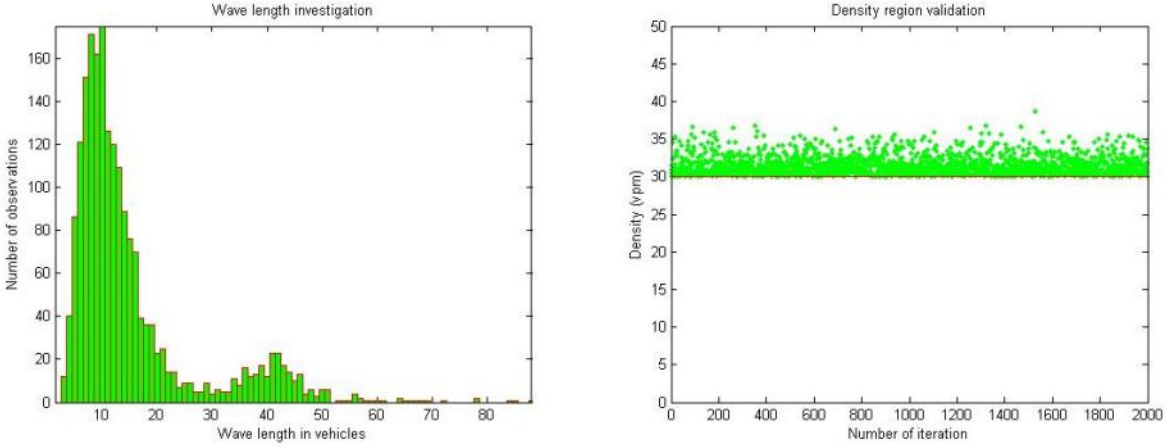

Figure 126. Resulting shockwave histogram for 100 % increase in density

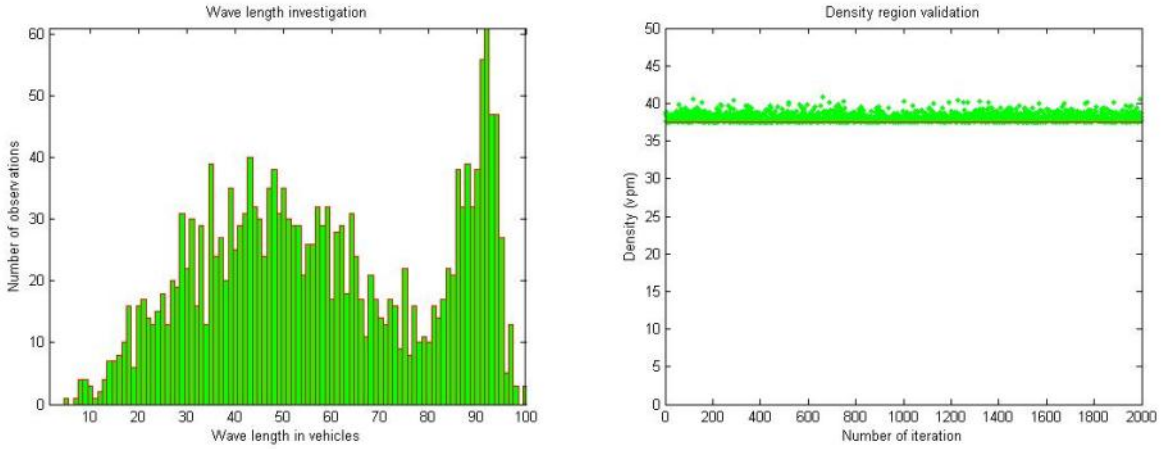

Figure 127. Resulting shockwave histogram for 150 % increase in density

It can be seen once again that for the uninterrupted initial conditions and the smallest of the tested increased demand levels (50 %), the resulting histograms depict an exponential distribution governed by the random character of the event. A further increase in the demand results in shrinking the following distances and develops second peak in the shockwave length distribution in the range of 25 and 35 vehicles. When the increase reaches a region that is significantly over 32 vpm the second peak shifts to the right and includes a larger proportion of the simulated shockwaves. The observed second peak occurring when density is increased by 100 % is significantly milder than that in the case of the Cliff road segment. Finally for densities close to 40 vpm (exceeding the critical density of the facility) a different distribution is observed with most of the observations being in the right section of the histogram indicating the expected flow breakdown.

The comparison between the various levels is illustrated in Figure 128 and Figure 129 by comparing the corresponding cumulative distribution function and the corresponding boxplots. It can be seen that for small increases reaching the operational boundary of the facility the length of the shockwaves does not reach concerning values while after the boundary it appears to become unstable and this results in the observed second peak on the right of the histograms of the simulated distributions.

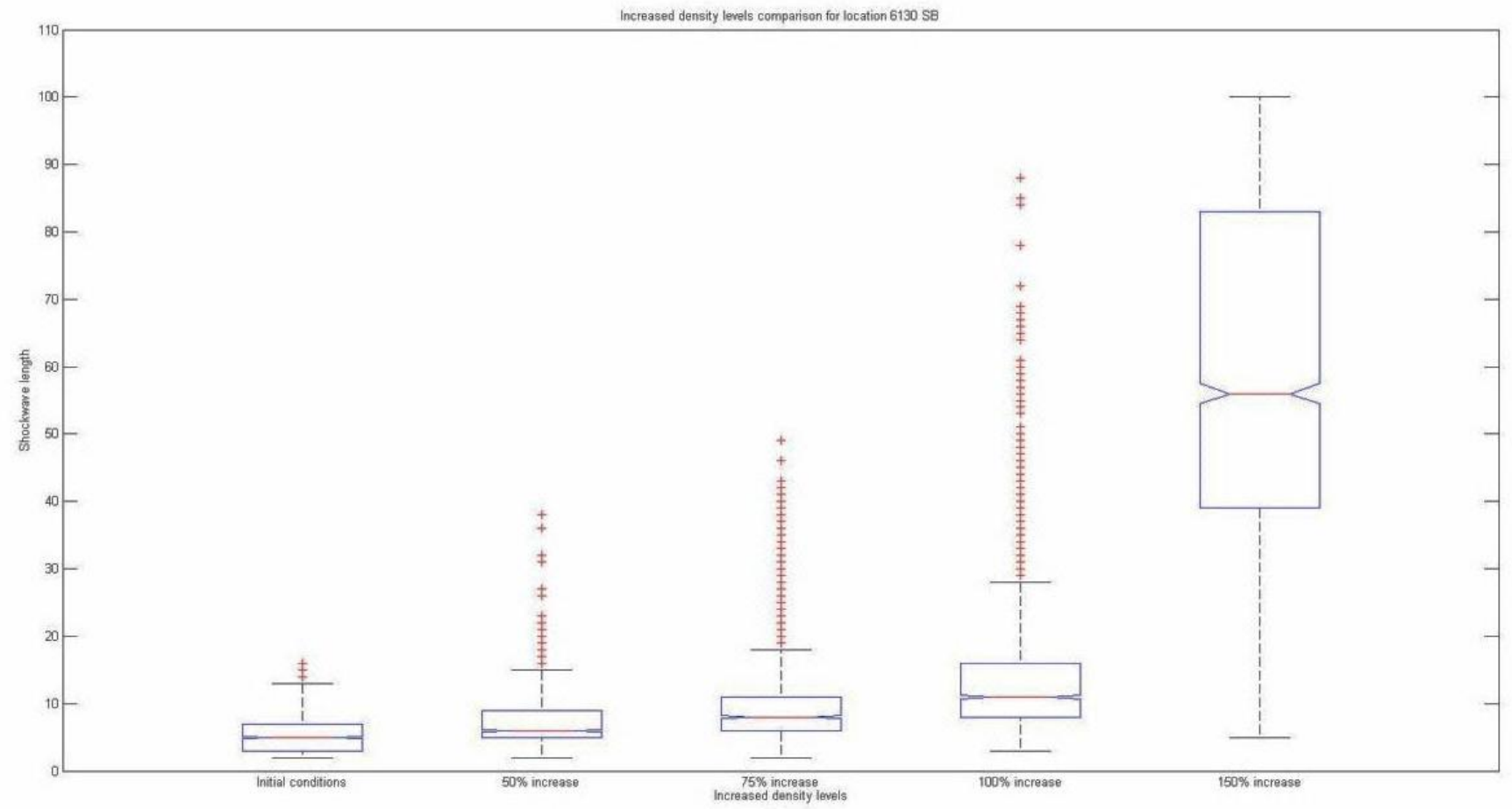

Figure 128. Boxplots of simulated shockwave lengths

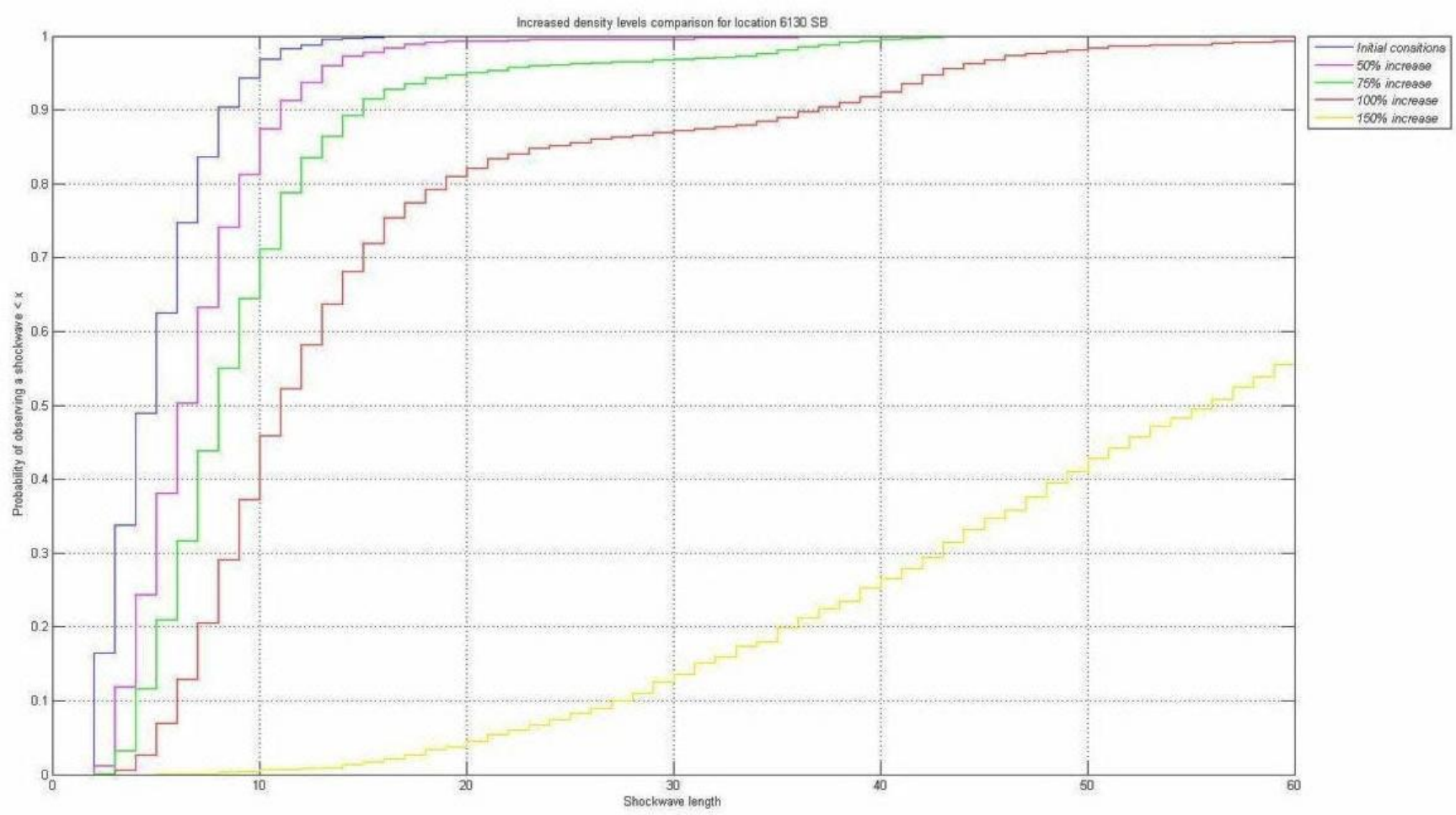

Figure 129. Cumulative distribution functions of simulated shockwave lengths

Southbound between 98th street and 106th street

The same steps performed in the previous two locations were also performed for the segment between 98th street and 106th street. Figure 130 presents a comparison between the simulated and the observed shockwave lengths. In this case the model did not capture the observed lengths at the detail that it did for the case of Cliff road. Once again the boxplots indicate that the general character of the wave propagation was captured. Figure 131 demonstrates the histogram of the simulated wave lengths and the density region validation. Once again in order to make conclusions about the simulated results the two-sample Kolmogorov Smirnov was used. The model did not capture the observed shockwave lengths at a 90% confidence interval but it was concluded that the ability of the model to describe the observations was satisfactory.

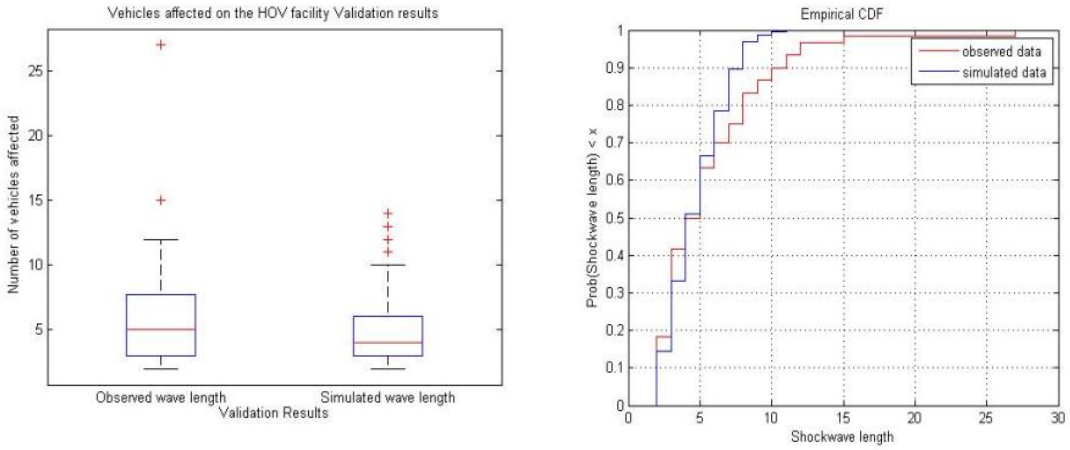

Figure 130. Validation results

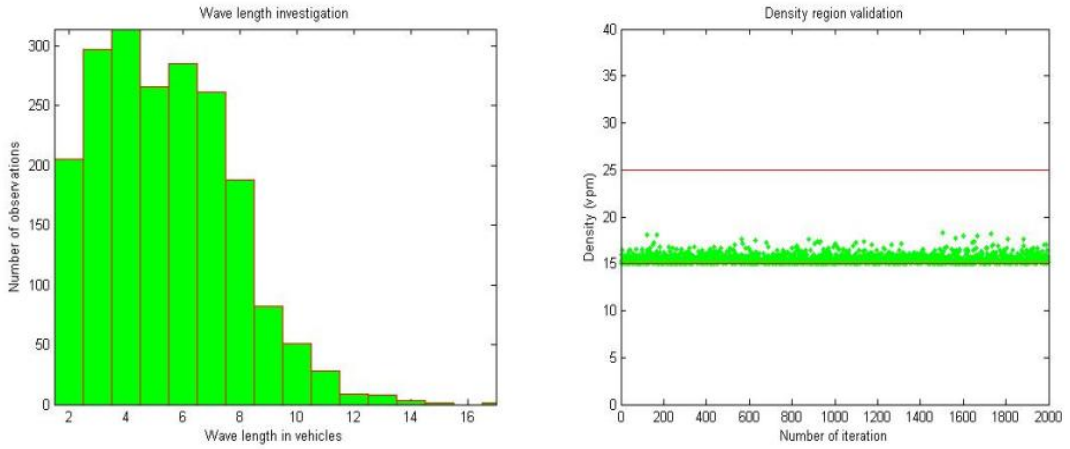

Figure 131. Shockwave length histogram and density region validation

Figure 132, Figure 133 and Figure 134 present the obtained histograms for the various density levels that the location was tested for; starting with a 50 % increase, then implementing a 75 % increase and finally a 100 % increase. The gap acceptance model limited the method's ability to increase density by 150 % since the headway characteristics of the location would result in cases that no gap would be accepted.

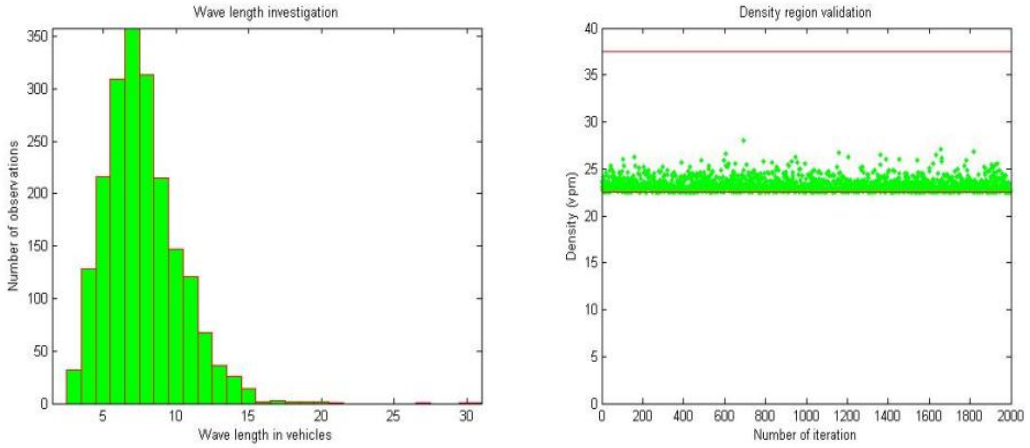

Figure 132. Resulting shockwave histogram for 50 % increase in density

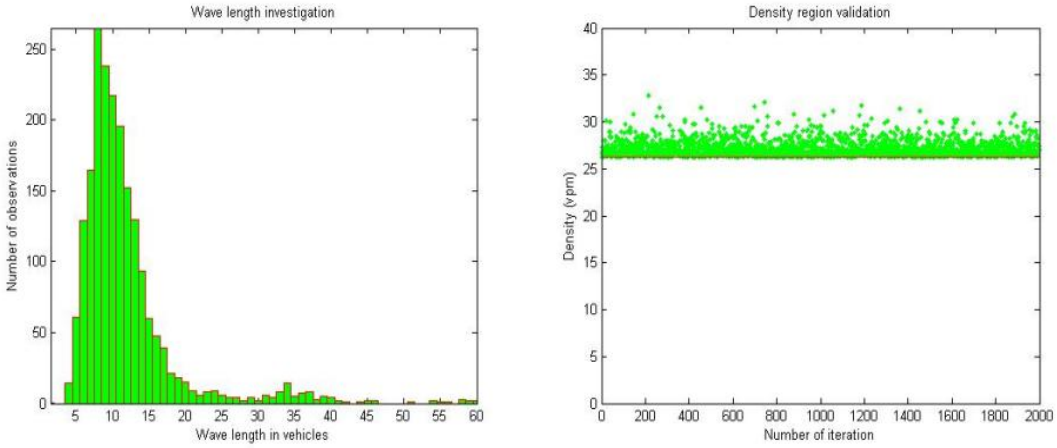

Figure 133. Resulting shockwave histogram for 75 % increase in density

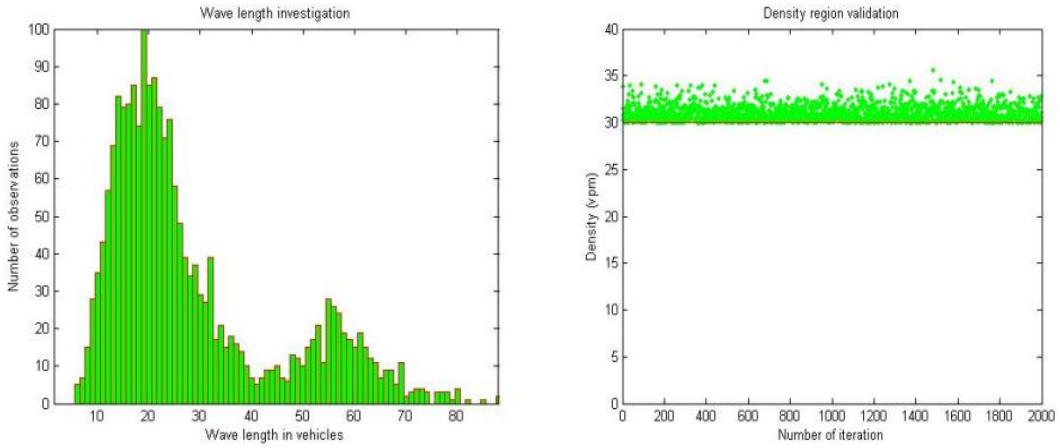

Figure 134. Resulting shockwave histogram for 100 % increase in density

It can be seen that the resulting histograms, for the uninterrupted initial conditions and the smallest of the tested increased demand levels (50 %), result in an exponential shape governed by the random character of the event. Even though a second peak is observed when the density region is increased by 100 %, the proportion of the simulated shockwaves in the right (severe) part of the histogram is a significantly smaller than that corresponding to the previous two locations.

The comparison between the various levels is illustrated in Figure 135 and Figure 136 by comparing the corresponding cumulative distribution functions and the corresponding boxplots. For this location even at increased levels the shockwave lengths do not approach concerning levels except for the case of the maximum examined increase of 100 %.

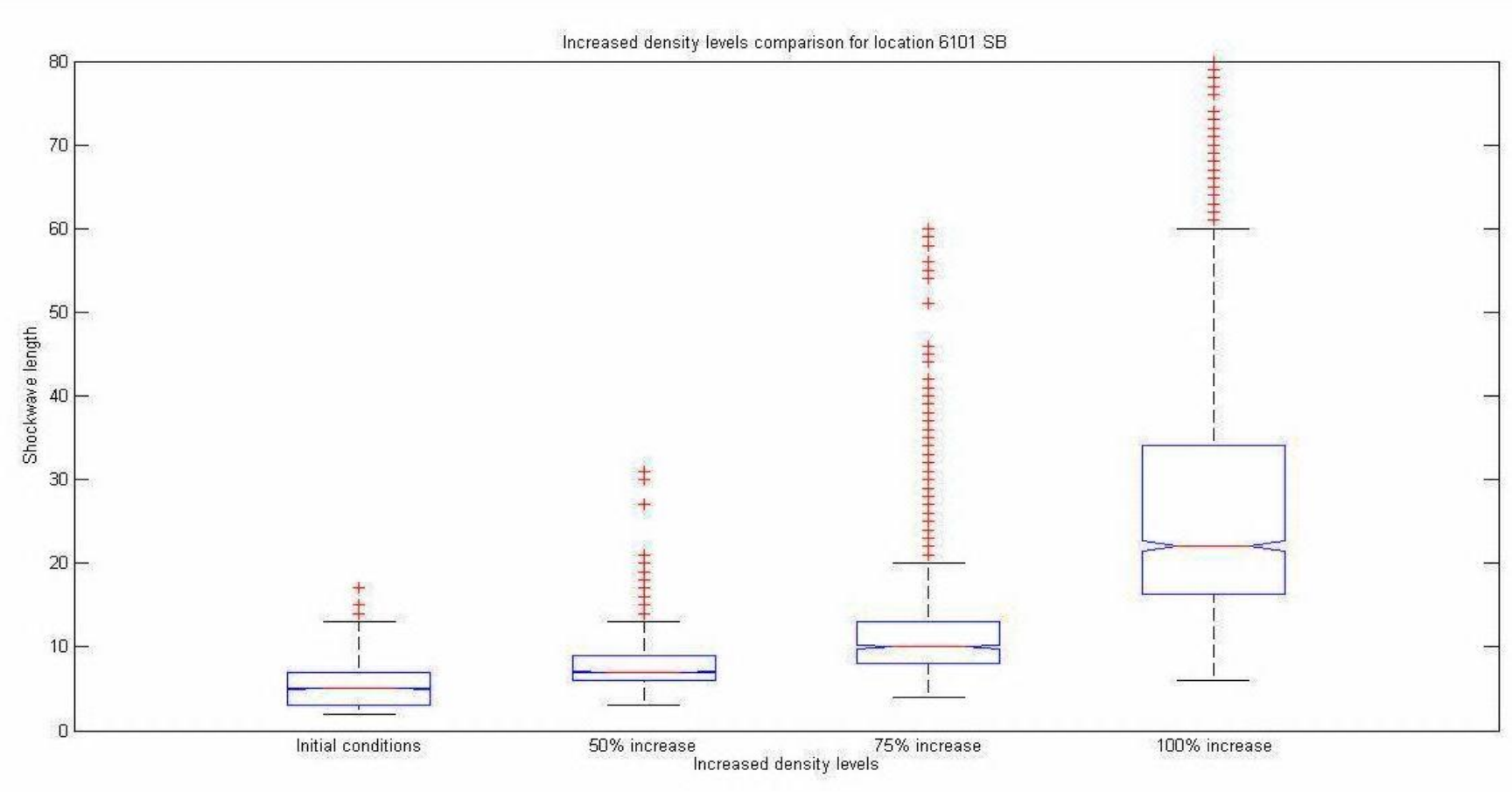

Figure 135. Boxplots of simulated shockwave lengths

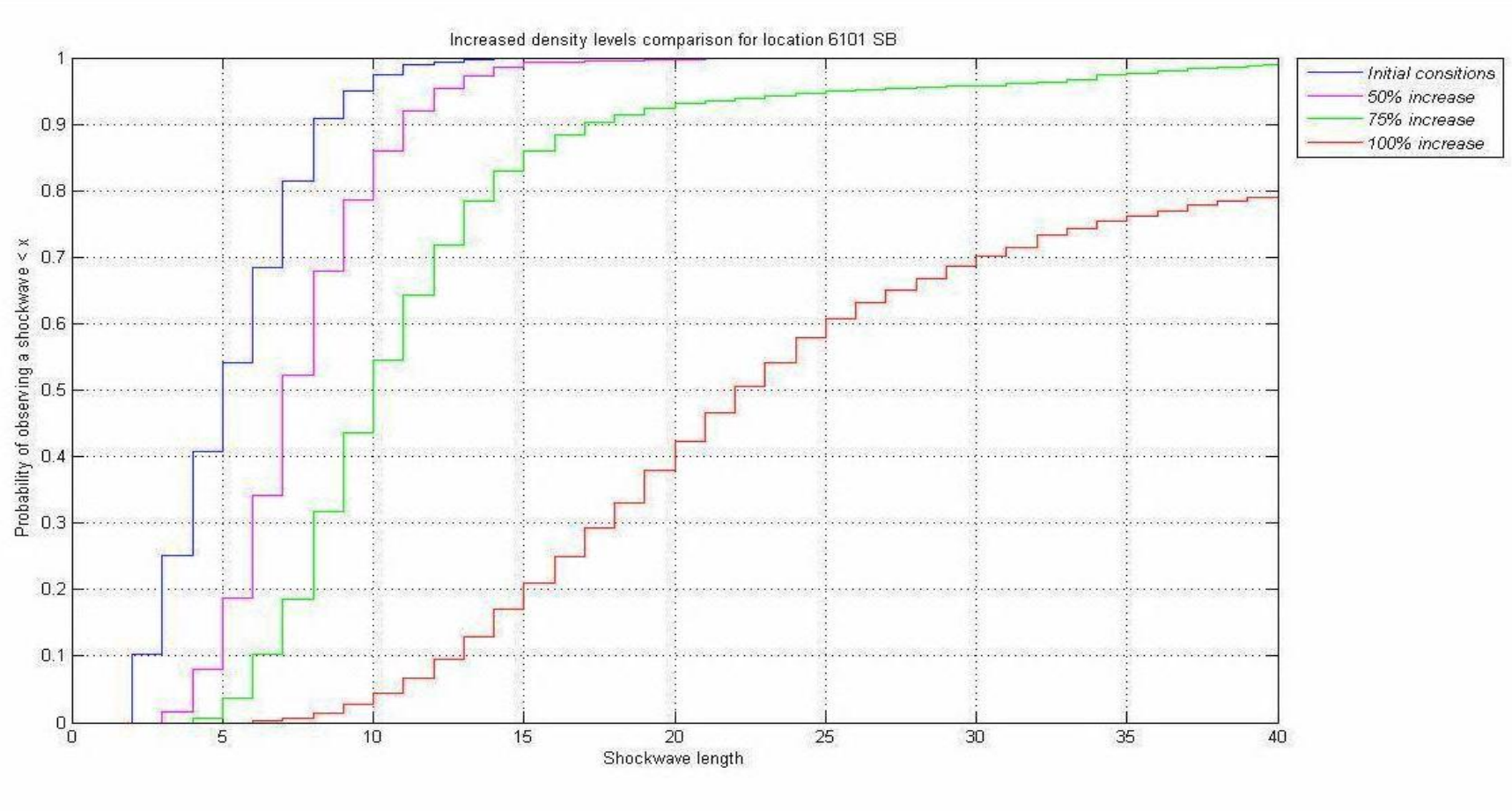

Figure 136. Cumulative Distribution Functions of simulated shockwave lengths

9. Conclusion

This study focused on operational and design features of HOT lanes. HOT lanes' mobility and safety are heavily contingent on the design of zones ("gates") that drivers can use to merge in or out of the facility. During high demand periods, due to the increased friction in these locations, a large speed differential can be observed between the HOT lane and its adjacent lane. Existing methodologies for the design of access zones are limited to engineering judgment or studies that take into consideration an undersized sample of observations. Case in point is the fact that the design philosophes between the two HOT facilities in Minnesota are diametrically opposed. Specifically, the I-394 freeway, the first dynamically priced HOT lane, was designed with a closed access philosophy, meaning that for the greater length of the roadway access to the HOT lane is restricted with only specific short-length sections where access is allowed. In contrast I-35W, the second HOT corridor, was designed with an open access philosophy where lane changes between the HOT and the GPLs are allowed everywhere except for a few specific locations. Naturally this contradiction generates questions as to which design method is better and more importantly what are the safety and mobility considerations in each case.

This project was established to investigate these considerations. The approach followed aimed to observe traffic patterns, selecting ones that can serve as quantifying measurements for mobility and safety. Shockwaves were selected to serve as these surrogate measures. Specifically, shockwave characteristics like frequency and length were utilized as surrogates for mobility and safety. Shockwave length was selected as a surrogate of safety based on the assumption that the more vehicles involved in a slow-and-go maneuver, the higher the possibility a driver will fail to react in a timely manner. Shockwave frequency was selected as a surrogate for mobility under the assumption that the more frequent such cycles are, the greater the impact on the HOT lanes average speed and travel time.

The two facilities of I-394 and I-35W have been operating with no great safety or operational concerns; therefore, this study utilized the patterns of shockwave activity to uncover differences between the two design philosophies and potentially uncover areas of improvement now or in the future. With the help of MnDOT's Regional Traffic Management Center surveillance infrastructure combined with the advanced detection and measurement capabilities of the Minnesota Traffic Observatory (MTO), the length and breadth of the two corridors was observed and analyzed. Finally focusing on specific locations of interest, this study showed that traffic on both HOT facilities can be disrupted by deteriorating conditions on the adjacent GPL although in the current levels of HOT lane utilization such disruptions are minimal. Specifically, the average size of observed shockwaves in any location did not exceed four vehicles with maximums not exceeding 15 vehicles. Although not directly related, observations on the high crash area on I-94 have shown that for the probability of crash to increase to levels requiring attention, shockwaves of 25 vehicles or more are needed.

It is difficult to compare the two design philosophies because they were designed to serve the needs of two distinct roadways. I-394 is operating very well with the closed access

design mainly because the majority of the demand originates from three specific interchanges, I-494, TH-169, and TH-100. The rest of the ramps, comparatively speaking, have much lower demands. As illustrated in this report, this is not the case on I-35W. The interchange density is much higher with entrance ramps very closely spaced and with the majority of those ramps carrying large numbers of HOT eligible vehicles. It would have been very difficult to follow a closed access design on I-35W and preserve the current level of service to the users. Therefore, given the results presented in this report, it would have made little difference in terms of mobility and safety.

The second objective of this study was to develop methodologies that address design issues related to forthcoming and existing HOT facilities. Two such methodologies were developed. The first methodology targeted forthcoming HOT facilities that adopt a closed access philosophy and formed the basis for a software tool capable of defining the OLCRs. The methodology is capable of defining the OLCRs on forthcoming HOT facilities with respect to the positions of entrance or exit ramps. Although the OLCR methodology and tool is primarily useful during the design stage of a HOT, the second tool focuses on existing HOT facilities that follow an open access philosophy and supports operational decisions to allow or restrict access for locations that have been or will reach their operational boundary in the near future. In particular, a shockwave propagation model was developed and captured the shockwave activity on three selected locations of interest on I-35W. After the model was calibrated to reproduce shockwave activity (shockwave lengths) at current traffic conditions, the same activity was reproduced for future demand levels until the examined facilities reached their operational boundary. The results support the validity of the process as the model replicated the distributions of shockwave lengths even at a 90% confidence interval. The developed mechanism was able to force the examined locations up to the boundary by increasing the density of the simulated streams. The boundary was identified as the point in the density domain that the entire simulated stream experienced a disturbance after it was introduced.

The developed methodologies were derived so that their transferability is not affected, and hence they can potentially be used by agencies to design HOT lanes without compromising mobility or safety. Both methodologies were driven by an extensive and diverse data collection process and validated against actual observations.

References

AASHTO, (2004), "Guide for High-Occupancy Vehicle (HOV) Facilities," Washington, D.C.: American Association of State Highway and Transportation Officials.

Ahn, S., Cassidy, M. J., and Laval, J. (2004), "Verification of a Simplified Car-Following Theory," *Transportation Research Part B: Methodological*, 38, 431-440.

Athol, P. (1965), "Headway Groupings," *Chicago Area Expressway Surveillance Project Report, Iss. 14*.

Benekohal, R. F., Kaja-Mohideen, A.-Z., and Chitturi, M. V. (2004), "Methodology for Estimating Operating Speed and Capacity in Work Zones," *Transportation Research Record*, 1883, 103-111.

Box, G. E., Jenkins, G. M., and Reinsel, G. C. (2011), *Time Series Analysis: Forecasting and Control* (Vol. 734), Hoboken, NJ: Wiley.

California Department of Transportation (1991), *High Occupancy Vehicle Guidelines for Planning, Design, and Operations*, Sacramento, CA: State of California, Business, Transportation and Housing Agency.

Cassidy, M. J., Daganzo, C. F., Jang, K., and Chung, K. (2006), "Empirical Reassessment of Traffic Operations: Freeway Bottlenecks and the Case for HOV Lanes." *Research Reports*, Institute of Transportation Studies, University of California Berkeley.

Castillo, J. M. d. (2001), "Propagation of Perturbations in Dense Traffic Flow: A Model and Its Implications," *Transportation Research Part B: Methodological*, 35, 367-389.

Daganzo, C. F. (1994), "The Cell Transmission Model: A Dynamic Representation of Highway Traffic Consistent with the Hydrodynamic Theory," *Transportation Research Part B: Methodological*, 28, 269-287.

Federal Highway Administration (2008), *Managed Lanes: A Primer*, Washington, D.C.: US Department of Transportation.

Fuhs, C. A. (1990), "High-Occupancy Vehicle Facilities: A Planning, Design, and Operation Manual." New York, NY: Parsons Brinckerhoff Quade & Douglas, Inc.

Gaur, A., and Mirchandani, P. (2001), "Method for Real-Time Recognition of Vehicle Platoons," *Transportation Research Record*, 1748, 8-17.

Gazis, D. C., Herman, R., and Rothery, R. W. (1961), "Nonlinear Follow-the-Leader Models of Traffic Flow," *Operations Research*, 9, 545-567.

Gipps, P. G. (1981), "A Behavioural Car-Following Model for Computer Simulation," *Transportation Research Part B: Methodological*, 15, 105-111.

Godunov, S. K. (1959), "A Difference Method for Numerical Calculation of Discontinuous Solutions of the Equations of Hydrodynamics," *Matematicheskii Sbornik*, 89, 271-306.

Greenshields, B. D., Bibbins, J., Channing, W., and Miller, H. (1935), "A Study of Traffic Capacity," *Proceedings of the Annual Meeting - Highway Research Board*, 448-447.

Greenwood, M. (1926), "A Report on the Natural Duration of Cancer," *Reports on Public Health and Medical Subjects*, London: H.M.S.O.

Immers, L., and Logghe, S. (2002), "Traffic Flow Theory," Heverlee, Belgium: Katholieke Universiteit Leuven.

Jabari, S. E., and Liu, H. X. (2012), "A Stochastic Model of Traffic Flow: Theoretical Foundations," *Transportation Research Part B: Methodological*, 46, 156-174.

Johansson, G., and Rumer, K. (1971), "Driver's brake reaction time", *Human Factors*, Vol.13, No 1.

Kim, T., and Zhang, H. (2008), "A Stochastic Wave Propagation Model," *Transportation Research Part B: Methodological*, 42, 619-634.

Koopmans, L. H., Owen, D. B., and Rosenblatt, J. (1964), "Confidence Intervals for the Coefficient of Variation for the Normal and Log Normal Distributions," *Biometrika*, 51, 25-32.

Kuhn, B. T., et al. (2005), *Managed Lanes Handbook*, Technical, Texas Transportation Institute, Texas A&M University System.

Kuhne, R., and Michalopoulos, P. (1997), "Continuum Flow Models," *Traffic Flow Theory: A State of the Art Report—Revised Monograph on Traffic Flow Theory*, Oak Ridge National Laboratory, Oak Ridge, TN, 432.

Lighthill, M. J., and Whitham, G. B. (1955), "On Kinematic Waves. II. A Theory of Traffic Flow on Long Crowded Roads," *Proceedings of the Royal Society of London: Series A. Mathematical and Physical Sciences*, 229, 317-345.

Liu, X., et al. (2011), "Analysis of Operational Interactions between Freeway Managed Lanes and Parallel, General Purpose Lanes," *Transportation Research Record*, 2262, 62-73.

Liu, X. C., Wang, Y., Schroeder, B. J., and Rouphail, N. M. (2012), "Quantifying Cross-Weave Impact on Capacity Reduction for Freeway Facilities with Managed Lanes," *Transportation Research Record*, 2278, 171-179.

May, A. D. (1990), *Traffic Flow Fundamentals*, Englewood Cliffs, N.J.: Prentice Hall.

Menendez, M., and Daganzo, C. F. (2007), "Effects of HOV Lanes on Freeway Bottlenecks," *Transportation Research Part B: Methodological*, 41, 809-822.

Nelder, J. A., and Wedderburn, R. W. (1972), "Generalized Linear Models," *Journal of the Royal Statistical Society. Series A (General)*, 370-384.

Newell, G. F. (2002), "A Simplified Car-Following Theory: A Lower Order Model," *Transportation Research Part B: Methodological*, 36, 195-205.

Texas Transportation Institute (1998), *HOV Systems Manual*, Washington, D.C.: Transportation Research Board.

Transportation Research Board (2000), *Highway Capacity Manual,* Washington, D.C.: Transportation Research Board, National Research Council.

Wellner, J. A. (1977), "A Glivenko-Cantelli Theorem and Strong Laws of Large Numbers for Functions of Order Statistics," *The Annals of Statistics*, 473-480.

Williams, J. C., Mattingly, S. P., and Yang, C. (2010), "Assessment and Validation of Managed Lanes Weaving and Access Guidelines," Technical, Arlington, TX: University of Texas at Arlington.

Windover, J. R., and Cassidy, M. J. (2001), "Some Observed Details of Freeway Traffic Evolution," *Transportation Research Part A: Policy and Practice*, 35, 881-894.

Yang, C., Mattingly, S. P., Williams, J. C., and Kim, H. (2011), "Development of Managed-Lane Access Guidelines Based on Gap Acceptance Theory," *Transportation Research Record*, 2257, 95-102.

Appendix A – Optimal Lane Changing Tool

The following Matlab code represents the tool for the optimal lane changing region estimation. Two sets of data are required input: 1) time series information for each lane of the section starting about 500 feet upstream of the merge area describing the evolution of density in 5-minute increments, and 2) the parameters of a Greenshields fitted fundamental diagram for each lane based on several days' worth of volume and density measurements. After these two sets of data are read in, the script iterates internally to generate traffic streams and create trajectories for vehicles seeking to enter the HOT lane. The script terminates when sufficient sample trajectories have been generated such that the distribution of trajectory lengths is stable. The function outputs histogram data of trajectory lengths. All simulated trajectories are binned into 50-foot groups up to roughly 1 mile in length.

```
% Code for determining gate locations for closed access design
% ------------------------------------------------------------------------------
% Inputs to the program:
%         LaneDensityTimeSeries.xlsx – Density (veh/mi/lane) for each lane in 5-minute blocks
%         FDparam.xlsx – Fundamental diagram parameters for each lane: freeflow speed and jam density
% ------------------------------------------------------------------------------

% Create Blocks of iterations and check with the two sample Kolmogorov-
% Smirnov Test about the stability of the outputted distribution
total = 0;
blockiter = 0;
densevol1 = xlsread('LaneDensityTimeSeries.xlsx');
serend = length(densevol1);
kappa = 1;

for kappa = 1:max(serend)
   h = 1;
   clearvars blockiter
   blockiter = 0;
   while h > 0;
      blockiter = blockiter + 1;
      % Load Fundamental diagram parameters
      fdparam = xlsread('FDparam.xlsx');
      fdparam1 = fdparam(1,:);
      fdparam2 = fdparam(2,:);
      fdparam3 = fdparam(3,:);
      fdparam4 = fdparam(4,:);
      fdparamhot = fdparam(5,:);
      % Constructing the other lanes time series and rimming the over capacity states
      density(:,1:5) = densevol1(kappa,1:5);

      % Trimming the over capacity values && Define speeds for all intervals
      a = 1;
      b = 3000;
      dso = size(density);
      for i = 1:dso(1)
         for f = a:b;
            speeds(f,1) = 1.4667*(fdparam1(1,1) - fdparam1(1,1)/fdparam1(1,2)* density(i,1));
         end
         a = a + 3000;
         b = b + 3000;
```

```
end
a = 1;
b = 3000;
for i = 1:1:dso(1)
   for f = a:b;
      speeds(f,2) = 1.4667 * (fdparam2(1,1) - fdparam2(1,1)/fdparam2(1,2)* density(i,2));
   end
   a = a + 3000;
   b = b + 3000;
end
a = 1;
b = 3000;
for i = 1:1:dso(1)
   for f = a:b;
      speeds(f,3) = 1.4667 * (fdparam3(1,1) - fdparam3(1,1)/fdparam3(1,2)* density(i,3));
   end
   a = a + 3000;
   b = b + 3000;
end
a = 1;
b = 3000;
for i = 1:1:dso(1)
   for f = a:b;
      speeds(f,4) = 1.4667 * (fdparam4(1,1) - fdparam4(1,1)/fdparam4(1,2) * density(i,4));
   end
   a = a + 3000;
   b = b + 3000;
end
a = 1;
b = 3000;
for i = 1:1:dso(1)
   for f = a:b;
      speeds(f,5) = 1.4667*(fdparamhot(1,1) - fdparamhot(1,1)/fdparamhot(1,2)* density(i,5));
   end
   a = a + 3000;
   b = b + 3000;
end

% set the counters for matrix construction
residtrim = zeros(5,1);
legbeg = ones(5,1);
legennd = zeros(5,1);
timecount = zeros(5,1);

% Generate headways for the whole time series
for i = 1:dso(1)
   %Lane1
   intervln1 = procdecfun(density(i,1),residtrim(1,1),fdparam1);
   legennd(1,1) = legennd(1,1) + length(intervln1) - 1;
   headway(legbeg(1,1):legennd(1,1),1,1) = round(intervln1(1:(end-1),1)*10)/10;
   legbeg(1,1) = legennd(1,1) + 1;
   residtrim(1,1) = intervln1(end,1);

   %Lane2
   intervln2 = procdecfun(density(i,2),residtrim(2,1),fdparam2);
```

```
    legennd(2,1) = legennd(2,1) + length(intervln2) - 1;
    headway(legbeg(2,1):legennd(2,1),2,1) = round(intervln2(1:(end-1),1)*10)/10;
    legbeg(2,1) = legennd(2,1) + 1;
    residtrim(2,1) = intervln2(end,1);

    %Lane3
    intervln3 = procdecfun(density(i,3),residtrim(3,1),fdparam3);
    legennd(3,1) = legennd(3,1) + length(intervln3) - 1;
    headway(legbeg(3,1):legennd(3,1),3,1) = round(intervln3(1:(end-1),1)*10)/10;
    legbeg(3,1) = legennd(3,1) + 1;
    residtrim(3,1) = intervln3(end,1);

    %Lane4
    intervln4 = procdecfun(density(i,4),residtrim(4,1),fdparam4);
    legennd(4,1) = legennd(4,1) + length(intervln4) - 1;
    headway(legbeg(4,1):legennd(4,1),4,1) = round(intervln4(1:(end-1),1)*10)/10;
    legbeg(4,1) = legennd(4,1) + 1;
    residtrim(4,1) = intervln4(end,1);

    %Lane5
    intervln5 = procdecfun(density(i,5),residtrim(5,1),fdparamhot);
    legennd(5,1) = legennd(5,1) + length(intervln5) - 1;
    headway(legbeg(5,1):legennd(5,1),5,1) = round(intervln5(1:(end-1),1)*10)/10;
    legbeg(5,1) = legennd(5,1) + 1;
    residtrim(5,1) = intervln5(end,1);
end
% After the initial conditions are defined create a sequence and assign a time stamp
timedim = cumsum(headway)*10;
timedim = round(timedim);
stdev1 = 3;
horiz = 5*60*10;% define the length of the time
timecount = 0;
thres = exprnd(1,[1000,5]);

% Lane 1 massive trajectory generation
b = 1;
for i = timedim(1,1):(horiz-200)
    if timedim(b,1) == i
        Xone(i-1,b,1) = 10;
        speed1(1,b) = speeds(i,1) + 10;
        % Select a region around the macro speed and let the individual speeds fluctuate around it.
        while (speed1(1,b) >= speeds(i,1) + stdev1 || speed1(1,b) <= speeds(i,1) - stdev1)
            speed1(1,b) = normrnd(speeds(i,1),3);
        end
        b = b + 1;
    end
    % update the X matrix based on the assigned speeds
    dimone = size(Xone);
    Xone(i,:,1) = Xone(i-1,:,1) + 0.1 * speed1(1,:);

    % match the speed of the proceeding vehicles if we have the chance of a collision
    for kl = 2:(dimone(2))
        if abs(Xone(i,kl,1) - Xone(i,kl-1,1)) <= thres(kl,1) * (speed1(1,kl)+speed1(1,kl-1))/2;
            speed1(1,kl) = speed1(1,kl-1);
        end
```

```
   end
end

% Lane 2 massive trajectory generation
b = 1;
for i = timedim(1,2):(horiz-200)
   if timedim(b,2) == i
      Xtwo(i-1,b,1) = 0;
      speed2(1,b) = speeds(i,2) + 10;
         % Select a region around the macro speed and let the individual speeds fluctuate around it.
      while (speed2(1,b) >= speeds(i,2) + stdev1 || speed2(1,b) <= speeds(i,2) - stdev1)
            speed2(1,b) = normrnd(speeds(i,2),3);
         end
      b = b + 1;
   end
   % update the X matrix based on the assigned speeds
   dimone = size(Xtwo);
         Xtwo(i,:,1) = Xtwo(i-1,:,1) + 0.1 * speed2(1,:);

      % match the speed of the proceeding vehicles if we have the chance of a collision
      for kl = 2:(dimone(2))
         if abs(Xtwo(i,kl,1) - Xtwo(i,kl-1,1)) <= thres(kl,2) *(speed2(1,kl)+speed2(1,kl-1))/2;
            speed2(1,kl) = speed2(1,kl-1);
         end
      end
end

% Lane 3 massive trajectory generation
b = 1;
for i = timedim(1,3):(horiz-200)
   if timedim(b,3) == i
      Xthree(i-1,b,1) = 0;
      speed3(1,b) = speeds(i,3) + 10;
      % Select a region around the macro speed and let the individual speeds fluctuate around it.
      while (speed3(1,b) >= speeds(i,3) + stdev1 || speed3(1,b) <= speeds(i,3) - stdev1)
         speed3(1,b) = normrnd(speeds(i,3),3);
      end
      b = b + 1;
   end
   % update the X matrix based on the assigned speeds
   dimone = size(Xthree);
         Xthree(i,:,1) = Xthree(i-1,:,1) + 0.1 * speed3(1,:);

      % match the speed of the proceeding vehicles if we have the chance of a collision
      for kl = 2:(dimone(2))
         if abs(Xthree(i,kl,1) - Xthree(i,kl-1,1)) <= thres(kl,3) *(speed3(1,kl)+speed3(1,kl-1))/2;
            speed3(1,kl) = speed3(1,kl-1);
         end
      end
end

% Lane 4 massive trajectory generation
b = 1;
for i = timedim(1,4):(horiz-200)
   if timedim(b,4) == i
```

```
      Xfour(i-1,b,1) = 0;
      speed4(1,b) = speeds(i,4) + 10;
        % Select a region around the macro speed and let the individual speeds fluctuate around it.
        while (speed4(1,b) >= speeds(i,4) + stdev1 || speed4(1,b) <= speeds(i,4) - stdev1)
        speed4(1,b) = normrnd(speeds(i,4),3);
        end
      b = b + 1;
    end
    % update the X matrix based on the assigned speeds
    dimone = size(Xfour);
        Xfour(i,:,1) = Xfour(i-1,:,1) + 0.1 * speed4(1,:);

      % match the speed of the proceeding vehicles if we have the chance of a collision
      for kl = 2:(dimone(2))
        if abs(Xfour(i,kl,1) - Xfour(i,kl-1,1)) <= thres(kl,4) *(speed4(1,kl)+speed4(1,kl-1))/2;
          speed4(1,kl) = speed4(1,kl-1);
        end
      end
end

% Lane 5 massive trajectory generation
b = 1;
for i = timedim(1,5):(horiz-200)
    if timedim(b,5) == i
      Xfive(i-1,b,1) = 0;
      speed5(1,b) = speeds(i,5) + 10;
        % Select a region around the macro speed and let the individual speeds fluctuate around it.
        while (speed5(1,b) >= speeds(i,5) + stdev1 || speed5(1,b) <= speeds(i,5) - stdev1)
        speed5(1,b) = normrnd(speeds(i,5),3);
        end
      b = b + 1;
    end
    % update the X matrix based on the assigned speeds
    dimone = size(Xfive);
        Xfive(i,:,1) = Xfive(i-1,:,1) + 0.1 * speed5(1,:);

      % match the speed of the proceeding vehicles if we have the chance of a collision
      for kl = 2:(dimone(2))
        if abs(Xfive(i,kl,1) - Xfive(i,kl-1,1)) <= thres(kl,5) *(speed5(1,kl)+speed5(1,kl-1))/2;
          speed5(1,kl) = speed5(1,kl-1);
        end
      end
end
disp('General Purpose lanes trajectory extraction completed')

%% start dropping vehicles from the ramp
a = 1;
b = 1;
Tveh1(200,1) = 1;
Tveh2(199,1) = 300;
tou = zeros(5,5000);
testspeed(2:6,1) = speeds(1,1:5) + 10;
% Select a region around the macro speed and let the individual speeds fluctuate around it.
for i = 2:6
```

```
        while (testspeed(i,1) >= (speeds(200,i-1) + stdev1) || testspeed(i,1) <= speeds(200,i-1) - stdev1 &&
testspeed(i,1) >= speeds(200,i-1))
            testspeed(i,1) = normrnd(speeds(200,i-1),2);
          end
      end

      % Unimodal TAP
      flat = [-1;-1;-1;-1;-1];
      while flat <= 1
        flat = normrnd(0,2.2,[5,1]);
      end

      reac(1:5,1) = round(flat * 10);

      % Sample a vehicle length for the test vehicle
      g = randi([1 100]);
      perclan = [52 95 100];
      if g <= perclan(1);
        testlength(1) = 14;
      elseif perclan(1) < g <= perclan(2);
        testlength(1)= 17;
      elseif  perclan(2) < g <= perclan(3)
        testlength(1) = 40;
      end

      upbod(1) = testspeed(2,1);
      testspeed(1,1) = 10 * 1.4667;

      for i = 200:(horiz-200)
        for k = a:b;
          clear targpos gap

          % Time on lane 0
          if (Tveh1(i,k) == 1 && tou(1,k) == 0)
            if testspeed(1,k) >= upbod(k)
            Tveh2(i,k) = Tveh2(i-1,k) + testspeed(1,k) * 0.1;
            else
              Tveh2(i,k) = Tveh2(i-1,k) + testspeed(1,k) * 0.1 + 0.5 * 7 * 0.01;
              testspeed(1,k) = testspeed(1,k) + 0.1 * 7;
            end
            targpos(:,1) = Xone(i,:)';
            targpos(targpos == 0) = [];
            gap = leadlag(targpos,Tveh2(i,k),testlength(k));
              % Gap acceptance for lane 1
                gappacc = gapeval(gap,speeds(i,1)/1.4667,testspeed(1,k)/1.4667);
                % If the gap is accepted
                if gappacc >= 0.5;
                  % Find the time that the lane change will take after the driver accepts a gap.
                  lagt = 20;
                  while (lagt >= 10 || lagt<=1);
                  lagt = normrnd(2.8,0.6);
                  end
                  lagt = round(lagt*10);
                  for p = 1:lagt
                    Tveh1(i+p,k) = 1;
```

```
            Tveh2(i+p,k) = Tveh2(i+p-1,k) + 0.1 * testspeed(1,k);
          end
          tou(1,k) = 1;
          Tveh1(i+p+1,k) = 2;
        else Tveh1(i+1,k) = 1;
        end

% Time on lane 1
elseif  (Tveh1(i,k) == 2 && tou(2,k)==0);
   Tveh2(i,k) = Tveh2(i-1,k) + testspeed(2,k) * 0.1;
   targpos(:,1) = Xtwo(i,:);
   targpos(targpos == 0) = [];
   gap = leadlag(targpos,Tveh2(i,k),testlength(k));
      % Gap acceptance for lane 2
        gappacc = gapeval(gap,speeds(i,2)/1.4667,testspeed(2,k)/1.4667);
        % Hold the vehicle for one reaction time before looking for a gap
        lad = Tveh1(:,k);
        lad = lad(lad == 2);
        if length(lad)<=reac(2,k)
           gappacc = 0;
        end
        % If the gap is accepted
        if gappacc >= 0.5;
          lagt = 20;
          while (lagt >= 10 || lagt <= 1);
          lagt = normrnd(2.8,0.6);
          end
          lagt = round(lagt*10);
          for p = 1:lagt
             Tveh1(i+p,k) = 2;
             Tveh2(i+p,k) = Tveh2(i+p-1,k) + 0.1 * testspeed(2,k);
          end
          tou(2,k) = 1;
          Tveh1(i+p+1,k) = 3;
        else Tveh1(i+1,k) = 2;
        end
% Time on lane 2
elseif  (Tveh1(i,k) == 3 && tou(3,k)==0);
   Tveh2(i,k) = Tveh2(i-1,k) + testspeed(3,k) * 0.1;
   targpos(:,1) = Xthree(i,:);
   targpos(targpos == 0) = [];
   gap = leadlag(targpos,Tveh2(i,k),testlength(k));
      % Gap acceptance for lane 1
        gappacc = gapeval(gap,speeds(i,3)/1.4667,testspeed(3,k)/1.4667);
        % Hold the vehicle for one reaction time before looking for a gap
        lad = Tveh1(:,k);
        lad = lad(lad == 3);
        if length(lad) <= reac(3,k)
           gappacc = 0;
        end
        % If the gap is accepted
        if gappacc >=0.5;
          lagt = 20;
          while (lagt >= 10 || lagt<=1);
          lagt = normrnd(2.8,0.6);
```

```
            end
            lagt = round(lagt*10);
            for p = 1:lagt
               Tveh1(i+p,k) = 3;
               Tveh2(i+p,k) = Tveh2(i+p-1,k) + 0.1 * testspeed(3,k);
            end
            tou(3,k) = 1;
            Tveh1(i+p+1,k) = 4;
         else Tveh1(i+1,k) = 3;
         end
% Time on lane 3
elseif  (Tveh1(i,k) == 4 && tou(4,k)==0);
   Tveh2(i,k) = Tveh2(i-1,k) + testspeed(4,k)* 0.1;
   targpos(:,1) = Xfour(i,:);
   targpos(targpos == 0) = [];
   gap = leadlag(targpos,Tveh2(i,k),testlength(k));
      % Gap acceptance for lane 1
         gappacc = gapeval(gap,speeds(i,4)/1.4667,testspeed(4,k)/1.4667);
         % Hold the vehicle for one reaction time before looking for a gap
         lad = Tveh1(:,k);
         lad = lad(lad == 4);
         if length(lad) <= reac(4,k)
            gappacc = 0;
         end
         % If the gap is accepted
         if gappacc >= 0.5;
            lagt = 20;
            while (lagt >= 10 || lagt<=1);
            lagt = normrnd(2.8,0.6);
            end
            lagt = round(lagt*10);
            for p = 1:lagt
               Tveh1(i+p,k) = 4;
               Tveh2(i+p,k) = Tveh2(i+p-1,k) + 0.1 * testspeed(4,k);
            end
            tou(4,k) = 1;
            Tveh1(i+p+1,k) = 5;
         else Tveh1(i+1,k) = 4;
         end
% Time on lane 4
elseif  (Tveh1(i,k) == 5 && tou(5,k)==0);
   Tveh2(i,k) = Tveh2(i-1,k) + testspeed(5,k)* 0.1;
   targpos(:,1) = Xfive(i,:);
   targpos(targpos == 0) = [];
   gap = leadlag(targpos,Tveh2(i,k),testlength(k));
      % Gap acceptance for lane 1
         gappacc = gapeval(gap,speeds(i,5)/1.4667,testspeed(5,k)/1.4667);
         % Hold the vehicle for one reaction time before looking for a gap
         lad = Tveh1(:,k);
         lad = lad(lad == 5);
         if length(lad) <= reac(5,k)
            gappacc = 0;
         end
         % If the gap is accepted
         if gappacc >= 0.5;
```

```
                lagt = 20;
                while (lagt >= 10 || lagt<=1);
                lagt = normrnd(2.8,0.6);
                end
                lagt = round(lagt*10);
                for p = 1:lagt
                   Tveh1(i+p,k) = 5;
                   Tveh2(i+p,k) = Tveh2(i+p-1,k) + 0.1 * testspeed(4,k);
                end
                tou(5,k) = 1;
                Tveh1(i+p+1,k) = 6;
              else Tveh1(i+1,k) = 5;
              end
        % Reset the counters
        elseif Tveh1(i,a) == 6
            a = a + 1;
        end
      end

      if Tveh2(i-1,k) >= 500;
          b = b + 1;
          Tveh1(i+1,b) = 1;
          Tveh2(i,b) = 300;
          testspeed(2:6,b) = speeds(i,1:5) + 10;
          % Assign speed to the new vehicle for all the lanes
            for u = 2:6
              while (testspeed(u,b) >= (speeds(i,u-1) + stdev1) || testspeed(u,b) <= speeds(i,u-1) - stdev1 &&
testspeed(u,b) >= speeds(i,u-1))
                  testspeed(u,b) = normrnd(speeds(i,u-1),2);
              end
            end
            upbod(b) = testspeed(2,b);
            testspeed(1,b) = 10 * 1.4667;

            % Unimodal TAP
            flat = [-1;-1;-1;-1;-1];
                while flat <= 1
                flat = normrnd(0,2.2,[5,1]);
                end
            reac(1:5,b) = round(flat * 10);

          % Assign vehicle length
          g = randi([1 100]);
          perclan = [52 95 100];
            if g <= perclan(1);
              testlength(b) = 14;
            elseif perclan(1) < g <= perclan(2);
              testlength(b)= 20;
            elseif  perclan(2) < g <= perclan(3)
              testlength(b) = 40;
            end
      end
    end

    %% Counting the time spent on each lane
```

```
    marg = size(Tveh1);
    a = 1;
    for i = 1:marg(2)
      totaldist(i,1) = max(Tveh2(:,i)) - 300;
    testtraj = Tveh1(:,i);
    testtraj(testtraj == 0) = [];
      b = 0;
      if max(testtraj) == 6;
        for h = 1:length(testtraj)
         if testtraj(h,1) == a
           b = b + 1;
         else a = a + 1;
            increm(a-1,i) = b;
            b = 1;
         end
        end
      end
      % Reset the counter
      if a == 6;
        a = 1;
      end
      clear testtraj
    end
    disp('End of Block')
    disp(blockiter)
    base = total(:,kappa);
    base(base == 0) = [];
    % Perform the 2 sample Kolmogorov Smirnov Test
        if blockiter >= 2
          h = kstest2(base,[base;totaldist],0.95);
        end
        dim = length(totaldist) + length(base);
    total(1:dim,kappa) = [base;totaldist];
    clearvars -except total h blockiter densevol1 kappa serend
  end% end of while
  clc
  total = [total zeros(length(total),1)];
end % of second while

final_list = total(:);
out_data = histc(final_list,[50:50:5300]);
```

This second set of code covers the tool replicating shockwave generation at open access facilities. Four sets of data are needed at the start: a sample list of platoon sizes representative of the HOV lane, a sample list of follower headways for vehicles within those platoons, and a sample list of leader headways for those platoons. Using these lists of characteristics, traffic streams will be generated within the HOV lane. The fourth set of data is speed measurements on the HOT and the Adjacent PGL to identify the speed drop during the lane change. Based on a gap acceptance model, a vehicle is inserted into the HOV lane to generate a shockwave. The vehicles upstream react using kinematic relationships and the shockwave is tracked. The function outputs histogram data based on the shockwaves observed, with counts for every shockwave length from 1 up to the maximum observed shockwave.

```
% Code for determining high shockwave activity within open access system
% --------------------------------------------------------------------------
% Inputs to the program:
%       platoonsize.xlsx – List of platoon sizes representative of the HOV lane
%       followerheadways.xlsx – List of headways for followers
%       leaderheadways.xlsx – List of leader headways for platoons
%       speeddata.xlsx – List of speed measurements on the HOV and adjacent lanes when lane changes
%                        occur
%
% Outputs:
%       out_data – Histogram data of shockwave lengths
% --------------------------------------------------------------------------

% Code for estimating the length that a shockwave will propagate based on
% empirical distributions. A Monte Carlo sampling process constructs a
% sequence of vehicles based on the collected observations for the platoon
% sizes and headways with respect to the platoon sizes. Kinematic equations
% are the core of the experiment used in a new car following model.

% Panagiotis Stanitsas / John Hourdos
% University of Minnesota

count = input('How many iterations would you like?        ');

[~,~,all1] = xlsread('platoonsize.xlsx');
[~,~,all2] = xlsread('followerheadways.xlsx');
[~,~,all3] = xlsread('leaderheadways.xlsx');
[~,~,all4] = xlsread('speeddata.xlsx');

for i = 1:length(all1);
   platoonsize(i,1) = all1{i,1};
end

for i = 1:length(all2);
   for j = 1:7
      sepfolhead(i,j) = all2{i,j};
   end
end

for i = 1:length(all3);
   leaderheadway(i,1) = all3{i,1};
```

```
end

leaderheadway(leaderheadway == 0) = [];
platoonsize(platoonsize > 7) = [];

% The loop will terminate if one vehicle is not forced to decelerate.
kkk = 2;
test = 1;
mntcr = 1;
while test > 0;
   b = 100;
   disp(mntcr)
   sequencelength = 0;
   while b > 90;
      b = normrnd(57,6);
   end
   gapthreshold(mntcr) = normrnd(0.8,0.05);
   % Creating the initial matrices of zero to increase the speed of the experiment
   hd = zeros(1,1);
   maxacc = zeros(100,1);
   maxdec = zeros(100,1);

   vehlen = zeros(100,1);
   X = zeros(1000,100);
   V = zeros(1000,100);
   decstoppoint = zeros(100,1);
   accstoppoint = zeros(100,1);
   rt = zeros(100,1);
   rcomp = zeros(100,1);

   %% Generating values for the model variables using distribution number generators
   for i=1:100;
      maxacc(i) = normrnd(5.6,0.3^2);
      maxdec(i) = 2 * maxacc(i);
      vehlen(i) = normrnd(18,1.5^2);
      while rt(i) < 0.5
         rt(i) = normrnd(1,0.3);
      end
      rcomp(i) = normrnd(35,1.5^2);
   end

   %% Sampling from the empirical distribution for proper headways and
   % Creating the sequence of different platoons and assigning leader headways
   sum = 1;
   j = 1;
   while sum <= 93;
     plindex = randi(length(platoonsize),1,1);
     platoon(j,1) = platoonsize(plindex,1);
     ldhdindex = randi(length(leaderheadway),1,1);
     hd(sum,1) = leaderheadway(ldhdindex,1);
     if platoon(j,1) > 1;
        for i = 2:platoon(j,1);
           folheadcol = sepfolhead(:,i);
           folheadcol(folheadcol == 0) = [];
           flhdindex = randi(length(folheadcol),1,1);
```

```
        hd(sum + i-1,1) = folheadcol(flhdindex);
      end
    end
    sum = sum + platoon(j,1);
    j = j + 1;
end

% Aggregating headways
go = 0;
for i =1:length(hd)
    go = go + hd(i,1);
end

% Corresponding macro measurements
flow = 3600 * length(hd) / go;
spacmeanspeed = 65 / 1.02;
density = flow / spacmeanspeed;

%% Introducing the disturbance at a point that is derived based on the gap selection model
accprob = 0;
kk = 0;
while accprob < gapthreshold;
    kk = kk + 1;
    accprob = gapacc(hd(kk),kk-1,b);
end

hd = hd(kk:length(hd),1);

%% Validating the sequence
if (density < 25 && density > 15)
    %% Creating the leader's trajectory
    densitystored(mntcr,1) = density;
    densitystored(mntcr,2) = 15;
    densitystored(mntcr,3) = 25;
    X(1,1) = 1000;
    V(1,1) = 95.3355;
    % Point obtaining the minimum speed
    minspeed = sampleSpeeds(all4);
    decstoppoint(1) = round(10 * b/(0.5 * maxdec(1)));
    accstoppoint(1) = round(10 * b/(maxacc(1)));

    for i=2:1000;
        % First 0.5 secs of undisturbed movement
        if (i >= 1 && i <= 50);
            V(i,1)= V(1,1);
        X(i,1)= X(i-1,1) + V(i-1,1)*0.1;
        end
        % Decelerating part
        if (i > 50 && i <= 50 + decstoppoint(1));
            V(i,1) = V(i-1,1) - 0.5 * maxdec(1)*0.1;
            X(i,1) = X(i-1,1) + V(i-1,1) * 0.1 - 0.5 * 0.5 * maxdec(1) * 0.1^2;
        end
        % Acelerating part
        if (i > (50 + decstoppoint(1)) && i <= (50 + decstoppoint(1) + accstoppoint(1)));
            V(i,1) = V(i-1,1) + maxacc(1)*0.1;
```

```
    X(i,1) = X(i-1,1) + V(i-1,1) * 0.1 + 0.5 * maxacc(1) * 0.1^2;
  end
  % Second linear part
  if (i > 50 + decstoppoint(1) + accstoppoint(1))
    V(i,1) = V(i-1,1);
    X(i,1) = X(i-1,1) + V(i-1,1)*0.1;
  end
end

%% Creating the following vehicles trajectories according to kinematic equations.
agrt = 0;
h3 = 0;
i = 2;
while i < sum;
  h1 = 0;
  h2 = 0;
  % Initial position for the following vehicle
  V(1,i) = 95.3355;
  X(1,i) = X(1,i-1) - hd(i) * 95.3355;
  agrt = agrt + rt(i);
  % 1st part of undisturbed movement
  for j = 2:round(50 + agrt * 10);
    V(j,i) = V(1,i);
    X(j,i) = X(j-1,i) + V(j-1,i)*0.1;
  end
  % position at this point
  secondvehpos = X(round(50 + agrt * 10),i);
  % car following part beginning
  decthres = maxdec(i-1);
  for j = (round(50 + agrt * 10)+1):1000;
    % Estimated position of the leader given the speed at the previous interval;
    estposleader = X(j-1,i-1) + V(j-1,i-1) * 0.1;
    estposfol = X(j-1,i) + V(j-1,i)*0.1;
    % Implement the threshold deceleration
    V(j,i) = V(j-1,i);
    X(j,i) = X(j-1,i) + V(j-1,i) * 0.1;
    % check if the follower needs to decelerate or accelerate;
    if (estposleader-estposfol <= 3*rcomp(i) && estposleader-estposfol > rcomp(i) && V(j,i) > (V(j,i-1)));
      V(j,i) = V(j-1,i) - decthres * 0.1;
      X(j,i) = X(j-1,i) + V(j-1,i) * 0.1 - 0.5 * decthres * 0.1^2;
      h1 = 1;
    elseif (estposleader - estposfol <= rcomp(i) && V(j,i) > (V(j,i-1)))  ;
      V(j,i) = V(j-1,i) - maxdec(i) * 0.1;
      X(j,i) = X(j-1,i) + V(j-1,i) * 0.1 - 0.5 * 1.5 * maxdec(i) * 0.1^2;
      h2 = 1;
    % else check if the follower needs to accelerate
    elseif (estposleader - estposfol > rcomp(i) && V(j,i) < (V(j,i-1)));
      V(j,i) = V(j-1,i) + maxacc(1) * 0.1;
      X(j,i) = X(j-1,i) + V(j-1,i) * 0.1 + 0.5 * maxacc(1) * 0.1^2;
    elseif (V(j-1,i) >= V(1,1));
      V(j,i) = V(1,1);
      X(j,i) = X(j-1,i) + V(j-1,i) * 0.1;
    end
  end
  i = i + 1;
```

```
        j = i;
        if (h1 == 0 && h2 == 0)
          wavelength(mntcr,1) = j-1;
          meanwavelength(mntcr,1) = mean(wavelength);
          i = sum + 1;
        end
      end

      mntcr = mntcr + 1;
      if mntcr == kkk * 300;
        x1 = wavelength(1:(kkk-1)*300,1);
        x2 = wavelength(:,1);
        test = kstest2(x1,x2,0.95);
        kkk = kkk + 1;
        test = + test;
      end
    end
end

out_data = histc(wavelength,[0:(max(wavelength)+1)]);
```